

University of Nebraska - Lincoln

DigitalCommons@University of Nebraska - Lincoln

Civil and Environmental Engineering Theses,
Dissertations, and Student Research

Civil and Environmental Engineering

Spring 4-16-2021

A METHODOLOGY FOR ESTIMATING CAPACITY AND PASSENGER CAR EQUIVALENTS FOR CONNECTED AND AUTOMATED VEHICLES TRAVELING ON FREEWAYS

Antonio Hurtado Beltran
University of Nebraska-Lincoln

Follow this and additional works at: <https://digitalcommons.unl.edu/civilengdiss>



Part of the [Transportation Engineering Commons](#)

Hurtado Beltran, Antonio, "A METHODOLOGY FOR ESTIMATING CAPACITY AND PASSENGER CAR EQUIVALENTS FOR CONNECTED AND AUTOMATED VEHICLES TRAVELING ON FREEWAYS" (2021). *Civil and Environmental Engineering Theses, Dissertations, and Student Research*. 163.
<https://digitalcommons.unl.edu/civilengdiss/163>

This Article is brought to you for free and open access by the Civil and Environmental Engineering at DigitalCommons@University of Nebraska - Lincoln. It has been accepted for inclusion in Civil and Environmental Engineering Theses, Dissertations, and Student Research by an authorized administrator of DigitalCommons@University of Nebraska - Lincoln.

A METHODOLOGY FOR ESTIMATING CAPACITY AND PASSENGER CAR
EQUIVALENTS FOR CONNECTED AND AUTOMATED VEHICLES TRAVELING
ON FREEWAYS

by

Antonio Hurtado-Beltran

A DISSERTATION

Presented to the Faculty of:

The Graduate College at the University of Nebraska

In Partial Fulfillment of Requirements

For the Degree of Doctor of Philosophy

Major: Civil Engineering

(Transportation Engineering)

Under the Supervision of Professor Laurence R. Rilett

Lincoln, Nebraska

May, 2021

A METHODOLOGY FOR ESTIMATING CAPACITY AND PASSENGER CAR
EQUIVALENTS FOR CONNECTED AND AUTOMATED VEHICLES TRAVELING
ON FREEWAYS

Antonio Hurtado-Beltran, Ph.D.

University of Nebraska, 2021

Advisor: Laurence R. Rilett

Recently, there has been a significant amount of research related to heavy trucks operating as connected and autonomous vehicles (CAVs). In order to understand the potential impact on the freeway system of CAV technologies, analyses should be conducted using the standard US methodological framework. In the current version of the Highway Capacity Manual (HCM-6), equal-capacity passenger car equivalencies (EC-PCEs) are used to account for the effect of heavy trucks on capacity and quality of service analyses. It is argued in this dissertation the HCM-6 EC-PCE methodology for basic freeway and multilane highway segments can be used to explore a wide variety of traffic situations beyond the scope of the existing results including those related to CAV technologies. However, there are various shortcomings to address before applying the methodology for these purposes.

This dissertation develops new strategies to improve the current state-of-the-art methodology for estimating freeway capacity and PCEs. The end result is a new modeling methodology that can be used to analyze new traffic scenarios including connected and automated vehicles (CAVs). Specifically, this dissertation develops consistent metrics for the HCM-6, introduces simpler regression model structures for

fitting simulated and estimated data, and proposes a replicable microsimulation framework. The proposed improvements are examined for both CAV and non-CAV conditions on unidirectional two-lane and three-lane freeway segments. In general, it was found EC-PCE values for CAV trucks are, on average, between 24% and 34% lower compared to the values for non-CAV trucks, indicating that CAV platoons can have a positive effect on freeway capacity. Additionally, it was demonstrated the proposed approaches can be successfully applied to the estimation of EC-PCEs.

The new techniques proposed for capacity modeling and EC-PCE estimation can be used by engineers and traffic agencies for analyzing any traffic condition outside the HCM-6. It is vital all future EC-PCE analyses are performed using the same standard methodological framework to produce comparable results that can be applied consistently in the HCM-6.

To

My beloved family for supporting me all the way.

ACKNOWLEDGMENTS

First, I would like to deeply thank my advisor Dr. Laurence R. Rilett for all his guidance and support. His genuine passion for research has been one of my greatest inspirations along this journey, and it has been a real privilege and a very delightful experience working with him. I would also like to thank the Fulbright foundation for supporting my doctoral studies and making my dream of studying in the U.S. come true.

My sincere appreciations go to my advisory committee members Dr. Aemal J. Khattak, Dr. Kent M. Eskridge, and Dr. Ronald K. Faller for all their constructive suggestions, support, and encouragement to successfully complete this work.

Thanks to the Nebraska Transportation Center, the Mid-America Transportation Center, and the Department of Civil and Environmental Engineering for their additional financial support, infrastructure, and administration during my studies. My sincere gratitude to Santos, MM, Ernest, Li, Huong, Janet, Larissa, Madison, and all my fellow students and staff members for their friendship and assistance during my studies.

I would like to provide a special thanks to Dr. Hamid Vakilzadian and Dr. Yunwoo Nam for the extra hours in research advice and the encouragement to go further in my academic development.

I sincerely thank the contributions of Dr. Jianan Zhou for the replication analysis and the empirical data used in this research. I would also like to thank Dr. George List and his colleagues at North Carolina State University for their advice on the 2016 HCM EC-PCE estimation methodology and the background information they provided. It is greatly appreciated.

TABLE OF CONTENTS

List of Figures.....	xiv
List of Tables	xvii
Chapter 1	1
Introduction	1
1.1 Background	1
1.2 Passenger Car Equivalent (PCE) Concept	3
1.3 HCM-6 EC-PCE Procedure	8
1.4 Relationship with HCM Analyses.....	10
1.5 Problem Statement	11
1.5.1 Need for a Replicable Microsimulation Model	12
1.5.2 Model Version Compatibility	14
1.5.3 Model Calibration	14
1.5.4 Need for a Consistent Calculation of Capacity.....	15
1.5.5 Need for Alternative Regression Models for Calculating CAFs	17
1.6 Research Objectives	19
1.7 Research Contributions	20
1.8 Structure of the Dissertation.....	21
Chapter 2	24
Literature Review	24
2.1 Introduction	24
2.2 CAV Truck Platooning Research.....	24
2.3 Modeling the Traffic Demand in VISSIM	27
2.3.1 Microsimulation Model Architecture	27
2.3.2 Vehicle Generation Model	31

2.3.3	Vehicle Interaction Model	37
2.3.4	CAV Platoon-Forming Logic	52
Chapter 3	55
	Impact of CAV truck Platooning on HCM-6 Capacity and Passenger Car	
	Equivalent Values	55
3.1	Introduction	55
3.2	HCM-6 EC-PCE Procedure	57
3.2.1	HCM-6 Model Assumptions.....	58
3.2.2	Background Analysis	60
3.2.3	Step 1: Flow-density plots	61
3.2.4	Step 2: Computation of Capacity Adjustment Factors from Simulation	
	Output	65
3.2.5	Step 3: Regression Models Development for Estimated CAFs	68
3.2.6	Step 4: CAFs Estimation for Specific Conditions	71
3.2.7	Step 5: EC-PCEs Estimation.....	72
3.3	CAV Modeling Methodology	74
3.3.1	CAV Base Case.....	76
3.3.2	Modeling the CAV Base Case	76
3.4	Step 4: Estimated CAF Results for CAV Base Case	81
3.5	Step 5: EC-PCE Results for CAV Base Case	83
3.6	Sensitivity Analysis of CAV Operation Factors	85
3.6.1	Market Penetration Rate	86
3.6.2	Platoon Truck Type: Restricted vs Unrestricted.....	87
3.6.3	Platoon Size	88
3.6.4	Lane Restriction	89
3.7	Concluding Remarks	90

Chapter 4	94
An Alternative Regression Model Structure for the HCM-6 Equal Capacity Passenger Car Equivalency Methodology	94
4.1 Introduction	94
4.2 Regression Model Approach.....	96
4.3 Methodology	97
4.3.1 Step 1 and 2: HCM-6 EC-PCE Microsimulation Model Capacity	98
4.3.2 Step 3: Regression Model Development for Estimated CAFs.....	101
4.3.3 Step 4 and 5: CAF and EC-PCE Estimation.....	106
4.4 Calibrated Regression Model Results	107
4.4.1 NLRM Calibrated Models	107
4.4.2 MLRM Calibrated Models.....	107
4.4.3 NLRM _{red} Calibrated Models.....	108
4.5 Goodness-of-Fit Results.....	109
4.6 CAF Model Results.....	111
4.6.1 HCM-6 Replication.....	111
4.6.2 CAV Truck Platooning	114
4.7 EC-PCE Results	115
4.8 Concluding Remarks	117
Chapter 5	120
Proposed Equations for HCM-6 Passenger Car Equivalent Values.....	120
5.1 Introduction	120
5.2 Original Nonlinear Regression Model (NLRM) for Estimated CAFs	121
5.3 Proposed Nonlinear Regression Model (NLRM _{red}) for Estimated CAFs	122
5.4 Proposed Equations for Calculating HCM-6 EC-PCE Values.....	123

5.5	Analyzing the Marginal Effects in the Proposed CAF model.....	130
5.5.1	Marginal Truck Percentage Effect	131
5.5.2	Marginal Grade-Distance Effect	135
5.5.3	Additive Property of Marginal Effects	140
5.6	Concluding Remarks	141
Chapter 6	143
	Impact of Capacity Definition on the HCM-6 Passenger Car Equivalent	
Values...	143
6.1	Introduction	143
6.2	Issues with the HCM-6 EC-PCE Approach	144
6.2.1	HCM-6 Capacity Definition	145
6.2.2	Model Calibration	148
6.2.3	Number of Microsimulation Replications for Each Scenario	149
6.2.4	Layout of Microsimulation Model.....	150
6.3	Proposed Approach for EC-PCE Estimation	152
6.3.1	Microsimulation Framework	153
6.3.2	Model Calibration	154
6.3.3	Capacity Definition	156
6.3.4	CAF and PCE Estimation	157
6.4	Comparison of Estimated CAF Results	158
6.5	Comparison of EC-PCE Results	160
6.6	Concluding Remarks	164
Chapter 7	166
	Impact of CAV Truck Platooning on Four-Lane Freeway Segments in Western	
U.S.	166
7.1	Introduction	166

7.2	Operational Traffic Conditions in Western U.S.....	167
7.3	Data Description.....	168
7.4	Microsimulation Model.....	171
7.5	Model Calibration	172
7.6	Proposed Procedure for the EC-PCE Estimation	176
7.6.1	Step 1: Simulated Capacity Determination.....	179
7.6.2	Step 2: Simulated CAFs Computation.....	184
7.6.3	Step 3: Regression Models Development	186
7.6.4	Step 4: CAFs Estimation for Specific conditions	188
7.6.5	Step 5: EC-PCEs Estimation.....	188
7.7	Calibrated Regression Model Results	189
7.8	Comparison of Estimated CAF Results	191
7.9	Comparison of EC-PCE Results	192
7.10	Concluding Remarks	195
Chapter 8	200
	Concluding Remarks and Recommendations.....	200
8.1	Concluding Remarks	200
8.1.1	Use the Exact HCM-6 EC-PCE Methodology for Exploring CAV Truck Platooning	202
8.1.2	Assess the Convenience of Alternative Regression Model Structures	203
8.1.3	Propose Simpler Equations to Calculate and Interpret CAFs and EC- PCEs.....	203
8.1.4	Propose a New Microsimulation Framework and Evaluate its Impact on HCM-6 EC-PCEs.....	204
8.1.5	Develop an Improved EC-PCE Methodology for Novel Traffic Scenarios	205

8.2 Future Research.....	206
References	210
Glosary and Key Abbreviations	223
APPENDIX A	226
The Importance of Stochasticity on Microsimulation Model Output	226
A.1 Introduction.....	226
A.1 Underlying Theory of Stochasticity in Vehicle Generation.....	229
A.1.1 Scenario (1) for Exploring Stochasticity.....	229
A.1.2 Results of Distributions for Stochastic Volumes and Time Headways	231
A.1.3 Results of Variability of Stochastic Volumes	233
A.1.4 Results of Variability in Exact Volumes.....	236
A.2 Impact of Stochasticity on Performance Measures.....	238
A.2.1 Scenarios (2 & 3) for Assessing Impact on Performance Measures.....	238
A.2.2 Interrupted Flow Case (Scenario 2)	238
A.2.3 Uninterrupted Flow Case (Scenario 3).....	241
A.2.4 Results of the Impact of Stochasticity on Performance Measures.....	243
A.3 Concluding Remarks.....	247
APPENDIX B	250
Impact of the Entry Time Model on CAV Platoon Formation	250
B.1 Introduction	250
B.2 Methodology	251
B.2.1 Microsimulation Model and Testbed	251
B.2.2 Time Headway Models	254
B.2.3 Stochastic Attributes Definition	259
B.2.4 Simulation Runs	260

B.2.5 Simulation Output Processing	261
B.3 Results and Discussion	261
B.3.1 Platoon Formation	261
B.3.2 Platoon Frequency	263
B.3.3 Platoon Size	265
B.4 Concluding Remarks	267
APPENDIX C	269
Impact of the Simulation Resolution on Microsimulation model Output	269
C.1 Introduction	269
C.2 Methodology	270
C.2.1 Traffic Scenario Combinations	271
C.2.2 Simulation Resolution Sensitivity	272
C.2.3 Time per Run	272
C.3 Discussion and Results	273
C.3.1 Simulated Capacity Results	273
C.3.2 Flow-Density Scatterplots Results	277
C.3.3 Time per Simulation Run Results	279
C.4 Concluding Remarks	281

LIST OF FIGURES

Figure 1-1. Flow-impedance relationship (modified from Huber, 1982)	4
Figure 1-2. Process for EC-PCE estimation according to HCM-6	8
Figure 1-3. Schematic of the HCM-6 VISSIM model for EC-PCE estimation (modified from Zhou, 2018)	9
Figure 2-1. Building blocks of the microsimulation architecture (modified from Barceló, 2010)	29
Figure 2-2. Car following model by Wiedemann (PTV, 2012)	39
Figure 2-3. Wiedemann 74 thresholds	41
Figure 2-4. Wiedemann 99 thresholds	45
Figure 2-5. Gap definitions in the lane-changing process (modified from Fransson, 2018).	50
Figure 3-1. Passenger car only flow-density scatter plot (grade 3%, distance 1 mi).....	64
Figure 3-2. Mixed traffic flow-density scatter plot (grade 3%, distance 1 mi).	65
Figure 3-3. Estimated CAF for Each Scenario.	67
Figure 3-4. Original CAF from HCM-6 versus Estimated CAF derived from more recent VISSIM models.	71
Figure 3-5. Impact of the VISSIM version on the replication of HCM-6 EC-PCEs.....	73
Figure 3-6. Flow-density scatter plot for 20% CAVs (grade 3%, distance 1 mi).....	77
Figure 3-7. Goodness of fit between simulated and estimated CAFs for original and proposed model.	80
Figure 3-8. CAF values as a function of scenario number: CAV and non-CAV scenarios	82
Figure 3-9. EC-PCE values as a function of truck percentage: CAV and non-CAV scenarios.....	84
Figure 3-10. CAV EC-PCEs as a function of market penetration rate.	87
Figure 3-11. CAV EC-PCEs as a function of truck type platoon.	88
Figure 3-12. CAV EC-PCEs as a function of platoon size.	89
Figure 3-13. CAV EC-PCEs as a function of lane restriction.	90
Figure 4-1. Simulated CAFs for each scenario combination.....	100
Figure 4-2. Comparison of goodness-of-fit between regression models.	111

Figure 4-3. CAF values as a function of scenario number for the HCM-6 Replication .	113
Figure 4-4. CAF values as a function of scenario number for the CAV condition	115
Figure 4-5. EC-PCE values for the HCM-6 replication.....	116
Figure 4-6. EC-PCE values for the CAV condition.....	116
Figure 5-1. Goodness-of-fit of proposed equation for 30/70 SUT/TT truck composition.	126
Figure 5-2. Goodness-of-fit of proposed equation for 50/50 SUT/TT truck composition.	126
Figure 5-3. Goodness-of-fit of proposed equation for 70/30 SUT/TT truck composition.	127
Figure 5-4. Marginal Effect of Truck Percentage on CAFs.....	132
Figure 5-5. Marginal Effect of Truck Percentage on EC-PCEs.....	133
Figure 5-6. Marginal Effect of Truck Percentage on Freeway Capacity.....	134
Figure 5-7. Marginal Effect of Combined Grade and Distance on CAFs.	136
Figure 5-8. Marginal Effect of Combined Grade and Distance on EC-PCEs.	138
Figure 5-9. Marginal Effect of Combined Grade and Distance on Freeway Capacity... ..	140
Figure 6-1. Effect of capacity definition and aggregation level on simulated capacity.	147
Figure 6-2. Gap sensitivity results used for model calibration.	156
Figure 6-3. CAF values as a function of scenario number for the proposed and HCM-6 approaches.....	160
Figure 6-4. EC-PCE values for the proposed and HCM-6 approaches.	161
Figure 7-1. Truck attributes considered in the microsimulation model (Zhou, 2018; Dowling et al., 2014).	170
Figure 7-2. Schematic of the VISSIM model for EC-PCE estimation.	171
Figure 7-3. Gap sensitivity results used for the model calibration of: (a) non-CAV condition and (b) CAV truck platooning condition.	174
Figure 7-4. Proposed Process for EC-PCE estimation.....	177
Figure 7-5. Passenger car only flow-speed scatter plot (grade 3%, distance 1 mi).	182
Figure 7-6. Mixed traffic flow-speed scatter plot for non-CAV condition (20% truck percentage, 3% grade, and 1 mi distance).....	183

Figure 7-7. Mixed traffic flow-speed scatter plot for CAV condition (20% truck percentage, 3% grade, and 1 mi distance).....	184
Figure 7-8. CAF values for four lane freeways as a function of scenario number: CAV and non-CAV scenarios.	192
Figure 7-9. EC-PCE values for four-lane freeways as a function of truck percentage: CAV and non-CAV scenarios.....	193
Figure A-1. Example of histograms for (a) stochastic volumes and (b) time headways	232
Figure A-2. Variability of stochastic input volumes.....	234
Figure A-3. Example of existing stochasticity in fractions of the time interval.	237
Figure A-4. Schematic of scenarios for (a) interrupted and (b) uninterrupted flow (modified from Zhou, 2018).	239
Figure A-5. Means and standard deviations of average delay from scenario 2.....	245
Figure B-1. Schematic of the microsimulation model.	252
Figure B-2. Histograms for lognormal and exponential time headway models.	257
Figure B-3. Empirical CDFs of desired speed.	260
Figure B-4. Platoon formation for lognormal and exponential time headway models...	262
Figure B-5. Mean platoon frequency as a function of distance: exponential and lognormal models.....	264
Figure B-6. Mean platoon size as a function of distance: exponential and lognormal models.	266
Figure C-1 Impact of simulation resolution on simulated capacity (as 95 th percentile of maximum flow rate).....	274
Figure C-2 Impact of simulation resolution on simulated capacity (as maximum flow rate).	275
Figure C-3 Flow-density scatterplots as a function of simulation resolution.	278
Figure C-4. Relative time per run as a function of simulation resolution.....	280

LIST OF TABLES

Table 1-1. Impedance Metrics Used in the Literature	5
Table 2-1. Headway Distribution Models (modified from Roy & Saha, 2018).	36
Table 2-2. Lane-Changing Parameters in VISSIM.....	51
Table 3-1. CAV Driving Behavior Parameters in VISSIM 20.	75
Table 3-2. Goodness of Fit Results for CAV Analysis.....	79
Table 3-3. Parameters and their Estimates for various CAF Models	81
Table 3-4. List of Parameters Studied in the Sensitivity Analyses.....	85
Table 4-1. Explanatory Variables for the Regression Models.....	106
Table 4-2. Parameters in the NLRM for CAF Estimation	107
Table 4-3. Goodness-of-Fit Statistics for Estimated CAF values.....	110
Table 5-1. PCE Values from Trilinear Interpolation and HCM-6 CAF Model.....	128
Table 6-1. Independent versus Single Runs on Capacity Values for a Mixed Traffic Scenario.....	152
Table 6-2. Calibrated NLRM Models.....	159
Table 6-3. PCE Values for Proposed and Original Approaches.....	162
Table 7-1. Driving Behavior Parameters in VISSIM 20.....	174
Table 7-2. Goodness-of-Fit Statistics for Estimated CAF values.....	190
Table A-1. Applied Criteria for Best-fit Distributions on: (a) Stochastic Volume and (b) Time Headways.....	231
Table A-2. Descriptive Statistic of the Analyzed Stochastic Vehicle Input Combinations	233
Table A-3. Descriptive Statistic and Paired t-test of Performance Measures at Interrupted Flow Conditions.....	243
Table A-4. Descriptive Statistic and Paired t-test of Performance Measures at Uninterrupted Flow Conditions.	246
Table B-1. Summary Statistics for a Sample of Time Headways.....	256
Table C-1 Descriptive Statistics and two-sided t-test of Explored Simulation Resolutions.	276

CHAPTER 1

INTRODUCTION

1.1 Background

Passenger car equivalencies (PCEs) are used to account for the effect of different vehicle types on capacity and quality of service of a mixed traffic stream. These vehicle types include heavy vehicles, motorcycles, and recreational vehicles and the PCE accounts for differences in size and operational characteristics as compared to passenger cars. In effect, the PCE represents the number of passenger cars that would produce the same effect on the traffic flow as a given vehicle type. Transportation engineers use PCEs to convert traffic streams, measured in vehicles per hour (veh/h), to an ‘equivalent’ stream measured in passenger car units per hour (pcu/h). This allows various roadways, which have different proportions of vehicle types, to be analyzed and/or designed based on a single metric.

In the current version of the Highway Capacity Manual (HCM-6), PCEs for freeway and multilane highway segments are estimated using the equal-capacity method. The equal-capacity passenger car equivalences (EC-PCEs) are calculated using the estimated capacities of both mixed-flow and passenger car-only flow (HCM, 2016; Dowling et al., 2014a; Yang, 2013; Zhou, 2018). It is important to note that the HCM-6 equal capacity methodology for freeway segments is based completely on VISSIM microsimulation model results aggregated over one-minute intervals. This is important because up until the HCM-6, all HCM data aggregations levels were at the 15 minute

level. The HCM-6 includes EC-PCE values for 14 levels of truck percentage, 13 levels of grade, 7 levels of grade distance, and 3 levels of truck composition type.

The advantage of using a simulation model is obvious—it greatly reduces the amount of empirical data that needs to be collected and allows for a relatively quick analysis of many different situations. The disadvantages include complex and time-consuming model calibration and validation, considerable inputs and simulation parameters, and a need for a deep understanding of the underlying logic of the models (Hendrickson and Rilett, 2017; Rilett, 2020). It is argued in this dissertation the HCM-6 EC-PCE procedure can be used to explore a wide variety of traffic situations beyond the scope of the existing results. For example, the methodology allows a user to simulate disruptive technologies such as connected and autonomous vehicles (CAV) and use the resulting output to estimate capacity and PCE values. However, there are various shortcomings to address before applying the methodology for these purposes. Some of these shortcomings include the need for a calibration of the microsimulation model, compatibility issues between model versions, unclear consistency while computing metrics, and poor flexibility of the existing regression model for fitting data. Therefore, if analysts are going to use the HCM-6 EC-PCE procedure to model new traffic situations and use the output to estimate capacity and PCE values, they must ensure the experiments can be repeated and the results are consistent with the analytical methods contained in the HCM-6.

The research described in this dissertation will develop new strategies that improves the current state-of-the-art methodology for estimating freeway capacity and PCEs. The end result is a new modeling methodology that can be used to analyze new

traffic scenarios including connected and automated vehicles (CAVs). The primary aim is to develop an improved microsimulation-based methodology that can be used to the current Highway Capacity Manual (HCM-6) for capacity modeling and the estimation of EC-PCE values at freeway and multilane highway segments. The new methodology would allow for more accurate, replicable, consistent, and comparable results while exploring new traffic scenarios beyond the existing scope of the HCM-6. The improvements of the proposed approach are mostly related to three aspects of the current HCM-6 EC-PCE methodology: (1) create a new simulation framework for the traffic microsimulation model that will improve the repeatability of the results despite the compatibility of the microsimulation model versions and their inherent uncertainties, (2) develop consistent metrics between the microsimulation based methodology and the core methodologies contained in the HCM-6, and (3) develop alternative regression model structures to fit simulated and estimated data that will facilitate the process of reporting results.

In summary, this dissertation emphasizes the importance of having a standard methodological framework to estimate capacity and EC-PCE values for novel traffic situations in basic freeway and multilane highway segments. It is critical all future EC-PCE analyses produce comparable results that can be applied consistently to the core methodologies described in the HCM-6.

1.2 Passenger Car Equivalent (PCE) Concept

The PCE concept has been used for over 55 years in the Highway Capacity Manual (HCM) and other design guides (HCM, 1965; HCM, 2016; AASHTO, 2011; Urbanik et al., 2015). In the current HCM-6, the PCEs are defined as *factors that allow the analyst*

to convert a mixed traffic stream of cars and trucks to a single uniform PCE stream for purpose analysis.' They are used to account for the effect of heavy vehicles on capacity and level of service (LOS) on freeways in the HCM-6.

The concept was formally introduced by Huber (1982), who proposed a framework for estimating PCE values for vehicles under free-flow and multilane conditions considering various measures of impedance. According to this approach, the PCE formulation can be simplified into a ratio between the flow rate of a basic traffic stream composed by passenger cars, and the flow rate of a mixed traffic stream composed by passenger cars and trucks, where both traffic streams experience the same level of impedance as shown in **Figure 1-1**. Thus, the PCE values based on a measure of impedance are calculated using **Equation (1-1)**.

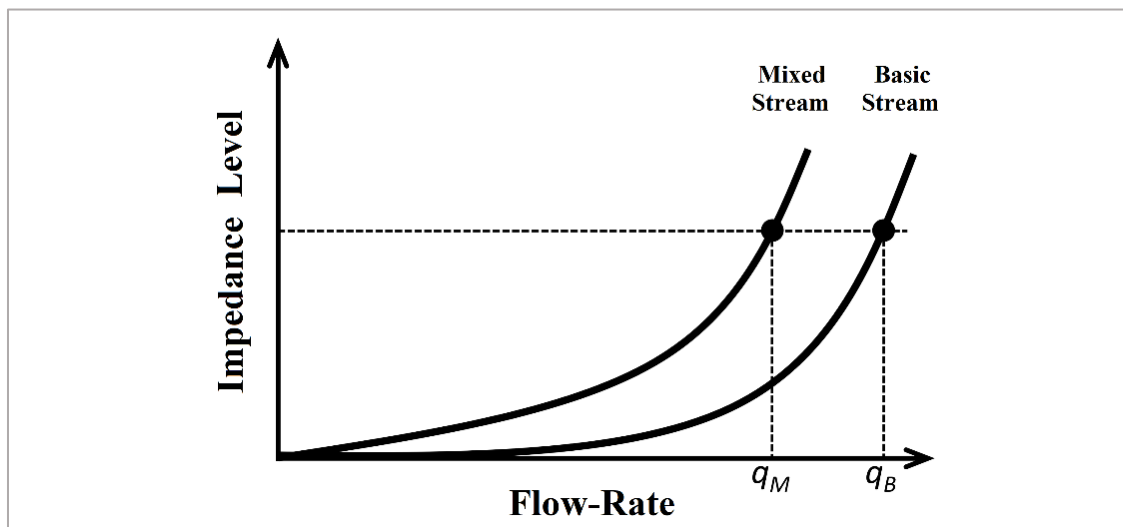


Figure 1-1. Flow-impedance relationship (modified from Huber, 1982)

$$PCE = \frac{1}{p} \left(\frac{q_B}{q_M} - 1 \right) + 1$$

(1-1)

Where:

PCE : Passenger car equivalence factor.

q_B : Basic flow-rate composed by passenger cars at common impedance level.

q_M : Mixed flow-rate composed by passenger cars and trucks at common impedance level.

p : Proportion of trucks in the mixed traffic flow.

Various metrics of impedance have been used in the literature along with different methods for estimating PCE values. Some of the impedance metrics that have served as a basis for the proposed methods are provided in **Table 1-1**. Typically, the PCE is defined as the ratio of the impedance metric for the passenger car flow and the mixed flow conditions. An extensive literature review about the PCE concept can be found elsewhere (Raj et al., 2019; Sharma & Biswas, 2020).

Table 1-1. Impedance Metrics Used in the Literature

Author (Year)	Impedance Metric	Traffic Flow Condition
Krammes & Crowley (1986); Okura & Sthapit (1995a)	Headways	Uninterrupted
Elefteriadou, Torbic, & Webster (1997)	Speed	Uninterrupted
Webster & Elefteriadou (1999); Rakha et al. (2007)	Density	Uninterrupted
Benekohal & Zhao (2000); Chitturi & Benekohal (2008)	Delay	Interrupted
Keller & Saklas (1984); Huber (1982)	Travel Time	Interrupted
Al-Kaisy, Jung, & Rakha (2005); Al-Kaisy, Hall, & Reisman (2002)	Queue Discharge Flow	Interrupted
Van Aerde, & Yagar (1984); Gunst & Webster (1975)	Platoon-based	Uninterrupted
Okura & Sthapit (1995b)	Volume to Capacity Ratio	Uninterrupted

Huber (1982)	Level of Service	Uninterrupted
Alecsandru, Ishak, & Qi (2012); Fan (1990); Yeung, Wong, & Secadiningrat (2015)	Capacity	Uninterrupted

In the current HCM-6, the PCE values were obtained using an equivalency method in which the capacity was the impedance metric of reference. The capacity is defined as the maximum sustainable hourly flow rate that can pass a given point of the road system during a given time period under prevailing roadway, environmental, traffic, and control conditions. Any change in the prevailing conditions (e.g., heavy vehicle percentage) changes the capacity of the system. The equal capacity passenger car equivalences (EC-PCEs) allow for the conversion of the mixed flow capacity values into passenger car-only capacity values and vice-versa. For obvious reasons, this equivalency method requires finding the capacities for the passenger car-only flow condition and the mixed traffic flow condition. These are then used to estimate the EC-PCE values. In the HCM-6 EC-PCE methodology, the capacity values were obtained using a microsimulation model approach explained in more detail later. The EC-PCE values are calculated using **Equation (1-2)**. Note this equation is based on the Huber's model (Huber, 1982).

$$EC - PCE_{p_s, m_s, g_s, d_s} = \frac{1}{p_s} * \left(\frac{C_{1, g_s, d_s}}{C_{2, p_s, m_s, g_s, d_s}} - 1 \right) + 1 \quad (1-2)$$

Where:

$EC - PCE_{2, p_s, m_s, g_s, d_s}$: EC-PCE for the mixed flow at truck percentage p_s , truck composition m_s , grade g_s , and distance d_s .

C_{2,p_s,m_s,g_s,d_s} : Capacity for the mixed flow at p truck percentage level, m truck composition level, g grade level, d distance level, (veh/h/ln).

C_{1,g_s,d_s} : Capacity for the passenger car-only flow at g grade level, d distance level, (veh/h/ln).

p_s : Truck percentage (between 0 and 1).

The HCM-6 methodology introduced the concept of the capacity adjustment factor (CAF) to represent the ratios between the capacities of both mixed traffic and passenger car-only conditions as shown in **Equations (1-3)** and **(1-4)**.

$$CAF_{2,p_s,m_s,g_s,d_s} = \frac{C_{2,p_s,m_s,g_s,d_s}}{C_{1,g_s,d_s}} \quad (1-3)$$

$$CAF_{1,g_s,d_s} = \frac{C_{1,g_s,d_s}}{C_{1,g_s,d_s}} = 1 \quad (1-4)$$

Where:

CAF_{2,p_s,m_s,g_s,d_s} : Capacity adjustment factor for the mixed flow at truck percentage p_s , truck composition m_s , grade g_s , and distance d_s .

CAF_{1,g_s,d_s} : Capacity adjustment factor for the auto-only flow at grade g_s , and distance d_s .

C_{2,p_s,m_s,g_s,d_s} : Capacity for the mixed flow at p truck percentage level, m truck composition level, g grade level, d distance level, (veh/h/ln).

C_{1,g_s,d_s} : Capacity for the passenger car-only flow at g grade level, d distance level, (veh/h/ln).

By considering the capacity adjustment factors, the EC-PCE values can be also estimated using **Equation (1-5)**, which is derived from **Equation (1-2)**.

$$EC - PCE_{2,p_s,m_s,g_s,d_s} = \frac{1 - (1 - p_s) * CAF_{2,p_s,m_s,g_s,d_s}}{p_s * CAF_{2,p_s,m_s,g_s,d_s}} \quad (1-5)$$

Where:

$EC - PCE_{2,p_s,m_s,g_s,d_s}$: EC-PCE for the mixed flow at truck percentage p_s , truck composition m_s , grade g_s , and distance d_s .

CAF_{2,p_s,m_s,g_s,d_s} : Capacity adjustment factor for the mixed flow at truck percentage p_s , truck composition m_s , grade g_s , and distance d_s .

p_s : Truck percentage (between 0 and 1).

1.3 HCM-6 EC-PCE Procedure

The HCM-6 EC-PCE values were obtained using a microsimulation-based methodology comprised of five main steps as shown in **Figure 1-2**.

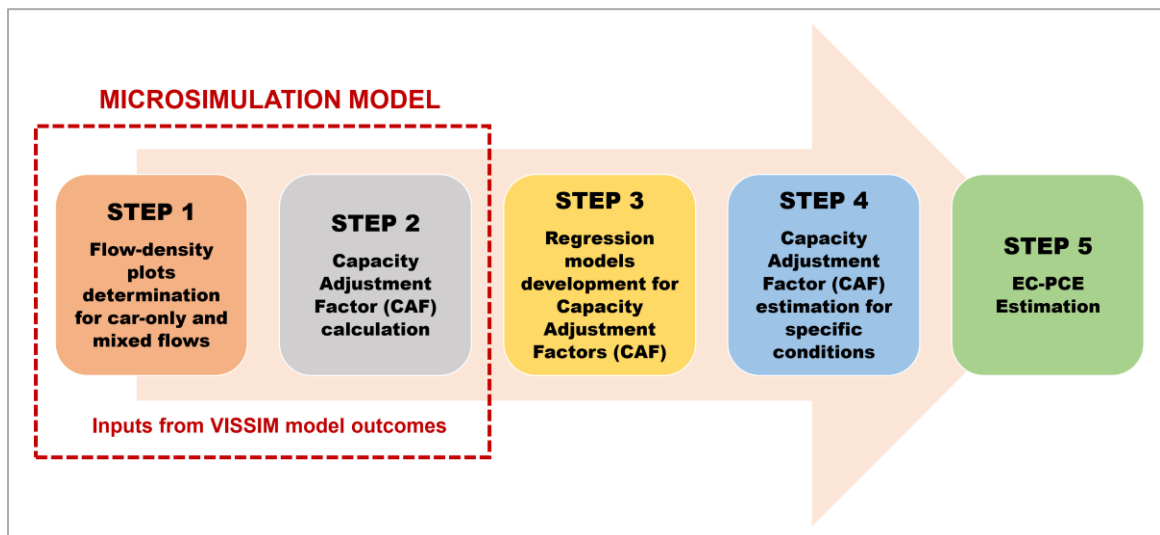


Figure 1-2. Process for EC-PCE estimation according to HCM-6

In Step 1, the simulated capacities for both passenger car-only flow and mixed flow are obtained for combinations of grade, grade length, truck percentage, and vehicle fleet composition. In Step 2, the Capacity Adjustment Factors (CAFs) for 1,274 scenarios are calculated. A nonlinear regression model is created in Step 3 that can predict the CAF value as a function of the parameters analyzed in Step 1. These calibrated models are used to estimate CAFs in Step 4. In Step 5, the EC-PCEs for specific combinations of truck percentage, grade, and grade distance are estimated based on the CAF estimates. These are the values provided in the HCM-6. A complete description of the HCM-6 EC-PCE methodology, including the key simulation parameters of the VISSIM model, can be found elsewhere (Zhou, Rilett, & Jones, 2019; Zhou, 2018; Dowling et al., 2014b).

As the process demonstrates, the microsimulation model is used in the HCM-6 EC-PCE methodology to obtain the capacity values for the 1,274 scenario combinations. The layout of the test network considered in the microsimulation model is depicted in **Figure 1-3**.

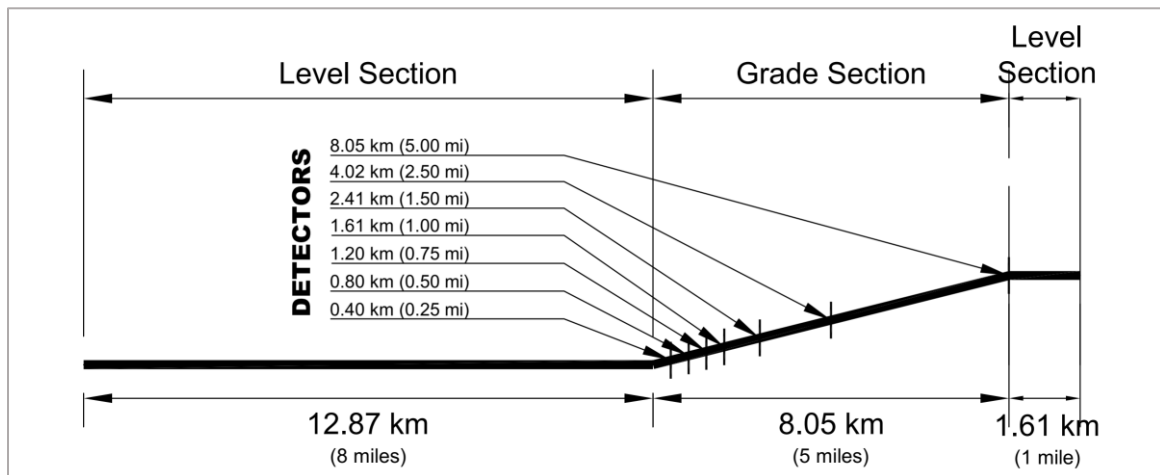


Figure 1-3. Schematic of the HCM-6 VISSIM model for EC-PCE estimation

(modified from Zhou, 2018)

This test network is a unidirectional freeway segment with a total length of 15 miles. The intermediate grade section of 6 miles contains seven data collection points used to obtain the inputs required for calculating the capacity values.

It is important to note the HCM-6 methodology has a large number of assumptions including those related to vehicle speed (e.g., all vehicles travel at the same uniform free-flow speed of 70 mph), vehicle type (e.g., single unit trucks and semitrailer trucks as heavy vehicles), weight and power, driving behavior (e.g., Wiedemann 99), operating conditions (e.g., three-lanes per direction, no lane restriction, etc.), and aggregation level (1 minute). A detailed description of the assumptions can be found elsewhere (Dowling et al., 2014a; Zhou, 2018). These assumptions define the scope of the existing results included in the HCM-6. Therefore, care must be taken in using the EC-PCE values obtained in the original research when the key assumptions are not met for a particular analysis.

1.4 Relationship with HCM Analyses

The EC-PCE values are used in various chapters of the HCM-6 to calculate the heavy vehicle adjustment factor f_{HV} given by **Equation (1-6)**. This factor converts the observed traffic demand (mixed traffic condition) into a standard flow-rate measured in passenger cars per hour (pc/h).

$$f_{HV} = \frac{1}{1 + P_T(E_T - 1)} \quad (1-6)$$

Where:

f_{HV} : Heavy vehicle adjustment factor (decimal).

E_T : Passenger car equivalent of one heavy vehicle in the traffic stream (PCEs).

P_T : Proportion of SUTs and TTs in the traffic stream (decimal).

In the HCM-6, the heavy vehicle adjustment factor is used in the calculation of the following metrics related to freeway and multilane highway facilities:

- Adjusted demand volume, v_p (*Chapter 12, Basic Segments, Equation 12-9*),
- Capacity of weaving segments, C_w (*Chapter 13, Weaving Segments, Equation 13-6*),
- Demand flow rate for subject movement, v_i (*Chapter 14, Merging & Diverging Segments, Equation 14-1*), and
- Demand flow rate in PCEs, $q_{i,t}$ (*Chapter 25, Planning-Level Methodology for Freeway Facilities, Equation 25-41*).

It is clear the EC-PCEs are of vital importance for analyzing the capacity and level of service of extended lengths of freeway composed of continuously connected basic freeway segments, weaving segments, and merging and diverging segments. These operational analyses are key for transportation agencies that prioritize upgrading and new construction projects based on forecasted demand and supply of the freeway system.

1.5 Problem Statement

As discussed above, the HCM-6 EC-PCE methodology for freeway and multilane highway segments represents an important and significant improvement for estimating freeway capacity and associated Passenger Cars Equivalents. To fully realize its potential, the modeling approach should be capable of analyzing a wide variety of local conditions and different traffic scenarios. This is important because a more robust

capacity and PCE estimation methodology could be used to explore not only different operational conditions (e.g., lane restrictions, traffic compositions, etc.) and geometric arrangements (e.g., number of lanes, steep grades, etc.) but also the impact of disruptive technologies (e.g., connected autonomous vehicles, battery-based electric vehicles, etc.) in which transportation agencies are especially interested. However, to meet these goals a number of improvements to the current HCM-6 methodology are required. Specifically, methodologies related to experimental replication, consistency while computing metrics, and more flexible regression model structures to fit simulated and estimated data will be required. These issues represent the motivation behind this dissertation and are explained in further detail in the following sections.

1.5.1 Need for a Replicable Microsimulation Model

The HCM-6 CAF/EC-PCE values are dependent on the VISSIM Version 4.4 simulation model that is no longer available. It is important to note no empirical data was used to calibrate or validate the results (Dowling et al., 2014a, 2014b; Yang, 2013; Zhou, 2018). This is a huge advantage from a modeling perspective; it takes significantly less time to model the 1,274 HCM-6 scenarios in comparison to collecting empirical data and developing statistically-based models. In addition, it also allows modelers to study new traffic situations. However, there are a number of issues related to the “all-simulation” approach adopted by the HCM-6 that require further analyses to ensure consistent and replicable results.

The HCM-6 included a section that provides recommendations for using alternative tools, such as microsimulation models, for analyzing freeway and multilane highway segments (HCM, 2016). Interestingly, the majority of these recommendations

were not observed in the original research (Dowling et al., 2014a, 2014b; Zhou, 2018).

These recommendations are listed below:

- **Assure compatibility between the capacity obtained from alternative tools and those of the HCM:** In the HCM-6 there is no consistency in capacity values and definitions between the original research and the core methodology of the HCM-6 (Dowling et al., 2014b). This point will be discussed in more detail later.
- **Determine the free-flow speed (FFS) of the study site by field data or estimation:** The original research behind the HCM-6 considered a constant speed of 70 mph for all vehicles instead of speed distributions (Zhou, Rilett, & Jones, 2019a). It is hypothesized this produces unrealistic driving behavior and, therefore, suspect results.
- **Calibrate the simulation model by modifying the parameters related to the minimum time headway so that the capacity obtained by the simulator closely matches the HCM estimate:** Interestingly, in the research conducted as part of the HCM-6, the default driving-behavior parameters were used in the original model without targeting an empirical capacity value (Yang, 2013; Dowling et al., 2014b).
- **Estimate the number of runs required for a statistically valid comparison:** In the original research only one simulation run was performed for each of the 1,274 simulated scenarios. This point is crucial because performing a single simulation run drastically increases the noise of the simulation results and

could potentially negatively impact the accuracy of the capacity estimates and the associated EC-PCE values.

1.5.2 Model Version Compatibility

The VISSIM developers acknowledge simulation results can differ among different versions due to changes and updates in the internal logic of the simulator (PTV, 2019b). Because of this, there is no guarantee newer versions of VISSIM will result in the same EC-PCE values obtained from earlier versions, making difficult the replication of the experiments. Since the HCM-6 was released in 2016, there have been no less than five versions of VISSIM released. For example, it was observed from preliminary experiments the simulated capacity for the passenger car-only condition, which is the basis for the CAF/EC-PCE calculation, was 6.54% lower, on average, for the VISSIM 20 results as compared to the VISSIM 9 results (Hurtado-Beltran & Rilett, 2021). A paired t-test at 0.05 level of significance showed that such a difference was statistically significant. Similar results were found by comparing the capacity results from other VISSIM versions. Therefore, assuming that the simulation logic underlying VISSIM release 4.4, used in the original research is the same as newer VISSIM versions would be a mistake. Moreover, the exact version VISSIM 4.4 is not available anymore, which represents a significant problem for replicating the results.

1.5.3 Model Calibration

Although some operational and geometric characteristics of the vehicles including acceleration profiles, weight and power distributions, and vehicle dimensions, were set in the HCM-6 EC-PCE model according to findings from previous research, no empirical

data was used to calibrate the driving-behavior of vehicles in the simulation. In the original research, the default Wiedemann 99 (car-following) and slow lane rules (lane-changing) were used to model the driving-behavior of the driver-vehicle units (Zhou, 2018). A user may obtain capacity values that differ greatly from the base capacity values included in the HCM-6 (*Exhibit 12-4*). The difference will be a function of the VISSIM version and the capacity definition used. For example, the HCM-6 capacity of basic freeway and multilane highway segments under base conditions ranges from 1,900 to 2,400 pc/h/ln and is a function of the free-flow speed and the facility type (HCM, 2016). These capacity values represent the national norm in the US. For example, the base capacity for a freeway segment at 70 mph of free-flow speed is 2,400 pc/h/ln; however, the microsimulation model of the original research may produce capacities as low as 2,059 pc/h/ln (VISSIM 11) or 2,275 pc/h/ln (VISSIM 20) for the same conditions and this can negatively affect the calculation of CAF/EC-PCE values.

It is hypothesized an adequate model calibration, targeting an empirical value of capacity (e.g., the HCM-6 base capacity), will improve the accuracy of the results. In addition, this will ensure the results can be reproduced and repeated by others regardless of the inherent uncertainties of the microsimulation model.

1.5.4 Need for a Consistent Calculation of Capacity

In the original EC-PCE research, the capacity is defined as the 95th percentile of the maximum one-minute average flow-rate for the given scenario (Dowling et al., 2014a, 2014b; Yang, 2013). This is the first instance, to the author's knowledge, that the HCM used an aggregation level other than 15-minutes to calculate a traffic flow metric. In fact,

the traffic demands used in HCM analyses are typically expressed as flow rates that represent four times the peak 15-minute traffic demand.

In the HCM-6, the capacity for basic freeway and multilane highway segments is defined as the maximum hourly flow rate related to some type of breakdown during a sustained period of 15 minutes. The same manual included a section to estimate the capacity in the field while taking into account the same capacity definition. Moreover, a similar capacity definition can be found for various transportation facilities in the manual. For example, in weaving segments, the capacity is defined as “*the maximum flow rate for a 15-min analysis period, as are all capacities*”.

On the other hand, previous studies have shown the EC-PCE values may differ depending on the data aggregation level used to estimate capacity. For example, it has been reported the EC-PCE values were, on average, 11% lower for data aggregation levels of 15 minutes as compared to the aggregation level of one-minute used in the original research (Zhou, Rilett, & Jones, 2019b). The authors found this difference was statistically significant at 5% level of significance. Similar results were found if different percentiles were used in the calculations. For example, the authors used the maximum flow rate (e.g., 100th percentile) instead of the 95th percentile used in the original research and they found greater capacity values that tended to produce greater CAF values.

It was recognized in the original research that the capacity should be defined as the maximum flow rate which would be in concordance with the theoretical definition (Dowling et al., 2014b; Yang, 2013). Nevertheless, due to the amount of noise found in the flow-density plots, it was decided to calculate the capacity as the 95th percentile of the average one-minute flow rate. It is hypothesized this noise was mainly due to the data

aggregation level of one-minute and/or the use of only one simulation run. This, in turn, resulted in atypical flow rate peaks. It should be noted the developers of the original HCM approach stated the reliability of the procedure may improve if capacity is calculated in a more accurate way (Yang, 2013).

Care must be taken in comparing the capacity values found in the EC-PCE research with other published capacity values based on larger aggregation levels. For example, in the HCM-6 mixed flow model, the estimated CAF values (one-minute aggregation level) of the EC-PCE research are used to compute the mixed-flow capacity (*Equation 26-5*, HCM, 2016). This mixed-flow capacity is compared with the auto-only capacity (*Exhibit 12-6*) that was based on a larger aggregation level (15 minutes). It is important to analyze the impact of using different percentiles of flow-rate and different aggregation levels on the EC-PCE estimation. It is expected by calculating the capacity, using a consistent percentile of flow-rate and aggregation level with those used in the core methodologies for basic freeway and multilane highway facilities, the approach will produce more reliable and comparable EC-PCE values as compared to the current values.

1.5.5 Need for Alternative Regression Models for Calculating CAFs

The capacity adjustment factors (CAFs) are defined as a ratio between the capacity of the mixed flow condition and the passenger car-only flow condition considering comparable scenario combinations. These CAFs are the main input to estimate EC-PCE values.

Because of the inherent variability of the CAF results from simulation, the HCM-6 developers chose not to use the CAF values for a given combination of parameters directly. Instead, they calibrated a nonlinear regression model that related the CAF value to the truck percentage, grade, distance, and free-flow speed parameters. The goal was to

mitigate the effect of the variability in the CAF results. The form for the HCM-6 analytical model was based on kinematic and resistance equations related to vehicles ascending and descending different grades (Dowling et al., 2014c). A heuristic optimization approach was used to calibrate the model where the aim was to identify the model parameters that minimized the error between the simulated CAFs and the estimated CAFs. The parameters of these equations were optimized, using an Excel Spreadsheet. A detailed description of the nonlinear regression model used in the HCM-6 EC-PCE methodology can be found elsewhere (Dowling et al., 2014b; List, et al., 2014) Zhou, Rilett, & Jones, 2019; Zhou, 2018).

The current CAF/EC-PCE values suggest the combined effect of grade and distance is significantly different for positive grade values as compared to negative values. Indeed, the original research reported grade is the main influencing factor (Dowling et al., 2014b). It is hypothesized a segmented function based on the grade conditions (positive and negative) could improve the model fitting for the estimation of CAF values using simpler regression models. However, this approach has not been explored in previous studies.

It is argued an analysis of the form and error of the regression models using fitting simulated and estimated data should be conducted. It is possible different model structures for the regression analysis might provide better results. In this regard, it is important to determine if simpler models may reasonably assist at this stage of the procedure while modeling novel traffic situations. This would represent an advantage for the analyst because the estimated CAFs could be calculated analytically through more

straightforward equations than those used in the HCM-6. This would facilitate the process of understanding and reporting the results.

1.6 Research Objectives

The primary goal of this dissertation is to develop an improved microsimulation-based methodology for capacity modeling. The new methodology will allow for more accurate, replicable, consistent, and comparable capacity results. This will, in turn, improve the estimation of equal capacity passenger car equivalences (EC-PCE) at freeway and multilane highway segments used in capacity and level of service analyses. Moreover, the dissertation will demonstrate how the approach can be further used to analyze new traffic situations such as the implementation of CAV technology. The specific objectives are:

1. Demonstrate that the HCM-6 EC-PCE methodology has the potential to be used for exploring new traffic situations such as disruptive technologies. In this case, the EC-PCE values for CAV truck platooning on basic freeway segments (e.g., unidirectional three-lanes) will be explored using the original HCM-6 approach.
2. Assess the convenience of alternative regression model structures to fit simulated and estimated data, especially while modeling disruptive technology such as CAVs.
3. Propose simpler equations that facilitate the computation and interpretation of the CAF and EC-PCE values for the HCM-6.
4. Propose a new simulation framework for the microsimulation model used in the EC-PCE methodology that provides results that can be replicated readily.

It is important to overcome issues principally related to model calibration and

consistency of the results with the core methodology of the HCM-6 (e.g., comparable capacity, CAF, and PCE values).

5. Propose an improved methodology to estimate EC-PCEs for freeway segments that overcomes the main issues identified in the original HCM-6 EC-PCE research. The proposed approach will be used to examine the effect of CAV truck platooning under the US Western conditions (e.g., unidirectional two-lanes) using empirical data.

1.7 Research Contributions

The new techniques proposed in this dissertation for capacity modeling and EC-PCE estimation are expected to be applied for any traffic condition beyond the scope of the HCM-6. The proposed approach will provide a more flexible and repeatable procedure usable by engineers and traffic agencies for generic purposes. The original HCM-6 methodology considered various assumptions (e.g., three-lanes per direction, no lane restriction, trucks and cars have the same free-flow speed, etc.) that can be easily violated. For these cases, the improved methodology allows repeating the procedure for the local conditions of interest to obtain more accurate, reliable, and comparable EC-PCE values.

To illustrate, the new methodological framework could be used to model and explore further traffic scenarios as those related to emerging and disruptive technologies. It is expected these technologies will transform the operational dynamics of the national highway system in the following decades producing a significant impact on freeway capacity (Hallmark, Veneziano, & Litteral, 2019; Fitzpatrick et al., 2016; Bujanovic & Lochrane, 2018). In this regard, the proposed framework could be used to analyze how

the deployment of CAVs will affect freeway capacity, especially during the transitional period in which the CAVs and non-CAVs will share the road system. Similarly, the methodology could be applied to estimate EC-PCE values for battery-based electric trucks expected to have different acceleration/deceleration profiles and weight to power ratios that will change their operational behavior as compared to conventional vehicles.

It is vital all the future capacity and EC-PCE analyses are performed using the same standard methodological framework to produce comparable results that can be applied consistently into the core methodologies described in the HCM-6.

1.8 Structure of the Dissertation

The remainder of this dissertation is organized into seven chapters. First, a literature review is included in Chapter 2 to provide background on the current state of the truck platooning research. Moreover, some key microsimulation models of special interest for the development of this research are exposed such as the vehicle generation model, the vehicle interaction model, and the CAV platoon forming logic.

Chapter 3 through 7 are the body of this research. These chapters provide an additional review of the literature on the background of each chapter's research objective. Chapter 3 to Chapter 7 are either peer-reviewed published technical papers or currently under preparation or consideration by a technical journal for publication.

Chapter 3 uses the exact Highway Capacity Manual, Sixth Edition (HCM-6) equal capacity passenger car equivalencies (EC-PCE) methodology to estimate capacity and EC-PCEs for CAV truck platoons on three-lane freeway segments. The original HCM-6 EC-PCE procedure is described step by step. A comparative analysis of the EC-PCE values estimated for CAV trucks and non-CAV trucks is discussed. In addition, a

sensitivity analysis explores some relevant CAV operational assumptions including market penetration rate, platoon size, truck type restriction, and lane restriction. This chapter also addresses some issues identified in the original HCM-6 methodology relative to experimental replication and regression models development. Note that a significant part of this chapter was published in the American Society of Civil Engineers Journal of Transportation Engineering (Hurtado-Beltran & Rilett, 2021).

Chapter 4 contributes to the dissertation narrative by assessing the performance of the original nonlinear regression model used in the HCM-6 EC-PCE research as compared to simpler regression model structures. The performance of the regression models is analyzed considering two traffic conditions, CAV truck platooning and conventional traffic. Note a significant part of this chapter will be published in a forthcoming edition of the Transportation Research Record journal (Hurtado-Beltran & Rilett, 2021).

Chapter 5 introduces a simpler nonlinear regression model used to develop equations for the estimation of CAF values and EC-PCE values for freeway and multilane highway segments. The benefits of the proposed equations and how they could be implemented in the HCM-6 are discussed in this chapter. Finally, the marginal effects of the main contributors in the proposed model are analyzed to better understand the relationship between the main influencing factors defined in the HCM-6 research and the traffic metrics.

Chapter 6 addresses some issues identified in the HCM-6 EC-PCE methodology including a new capacity definition and a new data aggregation level atypical of past HCM releases. This chapter compares the HCM-6 PCEs, and associated capacity

adjustment factors (CAFs), with values developed using the HCM-6 EC-PCE methodology with historic HCM assumptions. The proposed approach presented in this chapter is later used in Chapter 7.

The improved methodology developed in this dissertation for estimating capacity and EC-PCE values for traffic scenarios beyond the scope of the HCM-6 is presented in Chapter 7. The proposed methodology is illustrated using the Western U.S. conditions under the operation of CAV truck platooning as a case study. A comparative analysis of the results between the CAV condition and the non-CAV condition is also discussed.

The concluding remarks and future research recommendations of this dissertation are summarized in Chapter 8.

CHAPTER 2

LITERATURE REVIEW

2.1 Introduction

In this research, it is argued the HCM-6 EC-PCE methodology for basic freeway and multilane highway segments can be used to analyze different traffic situations beyond the scope of the HCM-6. In particular, the goal of this research is to examine the CAV truck platooning effect on the estimation of EC-PCE values using the existing HCM-6 approach. It is important to note the HCM-6 EC-PCE methodology is microsimulation-based where a VISSIM model is used for modeling the capacity of various traffic scenario combinations. As a result, the literature review is divided into two parts to provide a better background on these two main components of the research. The first part of the literature review provides a review of the state-of-the-art CAV truck platooning research. The second part provides a description of the microsimulation architecture of VISSIM with especial emphasis on the key models for traffic modeling such as the vehicle generation model and the vehicle interaction model that are of vital interest for the HCM-6 EC-PCE VISSIM model.

2.2 CAV Truck Platooning Research

This dissertation uses the ACEA truck platooning definition where truck platooning is defined as the “linking of two or more trucks in convoy, using connectivity technology and automated driving support systems.” Many researchers believe truck platooning will be one of the earliest CAV technologies to be deployed on the national highway system because of its lower operational complexity and the advantages offered to freight carrier

companies in terms of fuel savings, safety benefits, and labor costs, among others (Janssen, et al., 2015; ACEA, 2017). The Minnesota Department of Transportation reported local transportation agencies should prepare a plan for the gradual integration of automated technology and truck platooning in the next 5 to 10 years (Hallmark, Veneziano, & Litteral, 2019). The report “Challenges to CV and AV Applications in Truck Freight Operations” included an extensive discussion of the challenges and expected benefits of the truck platooning deployment in the US (Fitzpatrick et al., 2016). This report also listed various research needs including research on the impact of CAV platooning on transportation capacity.

Over the past few years, there have been a number of studies analyzing the effect of CAV technology on highway capacity. Kittelson & Associates (2019) derived capacity adjustment factors (CAFs), as a function of volume and market penetration rate, for CAVs on freeway segments that will be used in planning studies. This study utilized VISSIM and examined three different driving behaviors in VISSIM: AV Cautious, AV Normal, and AV All-knowing. The authors found that CAVs may increase freeway capacities by 30-40% at 100% market penetration rates with the caveat that these results would be a function of certain factors such as technology, legislation, and public acceptance.

Stanek (2019) proposed an adjustment factor to modify the adjusted demand volume (V_p in *Equation 12-9*) of the HCM procedure. This adjustment factor was based on VISSIM modeling and was used to account for the effect of passenger car AVs on freeway capacity. The microsimulation model was calibrated so the 15-minute capacity replicated the base capacity included in the HCM-6. This calibrated model was then used

to explore various AV scenarios. Similar to the previous study, a sensitivity analysis of the effect of market penetration rates on freeway capacity was conducted. It was found the AV capacity ranged from 2,350 to 3,200 veh/h/ln. Note the study did not analyze platoon formation nor analyze driver behavior logic.

Shi and Prevedouros (2016) explored the impact of CAV and AV technologies on freeway segment capacity by using a Monte Carlo simulation to estimate level of services (LOS) assuming AVs and CAVs headways (1.0 and 0.5 seconds respectively) and market penetration rates (0.1%, 1%, 5%, and 10% to 100% using 10% intervals). They used the HCM-5 macroscopic equations as a base situation. They found AVs can improve LOS at high density conditions. However, the scope of the study was limited in that they extrapolated existing HCM-5 equations to explore their AV/CAV scenarios. In addition, the HCM-5 capacity values were updated in the HCM-6.

Other studies have also found capacity improvements on freeways due to the deployment of CAV technology (Makridis et al., 2018; Rossen, 2018). It should be noted these studies used experimental data instead of empirical data and did not include an analysis of truck platooning. There were no studies in the literature that used the EC-PCE methodology, which is the standard for capacity analyses of freeways in the U.S. (Zhou et al., 2018; HCM, 2016; Dowling et al., 2014a; Yang, 2013), to analyze truck platooning effects.

The Truck Platooning Project in Japan (TTC, 2019) assessed the deployment CAV truck platooning on a Japanese highway. The platoons ranged in size from 2 to 4 trucks with truck spacing as small as 10 meters and speeds of 70 and 80 km/h. The authors reported successful operation of the platooning systems and identified issues

relative to visibility and merging points. Bevely and Ward (2019) assessed the feasibility of implementing driver assisted truck platooning using Cooperative Adaptive Cruise Control (CACC) and Vehicle to Vehicle (V2V) communication technology. The authors used computational fluid dynamics analysis and simulation models, which were validated using empirical data obtained from a test track. They found truck platooning resulting in fuel savings of between five and seven percent and the improvements were a function of the following distance of trucks in the platoons. The ENSEMBLE project (Konstantinopoulou, Coda, & Schmidt, 2019) identified V2V communication protocols for multi-brand truck platooning in Europe. Three platoon levels were defined based on automation capabilities and time gaps between vehicles. The FHWA Level 1 Truck Platooning Research Program is currently on-going and has the aim of exploring human factors and early deployment factors related to truck platooning operations in the U.S. (McHale, 2019). In addition to this, an extensive literature review relative to truck platooning control systems can be found elsewhere (Guanettia, Kima, & Borrelli, 2018; Li et al., 2016).

2.3 Modeling the Traffic Demand in VISSIM

2.3.1 Microsimulation Model Architecture

During recent years, microsimulation has become an increasingly common traffic analysis tool for planning, operating, and researching transportation engineering systems. A traffic microsimulation model is a virtual representation of a traffic system where the driver-vehicle unit represents the fundamental entity of analysis. According to Jaume Barceló (2010), the architecture system of a microsimulation model generally comprises

four main building blocks: (1) infrastructure, (2) traffic, (3) control, and (4) output. The infrastructure building block shapes the road network and comprises the static objects such as lanes, ramps, connectors, medians, islands, parking lanes, bus stops, sidewalks, crosswalks, buildings, poles, marks, and detectors. On the other hand, the traffic building block includes the dynamic elements of the traffic simulation and has the aim to provide traffic demand and govern its behavior. The entities that are part of the traffic building block may include the driver-vehicle units, pedestrians, bicycles, buses of the transit system, and trains. It is important to mention this building block is key for a reliable traffic simulation because it defines how the dynamic elements are going to behave in the road network. Regarding the control building block, this contains the elements that change the behavior of the dynamic entities in terms of traffic operations. The traffic signal controls, priority rules, and the speed controls are some examples of elements that pertain to the control block.

During the simulation process, the three blocks described above exchange information between each other, forming a loop as shown in **Figure 2-1**. In this loop, the output of one building block may be the input of another one. Within this process, the output building block saves the data derived from each block in the loop. This data collection can be done each tenth of a second or a greater time simulation unit (i.e., simulation time step) defined by the user. The output building block is responsible for processing the data to compute the performance measures or any relevant information requested by the user including a visual animation of the traffic simulation.

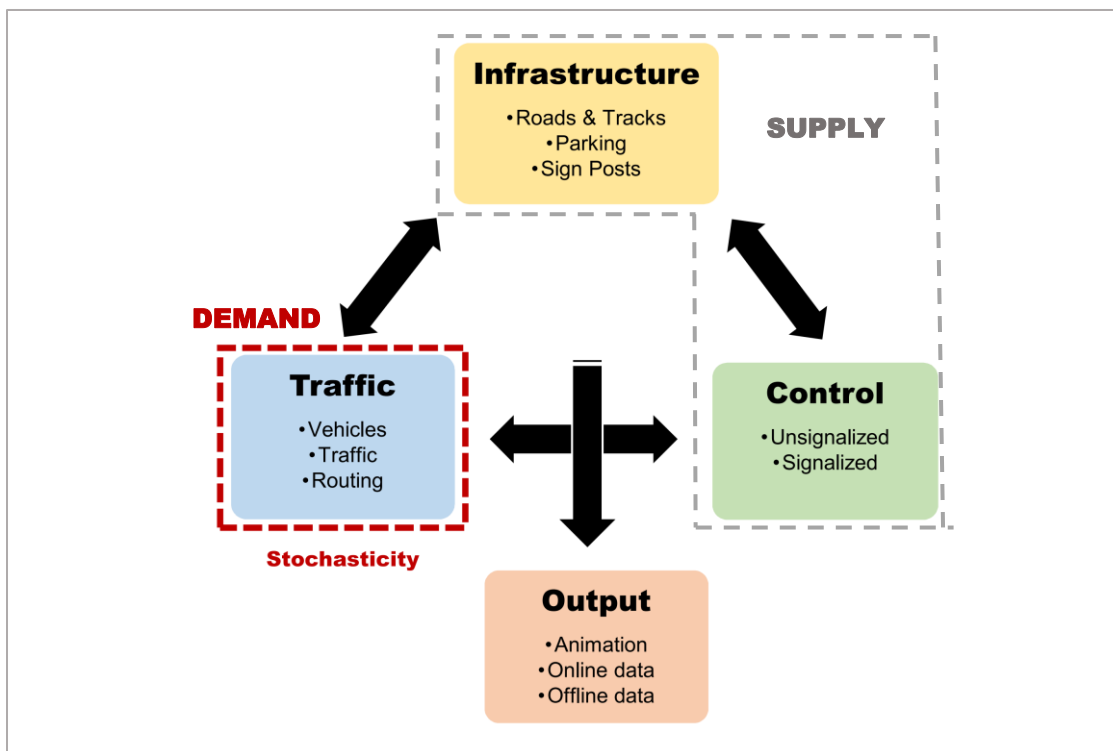


Figure 2-1. Building blocks of the microsimulation architecture (modified from Barceló, 2010)

The focus of this dissertation is closely related to the traffic building block. Here the traffic demand is generated through three key models: (1) vehicle generation (introduce the vehicles in the simulation), (2) vehicle movement (control the behavior and routes of vehicles in the network), and (3) vehicle interaction (govern the reaction of vehicles to other vehicles present in the traffic stream) (Dowling, Skabardonis, & Alexiadis, 2004).

The demand in a microsimulation model is often represented by an origin-destination (OD) matrix, which lists the volume of vehicles traveling between all combinations of a given origin and a given destination over a set time period. For a given OD pair, the vehicle generation model takes the given OD volume and converts it into

simulated vehicles that enter the network at specific times. The OD volume may be treated as either static (e.g., exactly 200 vehicles from origin node A to destination node B) or stochastic (e.g., on average, 200 vehicles travel from origin node A to destination node B where the exact number is randomly chosen during the simulation). The simulated vehicles are assigned to enter the network from a link (e.g., road segment) that originates from the origin (e.g., parking lot). When a driver-vehicle unit is generated in the simulation process, all their attributes are defined as well. These attributes may be grouped into three categories: (1) vehicle characteristics (length, width, maximum/minimum acceleration/deceleration, maximum speed, maximum turn radius, etc.), (2) driver characteristics (aggressiveness, reaction time, desired speed, critical gaps, route, etc.), and (3) time headways between two successive vehicles. The driver-vehicle attributes may be modeled by constants, functional relationships with other attributes, or using probability distributions (Dowling, Skabardonis, & Alexiadis, 2004). The probability distributions are used to reflect the variability of the driver-vehicle characteristics in the real transportation system.

Usually, the traffic demand can be modeled from two main approaches: (1) static assignment (based on vehicle inputs and turning proportions), and (2) dynamic assignment (defined by traffic zones and origin-destination matrices) (Fellendorf & Vortisch, 2010). The first approach is more frequently applied because it is easy and quick to set when the network involves a limited number of turning movements, but here the routes followed by vehicles are randomly assigned. In contrast, the dynamic assignment provides more advantages when it is relevant in the study to track the vehicle path or deals with a more complex network, although obtaining the origin-destination

matrices, which are crucial for the reliability of this scheme, could represent extensive additional works.

The VISSIM models also allows users to introduce driver-vehicle units using the COM interface. The COM (component object model) interface is an add-on module useful for data preparation and processing, scenario management, and objects controlling (PTV, 2019b). The COM interface can execute external script files from a high-level programming language (e.g., Python®, Microsoft® Visual Basic®, MATLAB®, Java®, etc.). Through this module, the user can create vehicle inputs in the network while controlling some stochastic attributes of the driver-vehicle units such as entry times (e.g., arrivals), vehicle type, desired speed, link and lane selection, traffic interaction type, and link position. By controlling the key sources of stochasticity, the COM interface allows users to conduct more realistic experimental studies.

Due to the characteristics of the microsimulation model used in HCM-6 to analyze basic freeway segments, the vehicle generation model and the vehicle interaction model are of special interest for this dissertation. A brief discussion of these key models in VISSIM is provided in the following sections.

2.3.2 Vehicle Generation Model

The vehicle generation model determines how and when the driver-vehicle units are introduced in the simulation. Most microsimulation models include exact and stochastic options to vehicle generation (PTV, 2019b; TTS, 2016; Husch & Albeck, 2004; MnDOT, 2008). In the former, the user decides exactly how many vehicles will be generated, and in the latter, the user inputs the parameters of a predefined distribution and the microsimulation identifies the number of vehicles generated by sampling from this

distribution (Dowling, Skabardonis, & Alexiadis, 2004). In VISSIM, the vehicle generation model uses either vehicle inputs for static assignment or parking lots for dynamic assignment to introduce the traffic in the simulation (PTV, 2018).

2.3.2.1 Vehicle Generation Under Static Assignment

Under the static assignment scheme, the traffic demand is generated at the link entries instead of traffic zones as it occurs in the dynamic assignment. The vehicle input function allows defining a traffic volume (either stochastic or exact) and choosing a predefined vehicle composition. This function requires selecting a link in which the vehicle input is placed. It is important to add the vehicle input generates vehicles for all the lanes part of the link; in other words, vehicles cannot be introduced in individual lanes for multilane links. Here, the lane selection of each generated vehicle depends on the maximum collision time offered by the available lanes (PTV, 2018). When a driver-vehicle unit is generated in the simulation process, all their attributes are defined as well. Such attributes may be grouped into three categories: (1) vehicle characteristics (length, width, maximum/minimum acceleration/deceleration, maximum speed, maximum turn radius, etc.), (2) driver characteristics (aggressiveness, reaction time, desired speed, critical gaps, route, etc.), and (3) Time headways between two successive vehicles (key for the vehicle generation model). The driver-vehicle attributes may be modeled by constants, functional relationships with other attributes, or using probability distributions (Dowling, Skabardonis, & Alexiadis, 2004). The probability distributions are used to reflect the variability of the driver-vehicle characteristics in the real transportation system.

2.3.2.2 Vehicle Inputs in the Vehicle Generation Model

In some cases, the probability distributions used to generate stochasticity in the simulation are applied internally, and the user cannot change their parameters to reflect a specific condition, as occurs with the vehicle input function in VISSIM. According to the VISSIM manual (PTV, 2018), the model uses a seed number to generate a random number that serves as input for a probability distribution which defines the stochastic generation of vehicles at the link entry. The same manual also states the time headways are obtained from a negative exponential distribution (which relates to a Poisson distribution) where the average time gap comes from the hourly volume. For the vehicle input function, the user introduces the following parameters:

- Volume in vehicles per hour [vph], regardless of the length of the associated time interval.
- Volume type, stochastic or exact.
- Vehicle composition associated with the volume (set of vehicle types and their associated classes).
- Time interval in seconds [s] associated with the volume. Several time intervals with different volume and vehicle composition each may be introduced.
- Continued time interval [Boolean]. If selected, the successive time intervals work as a single time interval.
- Link in which the volume will be generated.

The stochastic vehicle input is the default volume type in VISSIM. The user changes this option if the analysis requires deploying exact volumes. For example, the microsimulation model used to estimate the PCEs for the HCM-6 considered exact

vehicle inputs instead of stochastic volumes (Zhou, 2018; Dowling et al., 2014; Yang, 2013). There is no discussion in the literature why this was chosen. In addition to this, some simulation guides also recommend applying exact volumes and a data aggregation interval of 15-min to calculate performance measures (Dowling, Skabardonis, & Alexiadis, 2004). However, in many simulation studies, only the more skilled users take care of the vehicle input type, while the impacts of this selection have not been entirely known. Therefore, volume type and data aggregation size are important aspects to consider while modeling the traffic demand to obtain reliable outputs from any microsimulation.

The associated time interval of the vehicle input is another significant aspect to consider while deploying the traffic volumes. For example, if the user input a traffic volume of 1,200 veh/h for a time interval of 15-minutes in the 'exact' vehicle input scheme, the microsimulator will generate exactly 300 vehicles each 15 minutes. Therefore, the exact volumes would be exact only for the whole associate time interval.

2.3.2.3 Entry Time Model

The entry time model, which is also known as the arrival model in the simulation literature, is part of the vehicle generation model. This model not only creates the driver-vehicle units but also sets the stochastic entry times for the driver-vehicle units by sampling from an input probability distribution.

In some cases, the probability distributions used to generate stochasticity in the simulation are applied internally, and the user cannot change their parameters. This is the case for the entry time model in VISSIM. According to the VISSIM manual, the seed number input to the model is used to generate a series of pseudo-random numbers. These

numbers are used for stochastic modeling of a number of variables including the probability distribution which defines the stochastic generation of vehicles at the link entry location (PTV, 2019b). In other words, the time a given vehicle is modeled as entering the network is generated in this model. If the seed number changes, so too does the simulated entry times. In VISSIM, the time headways of vehicles entering the network are obtained from an exponential distribution where the average time headway is derived from the volume input by the user.

The time headway is defined as the time that elapses between two successive vehicles passing a given point on a link where the reference is taken from the front bumper of those vehicles (HCM, 2016). One of the earliest headway models used in traffic flow theory was the exponential model (Roy & Saha, 2018; Li & Chen, 2017). In this model, the time headways of vehicles traveling on uninterrupted flow conditions relate to an exponential distribution while the number of the vehicles over a time interval fits a Poisson distribution. It has been found this model is more realistic for lightly congested traffic conditions where the variance of the time headways is approximately equal to the mean time headway (Mannering, Kilareski, & Washburn, 2007). However, for underdispersed or overdispersed traffic other headway models may provide better results.

Most of the commercial traffic microsimulation packages use the exponential distribution to model the stochasticity of time headways in vehicle generation because it is easy to code, has low processing demand, and if there are no platooning effects in the network, it fits standard traffic flow theory (PTV, 2019b; TTS, 2016; Husch & Albeck, 2004; MnDOT, 2008). However, various empirical studies have shown that time

headways can fit different statistical distributions (e.g., lognormal, log-logistic, gamma, Pearson, etc.) depending on the characteristics of the traffic demand (Maridpour, 2015; Maurya, Dey, & Das, 2015). **Table 2-1** shows various headway distributions that have been used to model different traffic operating conditions on highways in the literature. For example, the exponential distribution is considered suitable for modeling headways at low flow rates while the lognormal distribution is recommended when there are moderate to high levels of congestion (Roy & Saha, 2018; Li & Chen, 2017). It is important to note traffic microsimulation studies are often used to analyze transportation facilities when they are approaching or at congested conditions. Interestingly, the most recent version of the Highway Capacity Manual (HCM) has utilized the VISSIM microsimulation exclusively to identify capacity for freeways in the U.S. (HCM, 2016).

Table 2-1. Headway Distribution Models (modified from Roy & Saha, 2018).

Author (Year)	Distribution Function	Traffic Condition
Adams (1936)	Poisson	Arrivals in short periods
Greenberg (1966)		
Mei and Bullen (1993)	Lognormal	Moderate to heavy flow
Luttinen (1996)		Car-following models
Dey & Chandra (2009)		
Adams (1936)	Exponential	Low flow; small vehicles (e.g., two-wheelers)
Kumar and Rao (1998)		
Al-Ghamdi (2001)		
Arasan and Koshy (2003)		
Luttinen (1996)	Gamma	Low to moderate flow
Yin et al. (2007)	Log-logistic	Heavy flow, congestion status
Jang (2012)		
Riccardo and Massimiliano (2012)	Pearson 5, Person 6	Heavy flow

2.3.3 *Vehicle Interaction Model*

2.3.3.1 Car-Following Model

The car-following model defines the interaction between two successive vehicles traveling in the same lane. This model assumes the driver of the following vehicle will accelerate or decelerate as a response to the stimulus received from the leading vehicle. There are two main types of car-following models that have been used to represent this basic behavior: (1) stimulus-response models (Chandler et al., 1958) and (2) psycho-physical models (Wiedemann, 1974).

VISSIM uses a psycho-physical car-following model that incorporates a stochastic response of the driver depending on its prevailing driving state. The thresholds of the stimulus in which the driver takes an action are known as action points and they define different car following stages. According to Wiedemann (1974), there are four different car following stages: (1) no reaction, (2) unconscious reaction, (3) conscious deceleration, and (4) collision. These four stages of following a leading vehicle can also be understood as driving states: (1) free flow, (2) following, (3) approaching, (4) braking, and (5) collision (PTV, 2018). These driving states are defined below:

- Free flow: the leading vehicle does not influence the driving of the following vehicle. The target of the driver in the following vehicle is to reach its desired speed. This driving state is highlighted by a significant gap between both vehicles.
- Approaching: The driver in the following vehicle adapts its speed to the lower speed of the leading vehicle. The driver consciously perceives a significant difference of speed between both vehicles, so he decelerates the vehicle to

diminish that difference of speed until reaching the desired safety distance. In this case, the driver applies the desired deceleration assigned to the vehicle category.

- **Following:** The driver in the following vehicle maintains the desired safety distance between both vehicles without consciously accelerating or decelerating. The difference of speed oscillates around zero due to the imperfect throttle control.
- **Braking:** The gap between the following and leading vehicle falls below the desired safety distance. The driver in the following vehicle applies medium to high deceleration rates to increase the gap and recover the desired safety distance.

Figure 2-2 shows the four driving states and thresholds of Wiedemann's car following model. The thresholds that define each driving state are a function of the difference of speed and distance gap, which implies that different values of these parameters will generate different regions for each driving state. These thresholds are defined as follows:

- **AX:** desired distance between two successive vehicles in a standing queue.
- **ABX:** desired safety distance (or desired minimum following distance).
- **SDV:** approaching point when the driver consciously perceived a slower vehicle.
- **OPDV:** increasing speed difference when the drivers of the follower vehicles perceived they are traveling at a lower speed than the leading vehicle.
- **CLDV:** decreasing speed difference that accounts for small speed differences in short decreasing distances where additional deceleration is applied. In VISSIM this threshold is assumed to be equal to SDV.

- SDX: maximum following distance which varies between 1.5 and 2.5 times the minimum following distance.

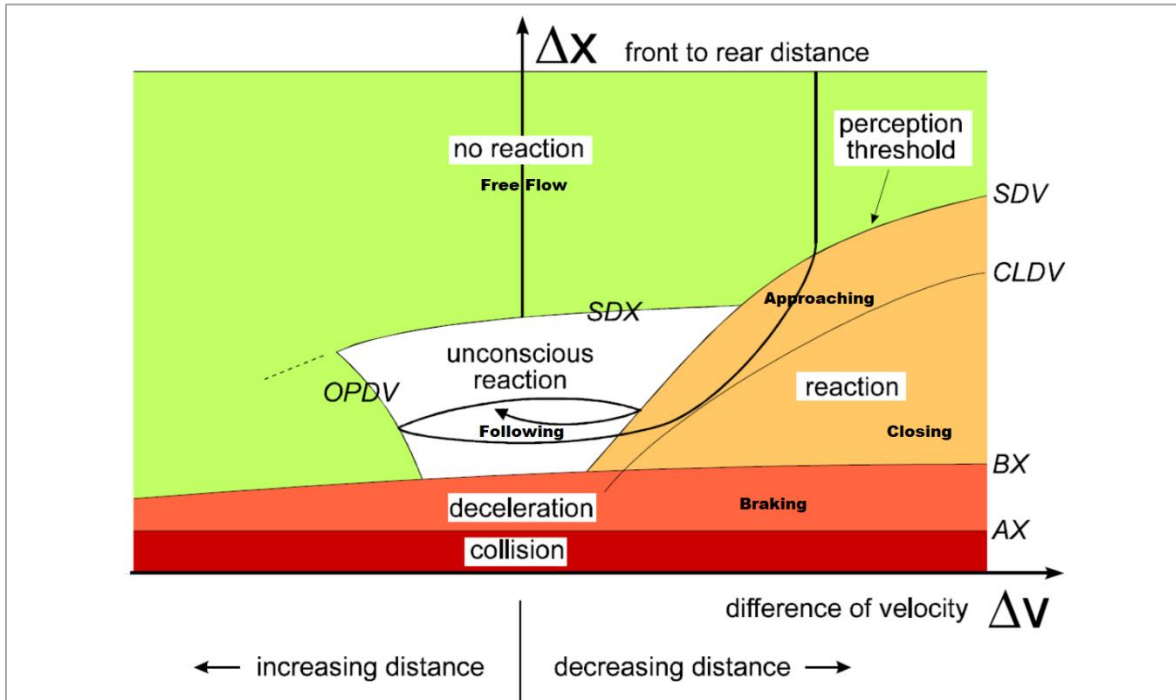


Figure 2-2. Car following model by Wiedemann (PTV, 2012)

According to the VISSIM manual (2018), if the following vehicle is driving below its desired speed during the free flow state, the acceleration is defined based on the following:

- 1) If the desired safety distance is reached, the following vehicle drives at the same speed as the leading vehicle;
- 2) If the desired safety speed is between 100% and 110%, the speed of the following vehicle is interpolated between its desired speed and the leading vehicle's desired speed;

- 3) If the safety distance is greater than 110%, the follower vehicle accelerates to its desired speed.

One of the challenges of the psycho-physical models is to define the distribution of the thresholds that produces representative results of real traffic scenarios. The VISSIM manual (2018) stated the car following model has been calibrated through several measurements developed at the Institute of Transport Studies of the Karlsruhe Institute of Technology in Germany. The thresholds that define the different driving states are a function of the difference of the speed and the distance gap (front to rear distance). The variability of the driver dependent characteristics such as perception abilities and willingness to risk is modeled by including random values normally distributed to the parameters. The Wiedemann model assumes that the desired speed of the driver, the desired safety distance, and the perception of speed differences are parameters that vary across the driver population.

In VISSIM, the user can select among three different types of car following models: (1) no interaction (vehicles do not recognize any other vehicles), (2) Wiedemann 74 (recommended for modeling urban traffic and merging areas), and (3) Wiedemann 99 (recommended for freeway traffic without merging areas). The formulas that provide the thresholds (action points) that define the different driving states in the Wiedemann 74 and Wiedemann 99 models are explained in the following sections.

2.3.3.2 Wiedemann 74

The Wiedemann 74 model considers six thresholds (action points) to define the four driving states. These thresholds are AX, ABX, SDV, OPDV, CLDV, and SDX. The equations to compute the thresholds were obtained from Olstam and Tapani (2004) who

refers to Wiedemann and Reiter (1992) for a complete explanation of the random numbers used in the model. It is important to note the exact difference between the car following model used in VISSIM and the model described by Wiedemann and Reiter (1992) has not been publicly known. The model parameters the user is able to change in VISSIM appear in red in **Equations (2-1) to (2-7)**. In contrast, the remaining parameters included in the equations are managed internally in VISSIM. **Figure 2-3** shows the Wiedemann 99 thresholds using **Equations (2-1) to (2-6)** assuming the default VISSIM parameters and a speed of 20 m/s (45 mph) for the leading vehicle.

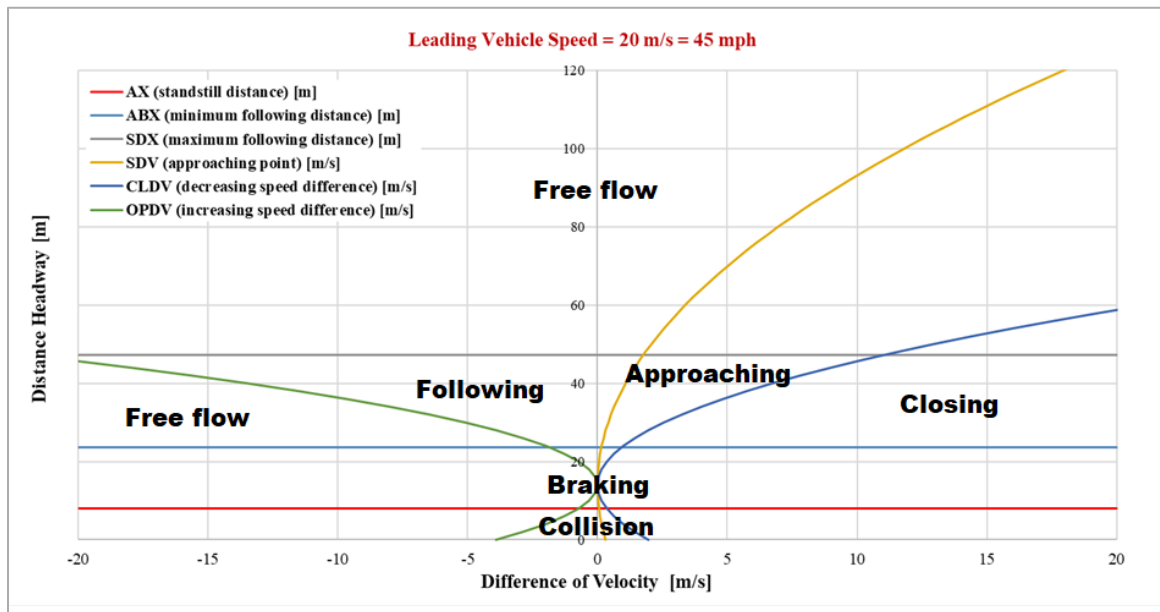


Figure 2-3. Wiedemann 74 thresholds.

$$AX = L_{n-1} + AX_{add} + RND1_n * AX_{mult} \quad (2-1)$$

Where:

AX : desired standstill distance.

L_{n-1} : length of the leading vehicle.

$RNDI_n$: normally distributed driver dependent parameter. Mean equal to zero and standard deviation of 0.3 m.

AX_{add} : calibration parameter. In VISSIM this parameter appears as W74ax (average standstill distance) and has a default value of 2.0 m with a tolerance that lies from -1.0 m to +1.0 m due to the values taken by the random parameter $RND1_n$.

AX_{mult} : calibration parameter. Due to the tolerance of the parameter AX_{add} , it is assumed the value for this parameter is equal to 1.0 m.

$$ABX = AX + BX \quad (2-2)$$

$$BX = (BX_{add} + BX_{mult} * RNDZ_n) * \sqrt{v}$$

$$v = \begin{cases} v_{n-1} & \text{for } v_n > v_{n-1} \\ v_n & \text{for } v_n \leq v_{n-1} \end{cases}$$

Where:

ABX : desired minimum following distance (desired safety distance d in the VISSIM manual).

BX_{add} : calibration parameter. In VISSIM this parameter appears as W74bxAdd (additive part of the safety distance) and has a default value of 2.0.

BX_{mult} : calibration parameter. In VISSIM this parameter appears as W74bxMult (multiplicative part of the safety distance) and has a default value of 3.0. Greater values produce a greater distribution of the safety distance.

$RNDZ_n$: normally distributed driver dependent parameter (appears as z in the VISSIM manual). The range of this value is [0,1] with mean equal to 0.5 and standard deviation of 0.15. This parameter was modified from Olstam & Tapani

(2004) in order to differentiate from the parameter $RND1_n$ that appears in the expression for the threshold AX .

v_{n-1} : current speed of the leading vehicle.

v_n : current speed of the follower vehicle.

$$SDX = AX + EX * BX \quad (2-3)$$

$$EX = EX_{add} + EX_{mult} * (NRND - RND2_n)$$

Where:

SDX : maximum following distance (varies from 1.5 to 2.5 times ABX).

EX_{add} , EX_{mult} : calibration parameters.

$NRND$: normally distributed random number.

$RND2_n$: normally distributed driver parameter.

$$SDV = \left(\frac{\Delta_x - L_{n-1} - AX}{CX} \right)^2 \quad (2-4)$$

$$CX = CX_{const} * (CX_{add} + CX_{mult} * (RND1_n + RND2_n))$$

Where:

SDV : approaching point.

Δ_x : front to rear distance (distance gap) between both vehicles.

CX_{const} , CX_{add} , CX_{mult} : calibration parameters.

$$CLDV = SDV \quad (2-5)$$

Where:

$CLDV$: decreasing speed difference.

$$OPDV = CLDV * (-OPDV_{add} - OPDV_{mult} * NRND) \quad (2-6)$$

Where:

$OPDV$: increasing speed difference.

$OPDV_{add}$, $OPDV_{mult}$: calibration parameters.

$NRND$: normally distributed random number.

The speed of the following vehicle in the Wiedemann 74 model is given by

Equation (2-7) (Gao, 2008).

$$u_n(t + \Delta t) = \min \begin{cases} 3.6 * \left(\frac{s_n(t) - s_j}{BX} \right)^2 \\ 3.6 * \left(\frac{s_n(t) - s_j}{BX * EX} \right)^2 \end{cases}, u_f \quad (2-7)$$

Where:

$u_n(t + \Delta t)$: speed of following vehicle at instant $t + \Delta t$, (km/h).

$s_n(t)$: vehicle spacing between the front bumper of the leading vehicle and front bumper of following vehicle at time t , (m).

s_j : vehicle spacing at complete stop in a queue (i.e., standstill distance), (m).

u_f : free-flow speed, (km/h).

2.3.3.3 Wiedemann 99

The Wiedemann 99 model considers the same six thresholds (action points) that appear in the Wiedemann 74 to define the four driving states. These thresholds are AX, ABX, SDV, OPDV, CLDV, and SDX. In Wiedemann 99, the thresholds depend on ten parameters, from CC0 to CC9, that can be adjusted by the user to calibrate a traffic

model, demonstrating is as a more flexible model compared to the Wiedemann 74. The parameters CC0 to CC6 are used to define the thresholds in the model. The remaining parameters, CC7 to CC9, are related to different acceleration conditions of the follower vehicle. The equations to compute the thresholds were obtained from Aghabayk et al. (2013) where one of the co-authors collaborated with the PTV group. As occurs with the Wiedemann 74 model, the exact expressions for the Wiedemann 99 model coded in VISSIM has not been publicly known. The model parameters the user is able to change in VISSIM appear in red in the equations. The rest of the parameters are managed internally in VISSIM. **Figure 2-4** shows the Wiedemann 99 thresholds using **Equations (2-8) to (2-13)** assuming the default VISSIM parameters and a speed of 20 m/s (45 mph) for the leading vehicle.

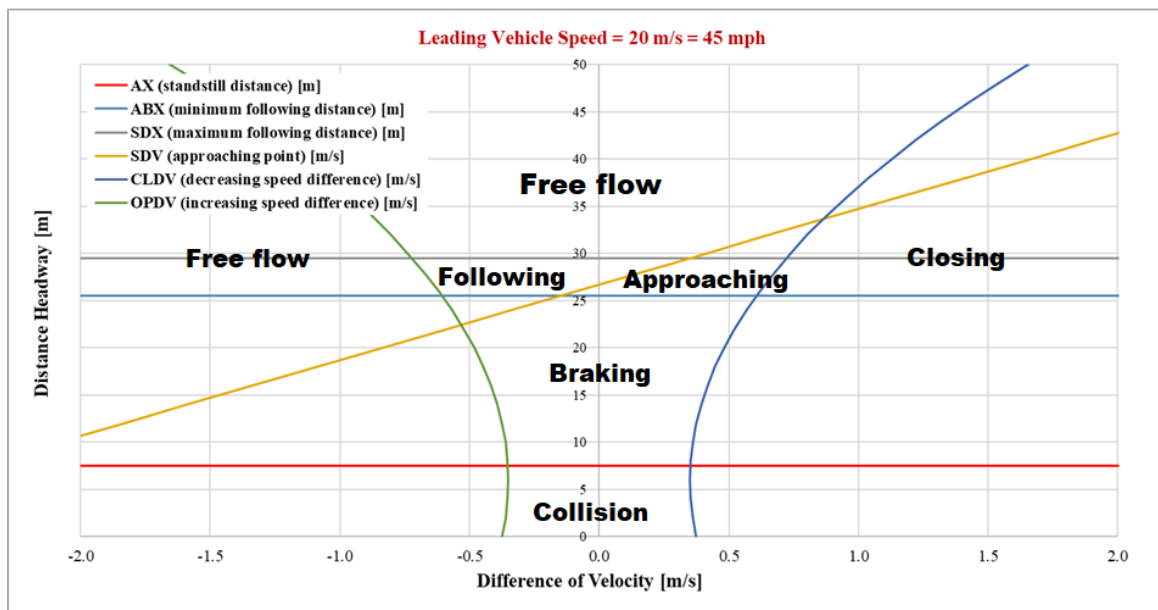


Figure 2-4. Wiedemann 99 thresholds.

$$AX = L_{n-1} + \text{CC0} \quad (2-8)$$

Where:

AX : desired standstill distance [m].

L_{n-1} : length of the leading vehicle.

$CC0$: standstill distance. This parameter has no variation and the default value is 1.5 m.

$$ABX = AX + CC1 * v \quad (2-9)$$

$$v = \begin{cases} v_{n-1} & \text{for } v_n > v_{n-1} \\ v_n & \text{for } v_n \leq v_{n-1} \end{cases}$$

Where:

ABX : desired minimum following distance (desired safety distance d in the VISSIM manual).

$CC1$: headway time [s]. This is the distance in seconds the driver in the follower vehicle desires to maintain from the leading vehicle. This parameter can be defined as a constant value or as a time distribution (users are able to define a new empirical or normal time distribution). The default value for this parameter is 0.9 seconds. According to the VISSIM manual (2018), the parameter $CC1$ has the most significant influence on capacity and saturation flow rate as compared to the other model parameters.

v : subject vehicle speed (follower vehicle).

v_{n-1} : current speed of the leading vehicle.

v_n : current speed of the follower vehicle.

$$SDX = ABX + CC2 \quad (2-10)$$

Where:

SDX: maximum following distance.

CC2: following variation [m]. This parameter restricts the distance difference (longitudinal oscillation) or the additional distance regarding the desired safety distance that a driver allows before he intentionally moves closer to the leading vehicle. The default value is 4.0 m.

$$SDV = -\frac{\Delta_x - SDX}{CC3} - CC4 \quad (2-11)$$

Where:

SDV: approaching point.

CC3: threshold for entering following [s]. This is the number of seconds before or after the start of the deceleration process when the driver perceived a slower leading vehicle. The default value is -8.0 seconds.

CC4: negative following threshold [m/s]. This is the negative speed difference during the following process. Low values produce a more sensitive driver reaction to the acceleration or deceleration of the leading vehicle. The default value is -0.35 m/s.

Δ_x : front to rear distance (distance gap) between both vehicles.

$$CLDV = \frac{CC6}{17000} * (\Delta_x - L_{n-1})^2 - CC4 \quad (2-12)$$

Where:

CLDV: decreasing speed difference.

CC6: speed dependency of oscillation [1/m*s]. This is the influence of distance on speed oscillation during the following driving state. Values greater than zero

produce greater speed oscillation with increasing distance. The default value is $11.44 \text{ m}^{-1} \cdot \text{s}^{-1}$.

$$OPDV = -\frac{CC6}{17000} * (\Delta_x - L_{n-1})^2 - \delta * CC5 \quad (2-13)$$

Where:

OPDV: increasing speed difference.

CC5: positive following threshold [m/s]. This is the positive speed difference during the following process in agreement to *CC4*. Low values produce a more sensitive driver reaction to the acceleration or deceleration of the leading vehicle.

The default value is 0.35 m/s.

δ : dummy variable [0-1]. If the subject vehicle speed v is greater than *CC5*, the dummy variable is equal to one, otherwise is equal to zero.

Additionally,

- *CC7*: oscillation acceleration [m/s^2]. This is the actual acceleration during the oscillation process. The default value is 0.25 m/s^2 .
- *CC8*: standstill acceleration [m/s^2]. This is the desired acceleration when starting from standstill limited by the maximum acceleration associated to the vehicle type. The default value is 3.50 m/s^2 .
- *CC9*: acceleration with 80 km/h [m/s^2]. This is the desired acceleration at 80 km/h limited by the maximum acceleration associated to the vehicle type. The default value is 1.50 m/s^2 .

The speed of the following vehicle in the Wiedemann 99 model is given by

Equation (2-14) (Gao, 2008).

$$u_n(t + \Delta t) = \min \left\{ \begin{array}{l} u_n(t) + 3.6 * \left(CC8 + \frac{CC8 - CC9}{80} * u_n(t) \right) * \Delta t \\ 3.6 * \left(\frac{s_n(t) - CC0 - L_{n-1}}{u_n(t)} \right)^2 \end{array} \right. , u_f \quad (2-14)$$

Where:

$u_n(t + \Delta t)$: speed of following vehicle at instant $t + \Delta t$, (km/h).

$u_n(t)$: speed of following vehicle at instant t , (km/h).

Δt : time step.

$s_n(t)$: vehicle spacing between the front bumper of the leading vehicle and front bumper of following vehicle at time t , (m).

L_{n-1} : length of leading vehicle, (m).

u_f : free-flow speed, (km/h).

2.3.3.4 Lane-Changing Model

The lane changing model is a decision-making process in which the driver has to decide if it is possible to change to the desired adjacent lane. There are two main types of lane changes: (1) free lane change and (2) mandatory lane change (Gao, 2008). The free lane change occurs when a subject vehicle wants to improve its current speed (based on its desired speed) by overtaking a slower vehicle traveling on the same lane. The mandatory lane change is produced when a vehicle has to follow its own route or due to the constrictions of the road network such as a lane drop. In both cases, the lane change decision is mainly a function of a gap acceptance (Barcelo, 2010). During the lane changing process, the subject vehicle accepts that it forces a lag vehicle on the desired lane to decelerate with the aim of creating a safe distance for allowing the incorporation

of the vehicle performing the lane change. The majority of the lane-changing models the total gap is a function of two sub-gaps, lead gap and lag gap, as shown in **Figure 2-5**. The total gap is accepted by the subject vehicle once both the lead gap and lag gap are acceptable.

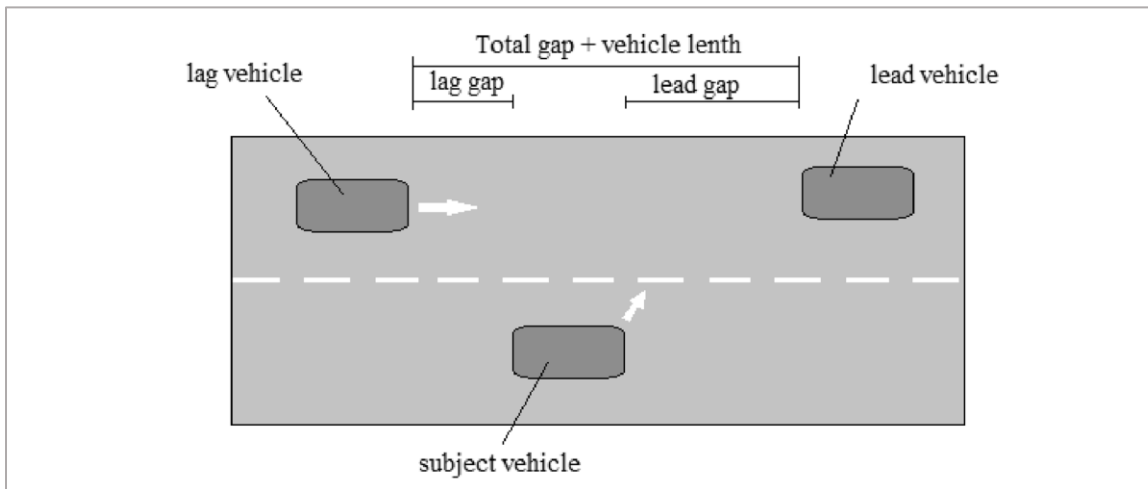


Figure 2-5. Gap definitions in the lane-changing process (modified from Fransson, 2018).

The lane-changing logic coded in VISSIM is based on the Sparmann model developed by Willmann and Sparmann (1978). In this model, there are two types of lane-changing behavior: (1) lane change to a faster lane, and (2) lane change to a slower lane. The lane-changing decision requires the evaluation of three hierarchical questions (Fransson, 2018):

- 1) Does the driver desire to change lane?
- 2) Are the driving conditions improved by a change to the adjacent lane?
- 3) Is it feasible to safely perform the desired lane change?

According to the VISSIM manual (2019), there are two types of lane change: free lane change and necessary lane change. For free lane change, VISSIM checks two desired safety distances (1) the desired safety distance of the trailing vehicle on the desired lane to the lane changing vehicle, and (2) the desired safety distance of the lane changing vehicle to its preceding vehicle on the desired lane. In this regard, a safety reduction factor is applied to both desired safety distance that serves as a calibration parameter to increase or reduce the frequency of the lane changing. For necessary lane change, VISSIM checks the maximum acceptable deceleration for both the lane changing vehicle and the trailing vehicle on the new lane. The deceleration is a function of the distance to the next connector in the route. In both cases of lane change (e.g., free or necessary), the minimum clearance distance must be respected. **Table 2-2** shows a description of the parameters used for the lane-changing model in VISSIM (PTV, 2019).

Table 2-2. Lane-Changing Parameters in VISSIM.

Parameter	Description
General behavior (lane change rule)	There are two types of lane change rules: 1) Free lane selection: overtaking is allowed in any lane. 2) Slow lane rule: overtaking occurs using the fast lane (e.g., left side in the US).
Necessary lane change (route)	The deceleration thresholds for the lane change vehicle (own) and trailing vehicle are defined to reflect the level of aggressiveness for the lane change. The maximum accepted deceleration determines the range of deceleration accepted for the lane change. The reduction rate 1 m/s^2 per distance defines the change rate for the maximum deceleration regarding the emergency stop distance.
Waiting time before diffusion	Maximum time a vehicle will stay at the emergency stop position waiting to perform a necessary lane change. The vehicle will be removed from the network if the waiting time exceeds this value.

Minimum clearance (front/rear)	Minimum distance between two vehicles after the lane change. The default value is 0.5 m.
To slower lane if collision time is above	Minimum time headway that must be available on the slower lane, so that an overtaking vehicle switches to the slower lane. Only for slow lane rule.
Safety distance reduction factor	The safety distance of the trailing vehicle and the lane change vehicle is reduced by this factor during the lane change. The default value of 0.6 represents a 40% reduction of the safety distance.
Maximum deceleration for cooperative braking	Determines to what extent the trailing vehicle in the new lane is braking cooperatively to help the lane change vehicle to incorporate to the new lane. A greater deceleration value will increase the lane-changing opportunities. Default value is -3 m/s^2 .
Overtake reduced speed areas	If selected, vehicles start a free lane change immediately upstream of a reduced speed area. The reduced speed area on the new lane is also observed.
Advanced merging	This option is considered for necessary lane change. If selected, the vehicles will change lane at an earlier point. This reduces the likelihood of stopped vehicles waiting for a gap. If not selected, the trailing vehicle will not break or cooperate with the lane change vehicle if it is within 50 m ahead.
Vehicle routing decisions look ahead	If selected, the vehicles identify routing decisions in advance and choose the lane accordingly.
Cooperative lane change	This option facilitates the lane changing by allowing the trailing vehicle on the new lane to detect the lane changing on the adjacent lane and then perform a lane change itself to accommodate the initial lane change. The trailing vehicle does not perform a cooperative lane change when the new lane is less suitable, the maximum speed difference is exceeded, or the maximum collision time is exceeded regarding the lane change vehicle.
Rear correction of lateral position	Ensures the lane change vehicle to be aligned to the middle of the lane at the end of the lane change. The rear correction occurs for slower vehicles than the specified maximum speed. The user can also define the elapsed time between the lane change and rear correction (active during time period from).

2.3.4 CAV Platoon-Forming Logic

Because of its widespread importance for many transportation planning agencies, many traffic microsimulation models have added features that allow for CAV modeling. For example, VISSIM 20 allows the user to model CAV platoons based on a preset platoon

forming logic and user-defined platoon properties. A comprehensive analysis of the platooning logic may be found elsewhere (PTV, 2019b). The platoon attributes defined by the user include the maximum number of vehicles in the platoon, the desired speed, and the intraplatoon spacing. Conversely, the platoon forming logic is defined by the following conditions:

- CAVs must travel on the same lane to join a platoon (no lane-changing is allowed).
- The headway must be shorter than the preset close-up distance.
- Only CAVs are allowed in the platoon.
- The desired speed of the following CAV must be higher than that of the preceding CAV.
- The leading CAV controls the platoon speed and does not travel faster than the desired platoon speed input by the user.
- Platoons cannot change lanes (e.g., they cannot pass).
- The vehicles leave the platoon based on their individual path or route.
- If a vehicle leaves the platoon, the original platoon is divided into two platoons.

For an adequate interpretation of the simulation results, the analyst must take into account the conditions listed above. Because CAV is a disruptive technology that has not yet been fully implemented, it is impossible to calibrate the simulation results to empirical data. However, the VISSIM models have been calibrated to non-CAV conditions including the HCM-6 EC-PCE model that has been used in the most recent version of the *Highway Capacity Manual* (PTV, 2019b; HCM, 2016).

In summary , the following points were identified from the literature review: (1) there is a general agreement about the early deployment of CAV truck platooning in the freeway system, (2) the potential effects of CAV technology on freeway capacity is considered a research need, (3) the HCM-6 EC-PCE methodology has not been used to explore the effect of CAV technology, (4) there is a lack of empirical data relative to truck platooning; (5) microsimulation models have started adding CAV modeling capabilities due to the interest of traffic agencies; (6) existing microsimulation models have been calibrated for non-CAV traffic; (7) some key models of the traffic building block have limitations that the analyst must consider while modeling traffic.

In the following chapter, the exact HCM-6 EC-PCE methodology will be used to explore the impact of CAV truck platooning on HCM-6 capacity and EC-PCE values. The original HCM-6 procedure will be described step by step and the identified shortcomings while modeling CAV traffic will be highlighted and discussed. These shortcomings are addressed in later chapters to provide support to the proposed methodology developed in this dissertation.

CHAPTER 3

IMPACT OF CAV TRUCK PLATOONING ON HCM-6 CAPACITY AND PASSENGER CAR EQUIVALENT VALUES

3.1 Introduction

The HCM-6 equal capacity methodology for freeway segments is based completely on VISSIM microsimulation model results aggregated over one-minute intervals. The HCM-6 includes EC-PCE values for 14 levels of truck percentage, 13 levels of grade, 7 levels of grade distance, and 3 levels of truck composition type. The advantage to using a simulation model is obvious — it greatly reduces the amount of empirical data that needs to be collected and allows for relatively quick analysis of many different situations. For example, on the surface it would be relatively easy to simulate connected and automated (CAV) vehicles and use the resulting output to estimate capacity and PCE values. The disadvantages are also obvious (Hendrickson and Rilett, 2017). In particular, the developers of the VISSIM model periodically update their model and do not guarantee backward compatibility. Therefore, if users are going to use later versions of VISSIM to model new situations, such as CAV vehicles, and use the output to estimate capacity and PCE values, they must ensure the results are compatible with the original VISSIM model used to calculate the values in the HCM-6.

Recently, there has been a significant amount of research related to heavy trucks operating as autonomous vehicles (AV) as well as connected and autonomous vehicles (CAV) (Bujanovic, & Lochrane, 2018; Kang, Ozer, & Al-Qadi, 2019; Mahdavian, Shojaei, & Oloufa, 2019). CAVs are defined as vehicles capable of both autonomous

driving and connectivity with other entities of the transportation system (e.g., vehicles, road infrastructure, etc.) (Guanetti, Kim, & Borrelli, 2018). These CAVs will form platoons where the lead vehicle “controls” the behavior of the following vehicles and the following vehicles are able to maintain time headways much smaller than those used by non-CAVs. It is hypothesized these CAV platoons will, among other benefits, reduce congestion, increase capacity, reduce pollution, and alleviate the U.S. commercial driver shortage. It has been argued heavy trucks will be the first CAVs on the national truck highway system because the driving environment is not as complex as urban arterial networks and because there are significant benefits in terms of increased fuel efficiency, reduced operating costs, and improved truck safety (Hallmark, Veneziano, & Litteral, 2019; Fitzpatrick et al., 2016; Janssen, et al., 2015).

It is important the effect of CAVs on the performance of these systems be determined. While there has been considerable work done on CAV modeling (Sukennik & PTV Group, 2018; Kittelson & Associates, 2019; Stanek, 2019; Shi & Prevedouros, 2016) none have used the HCM-6 methodology which is the national standard for estimating capacity and quality of service for freeways. Consequently, it is unclear exactly how the highway capacity metrics, including the HCM-6 PCE values, will need to change. It is argued in this chapter that to understand the potential impact on the freeway system of CAV technologies the analyses should be conducted using the standard U.S. methodological framework. This is the motivation of this chapter.

Specifically, this chapter uses the exact HCM-6 EC-PCE methodology to estimate EC-PCEs for CAV trucks on freeway and multilane highway segments. The main objective is to analyze highway capacity under the interaction of CAV trucks and

conventional vehicles. In addition, sensitivity analyses are conducted in order to explore the effect of four factors considered critical in the operation of CAVs: (1) market penetration rate, (2) lane restriction, (3) platoon truck type, and (4) platoon size. It should be noted it is assumed that only trucks can operate in CAV mode in this chapter. Passenger cars will operate as conventional or non-CAVs. This assumption may be relaxed without changes to the methodology discussed in this chapter. Additionally, it is assumed the operational and geometric characteristics of the vehicles and testbeds used in the CAV analysis (e.g., acceleration/deceleration profiles, speed distributions, weight, and power distributions, vehicle lengths, etc.) are the same as those used in the original HCM-6 methodology.

The remainder of the chapter is laid out in four sections. First, the current HCM-6 EC-PCE values are estimated to ensure the current version of VISSIM can be used to replicate the existing HCM-6 values. Secondly, the VISSIM microsimulation model is run with a CAV base case scenario and the output is used to estimate Capacity Adjustment Factors (CAFs) following the HCM-6 estimation methodology. Next, the exact HCM-6 EC-PCE methodology is used to estimate EC-PCEs for CAV trucks interacting with conventional traffic. Lastly, a sensitivity analysis is performed to measure the effect of different operational CAV conditions on highway capacity.

3.2 HCM-6 EC-PCE Procedure

The HCM-6 EC-PCE methodology is comprised of five main steps as shown in **Figure 1-2**. In Step 1, the simulated capacities for both passenger car-only flow and mixed flow are obtained for various combinations of grade, grade length, truck percentage, and vehicle fleet composition. In Step 2, the Capacity Adjustment Factors (CAFs) for 1,274

scenarios are calculated. A nonlinear regression model is created in Step 3 that can predict the CAF value as a function of the parameters analyzed in Step 1. These calibrated models are used to estimate CAFs in Step 4. In Step 5, the EC-PCEs for specific combinations of truck percentage, grade, and grade distance are estimated based on the CAF estimates. These are the values provided in the HCM-6. A complete description of the HCM-6 EC-PCE methodology, including the key simulation parameters of the VISSIM model, can be found elsewhere (Zhou, Rilett, & Jones, 2019; Zhou, 2018; Dowling et al., 2014b). A brief description, which highlights issues critical for modeling the effects of CAV vehicles, is provided below.

3.2.1 HCM-6 Model Assumptions

It is important to note the HCM-6 CAF/EC-PCE values are dependent on the VISSIM Version 4.4 simulation model—to the author’s knowledge no empirical data was used to calibrate and validate the HCM-6 capacity and EC-PCE values (Dowling et al., 2014a, 2014b; Yang, 2013; Zhou, 2018). This approach is a huge advantage from a modeling perspective; it takes significantly less time to model the 1,274 HCM-6 scenarios in comparison to collecting empirical data and developing statistically-based models. In addition, it also allows modelers to study new technologies, such as CAV truck platooning. However, there are a number of issues related to the “all-simulation” approach adopted by the HCM-6 (Hendrickson and Rilett, 2017). For example, the VISSIM developers do not guarantee backward compatibility so there is no guarantee the current version, VISSIM 20, will result in the same EC-PCE values as shown in the HCM-6. Since the HCM-6 was released in 2016, there have been no less than five updated versions of VISSIM released. Due to its CAV and platoon modeling capabilities,

VISSIM 20 was used in this research. Consequently, a considerable amount of effort was spent ensuring the reasonableness of using this version of VISSIM in this research.

The layout of the HCM-6 test network is depicted in **Figure 1-3**. This test network is a unidirectional freeway segment with 3-lanes of 3.66 m (12 ft) width each. The total length of 24.1 km (15 mi) is divided in three sections: (1) an initial level section of 12.9 km (8 mi) to assure all vehicles may enter in the link regardless the congestion level, (2) an intermediate grade section of 9.7 km (6 mi) for data collection, and (3) a final level section of 1.6 km (1 mi). The intermediate grade section contains seven data collection points (each covering the 3 lanes). The traffic information obtained at these locations are used as input to the HCM-6 methodology.

The HCM-6 methodology has a large number of assumptions including those related to vehicle speed (e.g., all vehicles travel at the same uniform free-flow speed of 112.7 km/h (70 mph)), vehicle length, weight and power, and driving behavior. A detailed description of the assumptions can be found elsewhere (Dowling et al., 2014a; Zhou, 2018). Unless otherwise noted, all the assumptions in the original HCM-6 research were followed in this chapter.

Note that four factors (e.g., truck percentage, grade, distance, and truck composition type) were examined in the original HCM-6 research. The same factors and scenarios were examined in this chapter. In the original research, three truck composition percentages also were explored: (1) 30/70 Single Unit Truck (SUT)/Tractor Trailer (TT), (2) 50/50 SUT/TT, and (3) 70/30 SUT/TT. In this chapter, only the former scenario was studied as it is the most common on the U.S. highway system (HCM, 2016).

3.2.2 Background Analysis

The most recent version of VISSIM, VISSIM 20, has CAV platoon modeling capabilities. However, the HCM-6 EC-PCE values were calculated using VISSIM 4.4 (Yang, 2013). Recent studies have shown that the HCM-6 EC-PCE results can be replicated using VISSIM 9 (Zhou, 2018, Zhou et al, 2019). However, it would be a mistake to assume the simulation logic underlying VISSIM releases 4.4 and 9 is the same as VISSIM 20. It is important to note the VISSIM developers acknowledge simulation results can differ among different versions due to changes and updates in the internal logic of the simulator (PTV, 2019b). Consequently, the first step was to ensure the HCM-6 EC-PCE values can be replicated using VISSIM 20. If true, then the results of this CAV analysis in this chapter can be compared directly to the HCM-6 results.

The first step was to compare the capacity values obtained from VISSIM 20 and 9 for all scenarios included in the HCM-6. In these experiments, all the simulation parameters were set equal to the HCM-6 values and both passenger cars and mixed-flow traffic were analyzed. The results showed the capacity, which is defined in the HCM-6 as the 95th percentile of the 1-minute average flow-rate, of the passenger car-only condition was 6.54% lower, on average, for the VISSIM 20 results as compared to the VISSIM 9 results. A paired t-test at 0.05 level of significance showed this difference was statistically significant. In contrast to the passenger car-only condition, the difference between VISSIM 20 and 9 for the mixed-traffic condition was only 0.60%, on average, and this was not statistically significant at the 0.05 level of significance.

Based on the above results, it was decided to use VISSIM 20 for the mixed-flow simulations and VISSIM 9 for the passenger car-only flow condition because it was

assumed this would give the best chance for replicating the HCM-6 results. This assumption will be checked later in this chapter. The steps for replicating the HCM-6 EC-PCE values are described below.

3.2.3 Step 1: Flow-density plots

In Step 1, the flow-density plots of each scenario are created based on output from the VISSIM model. Following HCM-6 protocols, each scenario is simulated using one single run and the same seed number. There are nine volume levels (e.g., 240, 600, 1200, 1800, 1920, 2040, 2160, 2280, and 2400 veh/h/ln) in every run and these correspond to volume-to-capacity ratios from 10% to 100% based on an assumed theoretical capacity of 2,400 veh/h/ln. Each volume level consists of one-hour of vehicle loading to achieve a steady-state condition, one-hour of steady-state for data collection, and one-hour of vehicle unloading. As a result, the simulation period comprises a total of 27 hours per scenario (e.g., 3 hours per volume level by 9 volume levels). The scenarios are defined by a combination of the following factors:

- 2 flow-rate types (f) either passenger car-only or mixed traffic flow,
- 13 levels of truck percentage (p) from 2% to 100%,
- 13 levels of grade (g) from -6% to 6%, and
- 7 levels of grade distance (d) from 0.40 km (0.25 mi) to 8.05 km (5.00 mi).

In total, there are 91 scenarios for the passenger car-only flow condition (e.g., 13 levels of grade x 7 levels of distance), and 1,183 scenarios for the mixed-traffic flow condition (e.g., 13 levels of truck percentage x 13 levels of grade x 7 levels of distance). The VISSIM model output consisted of the space mean speed and the flow rate collected

at each detector per one-minute interval. These outputs are used to compute the hourly flow rate and density, at one-minute averages, for each combination using **Equations (3-1)** and **(3-2)**, respectively.

$$q_{f,t,p,m,g,d,r} = V_{f,t,p,m,g,d,r} * 60 \quad (3-1)$$

$$k_{f,t,p,m,g,d,r} = \frac{q_{f,t,p,m,g,d,r}}{\bar{v}_{f,t,p,m,g,d,r}} \quad (3-2)$$

Where:

$q_{f,t,p,m,g,d,r}$: Flow rate for the f flow type at t time interval, p truck percentage level, m truck composition level, g grade level, d distance level, and r simulation flow-rate level based on 1-min interval traffic volume recorded by the detector, (veh/h/ln).

$V_{f,t,p,m,g,d,r}$: 1-min interval traffic volume recorded by the detector for the f flow type at t time interval, p truck percentage level, m truck composition level, g grade level, d distance level, and r simulation flow-rate level, (veh/min/ln).

$k_{f,t,p,m,g,d,r}$: Density for the f flow type at t time interval, p truck percentage level, m truck composition level, g grade level, d distance level, and r simulation flow-rate level, (veh/mi/ln).

$\bar{v}_{f,t,p,m,g,d,r}$: 1-min interval space mean speed for the f flow type at t time interval, p truck percentage level, m truck composition level, g grade level, d distance level, and r simulation flow-rate level, (mph).

The hourly flow-rate and density values populate the scatter plots for each scenario. There are 1,274 scatter plots in total. Each flow-density scatter plot for a given

scenario contains 540 pairs of flow-rate and density values (e.g., 60 minutes x 9 volume levels). Each scatter plot is used to identify the capacity value for a given scenario. Note in the HCM-6 capacity is defined as the 95th percentile of the maximum one-minute average flow-rate for the given scenario (Dowling et al., 2014a, 2014b; Yang, 2013). To the author's knowledge, this is the first time the HCM has used an aggregation level other than 15 minutes to calculate a traffic flow metric. Therefore, care must be taken in comparing the capacity values found in the HCM-6, and by definition in this chapter, with other published capacity values based on larger aggregation levels. The simulated capacity for each of the 1,274 scenarios is calculated using **Equation (3-3)**. Note if the 540 observations from each scenario were ordered from smallest to largest, the 95th percentile value will be the 513th largest observation.

$$C_{f,p,m,g,d} = \underset{r=1,9}{\overset{P95}{\text{P95}}}_{t=1,60} \{q_{f,t,p,m,g,d,r}\} \quad (3-3)$$

Where:

$C_{f,p,m,g,d}$: Capacity for the f flow type at p truck percentage level, m truck composition level, g grade level, d distance level, (veh/h/ln).

$P95$: 95th percentile.

$q_{f,t,p,m,g,d,r}$: Flow rate for the f flow type at t time interval, p truck percentage level, m truck composition level, g grade level, d distance level, and r simulation flow-rate level, based on 60 1-min interval traffic volume recorded by the detector (veh/h/ln).

To illustrate, **Figure 3-1** shows the flow-rate versus density graph for the passenger car-only flow, 3% grade, and 1.61 km (1.0 mi) distance scenario. It may be seen that the relationship between flow rate and density is linear. Using **Equation (3-3)**, the definition of the HCM-6 EC-PCE methodology, the capacity is found to be 2,260 veh/h/ln.

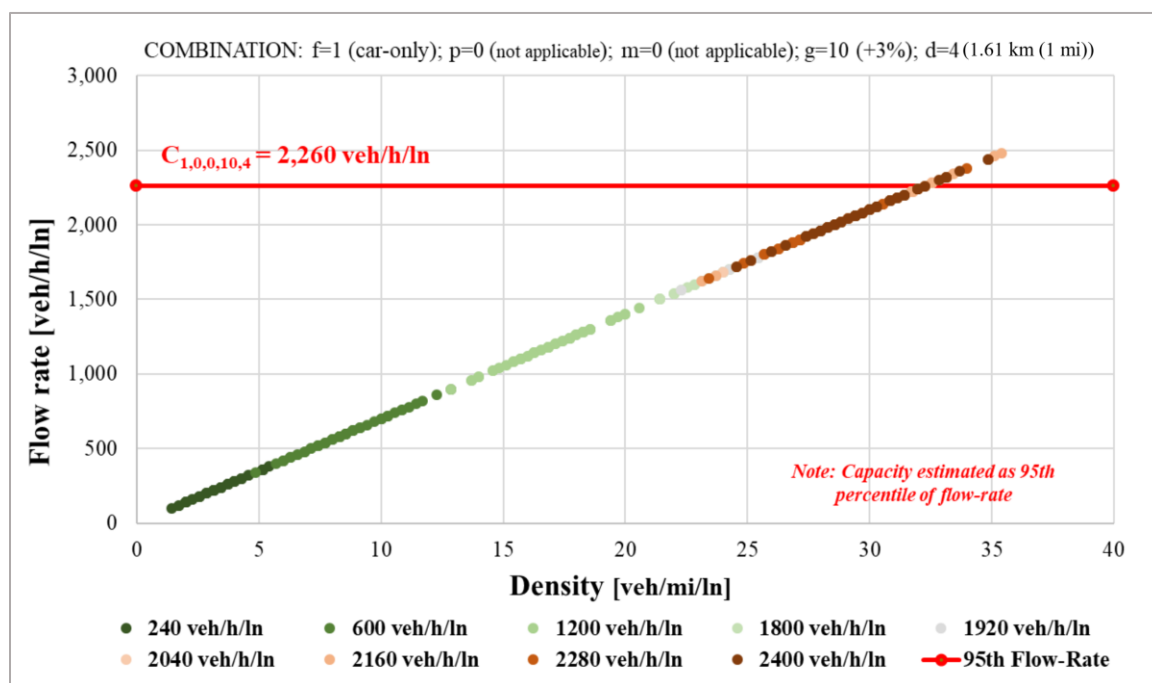


Figure 3-1. Passenger car only flow-density scatter plot (grade 3%, distance 1 mi).

Figure 3-2 shows the flow-rate versus density graph for the same conditions as **Figure 3-1** but for the mixed-traffic flow condition and a 20% truck percentage. It may be seen that at low density the flow-rate density relationship is linear. A breakpoint occurs at approximately 25 veh/mi/ln and the capacity value is estimated to be 1,780 veh/h/ln.

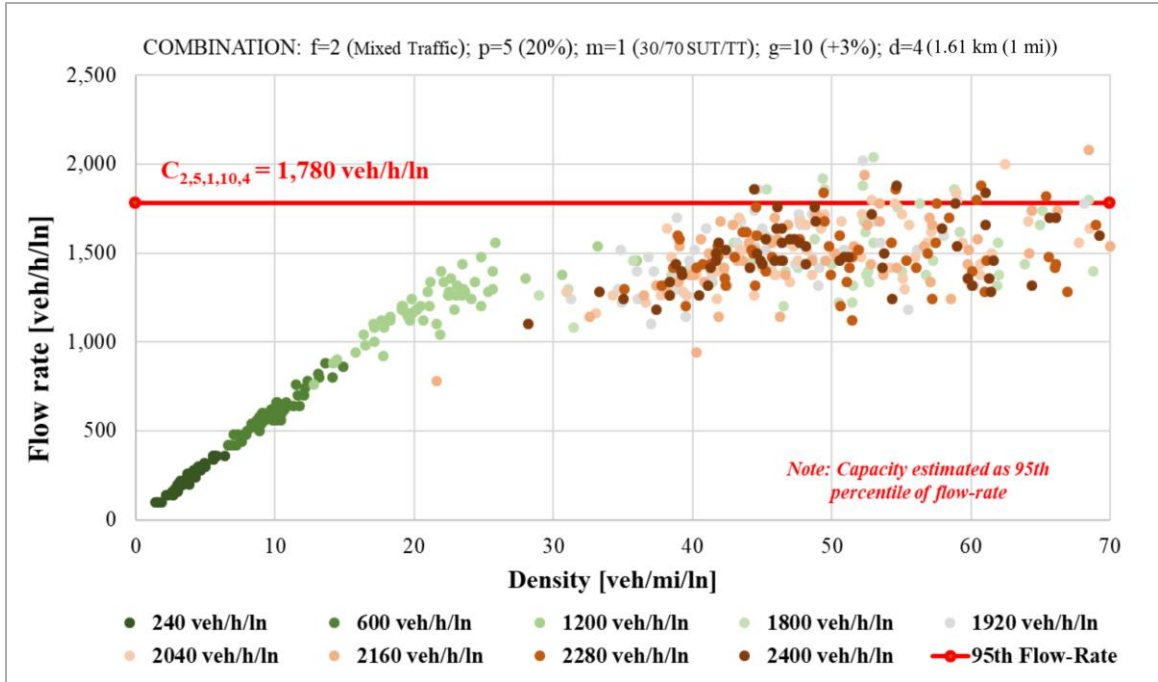


Figure 3-2. Mixed traffic flow-density scatter plot (grade 3%, distance 1 mi).

3.2.4 Step 2: Computation of Capacity Adjustment Factors from Simulation Output

In this step, the capacity adjustment factors (CAFs) for each scenario are calculated using the simulation results from Step 1. These are calculated for the mixed flow and passenger car-only flow scenarios using **Equations (3-4)** and **(3-5)**, respectively. These equations use the capacity of each scenario obtained from the flow-density scatter plots from Step 1.

$$CAF_{2,p,m,g,d} = \frac{C_{2,p,m,g,d}}{C_{1,0,0,g,d}}; \forall p = 1, P; \forall m = 1, M; \forall g = 1, G; \forall d = 1, D \quad (3-4)$$

$$CAF_{1,0,0,g,d} = \frac{C_{1,0,0,g,d}}{C_{1,0,0,g,d}} = 1; \forall g = 1, G; \forall d = 1, D \quad (3-5)$$

Where:

$CAF_{2,p,m,g,d}$: Capacity adjustment factor for the mixed flow at p truck percentage level ($P = 13$), m truck composition level ($M = 3$), g grade level ($G = 13$), d distance level ($D = 7$).

$CAF_{1,0,0,g,d}$: Capacity adjustment factor for the auto-only flow at g grade level ($G = 13$), d distance level ($D = 7$).

$C_{2,p,m,g,d}$: Capacity for the mixed flow at p truck percentage level, m truck composition level, g grade level, d distance level, (veh/h/ln).

$C_{1,0,0,g,d}$: Capacity for the auto-only flow at g grade level, d distance level, (veh/h/ln).

To illustrate, consider the scenario defined by mixed flow ($f=2$), 20% truck percentage ($p=5$), 30/70 SUT/TT truck composition ($m=1$), +3% grade ($g=10$), and 1.61 km (1.0 mi) distance ($d=4$). Note the passenger-car only and mixed traffic scatter plots for this situation were shown in **Figure 3-1** and **Figure 3-2**, respectively. Using **Equation (3-4)** the Capacity Adjustment Factor for this situation ($CAF_{2,5,1,10,4}$) is 0.788 (1,780/2,260). This calculation is repeated for the other 1,273 scenarios using either **Equation (3-4)** or **(3-5)**, as appropriate, for the given flow type.

The CAFs for all 1,274 scenarios are shown in **Figure 3-3**. The x-axis represents the scenario number. Each specific scenario number is calculated using **Equation (3-6)** and is a function of the truck percentage, grade, and distance. There were 14 truck percentage values (including 0%) and these are shown on the top of **Figure 3-3**. The red line represents the simulated CAFs from this chapter and the orange line the estimated CAFs obtained in the original HCM-6 research. The blue line will be discussed in Step 4. For a given truck percentage, the CAFs for grade and grade distance are shown in order.

The general form is a flat straight line for the negative and zero grade scenarios, followed by decreasing CAF values for the positive grade values.

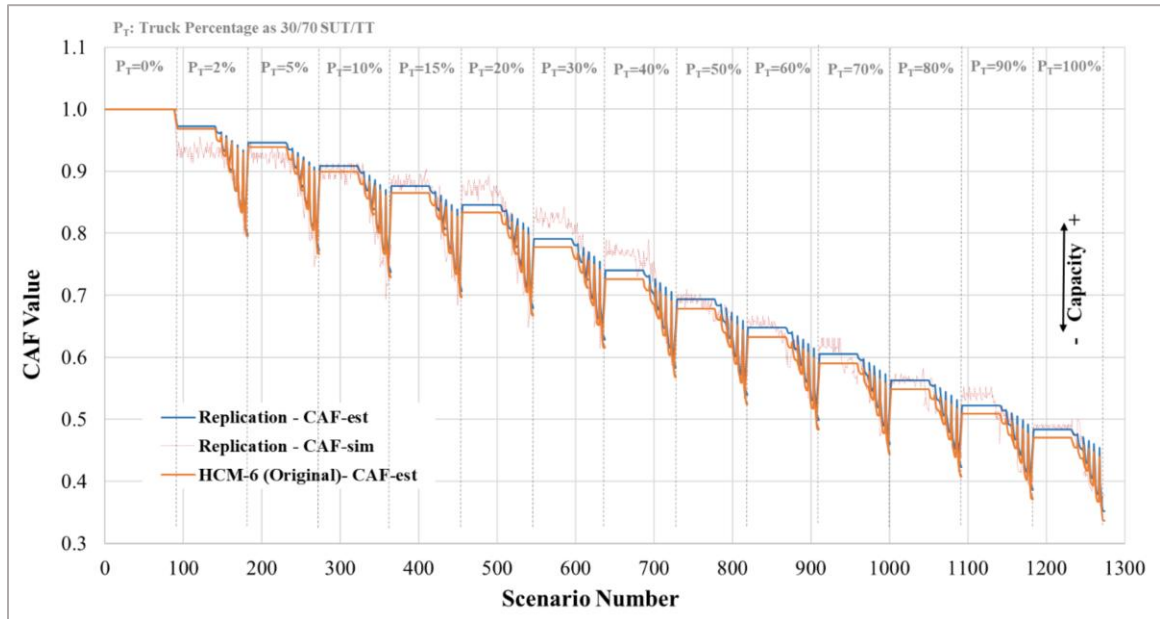


Figure 3-3. Estimated CAF for Each Scenario.

$$n = 91 * p + (g - 1) * 7 + d \quad (3-6)$$

Where:

n : Scenario number.

p : Ordinal number of truck percentage level, $p = 1, 2, \dots, P$, means 2-100% truck percentage.

P : Total levels of truck percentage, $P = 13$.

g : Ordinal number of grade level, $g = 1, 2, \dots, G$, means -6% to 6% grade.

G : Total levels of grade, $G = 13$.

d : Ordinal number of distance level (the level of detector location), $d = 1, 2, \dots, D$, means 0.40-8.05 km (0.25-5.00 mi).

D : Total levels of distance (detector location), $D = 7$.

All else being equal a greater CAF value indicates a higher capacity of the freeway segment. A visual analysis suggests there is a good match between the estimated CAF values from the two sources. This closeness will be examined statistically in the next section. Note the CAF values from the HCM-6 are fairly stable while the simulation values tend to have considerable variability. This difference will be explained in the following section.

3.2.5 Step 3: Regression Models Development for Estimated CAFs

Because of the inherent variability of the CAF results from the simulation, the HCM-6 developers chose not to use the simulated CAF values directly. Instead, they calibrated a regression model relating the simulated CAF values to the truck percentage, grade, and distance parameters. The goal was to lessen the variability in the CAF results.

The CAF values from Step 2 are used as input and statistical regression techniques are used to calibrate the model. The nonlinear regression model used in the HCM-6 are shown in **Equations (3-7) to (3-11)** (Dowling et al., 2014b; Zhou, Rilett, & Jones, 2019; Zhou, 2018).

$$CAF_{2,p,m,g,d} = CAF_{1,0,0,g,d} - CAF_{2,p,m}^{T_a} - CAF_{2,p,m,g,d}^{G_a} - CAF_{2,p,m}^{FFS_a} \quad (3-7)$$

$$CAF_{2,p,m}^{T_a} = \alpha_{12,m}^{T_a} * P_T^{\beta_{12,m}^{T_a}} \quad (3-8)$$

$$\rho_{2,p,m}^{G_a} = \begin{cases} \gamma_{2,m}^{G_a} * (p_s)_p; & \text{if } (p_s)_p < p^* \\ \theta_{2,m}^{G_a} - \mu_{2,m}^{G_a} * (p_s)_p; & \text{if } (p_s)_p \geq p^* \end{cases} \quad (3-9)$$

$$\begin{aligned}
CAF_{2,p,m,g,d}^{G_a} &= \rho_{2,p,m}^{G_a} * \max \left\{ 0, \alpha_{2,m}^{G_a} * \left[e^{\phi_{2,m}^{G_a} * (g_s)_g} - \eta_{2,m}^{G_a} \right] \right\} \\
&\quad * \max \left\{ 0, \beta_{2,m}^{D_a} * \left[1 - \alpha_{2,m}^{D_a} * e^{\phi_{2,m}^{D_a} * (d_s)_d} \right] \right\}
\end{aligned}
\tag{3-10}$$

$$CAF_{2,p,m}^{FFS_a} = \mu_{2,m}^{FFS_a} * \left[1 - \rho_{2,p,m}^{FFS_a} * (p_s)_p^{\beta_{2,m}^{FFS_a}} \right] * [(70 - FFS_1)/100]^{\phi_{2,m}^{FFS_a}}
\tag{3-11}$$

Where:

$CAF_{2,p,m,g,d}$: Capacity adjustment factor for the mixed flow at p truck percentage level, m truck composition level, g grade level, d distance level.

$CAF_{1,0,0,g,d}$: Capacity adjustment factor for the auto-only flow at g grade level, d distance level. This value is assumed to be 1.

$CAF_{2,p,m}^{T_a}$: Capacity adjustment factor for truck percentage effect for the mixed flow at p truck percentage level, m truck composition level.

$CAF_{2,p,m,g,d}^{G_a}$: Capacity adjustment factor for grade effect for the mixed flow at p truck percentage level, m truck composition level.

$CAF_{2,p,m}^{FFS_a}$: Capacity adjustment factor for free-flow speed effect for the mixed flow at p truck percentage level, m truck composition level.

$\rho_{2,p,m}^{G_a}$: Coefficient for capacity adjustment factor for grade effect for the mixed flow at p truck percentage level, m truck composition level.

$(p_s)_p$: Truck percentage at p truck percentage level (between 0 and 1).

p^* : Threshold of truck percentage for calculating coefficient for capacity adjustment factor related to grade with default value 0.01.

$(g_s)_g$: Grade at g grade level (between -0.06 and 0.06).

$(d_s)_d$: Distance of grade at d distance level (mile).

FFS_1 : Free-flow speed for auto-only flow (mph).

$\alpha_{1,2,m}^{Ta}, \beta_{1,2,m}^{Ta}$: Parameters for capacity adjustment factor for truck percentage effect.

$\gamma_{2,m}^{Ga}, \theta_{2,m}^{Ga}, \mu_{2,m}^{Ga}, \alpha_{2,m}^{Ga}, \phi_{2,m}^{Ga}, \eta_{2,m}^{Ga}, \beta_{2,m}^{Da}, \alpha_{2,m}^{Da}, \phi_{2,m}^{Da}$: Parameters for capacity adjustment factor for grade effect.

$\mu_{2,m}^{FFSa}, \rho_{2,p,m}^{FFSa}, \beta_{2,m}^{FFSa}, \phi_{2,m}^{FFSa}$: Parameters for capacity adjustment factor for free-flow speed effect.

This chapter adopted the same form of the nonlinear model (i.e., **Equation (3-7)**) as was used in the HCM-6. The parameters were estimated using a Generalized Reduced Gradient (GRG) approach. This is a nonlinear optimization method which uses an iterative process to optimize a target value. In this chapter, the target goal was to minimize the sum of squared errors between the simulated CAFs from Step 2 and the estimated CAFs from the non-linear regression model. A detailed description of the method can be found elsewhere (Lasdon, Fox, & Ratner, 1974). Note the original research did not mention the optimization technique that was applied to find the best estimates of the model parameters.

Table 3-3 shows the values of the parameters in the CAF model for the original research and for this chapter in rows 1 and 2, respectively. It may be seen the estimators between both cases are very similar. It is hypothesized the small differences found are due to the different versions of the simulator.

3.2.6 Step 4: CAFs Estimation for Specific Conditions

In this step, the CAFs for the mixed flow scenarios (CAF_{2,p_s,m_s,g_s,d_s}) are estimated for the specific conditions listed in the HCM-6. The parameters of interest are truck percentage p_s , grade g_s , and distance d_s . These estimated CAFs are obtained using **Equation (3-7)** based on the calibrated parameters shown in **Table 3-3** (Row 2).

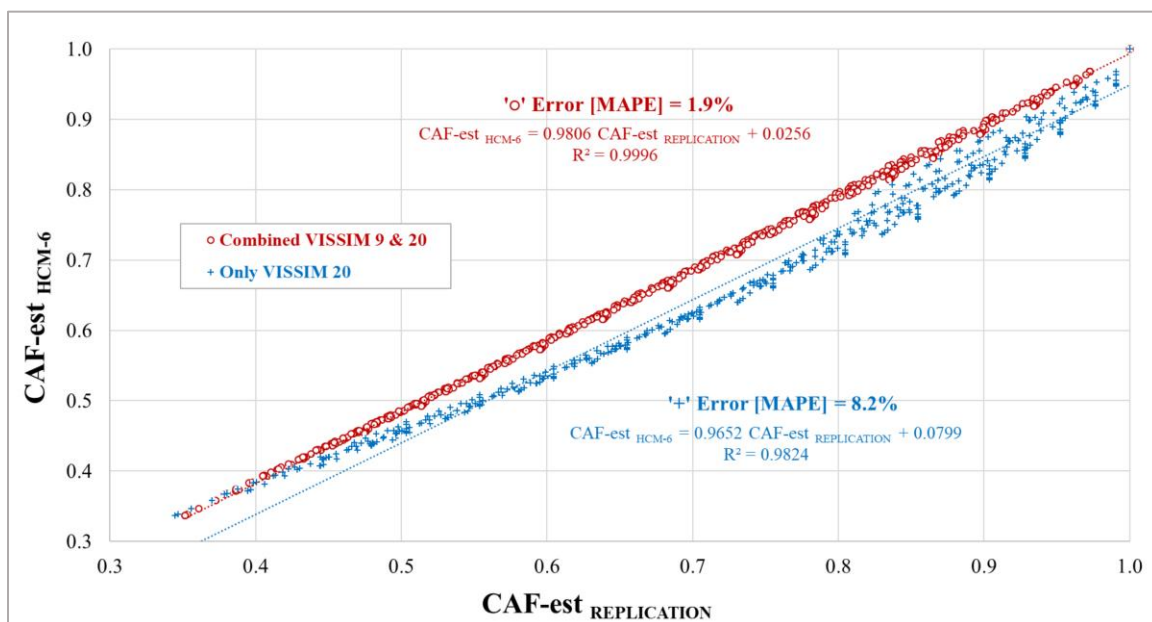


Figure 3-4. Original CAF from HCM-6 versus Estimated CAF derived from more recent VISSIM models.

Figure 3-4 shows a scatter plot of the estimated CAF value from the original HCM research as a function of the estimated CAF value from this chapter. There are a total of 1,274 points or comparisons in this figure. It may be seen the approach adopted in this chapter resulted in a linear relationship with a very high R-squared value of 0.99.

Figure 3-3 shows a direct comparison between the CAF values calculated in this chapter (blue line) and the CAF values from the HCM-6 (orange line). Not surprisingly, the CAF

values are generally in agreement. It was concluded using a VISSIM 9 model for passenger cars and a VISSIM 20 model for mixed traffic allowed for an accurate estimation of the HCM-6 values.

Figure 3-4 also shows the relationship between the HCM-6 CAF values and the values obtained if all the simulation data was obtained from VISSIM 20. While the relationship is generally linear, there is considerably more scatter as evidenced by the MAPE value of 8.2%. In addition, the VISSIM 20 CAF results tended to underestimate the CAF values used in the HCM-6. This was why a combination of VISSIM 9 and 20 was used in this chapter. Because VISSIM 20 limits lane changing for vehicles traveling at the same speed, it is hypothesized this adversely affected the passenger car only simulations (PTV, 2019b). With respect to mix-traffic conditions, this is not as critical as the vehicle characteristics that create more lane changing opportunities. This also illustrates a danger in using simulation models for national design guides without adequate controls such as clearly defining simulation logic and parameters (Hendrickson and Rilett, 2017; Rilett, 2020).

3.2.7 Step 5: EC-PCEs Estimation

In the last step of the methodology, the EC-PCEs ($EC - PCE_{2,p_s,m_s,g_s,d_s}$) at specific conditions of truck percentage p_s , grade g_s , and distance d_s , are calculated using **Equation (3-12)**.

$$EC - PCE_{2,p_s,m_s,g_s,d_s} = \frac{1 - (1 - p_s) * CAF_{2,p_s,m_s,g_s,d_s}}{p_s * CAF_{2,p_s,m_s,g_s,d_s}} \quad (3-12)$$

Where:

$EC - PCE_{2,p_s,m_s,g_s,d_s}$: EC-PCE for the mixed flow at truck percentage p_s , truck composition m_s , grade g_s , and distance d_s .

CAF_{2,p_s,m_s,g_s,d_s} : Capacity adjustment factor for the mixed flow at truck percentage p_s , truck composition m_s , grade g_s , and distance d_s .

p_s : Truck percentage (between 0 and 1).

The estimated EC-PCEs as a function of the HCM-6 EC-PCEs are shown in **Figure 3-5**. It may be seen that the relationship is approximately one to one with an R-squared value of 0.997 and a MAPE of 3.9%. It was concluded the simulation approach adopted in this chapter 1) can replicate the current HCM-6 values using the HCM-6 assumptions, and 2) can be used to model the effect of CAVs on capacity and PCE values using the same HCM-6 approach.

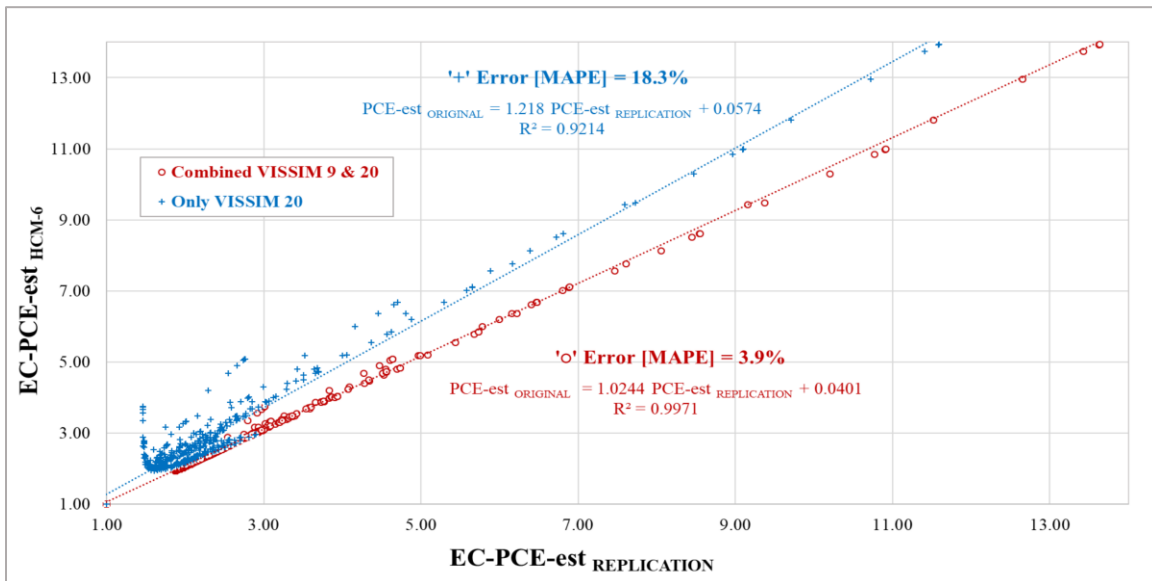


Figure 3-5. Impact of the VISSIM version on the replication of HCM-6 EC-PCEs.

Also shown in **Figure 3-5** is the relationship between the HCM-6 EC-PCE values and the estimated EC-PCE values if only VISSIM 20 were used. While linear, the fit is not nearly as good as evidenced by the MAPE value of 18.3%.

3.3 CAV Modeling Methodology

The HCM-6 methodology, using VISSIM 20 with the parameter sets described above, was applied to estimate the EC-PCEs when the trucks have CAV capabilities. Because the goal of this dissertation is to explore the effect of CAV truck platooning on the capacity of freeway segments, it was assumed only trucks could operate in CAV mode and the truck operational characteristics were the same as in the HCM-6. In other words, the only difference between the trucks in the HCM-6 and the trucks in the CAV analysis is the trucks in the latter scenario could form platoons based on CAV logic.

The VISSIM CAV-related parameter values are based on the CoExist project (Sukennik & PTV Group, 2018). The CoExist project is one of the largest research projects relative to CAV technology that have been developed to date. This project was funded by the European Union to prepare the transitional period in which CAVs and conventional vehicles will share the road system. The developers of VISSIM, the PTV Group, were responsible for the traffic operation section of the project.

Table 3-1 shows the parameter set for the CAV vehicles used in this chapter. The default driving behavior was ‘AV aggressive (CoExist)’, which is recommended for CAV that have full automation (Sukennik & PTV Group, 2018). It should be noted some of the driving behavior parameters were modified in order to be consistent with the calibrated safety distance parameters (e.g., CC0 + CC1) used in the original research. Specifically, the headway time parameter CC1 was set to 0.5 seconds, instead of the default value of

0.6 seconds, as this was the value used in the original research. Similarly, the minimum clearance distance was set to 1.5 meters, instead of the default value of 2.0 meters as this was the value used in the CoExist project. The analysis in this chapter was repeated without making these two minor changes and the results in this chapter were not changed appreciably.

Table 3-1. CAV Driving Behavior Parameters in VISSIM 20.

Model	Parameter	Setting
Autonomous Driving	Enforce absolute braking distance	Unselected
	Use implicit stochasticity	Unselected
	Platooning possible	Selected
	Max. number of vehicles	7
	Max. desired speed	112.65 km/h (70 mph)
	Max. distance for catching up to a platoon	250 m
	Gap time	0.5 s
	Minimum clearance	1.50 m
Following	Look ahead	Min 0 m; Max 300 m
	Number of interaction objects & vehicles	10 & 8
	Look back distance	Min 0 m; Max 150 m
	Behavior during recovery from speed breakdown	
	Slow recovery	Unselected
	Speed	60%
	Acceleration	40%
	Safety Distance	110%
	Distance	200 m
	Standstill distance for static obstacles	Unselected
Car Following	Wiedemann 99	
	CC0 standstill distance	1.0 m
	CC1 gap time	0.5 s (constant)
	CC2 following variation	0.0 m
	CC3 threshold for entering following	-6.0
	CC4 negative following threshold	-0.10
	CC5 positive following threshold	0.10
	CC6 speed dependency of oscillation	0.0
	CC7 oscillation acceleration	0.10 m/s ²
	CC8 standstill acceleration	4.0 m/s ²
CC9 acceleration with 80 km/h	2.0 m/s ²	
	Following behavior depending on the vehicle class	Same as conventional traffic
Lane Change	General behavior	Free lane selection
	Necessary lane change (own & trailing vehicle)	
	Maximum deceleration	-4.0 m/s ² & -4.0 m/s ²
	-1 m/s ² per distance	100 m & 100 m
	Accepted deceleration	-1.0 m/s ² & -1.5 m/s ²
	Waiting time before diffusion	60 s
	Min. clearance (front/rear)	0.5 m
	Safety distance reduction factor	0.75
	Maximum deceleration for cooperative braking	-6.0 m/s ²
	Overtake reduced speed areas	Unselected
Advanced merging	Selected	
Vehicle routing decisions look ahead	Selected	

	Cooperative lane change	Selected
	Maximum speed difference	10.8 km/h
	Maximum collision time	10.0 s
	Rear correction of lateral position	Unselected
	Desired position at free flow	Middle of lane
Lateral behavior	Observed adjacent lane(s)	Unselected
	Overtake on same lane	Unselected
	Exceptions for overtaking vehicles	None

3.3.1 CAV Base Case

There were four major CAV factors studied. The market penetration rate parameter is defined as the percentage of trucks in the traffic stream with CAV capabilities that will allow CAV platoons to form. The value for the base case was 100 percent. The lane restriction parameter refers to the number of lanes, starting from the median lane, in which CAV trucks were prohibited from traveling. For the base case, it was assumed there were no lane restrictions. The platoon truck type factor is related to which truck types, either SUT or TT or both, are allowed to join a CAV truck platoon. For the base case, platoons could only form using trucks of the same type. Lastly, the platoon size parameter is defined as the maximum number of trucks that can be part of a given CAV truck platoon. For the base case, this value was set to seven. Sensitivity analyses were used to explore the effect of changing market penetration rate, lane restriction rules, truck platoon vehicles and truck platoon size on the EC-PCE values.

3.3.2 Modeling the CAV Base Case

The EC-PCE values for the CAV base case scenario were developed using the HCM-6 procedure shown in **Figure 1-2**.

3.3.2.1 Steps 1 and 2: Simulated CAFs

The 91 passenger car only scenarios, and their associated flow-density plots, were developed using VISSIM 9 as described previously. Next, the flow-density plots were developed for the 1,183 CAV scenarios using VISSIM 20. From these plots the HCM-6 capacity, defined as the 95% maximum flow rate using 1-minute aggregation, was identified. These capacities were then used in Step 2 to calculate the CAF values of the CAV condition for each of the 1,274 combinations.

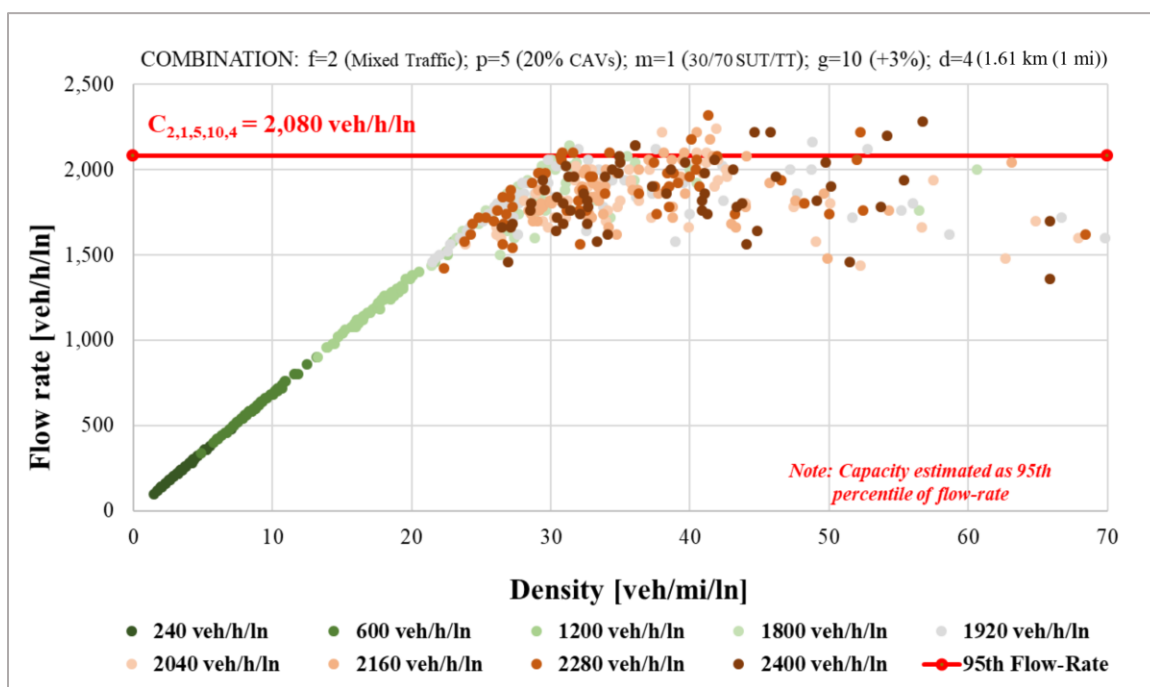


Figure 3-6. Flow-density scatter plot for 20% CAVs (grade 3%, distance 1 mi)

For illustrative purposes, **Figure 3-6** shows the flow-density curve for the baseline CAV condition for the same conditions as **Figure 3-2**. It may be seen the breakpoint occurs at a higher density value (e.g., 30 veh/mi/ln). The figure also shows the CAV capacity (e.g., 2,080 veh/h/ln) is approximately 10 percent higher than the

equivalent non-CAV capacity (e.g., 1,780 veh/h/ln). It is hypothesized the higher capacity occurs due to the deployment of CAV truck platoons in the traffic stream, which vehicles present shorter headways and reduced stochasticity as compared to non-CAVs.

3.3.2.2 Step 3: Nonlinear model development

In the original HCM-6 research, a nonlinear regression model was used in Step 3. The form for the HCM-6 analytical model was based on kinematic and resistance equations related vehicles ascending and descending different grades (Dowling et al., 2014b). A heuristic optimization approach was used to calibrate the model where the goal was to identify the model that minimized the error between the simulated CAFs and the estimated CAFs. The parameters of these equations were optimized using an Excel Spreadsheet. The final model consisted of a combined grade and distance effect parameter, a free-flow speed effect parameter, and truck percentage effect parameter (Dowling et al., 2014b; Zhou, 2018) as shown in **Equations (3-7) to (3-11)**.

In this chapter, the same model structure was assumed. However, the truck percentage effect ($CAF_{2,p,m}^{Ta}$) parameter could not be calibrated to an acceptable level. Therefore, it was decided to use four parameters to model this effect. No changes in model format were performed for combined grade and distance effect ($CAF_{2,p,m,g,d}^{Ga}$) and free flow speed effect ($CAF_{2,p,m}^{FFS_a}$). The statistic used to assess model fitting was the standard error of the regression (S) as shown in **Equation (3-13)**. The advantage to the S metric is it can be applied for both nonlinear and linear models in contrast to the R-squared that is only valid for linear models (Spiegelman, Park, & Rilett, 2011).

$$S = \sqrt{\frac{SSE}{N - P}}$$

(3-13)

Where:

S : standard error of the regression.

SSE : sum of squared errors.

N : number of observations.

P : number of parameters in the model.

Seven potential models attempting to capture the truck percentage effect were analyzed in **Table 3-2**. The HCM-6 model, shown as model 1, is a power function with two parameters. It had an S value of 0.0578. Model 4, which is a polynomial model, had an S value approximately a sixth of the size of Model 1. This model was chosen because it had a low S value and fewer parameters as compared with other models. Once the final model structure was chosen, the same approach used in the HCM-6 methodology, was adopted to find the best estimators for the parameters of the nonlinear regression model.

Table 3-2. Goodness of Fit Results for CAV Analysis

No.	Model for Truck Percentage Effect	P	$S = \sqrt{MSE}$
1*	$CAF_{2,p,m}^{Ta} = \alpha_{12,m}^{Ta} * P_T^{\beta_{12,m}^{Ta}}$	15	0.0578
2	$CAF_{2,p,m}^{Ta} = \alpha_{12,m}^{Ta} * P_T^{\beta_{12,m}^{Ta}} + \alpha_{22,m}^{Ta}$	16	0.0215
3	$CAF_{2,p,m}^{Ta} = \alpha_{12,m}^{Ta} * P_T^{\beta_{12,m}^{Ta}} + \alpha_{22,m}^{Ta} * P_T$	16	0.0257
4**	$CAF_{2,p,m}^{Ta} = \alpha_{12,m}^{Ta} * P_T^{\beta_{12,m}^{Ta}} + \alpha_{22,m}^{Ta} * P_T^{\beta_{22,m}^{Ta}}$	17	0.0105
5	$CAF_{2,p,m}^{Ta} = \alpha_{12,m}^{Ta} * P_T^{\beta_{12,m}^{Ta}} + \alpha_{22,m}^{Ta} * P_T^{\beta_{22,m}^{Ta}} + \alpha_{32,m}^{Ta}$	18	0.0103
6	$CAF_{2,p,m}^{Ta} = \alpha_{12,m}^{Ta} * P_T^{\beta_{12,m}^{Ta}} + \alpha_{22,m}^{Ta} * P_T^{\beta_{22,m}^{Ta}} + \alpha_{32,m}^{Ta} * P_T$	18	0.0127

$$7 \quad CAF_{2,p,m}^{Ta} = \alpha_{1,2,m}^{Ta} * P_T^{\beta_{1,2,m}^{Ta}} + \alpha_{2,2,m}^{Ta} * P_T^{\beta_{2,2,m}^{Ta}} + \alpha_{3,2,m}^{Ta} * P_T^{\beta_{3,2,m}^{Ta}} \quad 19 \quad 0.0096$$

Note: P = total number of parameters in the full nonlinear model; S = standard error of the regression in CAF units; P_T = truck percentage value; $\alpha_{i,2,m}^{Ta}$ and $\beta_{i,2,m}^{Ta}$ = model parameters relative to truck percentage effect. (*) original model; (**) proposed model.

Figure 3-7a and **Figure 3-7b** show the simulated CAF values versus the estimated CAF values for the original HCM-6 model formulation and the revised model formulation, respectively. It may be seen the revised model formulation performed much better at predicting the CAF value for a given scenario as evidenced by the linear relationship shown in **Figure 3-7b** and the very high R-squared statistic of 0.971.

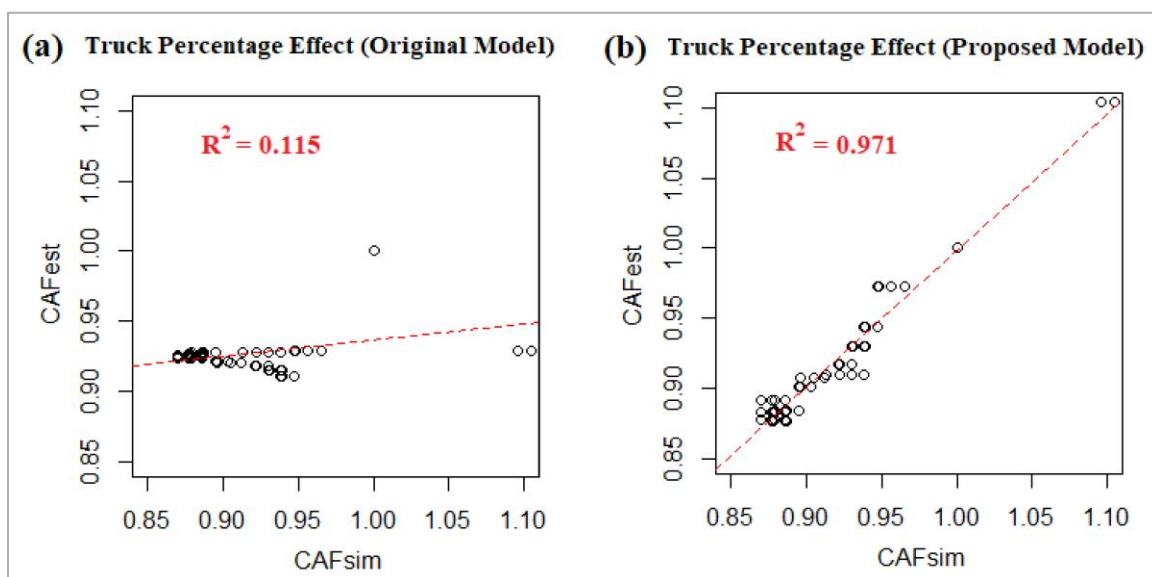


Figure 3-7. Goodness of fit between simulated and estimated CAFs for original and proposed model.

Table 3-3 shows the model parameters used to calculate the estimated CAFs using **Equations (3-7) to (3-11)** for each scenario. Row 1 corresponds to the HCM-6 research, row 2 to the HCM-6 replication described earlier, and row 3 to the CAV base case described above.

Table 3-3. Parameters and their Estimates for various CAF Models

Condition (30/70 SUT/TT)	Nonlinear Model Parameter												
	$\alpha_{1,2,m}^{T_a}$	$\beta_{1,2,m}^{T_a}$	$\alpha_{2,2,m}^{T_a}$	$\beta_{2,2,m}^{T_a}$	$\gamma_{2,m}^{G_a}$	$\theta_{2,m}^{G_a}$	$\mu_{2,m}^{G_a}$	$\alpha_{2,m}^{G_a}$	$\phi_{2,m}^{G_a}$	$\eta_{2,m}^{G_a}$	$\alpha_{2,m}^{D_a}$	$\beta_{2,m}^{D_a}$	$\phi_{2,m}^{D_a}$
HCM-6 original	0.53	0.72	-	-	8.0	0.126	0.030	0.69	12.9	1.0	1.71	1.72	-3.16
Non-CAV replication	0.52	0.75	-	-	8.0	0.211	0.052	1.36	5.4	1.0	1.71	1.72	-3.16
CAV base case	0.15	0.24	-0.25	7.37	8.0	0.211	0.052	1.36	5.4	1.0	1.71	1.72	-3.16
Penetration rate 100%*	0.15	0.24	-0.25	7.37	8.0	0.211	0.052	1.36	5.4	1.0	1.71	1.72	-3.16
Penetration rate 75%	2.41	0.30	-2.26	0.30	8.0	0.211	0.052	1.36	5.4	1.0	1.71	1.72	-3.16
Penetration rate 50%	0.33	0.62	-0.04	10.80	8.0	0.211	0.052	1.36	5.4	1.0	1.71	1.72	-3.16
Penetration rate 25%	0.49	0.81	-0.09	10.64	8.0	0.211	0.052	1.36	5.4	1.0	1.71	1.72	-3.16
Two-lane restriction	0.02	-0.35	0.65	1.41	8.0	0.211	0.052	1.36	5.4	1.0	1.71	1.72	-3.16
One-lane restriction	0.27	5.94	0.06	-0.12	8.0	0.211	0.052	1.36	5.4	1.0	1.71	1.72	-3.16
Non-lane restriction*	0.15	0.24	-0.25	7.37	8.0	0.211	0.052	1.36	5.4	1.0	1.71	1.72	-3.16
Platoon per truck type*	0.15	0.24	-0.25	7.37	8.0	0.211	0.052	1.36	5.4	1.0	1.71	1.72	-3.16
Platoon any truck type	0.22	0.36	-0.34	1.88	8.0	0.211	0.052	1.36	5.4	1.0	1.71	1.72	-3.16
Platoon size 9	0.39	0.69	-15.1	26.19	8.0	0.211	0.052	1.36	5.4	1.0	1.71	1.72	-3.16
Platoon size 7	0.33	0.62	-0.04	10.80	8.0	0.211	0.052	1.36	5.4	1.0	1.71	1.72	-3.16
Platoon size 5	0.38	0.69	-0.05	6.99	8.0	0.211	0.052	1.36	5.4	1.0	1.71	1.72	-3.16
Platoon size 3	0.39	0.70	-0.11	5.89	8.0	0.211	0.052	1.36	5.4	1.0	1.71	1.72	-3.16

Note: The capacity adjustment factor for free-flow speed effect for the mixed flow is given by the following parameters: $\mu_{2,m}^{FSSa}=0.25$; $\rho_{2,m}^{FSS}=0.70$; $\beta_{2,m}^{FSS}=1.0$; $\phi_{2,m}^{FSS}=1.0$. This factor is equal to zero when the assumed free-flow speed is 112.65 km/h (70 mph), as the case in the original research. * Base case scenario.

3.4 Step 4: Estimated CAF Results for CAV Base Case

Once the regression models were calibrated in Step 3, the CAFs were then estimated. A comparison between the estimated CAFs for the CAV condition (base case) and the estimated CAFs for the non-CAV condition (e.g., HCM-6 results) are shown in **Figure 3-8**.

3-8.

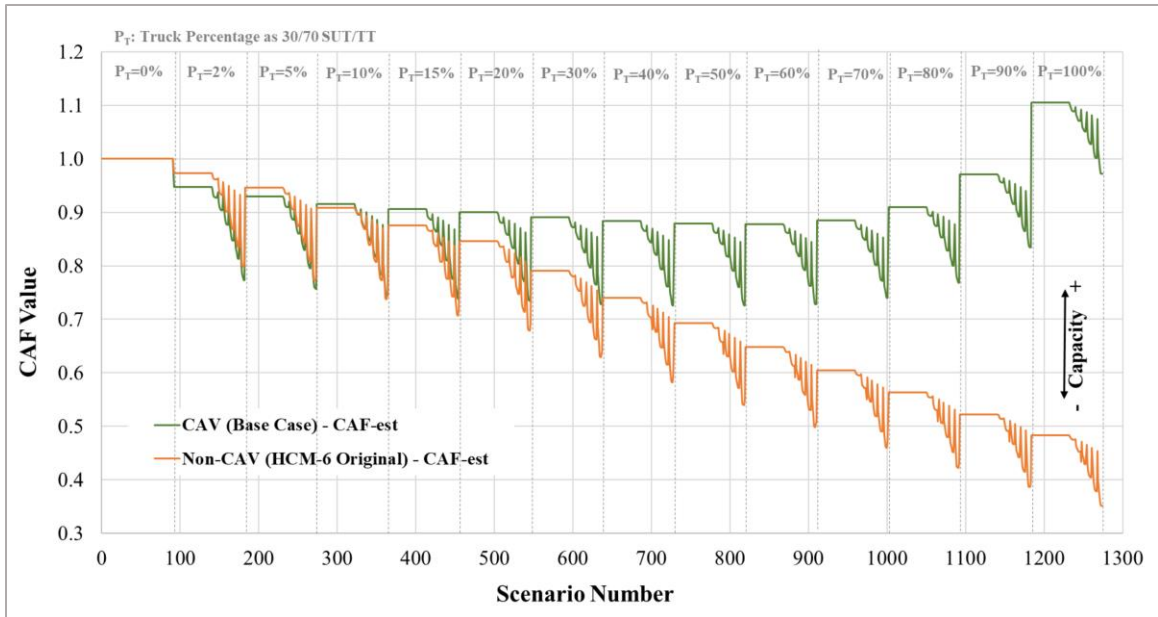


Figure 3-8. CAF values as a function of scenario number: CAV and non-CAV scenarios

The green line represents the CAV condition and the orange line the non-CAV condition. The scenario number (horizontal axis) is given by **Equation (3-6)** and corresponds to a particular combination of truck percentage, grade, and distance used to compute the corresponding CAF. For the non-CAV condition, the CAF values decrease as truck percentage increases and this decrease is at a fairly linear rate. In contrast, for the CAV condition the CAF values increase as the percentage of trucks increase. For truck percentages of less than 10 percent, the CAF values are similar to the HCM-6. It is hypothesized this occurs because there are less opportunities for truck platoon formation. Interestingly, when trucks are 100 percent of the vehicle stream the CAF values are approximately 10.5 percent higher than the CAF for passenger cars. That is, a traffic stream with 100% CAV will have a higher vehicle flow rate than a traffic stream with 100% passenger cars. Taking as reference the truck percentage interval from 10% to

100% (scenarios 274 to 1274), the CAF values for the CAV condition are, on average, 41.0% higher (ranging from 0.1% to 176.5%) than those of the non-CAV condition.

3.5 Step 5: EC-PCE Results for CAV Base Case

Similar to the HCM-6, the EC-PCE values were estimated for ten levels of truck percentage (i.e., 10% to 100% in 10% increments), grade (i.e., 0%, +3%, and +6%), and distance (i.e., 0.8 km (0.5 mi), 1.61 km (1.0 mi), and 2.42 km (1.5 mi)). **Figure 3-9** shows the corresponding EC-PCE values as a function of truck percentage for the three levels of grade and three levels of distance for both the CAV condition (base case) and the HCM-6 values. The solid lines represent the CAV EC-PCE values and the dotted lines the HCM-6 (e.g., non-CAV) EC-PCE values. The EC-PCE values were calculated using **Equation (3-12)**. Note any specific condition within the explored range of truck percentage, grade, and distance considered in the HCM-6 methodology can be computed using the model parameters provided in **Table 3-3**. On average, the EC-PCE values for the CAV condition are 34.3% lower than those of the non-CAV condition indicating the CAV technology lessens the impact of heavy trucks on traffic operations. For both the CAV and non-CAV conditions, the maximum EC-PCE values occur at a truck percentage of 10%. These values range from 2.0 to 4.5. In general, as grade and distance increase so does the EC-PCE. For higher truck percentages, the EC-PCE values for the non-CAV condition tend to decrease as truck percentages increases until the 30 percent value is reached. After this point, the EC-PCE values tend to increase at a decreasing rate with truck percentage. In general, the EC-PCE ranges from 2.0 to 4.5 for the non-CAV condition. In contrast, for the CAV condition the EC-PCE decrease at a smaller rate as

percentage of trucks increases. As would be expected from the earlier analysis, as truck percentage approaches 100 percent the EC-PCE value approaches 1.

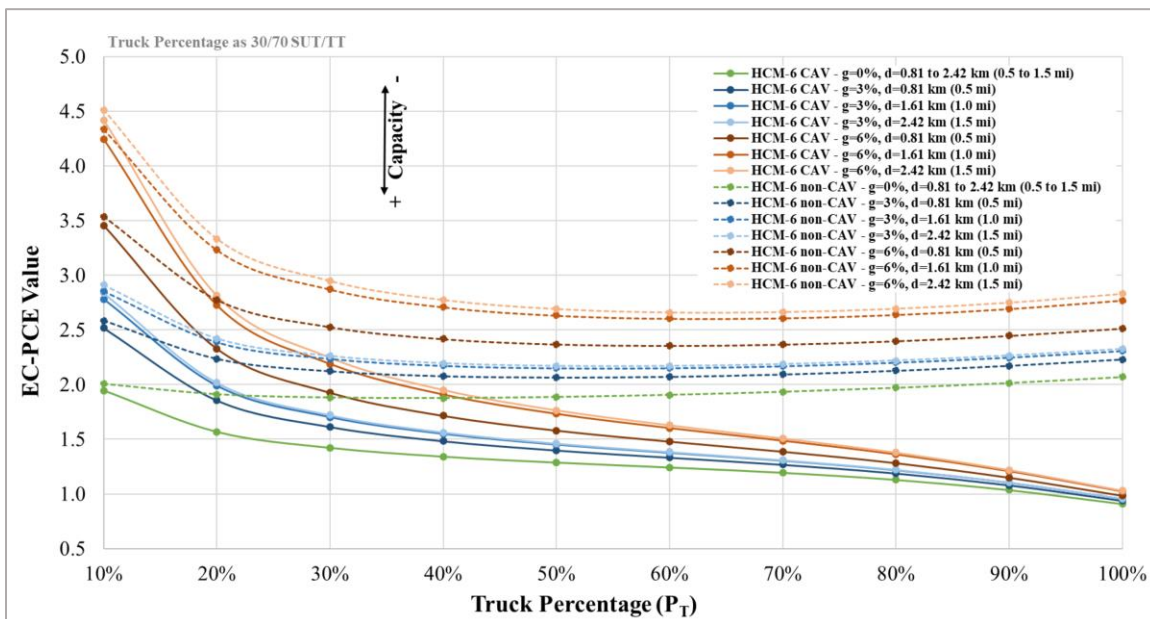


Figure 3-9. EC-PCE values as a function of truck percentage: CAV and non-CAV scenarios.

In summary, the CAV technology increases capacity for a given scenario, all else being equal, and this results in corresponding lower EC-PCE values. The increase in capacity for a given scenario is a function of the grade, grade length, and percentage trucks in the scenario. It should be noted this comparison is for trucks equipped with CAV technology. It is hypothesized that if the passenger cars also had CAV platoon technology then the capacity increase shown in **Figure 3-9** would be even greater. However, it is unclear how the EC-PCE values would change without a detailed simulation study, which is beyond the scope of this chapter.

3.6 Sensitivity Analysis of CAV Operation Factors

The parameters studied in the sensitivity analysis were market penetration rate, lane restriction, platoon truck type, and platoon size as shown in **Table 3-4**. Note the values with the asterisk (e.g., *) were considered in the base case scenario described earlier.

Table 3-4. List of Parameters Studied in the Sensitivity Analyses.

Factor	Scenarios
Market penetration rate parameter	0%, 25%, 50%, 75%, 100% *
Lane restriction parameter	No lane restriction*, 1-lane restriction, 2-lanes restriction
Platoon truck type parameter	Restricted (only similar truck types)*, Unrestricted (Any truck type)
Platoon size parameter	3, 5, 7*, 9

*Base case

The market penetration rate parameter is defined as the percentage of trucks in the traffic demand with CAV capabilities. Four other values, in addition to the base case value of 100 percent, were analyzed. Three lane restriction parameters values were analyzed including the base case value of “No lane restriction”. The “1-lane restriction” case meant the leftmost lane could not be used by trucks, while the “2-lanes restriction” meant the two leftmost lanes could not be used by trucks. The platoon truck type parameter included both the “Any truck type” meaning that platoons had no restriction on truck type and the “Per truck type” indicating platoons could only consist of similar truck types (e.g., base case). Lastly, four ‘platoon size’ parameter values were utilized, and these consisted of 3, 5, 7 (e.g., base case), and 9 for the maximum number of trucks that can be part of a CAV truck platoon.

The EC-PCE values as a function of scenario number for each of the four sensitivity analyses are shown in **Figure 3-10** through **Figure 3-13**. The scenario number is calculated using **Equation (3-6)** and represents the combination of truck percentage, grade, and distance that was used to compute the corresponding EC-PCE. The EC-PCE values were calculated using the model parameters provided in **Table 3-3**, which were obtained following the same HCM-6 methodology used for the CAV base case.

3.6.1 Market Penetration Rate

As may be seen in **Figure 3-10**, the EC-PCE values tend to decrease as market penetration rate increases and this holds true for all truck percentage rates. For truck percentage in the range from 10% to 20% the EC-PCE values for the CAV scenarios are, on average, 15.8% lower compared to the non-CAV condition (0% market penetration rate). For truck percentages in the range from 30% to 100%, the EC-PCE values decrease as market penetration rate increases. The decrease for the 25%, 50%, 75%, and 100% market penetration rate is, on average, 12.9%, 25.2%, 37.6%, and 41.3% lower than the corresponding non-CAV scenario, respectively. Interestingly, the market penetration rates of 75% and 100% produce similar EC-PCE values up to the 70% truck percentage level. After this point the 100% market penetration rate scenario performs better with EC-PCE values being, on average, 12.4% lower.

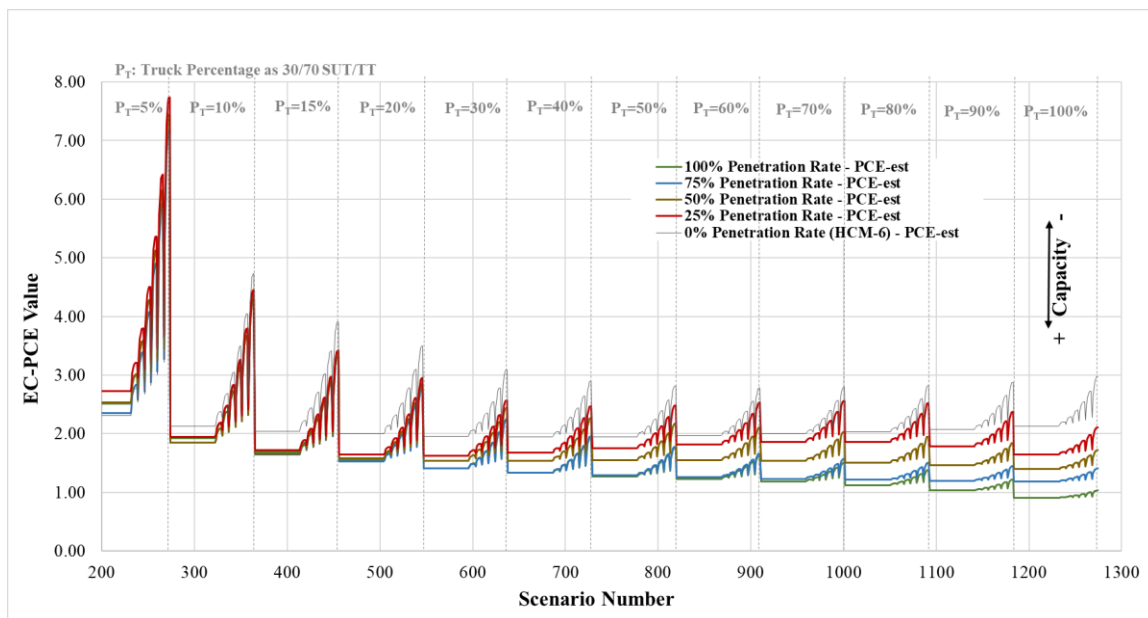


Figure 3-10. CAV EC-PCEs as a function of market penetration rate.

In summary, higher market penetration rates tend to produce lower EC-PCE values, indicating as market penetration rates increase the impact of trucks on freeway capacity decreases, all else being equal.

3.6.2 Platoon Truck Type: Restricted vs Unrestricted

Figure 3-12 shows the EC-PCE values as a function of scenario for the truck type parameter. There are only small differences between the results for the restricted and unrestricted platoon types. For lower truck percentages (e.g., 0% to 30%) and the highest truck percentage (e.g., 100%), the EC-PCE values are approximately the same for both scenarios. For truck percentages in the range of 40% to 90% the EC-PCE values for the restricted platoon scenario were, on average, 10.6% greater than the unrestricted platoon scenario. This indicates that limiting platoons to a specific type of truck type could negatively affect freeway capacity as compared to the unrestricted implementation. It

must be noted this factor can be affected by the truck composition type, and for this analysis, only one truck composition type was explored (30/70 SUT/TT). It is expected the differences found would be greater if a different proportion of truck types (e.g., 50/50 SUT/TT) were considered in the analysis.

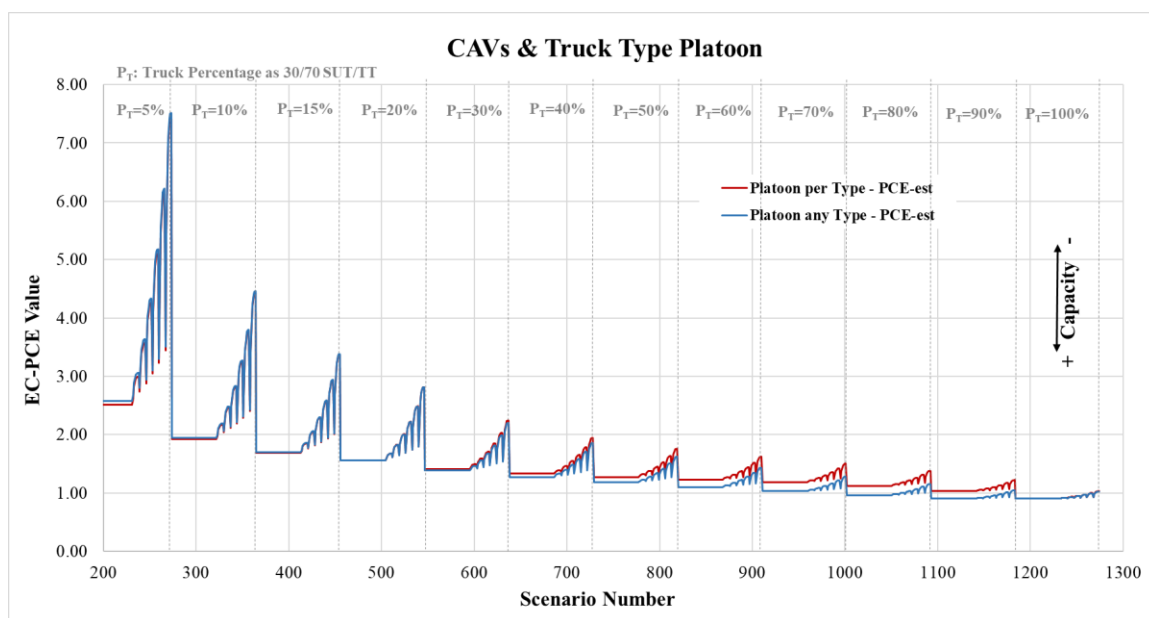


Figure 3-11. CAV EC-PCEs as a function of truck type platoon.

3.6.3 Platoon Size

Figure 3-11 shows the relationship between EC-PCE and platoon size. It can be seen the maximum platoon size has only a marginal effect on the EC-PCE values. For example, the largest difference between the three truck platoon value and the nine truck platoon value is on the order of 4%. It is hypothesized this result occurred because the interplatoon spacing and the intraplatoon spacing tend to be equivalent near or at capacity conditions. Note if merging and diverging zones, which are not part of the HCM-6 methodology studied in this chapter, were considered it is easy to envision that platoon

size would affect the EC-PCE values. However, the analysis of this aspect was beyond the scope of this chapter.

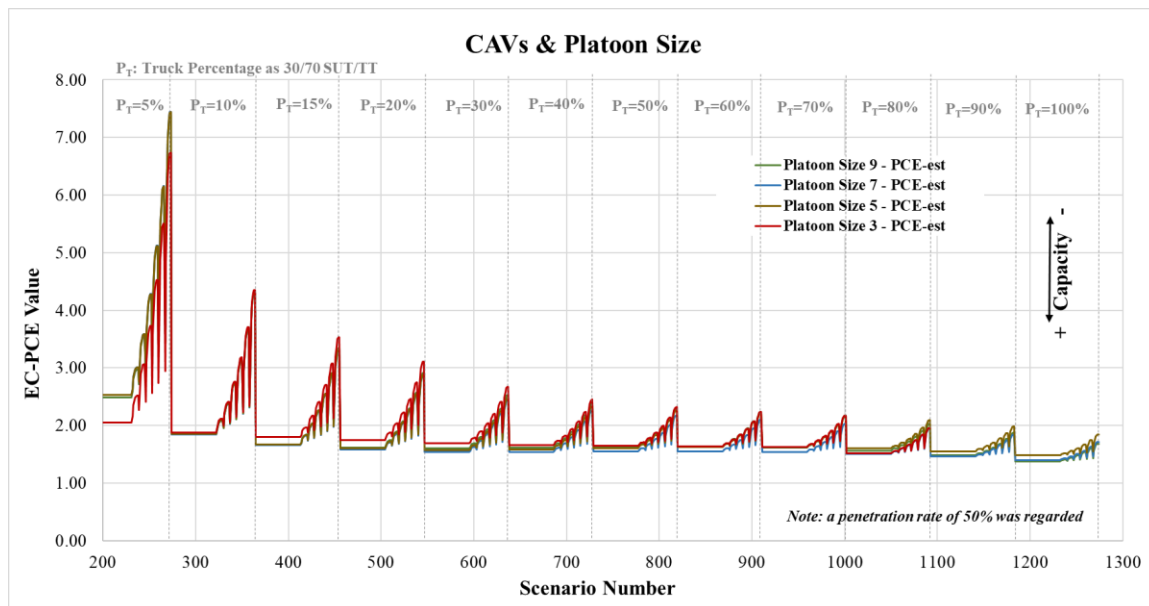


Figure 3-12. CAV EC-PCEs as a function of platoon size.

3.6.4 Lane Restriction

Figure 3-13 shows the EC-PCE values as a function of scenario number for the three lane restriction scenarios. Lane restriction had the greatest effect, in comparison to the other three sensitivity analysis parameters, on EC-PCE values. For truck percentages less than 20%, the three scenarios (e.g., no lane restriction, one-lane restriction, and two-lane restriction), had approximately similar EC-PCE values. However, as truck percentage increased past the 20 percent level so too did the EC-PCE values. The two-lane restriction scenario had EC-PCE values that were, on average, 91.8% higher than the base case (e.g., no lane restriction). Conversely, for truck percentages in the range of 20% to 80% the one-lane restriction scenario had EC-PCE values that were, on average 11.5%,

lower than the non-lane restriction scenario. It was hypothesized this occurred because there was still sufficient room in the traffic stream for platoons to form and operate. For truck percentages in the range from 80% to 100%, the one-lane restriction has on average 33.4% greater EC-PCE values compared to the non-lane restriction scenario.

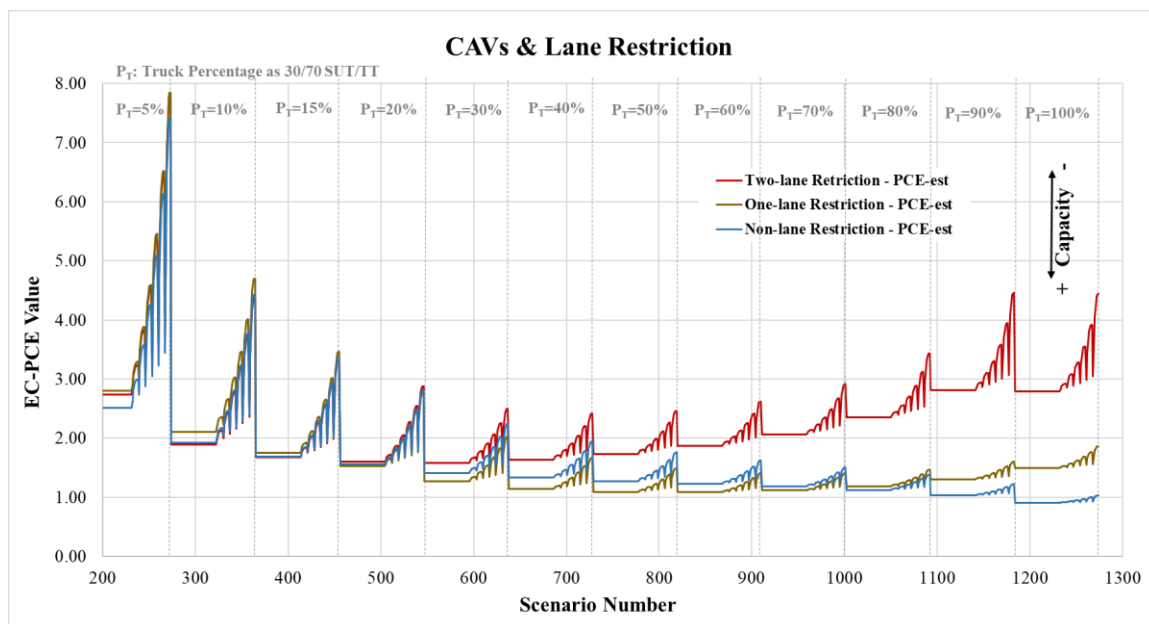


Figure 3-13. CAV EC-PCEs as a function of lane restriction.

In summary, the effect of lane restriction on capacity is dependent on the truck percentage. The effect of lane restriction is negligible for low truck percentages (20% or below), but it can negatively affect capacity for moderate to high truck percentages (30% or above) particularly if two of the three lanes are restricted.

3.7 Concluding Remarks

The objective of this chapter was to analyze the effect of CAV trucks on freeway segments using the HCM-6 methodology. In particular, the changes in CAF and EC-PCE values for different operating characteristics were compared. CAV truck platoons are

expected to be one of the first technologies deployed on the national highway system. First, the HCM-6 EC-PCEs were replicated using a microsimulation model in VISSIM 20. This VISSIM version was chosen because it can model explicitly CAV trucks and their associated platoons. Note the original CAF regression model was recalibrated to obtain a better fit between the simulated and estimated results. The impact of CAV technology on freeway capacity was then quantified using the estimated CAF values and the resulting EC-PCE values. Additionally, a sensitivity analysis of four CAV operational factors (e.g., market penetration rate, platoon truck type, platoon size, and lane restriction) was conducted to measure how these parameters affected the results.

Not surprisingly, it was found CAV truck platoons have the potential to increase capacity on freeway segments, all else being equal. The EC-PCE values for the CAV base case condition, which assumed a 100% CAV market penetration rate for trucks, were approximately 34.3 % lower, on average, than those for the non-CAV condition. In other words, CAV trucks have a lower impact on freeway operations than non-CAV trucks. To date, there has been no other analysis of the effect of CAV operations based on the HCM-6 methodology, which is the standard analysis and operations guide for U.S. transportation agencies.

Another major finding is that operational factors examined in the sensitivity analysis tended to have their greatest effect when truck percentage is greater than 30%. For truck percentage values below this cut-off, the sensitivity analyses scenarios tended to show similar behavior in operating characteristics. It was hypothesized this occurred because the proportion of CAV trucks was such that the resulting truck platoons, and associated truck platoon size, were not enough to influence the capacity of the freeway

segment. This finding indicates that CAV trucks may have the greatest impact in areas that have higher percentage truck values such as in the U.S. Midwest.

Note that in the Western U.S., particularly in the rural areas, speed limits are higher, the maximum free flow speeds of trucks and cars are different, and most of the roads are only two lanes in each direction. It is hypothesized that in these areas the positive effect of CAV trucks on capacity will be different than those explained in this chapter. It was demonstrated in this chapter that conducting analyses for localized conditions is relatively straightforward because the HCM-6 approach is simulation-based. If the conditions assumed in the HCM-6 (e.g., three lanes in each direction, trucks and cars have the same free flow speed, etc.) are violated then it is recommended the procedure be repeated for local conditions. Note the effect of CAV truck platooning on four-lane freeways in the Western U.S. will be explored in Chapter 7 of this dissertation.

It was found the microsimulation approach, which the current HCM-6 EC-PCE method for freeway segments and multilane highways is based on, has a number of issues that should be addressed in further studies. Because it was needed to use different versions of the VISSIM microsimulation model than was used in the HCM-6, a recalibration of the nonlinear regression model was required in order to replicate the results of the original research. It was hypothesized this was a result of periodic updates and changes in the internal logic of the microsimulation model made by the developer. In addition, it is recommended calibrating the HCM-6 methodology with empirical data. This would also include a deeper assessment of the form and error of the regression models using fitting simulated and estimated data. It is possible different model structures might provide better results, which is explored in Chapter 4 of this dissertation.

An assessment of the existing microsimulation framework and assumptions of the current HCM-6 EC-PCE methodology should also be performed. Interestingly, in the original research, only one simulation run was performed for each scenario combination. This is important because performing a single simulation run increases the noise of the simulation results and potentially could negatively impact the accuracy of the capacity estimates and the associated EC-PCE values. This point will be addressed in more detail in Chapter 6 of this dissertation.

Finally, it is also recommended the effect of other variables related to driving behavior and operational characteristics such as interplatoon spacing, platoon forming logic, weight and power distributions, acceleration profiles, etc., be studied. These parameters were not studied in this chapter due to space limitations and the lack of empirical data related to these topics. This is an area of potential research that would further help transportation agencies as they begin the transition to CAV operations.

CHAPTER 4

AN ALTERNATIVE REGRESSION MODEL STRUCTURE FOR THE HCM-

6 EQUAL CAPACITY PASSENGER CAR EQUIVALENCY

METHODOLOGY

4.1 Introduction

The HCM-6 EC-PCEs for freeway segments were estimated using a microsimulation-based methodology. The HCM-6 includes EC-PCE values for 14 levels of truck percentage, 13 levels of grade, 7 levels of grade distance, and 3 levels of truck composition type. In particular, the VISSIM microsimulation model is used for modeling the capacity of 1,274 scenarios derived from these factors. The simulated capacity values are used to calculate capacity adjustment factors (CAFs), for various combinations of truck percentage, truck composition, grade, and grade length.

Because of the stochasticity of the microsimulation results, including the capacity values, these CAFs are not used to calculate the PCE values directly. Instead, the CAFs are used as input to a multiple linear regression modeling process. The HCM-6 EC-PCE developed a 15-parameter nonlinear regression model (NLRM) which is used to estimate the CAF values (Zhou, Rilett, & Jones, 2019; Dowling et al., 2014b, 2014c). These estimated CAFs, as opposed to the CAFs calculated from the simulation output, are then used to calculate the EC-PCE values found in the HCM-6. Because of the complexity of the existing NLRM model structure, the EC-PCE results are presented in the HCM-6 as a series of tables. Previous studies have shown the HCM-6 EC-PCE methodology is suitable for analyzing traffic situations beyond the scope of the HCM-6 such as CAV

truck platooning (Hurtado-Beltran & Rilett, 2021). However, for this situation the original HCM-6 model structure had to be modified. In this regard, it is important to evaluate if the existing NLRM approach is flexible enough for fitting simulation results derived from novel traffic scenarios.

The main objective of this chapter is to analyze the use of alternative regression models to fit simulated and estimated CAFs in the HCM-6 EC-PCE methodology for freeway and multilane highway segments. It is hypothesized simpler regression models could provide comparable results and would be easier for users to apply. This would allow the users to analyze specific applications using the calibrated models directly rather than using tables. This method would also make it simpler for users to develop their own localized CAF models for situations that do not conform to the HCM-6 assumptions.

Three regression models were explored in this chapter: (1) the original HCM-6 nonlinear regression model with 15 model parameters (NLRM), (2) a proposed multivariate linear regression model with 10 model parameters (MLRM), and (3) a proposed reduced nonlinear regression model with 8 model parameters (NLRM_{red}). Following the HCM-6 protocols, these regression models were used to estimate CAF and EC-PCE values for two traffic situations: (1) existing HCM-6 conditions, referred to as the HCM-6 replication, and (2) CAV truck platooning. Finally, the performance of the regression models was assessed using various goodness-of-fit statistics. It is hypothesized simpler regression models may facilitate capacity analyses and the process of reporting results. Moreover, this chapter will provide insight about the performance of the current nonlinear regression model used in the HCM-6 EC-PCE methodology when modeling novel traffic scenarios such as CAV truck platooning.

4.2 Regression Model Approach

Due to the inherent variability of the simulated capacity values, the HCM-6 developers chose not to use the CAF values developed from the simulated capacity values directly. Instead, they developed and calibrated a nonlinear regression model that related the simulated CAF values to the truck percentage, grade, distance, and free-flow speed parameters. The goal was to mitigate the effect of the variability in the CAF results. The structure of the nonlinear regression model will be discussed in more detail later.

Previous research used simpler linear regression models to estimate the PCE values directly. For example, Washburn and Ozkul (2013) obtained linear regression models to estimate PCEs based on equal-density as a function of distance, grade, free-flow speed, number of lanes, flow rate, truck percentage, and truck type. The model had a good R-squared value of approximately 0.72. Similarly, Bo (2013) proposed linear regression models to estimate PCEs based on equal-capacity as a function of truck type, weight to power ratio, truck percentage, and grade. In this case, the R-squared value was 0.90 indicating a very good model fitting. It must be noted in both studies a single equation was used to model the influence of trucks on the traffic stream for the full range of values of the parameters, including grade effect. Moreover, these regression models were used to estimate the PCEs directly and no CAFs were involved in the computation process. This is in contrast to the HCM-6 approach, where regression models were used to estimate CAFs based on simulated data. These CAF models were used subsequently to calculate the EC-PCEs.

The current HCM-6 CAF/EC-PCE values suggest the combined effect of grade and grade distance is significantly different for positive grade values as compared to

negative values. Indeed, the original research reported grade is the main influencing factor on capacity (Dowling et al., 2014). It is hypothesized a segmented function based on the grade conditions (e.g., positive or negative) could improve the model fitting for the estimation of CAF values while simultaneously employing a simpler format. This approach has not been explored in previous studies. It is important to determine if simpler models may be used in Step 3 of the HCM-6 procedure. There are two main advantages. The first is the simpler equations can be used to estimate the CAF, capacity, and PCE values directly. In other words, users would no longer need the HCM-6 tables and there would be no need to interpolate any results. Secondly, it would make it easier for users to calibrate models for their local conditions (Zhou, Rilett, & Jones, 2019).

4.3 Methodology

The main purpose of this chapter is to evaluate alternative regression models for fitting simulated and estimated capacity adjustment factors (CAFs) in the HCM-6 EC-PCE methodology for freeway and multilane highway segments. Two alternative regression models are proposed in this chapter: (1) a multivariate linear regression model (MLRM) and (2) a reduced nonlinear regression model (NLRM_{red}). The proposed regression models use a segmented model structure that depends on the grade parameter (e.g., value of the negative or positive grade). The proposed model structures are simpler than the original HCM-6 nonlinear regression model (NLRM), which is comprised of 15 model parameters.

The two proposed regression models were evaluated using two scenarios: (1) HCM-6 replication, and (2) CAV truck platooning. The goal of the HCM-6 replication was to replicate the CAF values and EC-PCE values reported in the HCM-6 following the

protocol of the HCM-6 EC-PCE methodology. If the simpler models are not satisfactory then the hypothesis of this chapter is incorrect. The CAV truck platooning scenario was developed to show the proposed approach can be used to model a new traffic situation. For this case, it was assumed only trucks operate in CAV mode and all truck operational characteristics were the same as in the HCM-6. In other words, the only difference between the trucks in the HCM-6 and the trucks in the CAV analysis is the trucks in the latter scenario could form platoons based on CAV technologies. Otherwise, both analyses followed the HCM-6 EC-PCE methodology.

The methodology applied in this chapter is comprised of three main steps. First, the microsimulation model in VISSIM was used to obtain the simulated capacity values and this corresponds to Steps 1 and 2 in the HCM-6 EC-PCE methodology. The next step was to develop the regression models for fitting the simulated and estimated CAF values. This corresponds to Step 3 in the HCM-6 EC-PCE methodology. Three regression models (NLRM, MLRM, and NLRM_{red}) were explored in this step. Lastly, the estimated CAF values and EC-PCE values for specific conditions of truck percentage, grade, and distance were calculated. This corresponds to Steps 4 and 5 in the HCM-6 EC-PCE methodology. The EC-PCE values from the proposed models were then compared directly to the HCM-6 results.

4.3.1 Step 1 and 2: HCM-6 EC-PCE Microsimulation Model Capacity

The HCM-6 EC-PCE methodology uses the VISSIM microsimulation model to obtain the capacity values for each scenario combination (Dowling et al, 2014; Zhou, Rilett, & Jones, 2019a). In this chapter, the capacity values from the VISSIM model were obtained following HCM-6 protocols described in Section 3.2.3. In the original research three

truck composition percentages were explored: (1) 30/70 SUT/TT, (2) 50/50 SUT/TT, and (3) 70/30 SUT/TT. In this chapter, only the former scenario was studied as it is the most common on the US highway system (HCM, 2016).

In the original research, the HCM-6 EC-PCE values were calculated using VISSIM 4.4 which is no longer available (Zhou, Rilett, & Jones, 2019; Yang, 2013). Previous research has shown the HCM-6 EC-PCE results can be replicated accurately using VISSIM 9 (Zhou, 2018). For the HCM-6 replication analysis the 1,274 scenario combinations and their associated flow-density plots were developed using VISSIM 9. The model assumptions and testbeds were the same as those used in the HCM-6 EC-PCE research. For the CAV truck platooning analysis, all the flow-density plots were developed using VISSIM 20 because this version can model CAV and their associated platoons. The original HCM-6 microsimulation model assumptions and testbeds were also observed. The only exception was in the mixed-traffic flow condition where all the trucks were modeled using CAV behavior. The maximum platoon size was set to 7 and the VISSIM ‘Aggressive CoExist’ protocol was used to model truck driver behavior (Hurtado-Beltran & Rilett, 2021; PTV Group, 2019; Sukennik, 2018).

Once the capacity values were identified, the capacity adjustment factors (CAFs) were calculated for the mixed flow and passenger car-only flow scenarios using the HCM-6 definitions shown in **Equations (3-4)** and **(3-5)**, respectively (see Section 3.2.4).

The simulated CAFs for all 1,274 scenarios, which were calculated using the capacity values from the microsimulation models, are shown in **Figure 4-1**. The x-axis represents the scenario number. Each specific scenario number is calculated using **Equation (3-6)** and is a function of the truck percentage, grade, and distance. The red

line represents the simulated CAFs obtained for the HCM-6 replication analysis using VISSIM 9. The blue line corresponds to the simulated CAFs for the CAV truck platooning analysis using VISSIM 20.

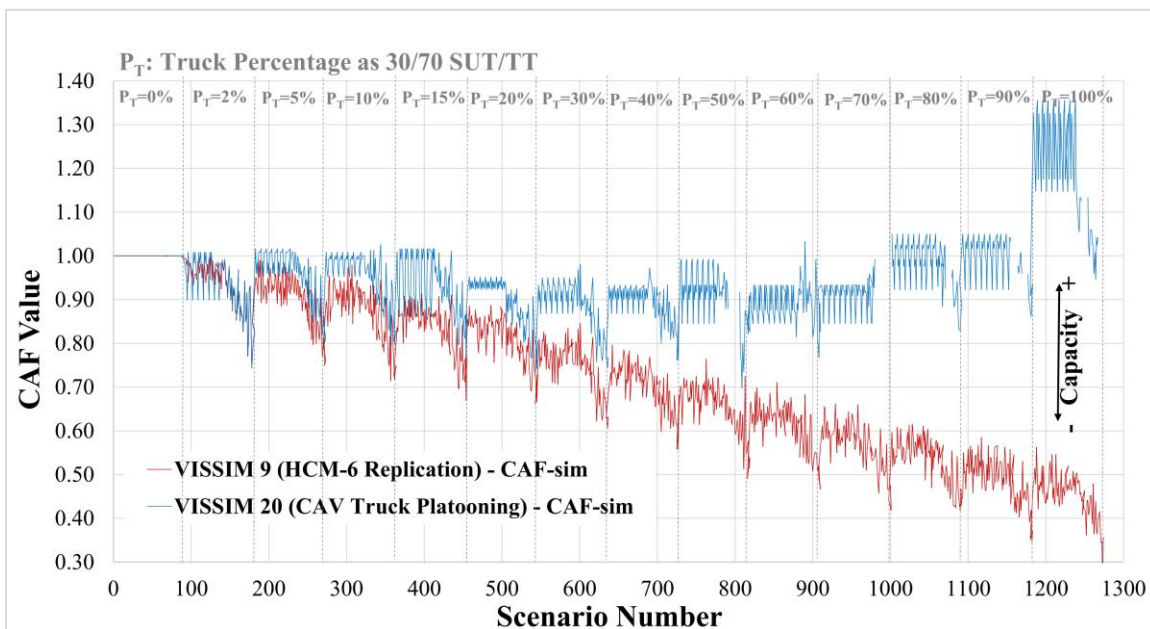


Figure 4-1. Simulated CAFs for each scenario combination.

It may be seen in **Figure 4-1** that, as expected, the simulated CAF values for the CAV truck platooning condition, characterized by shorter headways, tended to be higher than those of the HCM-6 replication based on conventional traffic. This was because the CAV scenarios had higher capacity values as a result of the truck platooning. It is also important to note that **Figure 4-1** demonstrates visually the inherent stochasticity in the CAF values. This stochasticity is directly attributable to the microsimulation-based approach defined in the HCM-6 research, which consisted of a single run with a single seed number for simulating each of the 1,274 scenario combinations (Dowling et al., 2014b, 2014c).

4.3.2 Step 3: Regression Model Development for Estimated CAFs

Because of the inherent variability of the microsimulation-based CAF results shown in **Figure 4-1**, the HCM-6 developers chose not to use the simulated CAF values for a given combination of parameters directly. Instead, they calibrated a regression model that related the CAF value to the truck percentage, grade, and distance parameters. The goal was to mitigate the variability in the CAF results. Consequently, the simulated CAF values from Step 2 were used as input and statistical regression techniques were used to calibrate the regression model. In this chapter, three regression models were explored: (1) the original nonlinear regression model (NLRM), (2) a proposed multivariate linear regression model (MLRM), and (3) a proposed reduced nonlinear regression model (NLRM_{red}). These regression models were developed for both the HCM-6 replication and CAV truck platooning analyses. Note all the models were a function of the same explanatory variables used in the original HCM-6 research (e.g., truck percentage, grade, and distance). A description of these regression models is provided below.

4.3.2.1 Original Nonlinear Regression Model (NLRM)

In the original HCM-6 research, a nonlinear regression model with 15 model parameters was used for fitting the simulated and estimated CAF values. The form for the HCM-6 analytical model was based on vehicle kinematic and resistance equations related to ascending and descending different grades (Dowling et al., 2014b). A heuristic optimization approach was used to calibrate the model where the goal was to identify the model parameter values that minimized the error between the simulated CAFs and the estimated CAFs. The explanatory variables were truck percentage, grade, and distance, while the truck composition type (m) and the free-flow speed (FFS) remained constant.

The parameters of these equations were optimized, using an Excel Spreadsheet. The final model consisted of a combined grade and distance effect parameter, a free-flow speed effect parameter, and truck percentage effect parameter (Zhou, Rilett, & Jones, 2019; Dowling et al., 2014b; List et al., 2014) as shown in **Equations (3-7)** through **(3-11)**.

In this chapter, the model parameters were estimated using a Generalized Reduced Gradient (GRG) approach (Lasdon, Fox, & Ratner, 1974). This is a nonlinear optimization method which uses an iterative process to optimize a target value. The target goal was to minimize the sum of squared errors between the simulated CAFs from the microsimulation output and the estimated CAFs from the non-linear regression model.

4.3.2.2 Multivariate Linear Regression Model (MLRM)

This chapter explored a multivariate linear regression model (MLRM) with 10 model parameters and a segmented model structure that was a function of grade condition (e.g., negative and level grade condition, or positive grade condition) as shown in **Equation (4-1)**. For the negative and level grade condition, truck percentage (p) was the only explanatory variable, while the truck composition type (m) and the free-flow speed (FFS) effects remained constant. The grade (g) and distance (d) variables were removed from the model because a partial F-test revealed the reduced model was preferred over the full model at $\alpha = 0.05$ ($F_{\text{stat}} = 0.39 < F_{\text{crit}} = 3.01$). For the positive grade condition, the explanatory variables were truck percentage (p), grade (g), and distance (d). All parameters are statistically significant at $\alpha = 0.05$. The free-flow speed (FFS) and the truck composition type (m) effects remain constant. Because the original research takes into account a similar criteria for exploring new truck composition types, and the free-

flow speed effect is null when the assumed free-flow speed is 70 mph, it is hypothesized the proposed model may provide comparable performance.

$$CAF_{2,p,m,g,d,FFS} = \begin{cases} \alpha_{2,m,FFS}^{0^-} + \alpha_{2,m,FFS}^{T_a^-} * (p_s)_p^{\beta_{2,m,FFS}^{T_a^-}} & \text{if } (g_s)_g \leq 0 \\ \alpha_{2,m,FFS}^{0^+} + \alpha_{2,m,FFS}^{T_a^+} * (p_s)_p^{\beta_{2,m,FFS}^{T_a^+}} & \text{if } (g_s)_g > 0 \\ + \alpha_{2,m,FFS}^{G_a^+} * (g_s)_g^{\beta_{2,m,FFS}^{G_a^+}} + \alpha_{2,m,FFS}^{D_a^+} * (d_s)_d^{\beta_{2,m,FFS}^{D_a^+}} & \end{cases} \quad (4-1)$$

Where:

$CAF_{2,p,m,g,d}$: Capacity adjustment factor for the mixed flow ($f = 2$) at p truck percentage level, m truck composition level, g grade level, d distance level, and FFS free-flow speed.

$(p_s)_p$: Truck percentage at p truck percentage level (between 0 and 1).

$(g_s)_g$: Grade at g grade level (between -0.06 and 0.06).

$(d_s)_d$: Distance of grade at d distance level (mile).

$\alpha_{2,m,FFS}^{0^-}$: Intercept parameter for capacity adjustment factor at level or negative grade.

$\alpha_{2,m,FFS}^{T_a^-}, \beta_{2,m,FFS}^{T_a^-}$: Parameters for capacity adjustment factor for truck percentage effect (T_a^-) at level or negative grade.

$\alpha_{2,m,FFS}^{0^+}$: Intercept parameter for capacity adjustment factor at positive grade.

$\alpha_{2,m,FFS}^{T_a^+}, \beta_{2,m,FFS}^{T_a^+}$: Parameters for capacity adjustment factor for truck percentage effect (T_a^+) at positive grade.

$\alpha_{2,m,FFS}^{G_a^+}, \beta_{2,m,FFS}^{G_a^+}$: Parameters for capacity adjustment factor for grade effect (G_a^+) at positive grade.

$\alpha_{2,m,FFS}^{D_a^+}$, $\beta_{2,m,FFS}^{D_a^+}$: Parameters for capacity adjustment factor for distance effect (D_a^+) at positive grade.

The model parameters of the multiple linear regression model were estimated using a multivariate Box-Cox transformation and the least square method for the statistically significant predictors (Sheather, 2009; Spiegelman, Park, & Rilett, 2011).

4.3.2.3 Reduced Nonlinear Regression Model (NLRM_{red})

This chapter also explored a new reduced nonlinear regression model (NLRM_{red}) with 8 model parameters and a segmented model structure that is a function of the grade condition as shown in **Equation (4-2)**. This model was derived from the previous multivariate linear regression model. Similarly, this model used truck percentage effect, grade effect, and distance effect as the explanatory variables and used the simulated CAF values as the dependent variable. However, this model assumed a combined effect of grade and distance similar to the original HCM-6 nonlinear regression model (NLRM). It should be noted only the model format for the distance effect was taken from the original nonlinear model. Preliminary analysis revealed this model format performs better for modeling the distance effect compared to the linear model.

$$CAF_{2,p,m,g,d,FFS} = \begin{cases} CAF_{1,0,0,g,d} + \alpha_{2,m,FFS}^{T_a^-} * (p_s)_p^{\beta_{2,m,FFS}^{T_a^-}} & \text{if } (g_s)_g \leq 0 \\ CAF_{1,0,0,g,d} + \alpha_{2,m,FFS}^{T_a^+} * (p_s)_p^{\beta_{2,m,FFS}^{T_a^+}} \\ + \alpha_{2,m,FFS}^{G_a^+} * (g_s)_g^{\beta_{2,m}^{G_a^+}} * \left[1 - \alpha_{2,m,FFS}^{D_a^+} * e^{\beta_{2,m,FFS}^{D_a^+} * (d_s)_d} \right] & \text{if } (g_s)_g > 0 \end{cases} \quad (4-2)$$

Where:

$CAF_{2,p,m,g,d}$: Capacity adjustment factor for the mixed flow ($f = 2$) at p truck percentage level, m truck composition level, g grade level, d distance level, and FFS free-flow speed.

$CAF_{1,0,0,g,d}$: Capacity adjustment factor for the auto-only flow at g grade level, d distance level. This value is assumed to be 1.

$(p_s)_p$: Truck percentage at p truck percentage level (between 0 and 1).

$(g_s)_g$: Grade at g grade level (between -0.06 and 0.06).

$(d_s)_d$: Distance of grade at d distance level (mile).

$\alpha_{2,m,FFS}^{T_a^-}, \beta_{2,m,FFS}^{T_a^-}$: Parameters for capacity adjustment factor for truck percentage effect (T_a^-) at level or negative grade.

$\alpha_{2,m,FFS}^{T_a^+}, \beta_{2,m,FFS}^{T_a^+}$: Parameters for capacity adjustment factor for truck percentage effect (T_a^+) at positive grade.

$\alpha_{2,m,FFS}^{G_a^+}, \beta_{2,m,FFS}^{G_a^+}$: Parameters for capacity adjustment factor for grade effect (G_a^+) at positive grade.

$\alpha_{2,m,FFS}^{D_a^+}, \beta_{2,m,FFS}^{D_a^+}$: Parameters for capacity adjustment factor for distance effect (D_a^+) at positive grade.

Similar to the NLRM, the model parameters of the NLRM_{red} were estimated using the Generalized Reduced Gradient (GRG) approach.

Table 4-1 summarizes the explanatory variables that were added and removed in the model formulation for the three regression models explored in this chapter.

Table 4-1. Explanatory Variables for the Regression Models

Regression Model		Explanatory Variable				
		$(p_s)_p$	$(g_s)_g$	$(d_s)_d$	FFS^*	m^*
NLRM		Yes	Yes	Yes	Yes	Yes
MLRM	$(g_s)_g \leq 0$	Yes	No	No	Yes	Yes
	$(g_s)_g > 0$	Yes	Yes	Yes	Yes	Yes
NLRM _{red}	$(g_s)_g \leq 0$	Yes	No	No	Yes	Yes
	$(g_s)_g > 0$	Yes	Yes	Yes	Yes	Yes

Note: NLRM = nonlinear regression model (original HCM-6 model); MLRM = multivariate linear regression model (proposed); NLRM_{red} = reduced nonlinear regression model (proposed); $(p_s)_p$ = truck percentage; $(g_s)_g$ = grade; $(d_s)_d$ = distance; FFS = free-flow speed; m = truck composition type; (*) treated as constant.

4.3.3 Step 4 and 5: CAF and EC-PCE Estimation

The CAFs for the mixed flow scenarios (CAF_{2,p_s,m_s,g_s,d_s}) were estimated for the specific conditions listed in the HCM-6. The parameters of interest were truck percentage p_s , grade g_s , and distance d_s . These estimated CAFs were obtained using the calibrated regression models described above. The CAF values were estimated for both the HCM-6 replication analysis and the CAV truck platooning analysis.

The last step was to calculate the EC-PCEs ($EC - PCE_{2,p_s,m_s,g_s,d_s}$) at specific combinations of truck percentage p_s , grade g_s , and distance d_s . These EC-PCE values were calculated using the HCM-6 method shown in **Equation (3-12)**.

4.4 Calibrated Regression Model Results

4.4.1 NLRM Calibrated Models

The calibrated model parameters of original nonlinear regression models (NLRM) are shown in **Table 4-2**. The calibrated model parameters were used in **Equations (3-7)** through **(3-11)**, to calculate the estimated CAFs for the mixed-flow condition. The calibrated model parameters for the original values of the HCM-6 research and the HCM-6 replication analysis are given in rows 1 and 2, respectively. It may be seen the calibrated parameters are relatively close. For the CAV truck platooning analysis, the calibrated model parameters are given in row 3. It is hypothesized the values in row 3 differ from the non-CAV models because they were fit to CAV traffic conditions which are considerably different than the HCM-6 assumptions.

Table 4-2. Parameters in the NLRM for CAF Estimation

Condition (30/70 SUT/TT)	Nonlinear Model Parameter (NLRM)														
	$\alpha_{2,m}^T$	$\beta_{2,m}^T$	$\gamma_{2,m}^G$	$\theta_{2,m}^G$	$\mu_{2,m}^G$	$\alpha_{2,m}^G$	$\phi_{2,m}^G$	$\eta_{2,m}^G$	$\alpha_{2,m}^D$	$\beta_{2,m}^D$	$\phi_{2,m}^D$	$\mu_{2,m}^{FSS}$	$\rho_{2,m}^{FSS}$	$\beta_{2,m}^{FSS}$	$\phi_{2,m}^{FSS}$
HCM-6 original	0.53	0.72	8.0	0.126	0.030	0.69	12.90	1.0	1.72	1.71	-3.16	0.25	-0.70	1.0	1.0
HCM-6 replication	0.52	0.72	8.0	0.785	0.186	0.70	2.79	1.02	1.81	2.00	-3.75	0.25	-0.70	1.0	1.0
CAV truck platooning	-0.32	7.63	8.0	0.398	-0.388	0.06	32.86	-3.35	0.54	3.21	-8.16	0.25	-0.70	1.0	1.0

Note: NLRM = nonlinear regression model (original mode); SUT = single unit truck; TT = tractor trailer.

4.4.2 MLRM Calibrated Models

The calibrated multivariate linear regression model (MLRM) for the HCM-6 replication analysis and the CAV truck platooning condition are shown in **Equations (4-3)** and **(4-4)**, respectively. These equations were used to calculate the estimated CAF values for the

mixed traffic condition for both analyses. Note that all the predictors included in the models were statistically significant at $\alpha = 0.05$.

- MLRM for HCM-6 replication: (4-3)

$$CAF_{2,p,m,g,d,FFS} = \begin{cases} 0.997 - 0.519 * (p_s)_p^{0.73} & \text{if } (g_s)_g \leq 0 \\ 0.884 - 0.514 * (p_s)_p^{0.66} - 0.828 * (g_s)_g^{0.68} + 0.141 * (d_s)_d^{-0.11} & \text{if } (g_s)_g > 0 \end{cases}$$

- MLRM for CAV truck platooning: (4-4)

$$CAF_{2,p,m,g,d,FFS} = \begin{cases} 0.943 - 0.315 * (p_s)_p^{13.27} & \text{if } (g_s)_g \leq 0 \\ 1.865 + 0.227 * (p_s)_p^{8.16} - 4.399 * (g_s)_g^{1.28} - 0.916 * (d_s)_d^{-0.01} & \text{if } (g_s)_g > 0 \end{cases}$$

Where:

$CAF_{2,p,m,g,d}$: Capacity adjustment factor for the mixed flow ($f = 2$) at p truck percentage level, truck composition level $m = 30SUT/70TT$, g grade level, d distance level, and free-flow speed $FFS = 70mph$.

$(p_s)_p$: Truck percentage at p truck percentage level (between 0 and 1).

$(g_s)_g$: Grade at g grade level (between -0.06 and 0.06).

$(d_s)_d$: Distance of grade at d distance level (miles).

4.4.3 $NLRM_{red}$ Calibrated Models

The calibrated models of the reduced nonlinear regression model ($NLRM_{red}$) for the HCM-6 replication and the CAV truck platooning are shown in **Equations (4-5)** and **(4-6)** respectively. The description of the model structure is analogous to the MLRM as discussed above.

- NLRM_{red} for HCM-6 replication: (4-5)

$$CAF_{2,p,m,g,d,FFS} = \begin{cases} 1 - 0.521 * (p_s)_p^{0.72} & \text{if } (g_s)_g \leq 0 \\ 1 - 0.501 * (p_s)_p^{0.73} - 3.456 * (g_s)_g^{1.10} * [1 - 1.786 * e^{-3.72*(d_s)_d}] & \text{if } (g_s)_g > 0 \end{cases}$$

- NLRM_{red} for CAV truck platooning: (4-6)

$$CAF_{2,p,m,g,d,FFS} = \begin{cases} 0.943 + 0.315 * (p_s)_p^{13.27} & \text{if } (g_s)_g \leq 0 \\ 1 + 0.205 * (p_s)_p^{7.14} - 1.162 * (g_s)_g^{0.66} * [1 - 1.893 * e^{-5.42*(d_s)_d}] & \text{if } (g_s)_g > 0 \end{cases}$$

Where:

$CAF_{2,p,m,g,d}$: Capacity adjustment factor for the mixed flow ($f = 2$) at p truck percentage level, truck composition level $m = 30SUT/70TT$, g grade level, d distance level, and free-flow speed $FFS = 70mph$.

$(p_s)_p$: Truck percentage at p truck percentage level (between 0 and 1).

$(g_s)_g$: Grade at g grade level (between -0.06 and 0.06).

$(d_s)_d$: Distance of grade at d distance level (miles).

4.5 Goodness-of-Fit Results

Table 4-3 shows the statistics calculated for assessing the goodness-of-fit of the regression models examined in this chapter. For the HCM-6 replication analysis, the statistics between the original NLRM and the proposed NLRM_{red} are, not surprisingly, exactly the same. Although the goodness-of-fit statistics for the proposed MLRM are slightly poorer, as revealed by the residual standard error (S) and the coefficient of determination (R^2), its performance is very close to the other two models. Interestingly, for the CAV truck platooning analysis, the proposed NLRM_{red} reveals a better goodness-

of-fit than both the original NLRM and the proposed MLRM as evidenced by a slightly higher R-squared value and a lower S value.

Note the goodness-of-fit statistics of all three regression models are poorer for the CAV truck platooning analysis as compared to the HCM-6 replication analysis. This issue will be discussed in more detail later.

Table 4-3. Goodness-of-Fit Statistics for Estimated CAF values

Statistic	HCM-6 Replication			CAV Truck Platooning		
	NLRM	NLRM _{red}	MLRM	NLRM	NLRM _{red}	MLRM
SSE	1.04	1.04	1.26	2.70	2.62	2.79
SST	39.73	39.73	39.73	10.85	10.85	10.85
N	1274	1274	1274	1204	1204	1204
P	15	8	10	15	8	10
S = $\sqrt{\text{MSE}}$	0.029	0.029	0.032	0.048	0.047	0.048
R ²	0.97	0.97	0.96	0.75	0.76	0.74
MAPE	3.4%	3.4%	3.7%	3.8%	3.8%	3.9%

Note: NLRM = nonlinear regression model; MLRM = multivariate linear regression model; SSE = sum of squared error; SST = sum of squared total; N = number of observations; P = number of regression parameters; S = residual standard error; R² = coefficient of determination; MAPE = mean absolute percentage error.

Figure 4-2 shows the relationship between the simulated CAF values (CAF-sim) and the estimated CAF values (CAF-est) for the calibrated regression models explored in this chapter. Note the goal of the regression model was to identify a CAF-est model that best replicates the CAF-sim values output from VISSIM. The left graph corresponds to the HCM-6 replication analysis, while the right graph corresponds to the CAV truck platooning analysis. In both graphs, the three regression models are depicted: (1) NLRM (blue circles), (2) proposed MLRM (green crosses), and (3) proposed NLRM_{red} (red Xs). For the HMC-6 replication the relationship is approximately one to one with an

approximate R-squared value of 0.97 for the three regression models. Note this R-squared value is higher than those obtained in previous related studies discussed in Section 4.2(Washburn & Ozkul, 2013; Yang, 2013). For the CAV truck platooning analysis, the fit is not nearly as good as evidenced by the R-squared value of approximately 0.75. Although all three regression models have a similar performance, the proposed $NLRM_{red}$ performs slightly better.

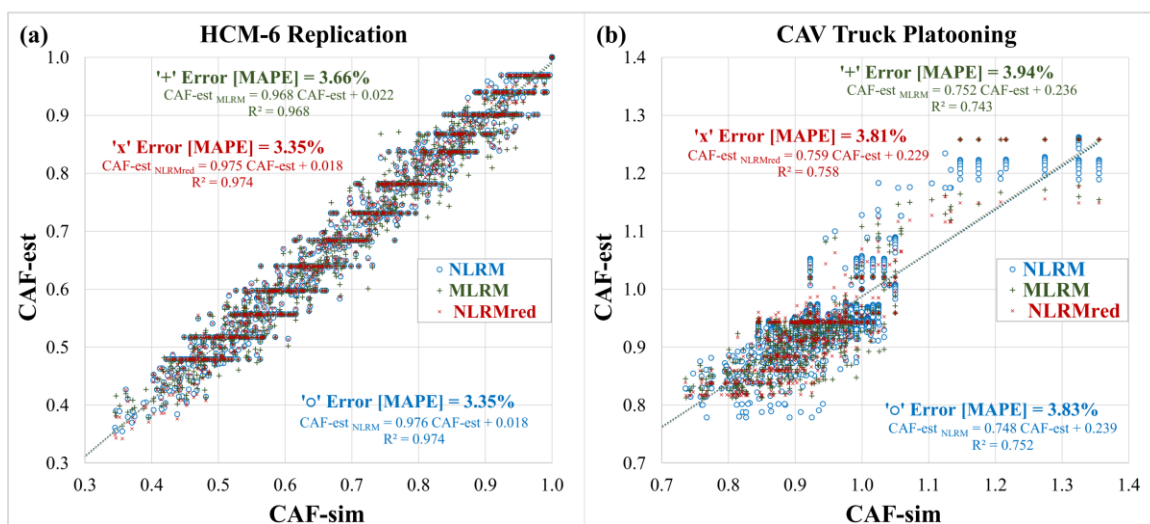


Figure 4-2. Comparison of goodness-of-fit between regression models.

4.6 CAF Model Results

4.6.1 HCM-6 Replication

The estimated CAF values for the HCM-6 replication are shown in **Figure 4-3**. These estimated CAF values were calculated using each of the three regression models explored in this chapter. The orange line represents the HCM-6 original values, the blue line the original NLRM, the red line the proposed $NLRM_{red}$, and the green line the proposed MLRM. Note the gray line in the background represents the VISSIM 9 simulated CAF

values used for fitting the regression models. For a given truck percentage, the CAFs for grade and grade distance are shown in order. The general form is a flat straight line for the negative and zero grade scenarios, followed by decreasing CAF values for the positive grade values. It may be seen the estimated CAF values decrease as truck percentage increases and this decrease is at a fairly linear rate. The estimated CAF values range from 1, which corresponds to the assumed value for the car-only flow condition (e.g., 0% truck percentage), to 0.34 for the 100% truck percentage. The mean absolute error between the estimated CAFs from the original HCM-6 results (orange line) and the estimated CAFs from the original NLRM (blue line) is only 0.006 with a maximum error of 0.018. Therefore, it was concluded the simpler models performed as well as the original, and more complex, HCM-6 model.

Figure 4-3 is a visual example of why the developers of the EC-PCE methodology adopted the modeling approach shown in **Figure 1-2**. Specifically, the CAF values calculated using the simulated capacity values have considerable variation as compared to the CAF values estimated using the models. This is particularly evident for the negative grade scenarios where the estimated CAF values are effectively horizontal. If the simulated CAF values were used to estimate the EC-PCE values, then this variability would be propagated to the EC-PCE results. For example, if the simulated CAF values were used directly, the EC-PCE values for 10%, 15%, and 20% truck percentage, 3 percent grade, and 1 mile grade length, would be 3.03, 2.13, and 2.59, respectively. When the estimated CAF values are used, the EC-PCE values are 2.95, 2.62, and 2.46. It may be seen the variability of the simulation results would cause counter intuitive EC-PCE results.

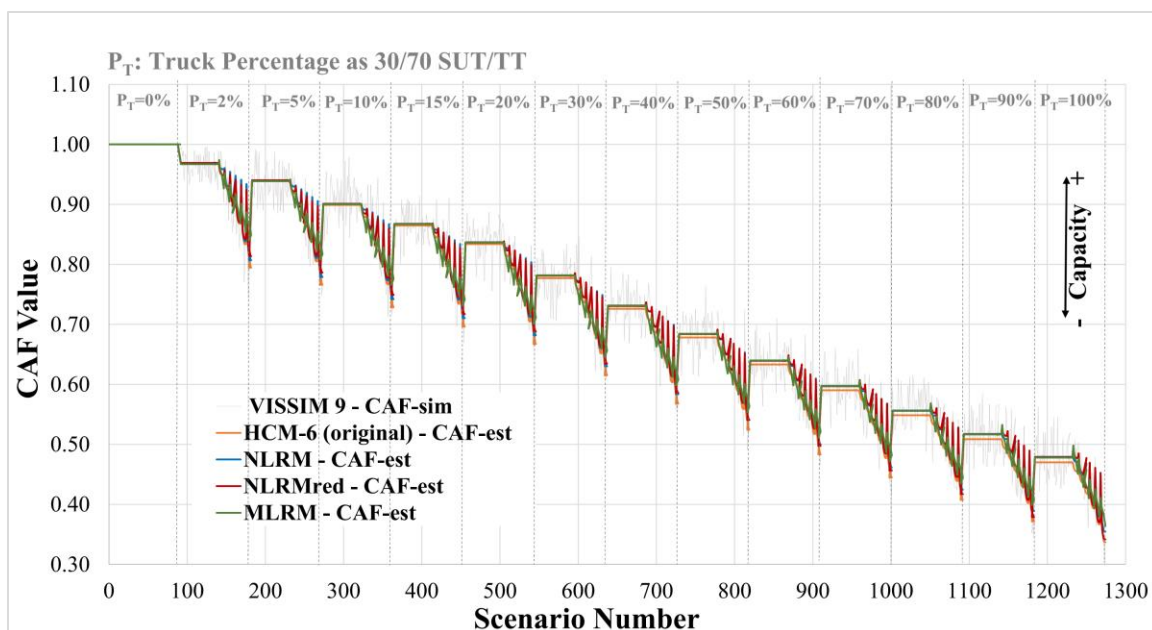


Figure 4-3. CAF values as a function of scenario number for the HCM-6 Replication

In general, the three regression models all estimated similar CAF values. The mean absolute error between the CAF values of the original NLRM (blue line) and the proposed NLRM_{red} (red line) is only 0.0016 (maximum error of 0.0153) which is outside the range of significant digits. A two-sided paired t-test on estimated CAFs revealed the difference between both models was not statistically significant at $\alpha=5\%$. In contrast, while the fitting is acceptable for most of the truck percentage and grade values, the proposed MLRM (green line) shows a consistent poor fitting for combinations that have high grade length values (e.g., greater than 0.75 miles). The mean absolute error between the CAF values of the original NLRM (blue line) and the proposed MLRM is 0.007 (maximum difference of 0.055). In this case, the two-sided paired t-test indicated the difference was statistically significant at $\alpha=5\%$.

4.6.2 CAV Truck Platooning

The estimated CAF values for the CAV truck platooning analysis are shown in **Figure 4-4**. The blue line represents the original NLRM, the red line the proposed NLRM_{red}, and the green line the proposed MLRM. Note the gray line in the background represents the simulated CAF values from VISSIM 20 used for fitting the regression models. For this analysis, the estimated CAF values range from approximately 0.80 to 1.25. Note the trend of the CAF values differs considerably from those based on conventional traffic.

Interestingly, in almost half of the 1,274 scenario combinations, the original NLRM (blue line) produces unrealistic CAFs for the scenarios at negative grade values as evidenced by the atypical peaks. Note the multiple linear regression analysis revealed the grade and distance predictors were not statistically significant at $\alpha = 0.05$ level for the simulated CAF values for negative and level grade conditions. Similar to the HCM-6 replication, the proposed MLRM (green line) shows a poor fitting for the scenario combinations at high distance values (e.g., greater than 0.75 miles). From the three regression models explored in this chapter, the proposed NLRM_{red} model was better at estimating the CAF values. It was concluded the simpler NLRM_{red} model can be used in place of the original HCM CAF model for modeling the new CAV scenarios. The model fitting process described in this chapter should be done when examining new traffic scenarios. In addition, it is clear the original HCM-6 model structure was not appropriate for the CAV scenarios. There is no guarantee the model form best for this CAV analyses will be best for other novel scenarios.

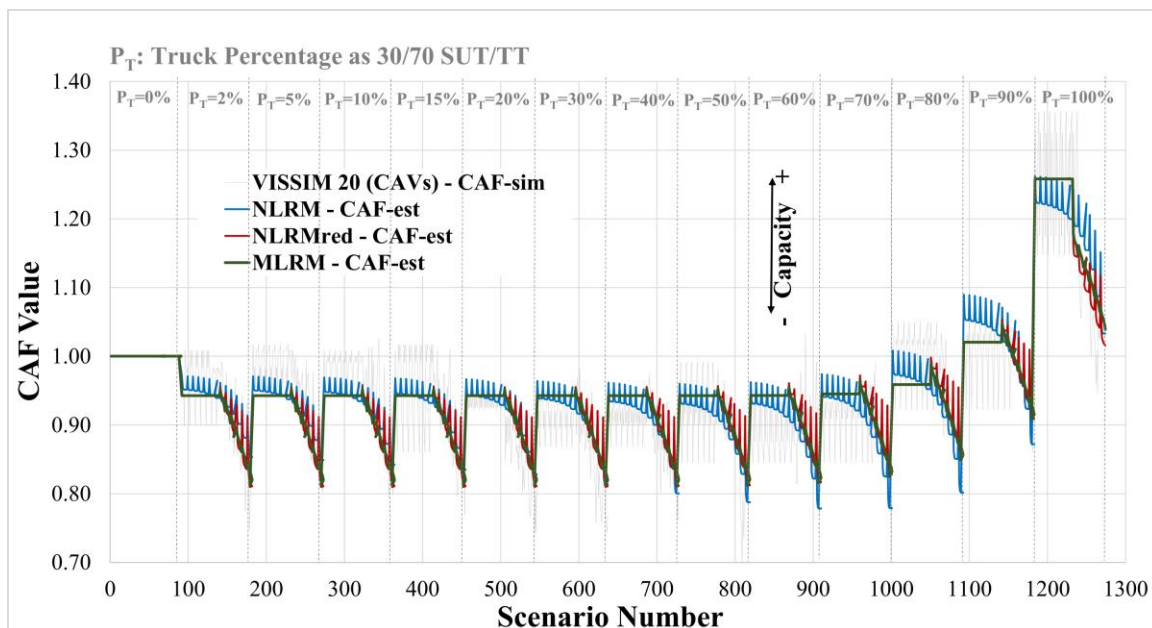


Figure 4-4. CAF values as a function of scenario number for the CAV condition

4.7 EC-PCE Results

The EC-PCE values at specific conditions were estimated for ten levels of truck percentage (i.e., 10% to 100% in 10% increments), grade (i.e., 0%, +3%, and +6%), and distance (i.e. 0.5, 1.0, and 1.5 mi). **Figure 4-5** and **Figure 4-6** show the corresponding EC-PCE values as a function of truck percentage for the three levels of grade and three levels of distance for the HCM-6 replication and the CAV truck platooning condition, respectively. The graph on the left side provides a comparison between the EC-PCE values from the original NLRM (dotted line) and the proposed MLRM (solid line). The graph on the right side compares the EC-PCE values from the original NLRM (dotted line) and the proposed NLRM_{red} (solid line). The EC-PCE values were calculated using **Equation (3-12)**.

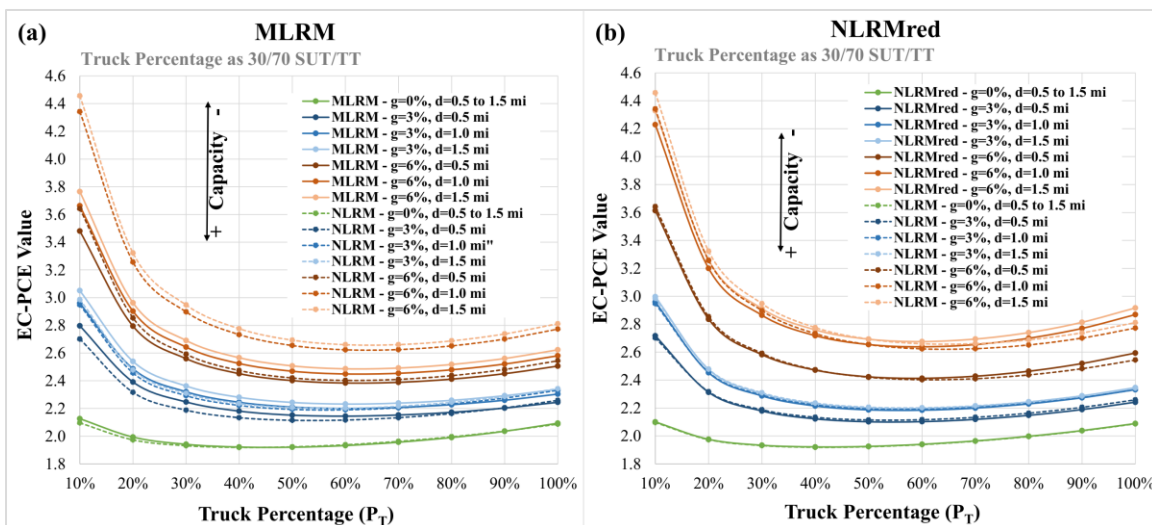


Figure 4-5. EC-PCE values for the HCM-6 replication

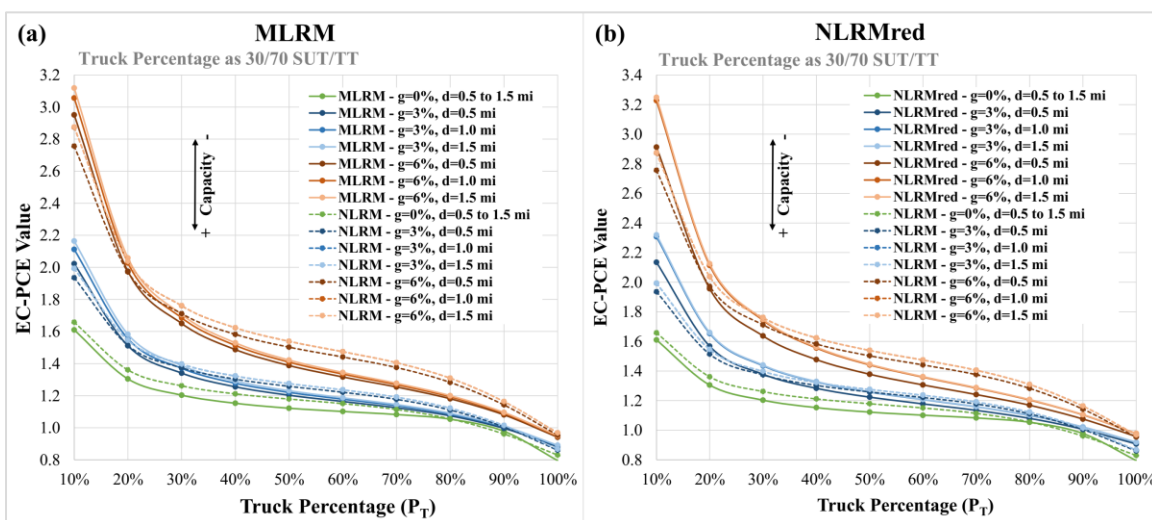


Figure 4-6. EC-PCE values for the CAV condition

In general, as grade and distance increase so does the EC-PCE. For the HCM-6 replication, the EC-PCE values tended to decrease as truck percentages increase until the 30 percent value is reached. After this point, the EC-PCE values tend to increase at a decreasing rate with truck percentage. In contrast, for the CAV truck platooning condition the EC-PCE decreases at a smaller rate as percentage of trucks increases.

For the HCM-6 replication, the EC-PCE values between the proposed MLRM and the original NLRM describe the same general form as shown in **Figure 4-5a**. However, the proposed MLRM may underestimate the distance effect by the producing lower EC-PCE values as evidenced by the conditions at +6% grade and distances of 1.0 and 1.5 miles. The same issue was observed for the CAV truck platooning analysis. The mean absolute error of the EC-PCE values between the original NLRM and the proposed MLRM is 0.094 (maximum value of 0.692). In contrast, **Figure 4-5b** shows the EC-PCE values between the original NLRM and the proposed $NLRM_{red}$ are approximately the same at any truck percentage, grade, and distance combination. The mean absolute error between the EC-PCE values from the original NLRM and the proposed $NLRM_{red}$ is 0.021 (maximum value of 0.105).

For the CAV truck platooning condition, the difference between the EC-PCE values produced by each regression model is more evident as shown in **Figure 4-6a** and **Figure 4-6b**. The mean absolute error between the original NLRM and the proposed MLRM is 0.065 (maximum error of 0.243). Similarly, the mean absolute error between the original NLRM and the proposed $NLRM_{red}$ is 0.073 (maximum error of 0.374). Note the $NLRM_{red}$ was the regression model that had the best goodness-of-fit for the CAV truck platooning condition.

4.8 Concluding Remarks

The objective of this chapter was to analyze the use of simpler regression models to fit simulated and estimated CAFs in the HCM-6 EC-PCE methodology for freeway and multilane highway segments. It was hypothesized simpler regression models could provide comparable results to the existing HCM-6 models and these models could be

used by HCM-6 users to estimate capacity, CAF, and PCE values directly. Moreover, the performance of the current nonlinear regression model when applied to new traffic situations such as CAV trucks has not been evaluated in previous studies.

One of the most significant findings to emerge from this chapter is that simpler regression models offer comparable results to those obtained with the original nonlinear regression model used in the HCM-6 EC-PCE methodology. For example, it was found that the difference of the results between the proposed $NLRM_{red}$ (8 model parameters) and the original NLRM (15 model parameters) was not statistically significant for the HCM-6 replication analysis. It was found that the $NLRM_{red}$ model is as accurate as the original HCM-6 model and can be used for exploring new traffic scenarios (e.g., CAVs, two-lanes, etc.) in the future with no loss in fidelity. In addition, the simpler model structure would facilitate the computations and the process of reporting results in HCM-6 applications. Chapter 5 of this dissertation will develop simpler equations to calculate CAF and EC-PCE values for the HCM-6 based on the regression model structures analyzed in this chapter.

Another major finding is the existing nonlinear regression model (NLRM) may not be adequate for analyzing CAV traffic conditions. It was found that the original NLRM overestimates the effect of the distance parameter at negative grade levels producing atypical CAF values in approximately half of the simulated scenario combinations. In this regard, the segmented model structure of the proposed $NLRM_{red}$ was found to outperform the original NLRM when modeling CAV traffic. However, both models showed a poor fitting with respect to the truck percentage effect as evidenced by the moderate R-squared value of 0.75. It is hypothesized the polynomial format for the

term related to the truck percentage effect developed in Chapter 3 would improve the fitting for the CAV condition. If the HCM-6 EC-PCE methodology is expected to be used to analyze traffic conditions beyond the scope of the HCM-6 (e.g., CAV traffic, two-lanes, etc.), it is important to perform a deeper assessment of the form and error of the regression models used for fitting the simulated and estimated data. It is possible different model structures might provide better results. In this regard, Chapter 7 of this dissertation will propose a simplified regression model structure that can be suitable for exploring CAV conditions.

CHAPTER 5

PROPOSED EQUATIONS FOR HCM-6 PASSENGER CAR EQUIVALENT VALUES

5.1 Introduction

The EC-PCEs for freeway segments were estimated using a microsimulation-based methodology where a nonlinear regression model (NLRM) with 15 model parameters was used to develop capacity adjustment factor (CAF) models using the microsimulation data as input (List, Roupail, & Yang, 2014; Zhou, Rilett, & Jones, 2019). It is hypothesized that because of the complexity of the existing 15 parameter model structure, the HCM-6 EC-PCE values were reported using a set of tables (e.g., *Exhibits 12-26, 12-27, and 12-28*, HCM, 2016). These tables are used to identify the required EC-PCE values for a given scenario (e.g., grade, grade distance, truck composition, and truck percentage). It is argued in this chapter a simpler regression model would allow HCM-6 users to calculate the CAF and EC-PCE directly and would eliminate the need for the HCM-6 tables.

The main objective of this chapter is to propose simpler equations to calculate the CAFs and EC-PCEs for basic freeway and multilane highway segments in the HCM-6. There are three main contributions of this chapter. The first is that simpler equations can be used to estimate the CAF and PCE values directly. In other words, users would no longer need to use the HCM-6 tables, there would be no need to interpolate any results, and more accurate EC-PCE values would be obtained for those situations where interpolation is currently required. Secondly, the simpler structure of the proposed model

allows a better understanding of the relationship between capacity, CAFs, and EC-PCEs and the main factors considered in the HCM-6 (e.g., truck percentage, grade, distance, and truck composition type). In addition, it is expected the proposed CAF model in this chapter would make it easier for users to calibrate the HCM-6 EC-PCE models for their local conditions (Zhou, Rilett, & Jones, 2019).

5.2 Original Nonlinear Regression Model (NLRM) for Estimated CAFs

Because of the inherent variability of the CAF results output from the simulation, the HCM-6 developers chose not to use the simulated CAF values for a given combination of parameters directly. Instead, they calibrated a nonlinear regression model that related the simulated CAF value to the truck percentage, grade, distance, and free-flow speed parameters. The goal was to mitigate the variability of the CAF results. This process is shown as Step 3 in **Figure 1-2**.

The original nonlinear regression model has a complex structure comprised of 15 model parameters. The form for the HCM-6 analytical model was based on vehicle kinematic and resistance equations related to trucks ascending and descending roadway sections of various grades and grade distance combinations (Dowling et al., 2014b). A heuristic optimization approach was used to calibrate the model where the goal was to identify the NLRM estimators that minimized the error between the simulated CAFs and the estimated CAFs. The final model consisted of a truck percentage effect parameter, a combined grade and distance effect parameter, and a free-flow speed effect parameter (List, Roupail, & Yang, 2014; Zhou, Rilett, & Jones, 2019) as shown in **Equations (3-7)** through **(3-11)**. It is clear from a quick examination of the original NLRM model it is very difficult to understand the relationship between CAF and truck percentage, traffic

stream composition, grade, and grade length. This was one of the motivating factors behind developing a simpler model structure.

5.3 Proposed Nonlinear Regression Model (NLRM_{red}) for Estimated CAFs

This chapter introduces a new reduced nonlinear regression model (NLRM_{red}) for estimating HCM-6 CAF values. The simplified model is shown in **Equation (5-1)**. The proposed model has six parameters and a dummy variable (D) related to whether the section being analyzed has a grade that is positive or non-positive. It may be seen when the grade is positive the explanatory variables are truck percentage (p), grade (g), and distance (d). Conversely, when the grade is negative or level, truck percentage (p) is the only explanatory variable. In addition, for all scenarios the effect of truck percentage is independent of the combined effect of grade and distance. These relationships will be examined in greater detail in a later section. The free-flow speed (FFS) and the truck composition type (m) effects are set constant for all situations, similar to the original HCM-6 nonlinear regression model (NLRM). The model format was motivated by a multivariate linear regression model. However, the proposed model assumed a combined effect of grade and distance and the model format for the distance effect was taken from the original HCM-6 model. Previous analysis revealed this model format performs better for modeling the distance effect as compared to a conventional multivariate linear model (Hurtado-Beltran & Rilett, 2021).

(5-1)

$$CAF_{2,p,m,g,d,FFS} = CAF_{1,0,0,g,d} + \alpha_{2,m,FFS}^{T_a} (p_s)_p^{\beta_{2,m,FFS}^{T_a}} + \alpha_{2,m,FFS}^{G_a} (g_s)_g^{\beta_{2,m}^{G_a}} * \left[1 - \alpha_{2,m,FFS}^{D_a} * e^{\beta_{2,m,FFS}^{D_a} * (d_s)_d} \right] * D$$

Where:

$CAF_{2,p,m,g,d}$: Capacity adjustment factor for the mixed flow ($f = 2$) at p truck percentage level, m truck composition level, g grade level, d distance level, and FFS free-flow speed.

$CAF_{1,0,0,g,d}$: Capacity adjustment factor for the auto-only flow at g grade level, d distance level. This value is assumed to be 1.

$(p_s)_p$: Truck percentage at p truck percentage level (between 0 and 1).

$(g_s)_g$: Grade at g grade level (between -0.06 and 0.06).

$(d_s)_d$: Distance of grade at d distance level (mile).

D : Dummy variable, if $(g_s)_g > 0$ then $D = 1$, otherwise $D = 0$.

$\alpha_{2,m,FFS}^{T_a}$, $\beta_{2,m,FFS}^{T_a}$, $\alpha_{2,m,FFS}^{G_a}$, $\beta_{2,m,FFS}^{G_a}$, $\alpha_{2,m,FFS}^{D_a}$, $\beta_{2,m,FFS}^{D_a}$: Parameters for capacity adjustment factor for truck percentage effect (T_a), grade effect (G_a), and distance effect (D_a).

5.4 Proposed Equations for Calculating HCM-6 EC-PCE Values

The proposed NLRM_{red} model was calibrated using the estimated CAF results obtained in the original HCM-6 EC-PCE research. The calibrated parameters were estimated using the Generalized Reduced Gradient (GRG) method (Lasdon, Fox, & Ratner, 1974) where the target goal was to minimize the sum of squared errors between the estimated CAF values given by the calibrated HCM-6 NLRM model and those estimated using the proposed model shown in **Equation (5-1)**. Specifically, CAF models for the 30/70 SUT/TT, 50/50 SUT/TT, and 70/30 SUT/TT truck composition levels were calibrated, and the results are shown in **Equations (5-2)**, **(5-3)**, and **(5-4)**, respectively. These equations can be used in combination with **Equation (5-5)** to estimate the EC-PCE value

for a given scenario. A paired t-test was conducted on 405 CAF values corresponding to the parameter variables shown in the HCM-6. It was found the differences between the original HCM-6 model CAF values and the proposed model CAF values were not statistically significant at the $\alpha = 5\%$ level. This was true for all three truck composition types.

- CAFs for a truck composition level $m = 30SUT/70TT$;

$$R_{adj}^2 = 0.999; \sqrt{MSE} = 0.0018:$$

$$CAF_{mix} = 1 - 0.530 * (p_s)^{0.72} - 6.881 * (g_s)^{1.30} * [1 - 1.381 * e^{-2.56*(d_s)}] * D \quad (5-2)$$

- CAFs for a truck composition level $m = 50SUT/50TT$;

$$R_{adj}^2 = 1.000; \sqrt{MSE} = 0.0011:$$

$$CAF_{mix} = 1 - 0.499 * (p_s)^{0.70} - 7.271 * (g_s)^{1.36} * [1 - 1.459 * e^{-3.01*(d_s)}] * D \quad (5-3)$$

- CAFs for a truck composition level $m = 70SUT/30TT$;

$$R_{adj}^2 = 1.000; \sqrt{MSE} = 0.0009:$$

$$CAF_{mix} = 1 - 0.472 * (p_s)^{0.73} - 6.180 * (g_s)^{1.30} * [1 - 1.239 * e^{-2.81*(d_s)}] * D \quad (5-4)$$

$$PCE = \frac{1 - (1 - p_s) * CAF_{mix}}{p_s * CAF_{mix}} \quad (5-5)$$

Where:

PCE : Passenger car equivalent for the mixed flow.

CAF_{mix} : Capacity adjustment factor for the mixed flow.

p_s : Truck percentage (between 0 and 1).

g_s : Grade (between -0.06 and 0.06).

d_s : Distance of grade (between 0 and 1.5 miles).

D : Dummy variable, if $g_s > 0$ then $D = 1$, otherwise $D = 0$.

An EC-PCE can be calculated for any combination of truck percentage, grade, and distance using the calibrated regression models. For example, consider the scenario defined by an 8% truck percentage ($p_s=0.08$), a +4.5% grade ($g_s=0.045$), a distance of 0.875 mi ($d_s=0.875$), and a truck composition of 30/70 SUT/TT. Using **Equation (5-2)** the Capacity Adjustment Factor for this situation ($CAF_{2,p,m,g,d,FFS}$) is 0.810. Using this value as input in **Equation (5-5)**, the EC-PCE is estimated to be 3.92. Note that the HCM-6 provides a value of 3.92 for the same scenario (*Exhibit 12-26*) (HCM, 2016).

The above EC-PCE estimation process was conducted for all entries in the corresponding HCM-6 PCE tables. The PCE values published in *Exhibits 12-26, 12-27, and 12-28* were plotted against the estimated values using **Equations (5-2), (5-3) and (5-4)** (HCM, 2016). These scatter plots are shown **Figure 5-1, Figure 5-2, and Figure 5-3**, respectively. It may be seen there is almost an exact one-to-one relationship between the original model and the simplified model. The Mean Absolute Percentage Error (MAPE) values were 0.64%, 0.46%, 0.42% for *Exhibits 12-26, 12-27, and 12-28*, respectively. The authors consider these errors to be negligible for practical purposes. Based on this analysis it was concluded the calibrated models developed in this chapter (e.g., **Equations (5-2) to (5-5)**) can be used to replace the corresponding HCM-6 PCE tables with only a negligible loss in fidelity.

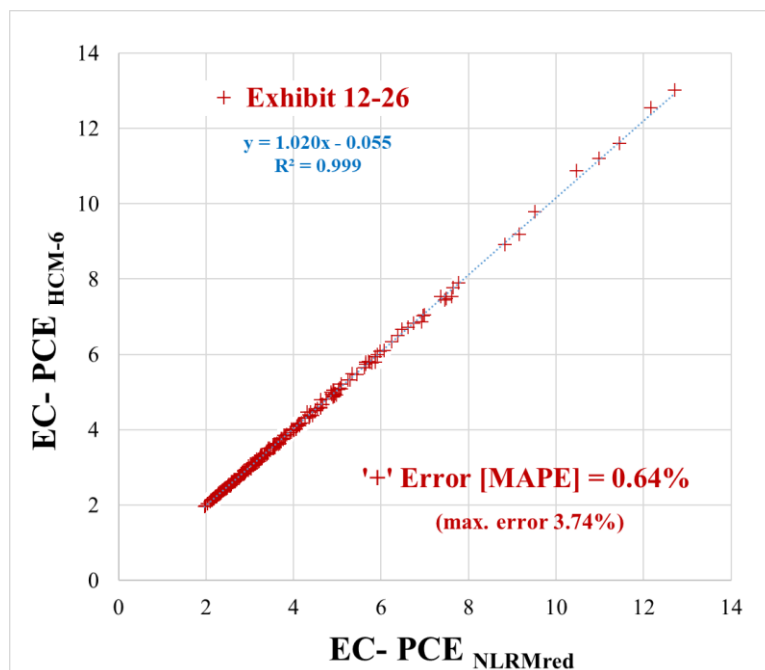


Figure 5-1. Goodness-of-fit of proposed equation for 30/70 SUT/TT truck composition.

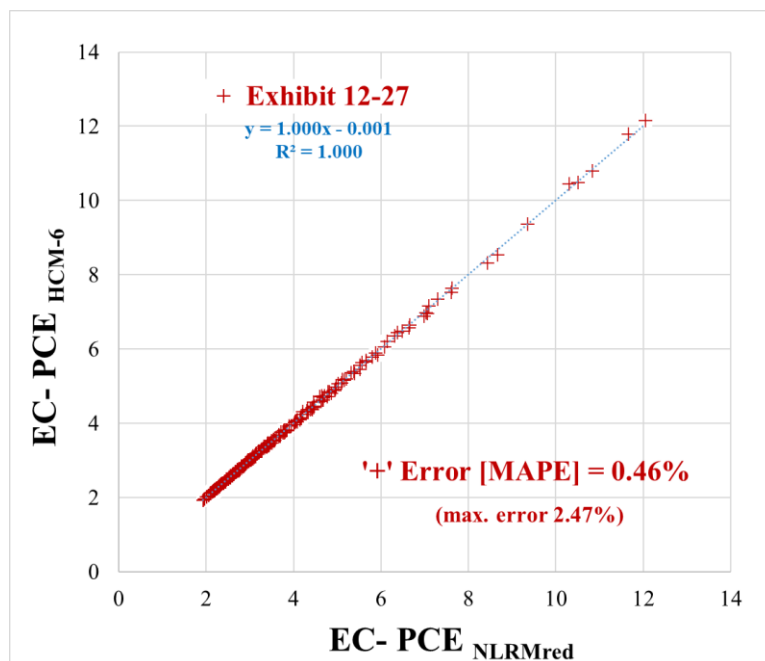


Figure 5-2. Goodness-of-fit of proposed equation for 50/50 SUT/TT truck composition.

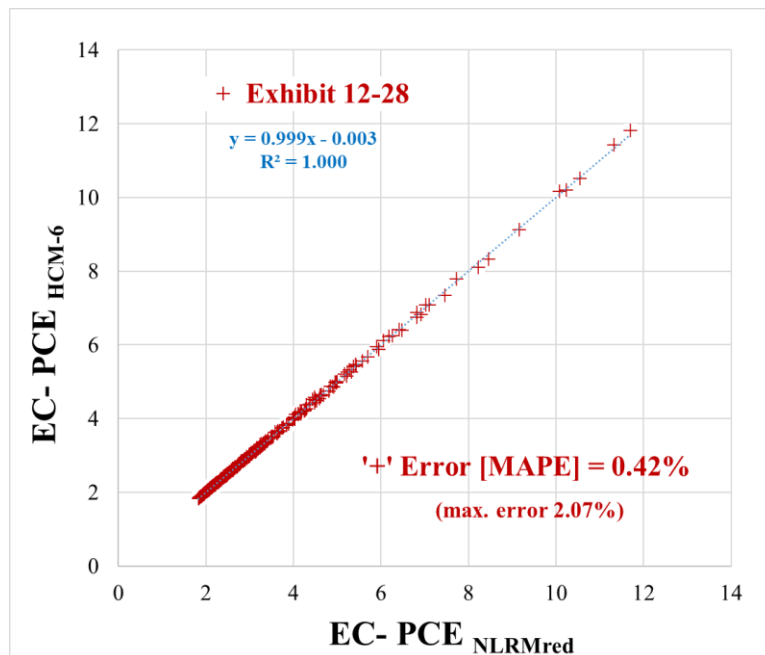


Figure 5-3. Goodness-of-fit of proposed equation for 70/30 SUT/TT truck composition.

The HCM-6 recommends a user should use interpolation when the HCM-6 PCE tables does not have the specific values for their analysis (HCM, 2016). Therefore, a comparison between the PCE values obtained from interpolation and those from the calibrated CAF model developed in this chapter was performed. In particular, the PCE values were calculated for 96 combinations of truck percentage, grade, and distance not listed in the HCM-6 PCE tables, as shown in **Table 5-1**. The combinations were selected to fall approximately midpoint between the HCM-6 table levels. Note that the interpolated values were obtained using a trilinear interpolation (Bourke, 1999). Intuitively, interpolation takes much more time when done manually, as compared to using the proposed equations directly. It was found the interpolation approach had an average error of 2.5% when the interpolated value was compared to the result of the 15

parameter HCM-6 model. The maximum error was 8.4%. In contrast, when the calibrated six parameter CAF model (i.e., **Equation (5-2)**) was compared to the 15 parameter HCM-6 CAF model the average error was 1.7%. This was an approximately 46.2% improvement. In summary, using the proposed 6-parameter model had more accurate results as compared to using interpolated values from the HCM-6 tables. The former was also much easier to calculate.

Table 5-1. PCE Values from Trilinear Interpolation and HCM-6 CAF Model.

Grade	Length		Percentage of Trucks (%)								
			3%			9%			12%		
%	km	(mi)	Intrpl	HCM-6	PropEq	Intrpl	HCM-6	PropEq	Intrpl	HCM-6	PropEq
1%	0.40	0.250	2.72	2.64	2.64	2.22	2.21	2.21	2.15	2.13	2.13
	0.80	0.500	3.07	2.97	2.86	2.34	2.33	2.29	2.24	2.22	2.19
	1.21	0.750	3.27	3.11	2.97	2.40	2.38	2.33	2.29	2.27	2.23
	1.61	1.000	3.36	3.18	3.03	2.43	2.41	2.35	2.32	2.29	2.25
	2.21	1.375	3.41	3.22	3.08	2.45	2.42	2.37	2.33	2.30	2.26
3%	0.40	0.250	3.22	3.06	3.19	2.39	2.36	2.41	2.28	2.25	2.29
	0.80	0.500	4.38	4.21	4.15	2.77	2.78	2.77	2.59	2.58	2.58
	1.21	0.750	5.04	4.76	4.68	2.99	2.99	2.97	2.77	2.74	2.73
	1.61	1.000	5.34	5.02	4.97	3.09	3.08	3.08	2.84	2.81	2.82
	2.21	1.375	5.53	5.16	5.17	3.16	3.14	3.15	2.90	2.86	2.88
4%	0.40	0.250	3.54	3.31	3.53	2.49	2.45	2.54	2.36	2.32	2.39
	0.80	0.500	5.24	5.01	4.97	3.06	3.08	3.08	2.82	2.81	2.82
	1.21	0.750	6.23	5.84	5.78	3.39	3.38	3.38	3.08	3.05	3.06
5%	0.40	0.250	3.91	3.61	3.90	2.62	2.56	2.68	2.47	2.41	2.50
	0.80	0.500	6.26	5.96	5.90	3.40	3.43	3.43	3.09	3.09	3.09
	1.21	0.750	7.66	7.14	7.05	3.87	3.87	3.86	3.47	3.43	3.44

Note: * = 30/70 SUT/TT truck composition type; Intrpl = PCE values from trilinear interpolation (*Exhibit 12-16*, HCM-6); HCM-6 = PCE values from calibrated NLRM from original HCM-6 EC-PCE research (*List, Roupail, & Yang, 2014*); PropEq = PCE values from calibrated proposed CAF model (**Equation (6-2)**).

It is also important to note some combinations cannot be interpolated because their bounds lie outside the PCE tables. This occurs even though the bounds may have been included in the original research. Specifically, the original HCM-6 VISSIM analyses were based on truck percentages that ranged from 0% to 100%, grades that ranged from -6% to 6%, grade distances that ranged from 0.25 miles to 5 miles, and the three truck composition levels discussed earlier. For example, a user cannot analyze a 4.0% grade and a 1.25 grade length using the HCM-6 tables even though this scenario was included in the original research. A major advantage of using the process developed in this chapter is that EC-PCE values can be calculated for any combination of factors including those not listed in the HCM-6 tables (e.g., truck percentage of 5.3%, +2.7% grade, and 0.9 miles distance). This would eliminate the need of interpolating the value from the appropriate HCM-6 tables since the EC-PCE values could be estimated directly. Moreover, as the HCM-6 EC-PCE methodology can be used to explore traffic conditions beyond the scope of the existing results, the proposed approach could be used to develop succinct and accurate equations for these novel conditions (Zhou, Rilett, & Jones, 2019; Hurtado-Beltran & Rilett, 2021).

Additionally, the calibrated CAF models shown in **Equations (5-2)** through **(5-4)** can also be used to estimate the mixed-flow capacity for the mixed flow model included in *Chapter 26* of the HCM-6 (e.g., *Equation 26-5*) (HCM, 2016). The HCM-6 recommends the mixed flow model be used when analyzing scenarios with high truck percentages and extended steep upgrade conditions. Specifically, the calibrated CAF models shown in **Equations (5-2)**, **(5-3)**, and **(5-4)** can be substituted for HCM-6 *Equations 26-1* through *26-4* when analyzing truck compositions of 30/70, 50/50 and

70/30, respectively. To illustrate, consider a scenario with a 30/70 SUT/TT truck composition. A comparison of the mixed-flow capacity values using the existing HCM model and the proposed model (e.g., **Equation (5-2)**) found the average error was 0.73% across all 1,183 mixed-flow scenarios explored in the HCM-6 EC-PCE methodology.

Interestingly, the mixed-flow model shown in *Chapter 26* of the HCM-6 was based on the original CAF model calibrated for the 30/70 SUT/TT truck composition. In other words, the developers assumed the relationship for other truck composition levels (e.g., 50/50 and 70/30 SUT/TT) were the same as the 30/70 SUT/TT relationship. It is hypothesized by the authors that using this approach may result in inaccurate capacity values for the other truck composition types (e.g., 50/50 and 70/30 SUT/TT). When the above analysis was repeated for the 50/50 SUT/TT and 70/30 SUT/TT truck composition levels the average error was found to be 2.05% and 4.61%, respectively. It is hypothesized that using the three proposed CAF equations calibrated in this model would result in much more accurate results for the mixed flow methodology outlined in *Chapter 26* of the HCM-6. This would be particularly true when the truck composition values are considerably different than the 30/70 SUT/TT scenario.

5.5 Analyzing the Marginal Effects in the Proposed CAF model

One of the main benefits of the simpler model proposed in this chapter is transportation engineers will find it easier to understand the relationship between EC-PCE values and the main influencing factors (e.g., truck percentage, grade, and grade distance). It must be noted that a greater PCE value indicates a lower capacity for a given freeway segment, all else being equal. In turn, greater PCE values are related to lower CAF values and a lower percentage of trucks. It may be seen in the proposed equations there are two main

contributors to the CAF values: (1) a truck percentage effect, and (2) a combined grade and distance effect. These main contributors are independent of each other in the proposed model. Note this assumption may not be valid for traffic conditions outside of the scope of the original HMC-6 research. The marginal effect of truck percentage effect and the combined effect of grade and distance are discussed below.

5.5.1 Marginal Truck Percentage Effect

Because the truck percentage effect is independent from the other exploratory variables in the CAF model, it is possible to quantify how the capacity, CAFs, and PCEs change as truck percentage changes. **Figure 5-4**, **Figure 5-5**, and **Figure 5-6** shows the marginal effect of truck percentage on CAF values, EC-PCE values, and capacity values, respectively. The relationships for all 3 truck composition types (e.g., 30/70, 50/50 and 70/30 SU/TT) are also shown in the graphs.

Figure 5-4 shows the marginal change in CAF values as truck percentage increases. This change is irrespective of grade and distance and as truck percentage increases the CAF values decrease at a slower rate. For example, when the truck percentage increases from 0 to 10 percent there is an approximately 0.101 drop in CAF values. However, from 10 to 20 percent the drop is approximately 0.065 and from 20 to 30 percent it is approximately 0.056. As would be expected for a given truck composition type, the higher the percentage of tractor trailers, the greater the effect of truck percentage on the CAF values of the freeway segment. The change in CAF values range from 0 (e.g., only passenger cars) to -0.530 (e.g., 100% truck percentage) where the highest impact is for the 30/70 SUT/TT truck percentage. This implies the potential drop in CAF values for

a given freeway segment can be as high as 0.530 due solely to the presence of trucks in the traffic stream.

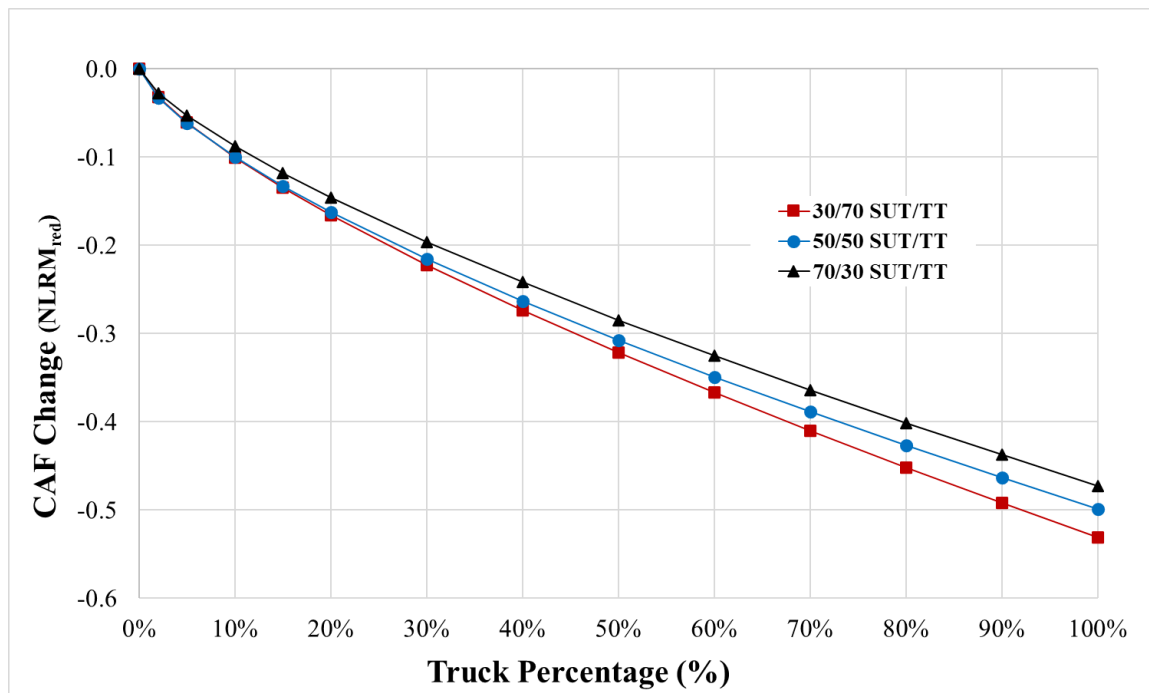


Figure 5-4. Marginal Effect of Truck Percentage on CAFs.

Figure 5-5 shows the marginal change in EC-PCE as the truck percentage increases. This change is irrespective of grade and distance and the relationship is parabola shaped. As truck percentage increases the EC-PCE value drops until it reaches a minimum (e.g., approximately at 40-50% truck percentage) and then increases again. This occurs because the EC-PCE values tend to have a minimum value when the product of truck percentage and CAF value is maximized, as shown in **Equation (5-5)**. As the CAF value decreases when the truck percentage increases, it is easy to envision there is an optimum combination that produces the lowest EC-PCE value for a mixed traffic stream. The EC-PCE values are highly sensitive to small variations of CAF values,

particularly when the truck percentage is 5% or lower. This explains why the highest EC-PCE values occur for these conditions.

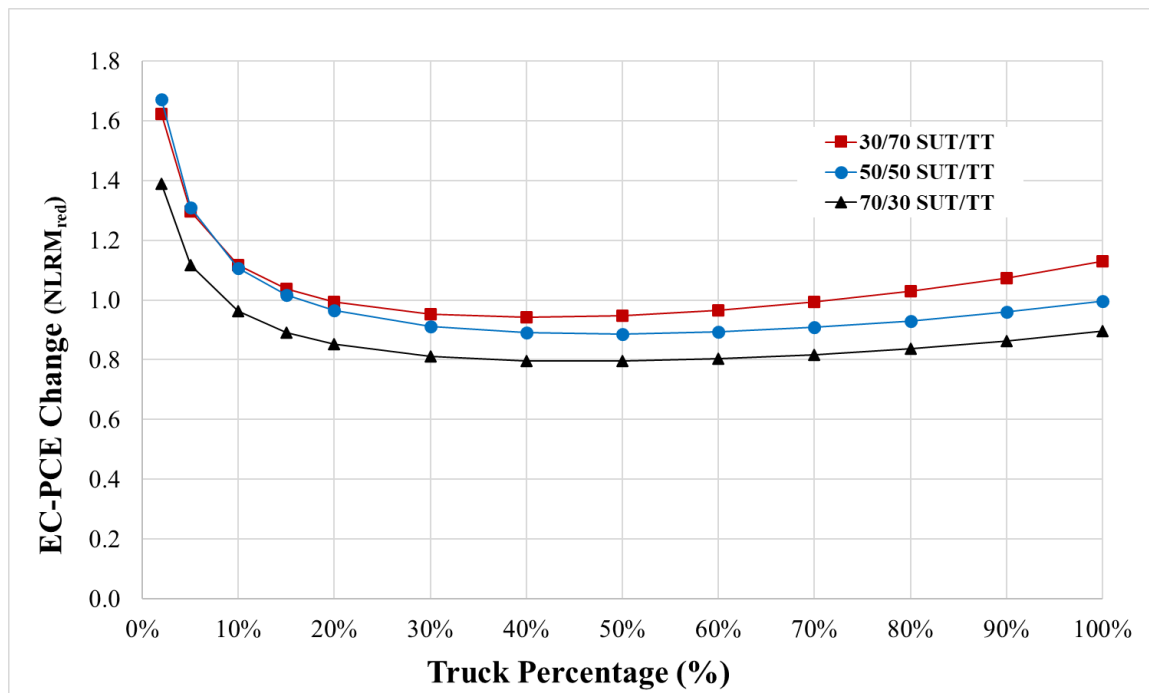


Figure 5-5. Marginal Effect of Truck Percentage on EC-PCEs.

Figure 5-6 shows the marginal change in freeway capacity as truck percentage increases. This change is irrespective of grade and distance. The marginal change in capacity was calculated using the CAF values from the calibrated proposed models. A base capacity of 2,400 pc/h/ln was assumed as indicated in the mixed flow model of the HMC-6. As truck percentage increases capacity decreases at a slower rate. For example, when the truck percentage increases from 0 to 10 percent there is an approximately 241 veh/h drop in capacity. However, from 10 to 20 percent the drop is approximately 157 veh/h, and from 20 to 30 percent it is approximately 136 veh/h. As would be expected for a given truck composition type, the higher the percentage of tractor trailers, the higher the

effect of trucks on the capacity of the freeway segment. The change in capacity ranges from 0 veh/h/ln (e.g., only passenger cars) to -1,273 veh/h/ln (e.g., 100% truck percentage) as a function of the truck percentage and the truck composition type. This implies the potential drop in capacity for a given freeway segment can be as high as 1,273 veh/h/ln due solely to the presence of trucks in the traffic stream.

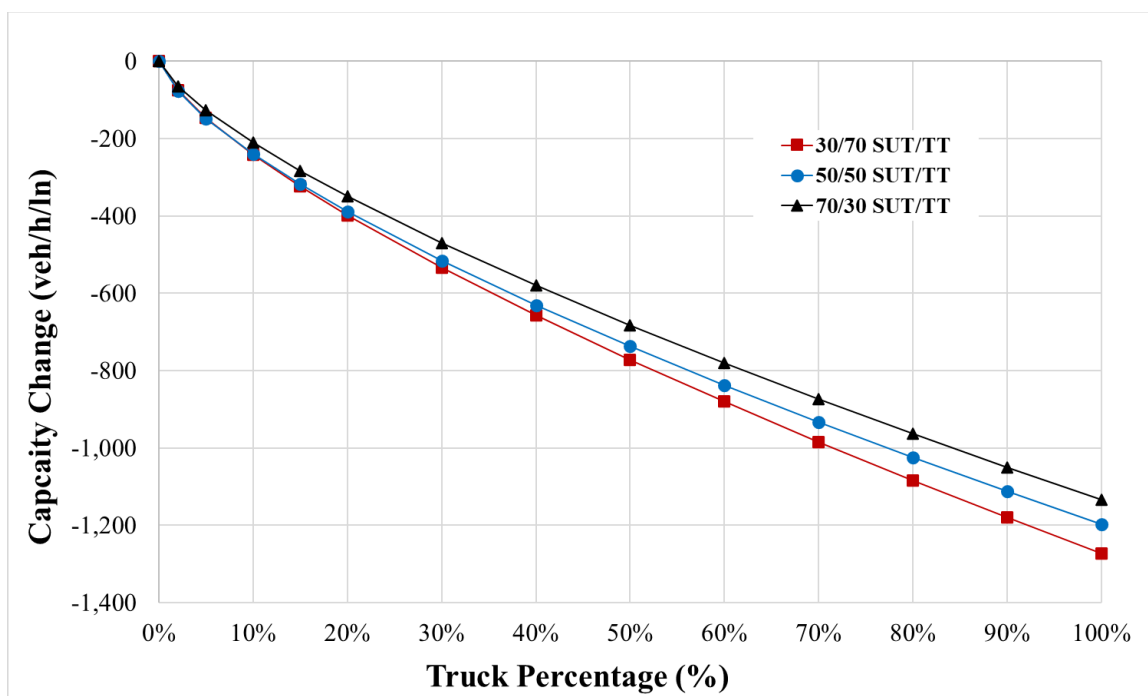


Figure 5-6. Marginal Effect of Truck Percentage on Freeway Capacity.

In general, **Figure 5-6** has the same form as **Figure 5-4**. This is because the CAF is a ratio of a mixed flow capacity to a passenger car-only flow capacity. Because, by definition, the passenger car-only flow capacity is not affected by the truck percentage, the values in **Figure 5-6** are essentially the values in **Figure 5-4** divided by a constant (e.g., base capacity value of 2,400 pc/h/ln). Therefore, the relationship between CAF

change and truck percentage is the same as the relationship between change in mixed flow capacity and truck percentage.

It may be seen in **Figure 5-4**, **Figure 5-5**, and **Figure 5-6** that there are only small differences between the three truck composition types considered in the HCM-6. It should be noted the 30/70 SUT/TT truck composition shows a slightly greater impact on the three traffic metrics analyzed. This is not surprising because this truck composition type was comprised of more tractor trailers (i.e., TT), the largest truck examined in the HCM-6 analysis. For all three truck composition scenarios, the maximum differences occur at 100% truck percentage value. The greatest differences were between the 30/70 SUT/TT and 70/30 SUT/TT scenarios and these differences were equal to 139 veh/h/ln, 0.058, and 0.23 for capacity, CAFs, and PCEs, respectively.

5.5.2 *Marginal Grade-Distance Effect*

Figure 5-7, **Figure 5-8**, and **Figure 5-9** show the marginal change of CAF values, EC-PCE values, and capacity values as a function of grade and distance. The grade-distance effect is independent of the truck percentage effect. The marginal change is only shown for the 30/70 SUT/TT truck composition scenario because of space limitation. This truck composition was chosen because it is the most common in the U.S. (*HCM, 2016*). Similar results were found for the remaining truck composition types (e.g., 50/50 SUT/TT and 70/30 SUT/TT).

Figure 5-7 shows the marginal change in CAF values as a function of grade and distance. The y-axis represents the change in CAF values while the x-axis represents the distance values (e.g., 0.25 to 5 miles). Each line corresponds to a different percentage of upgrade value (e.g., 0% to 6% in 1% increments). The marginal change in CAF was

calculated in the same manner as the truck percentage effect discussed in the previous section.

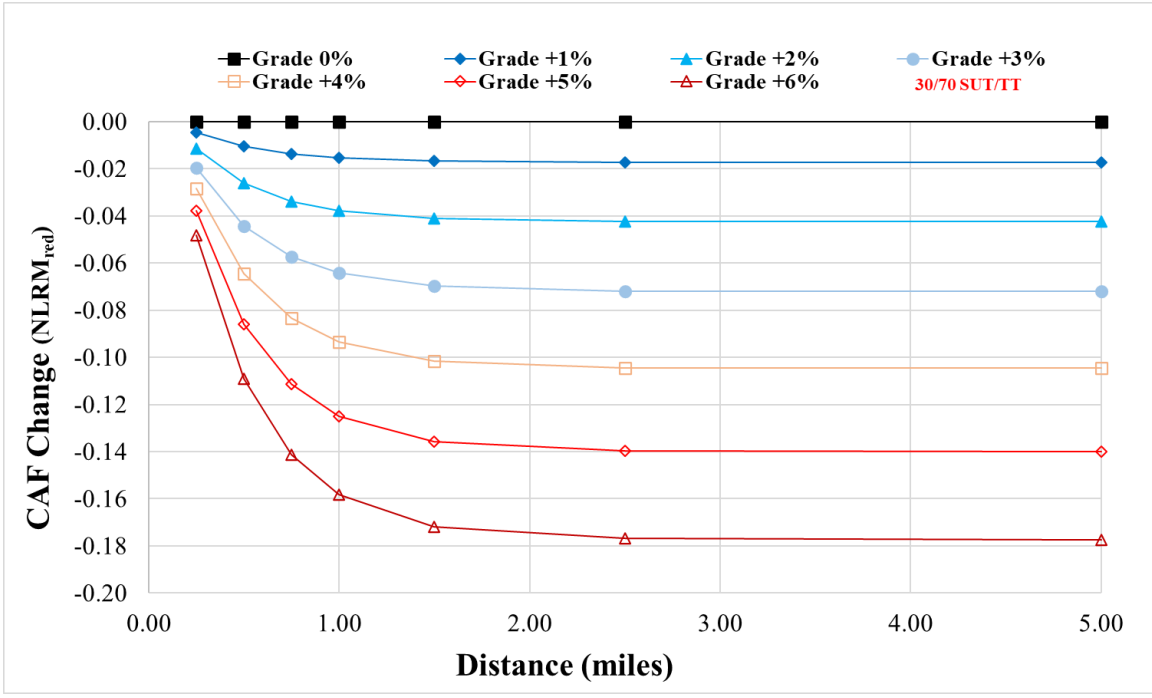


Figure 5-7. Marginal Effect of Combined Grade and Distance on CAFs.

CAF values tend to decrease as both grade and grade distance increases. The change in CAF ranges from 0 (e.g., 0% grade and any distance) to -0.177 (e.g., +6% grade and 5 miles distance). This implies the drop in CAF values for a given freeway segment can be as high as 0.177 due solely to the grade and distance conditions irrespective of the truck percentage.

However, the decrease in CAF produced by the combined effect of distance and grade occurs at a different rate when the variables are analyzed separately. For example, the effect on CAF increases with distance at a decreasing rate. The greatest effect occurs from 0 to 1.5 miles. After this point, increasing the distance value only produces a

minimal effect on CAF values. For example, approximately 97% of the potential CAF drop occurs by the 1.5 mile mark. This relationship is consistent for all the positive grade values explored for this analysis. On the other hand, in terms of grade effect, the decrease of CAF values occurs at a slightly increasing rate with the increase of the grade value. As would be expected, the maximum decrease corresponds to the +6% grade value, the steepest upgrade typically considered on freeways. In general, the potential change of the combined effect of truck and distance on the CAF values is lower than the potential truck percentage effect, all else being equal. However, the former may be more significant for lower values of truck percentage as can be observed by comparing **Figure 5-4** and **Figure 5-7**.

Figure 5-8 shows the EC-PCE values as a function of the grade and distance values for a scenario defined by a 10% truck percentage and a 30/70 SUT/TT truck composition type. The x-axis represents the EC-PCE value while the y-axis represents the distance value. Each line corresponds to a different grade value (e.g., 0% to 6% in 1% increments). In this case, the EC-PCE values range from 2.12 (e.g., 0% grade and any distance) to 4.85 (e.g., +6% grade and 5 miles distance) depending on the grade and distance combination. In general, the EC-PCE values tend to increase as both the grade and distance increase. However, this increase occurs at a decreasing rate with distance, while it occurs at a slightly increasing rate as grade increases. Similar to the CAF value analysis, the effect of distance on the EC-PCE values is minimal after 1.5 miles.

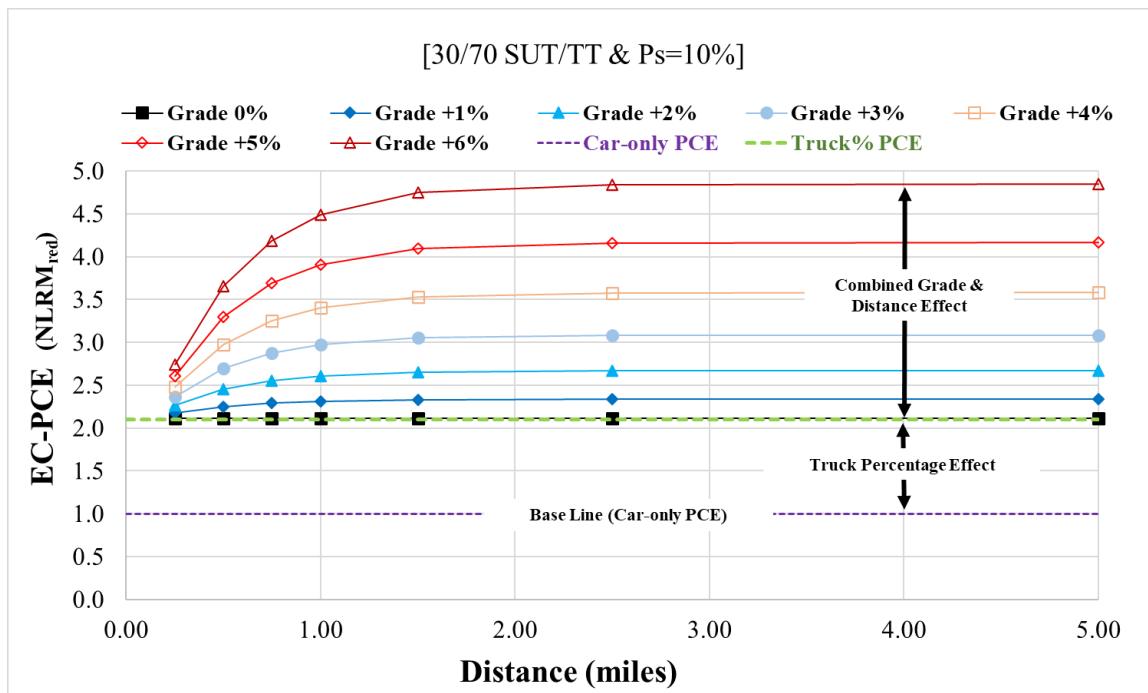


Figure 5-8. Marginal Effect of Combined Grade and Distance on EC-PCEs.

Figure 5-8 also illustrates how the EC-PCE values for trucks are comprised of three parts: (1) the EC-PCE value assumed for passenger-cars (assumed equal to one, see purple dotted line), (2) the marginal change produced by the truck percentage effect (green dotted line), and (3) the marginal change produced by the combined effect of grade and distance (solid lines). For example, consider the scenario defined by a 10% truck percentage, a +6% grade, a distance of 4.0 miles, and a truck composition of 30/70 SUT/TT. The EC-PCE value for this situation is 4.85 as shown in **Figure 5-8**. For this case, the marginal changes produced by the truck percentage effect and the combined effect of grade and distance are 1.12 and 2.37, respectively. This means that 67.9% of the EC-PCE value corresponds to the combined effect of grade and distance and the remaining 32.1% corresponds to the truck percentage effect. These percentages are a function of the truck percentage value as may be seen in **Equation (5-5)**. It would be

expected, for low truck percentage values (e.g., approximately less than 20%), the combined effect of grade and distance on the EC-PCE will be lower as compared to the truck percentage effect.

Figure 5-9 shows the marginal change in capacity of the combined effect of grade and distance. The y-axis represents the change in capacity values while the x-axis represents the distance values (e.g., 0.25 to 5 miles). Each line corresponds to a different percentage of upgrade value (e.g., 0% to 6% in 1% increments). The marginal change in capacity was calculated similar to that for the truck percentage effect. As both the grade and distance increase, capacity tends to decrease. The change in capacity ranges from 0 veh/h/ln (e.g., 0% grade and any distance) to -425 veh/h/ln (e.g., +6% grade and 5 miles distance) as a function of the grade and distance values. This implies the drop in capacity for a given freeway segment can be as high as 425 veh/h/ln due solely to the grade and distance conditions independent of the truck percentage.

However, the decrease in capacity produced by the combined effect of distance and grade occurs at different rates when the variables are analyzed separately. In general, **Figure 5-9** has the same form as **Figure 5-7** due to the same reasons discussed above for the marginal truck percentage effect. It may be seen the capacity values decrease as grade and distance increases. Although the potential change of the combined effect of truck and distance on capacity values is lower than the potential truck percentage effect, the former may be more significant for the lower values of truck percentage. This can be observed by comparing **Figure 5-6** and **Figure 5-9** for a given truck percentage value.

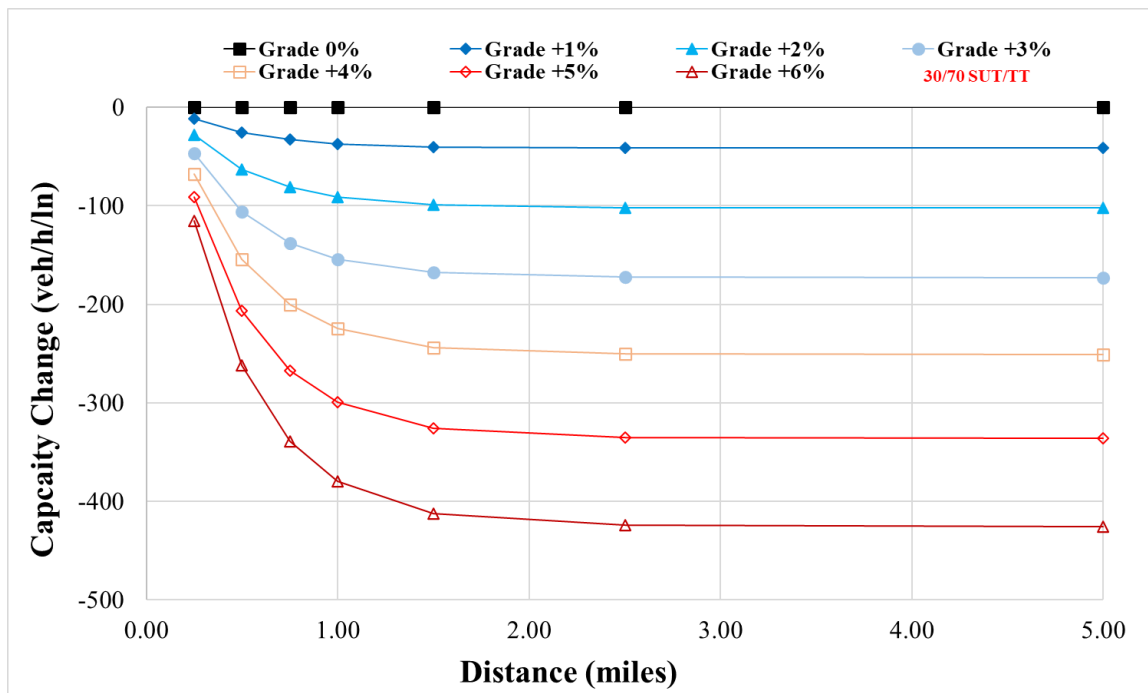


Figure 5-9. Marginal Effect of Combined Grade and Distance on Freeway Capacity.

5.5.3 Additive Property of Marginal Effects

Because the marginal effects discussed in this chapter are additive, the figures discussed above (e.g., **Figure 5-4** to **Figure 5-9**) can be combined, as appropriate, to estimate the capacity, CAF, and EC-PCE value for a given scenario combination. For example, consider the scenario defined by a 20% truck percentage, a +5% grade, a distance of 1 mile, and a 30/70 SUT/TT truck composition type. The analyst can estimate the drop in the mixed flow capacity by adding the marginal changes shown in **Figure 5-6** and **Figure 5-9**. In this case, the total drop in capacity is 700 veh/h/ln. This is 400 veh/h/ln from the truck percentage effect (**Figure 5-6**) plus 300 veh/h/ln from the combined grade and distance effect (**Figure 5-9**). The total drop in capacity of 700 veh/h/ln corresponds to a mixed flow capacity of 1,700 veh/h/ln, assuming a base capacity of 2,400 pc/h/ln for the freeway segment. A similar procedure can be used to estimate a specific CAF value. Of

course, the same result could be obtained by using **Equations (5-2), (5-3), and (5-4)** to calculate the CAF value and then using **Equation (5-5)** to estimate the corresponding EC-PCE value.

In summary, the proposed CAF model is comprised of two main contributors: (1) truck percentage effect, and (2) combined effect of grade and distance. The former has the greatest potential to impact on the operational performance of freeways, especially at moderate to high truck percentage values. However, the combined effect of grade and distance may be more critical than the truck percentage effect for steeper/longer grade values, especially when the truck percentage is lower than 20%. These findings can be useful for engineers and analysts to better understand the trade-off caused by key influencing factors such as the truck percentage, grade, distance, and truck composition type in the design and operation of freeways.

5.6 Concluding Remarks

The objective of this chapter was to propose simpler equations to calculate the EC-PCEs for basic freeway and multilane highway segments in the HCM-6. It was hypothesized simpler regression models could provide comparable results to the existing HCM-6 models and these models could be used by HCM-6 users to estimate CAF and PCE values directly.

One important finding to emerge from this chapter is that a proposed simpler regression model (NLRM_{red}) offers comparable results to those obtained with the original nonlinear regression model used in the HCM-6 EC-PCE methodology. For example, it was found the error between the PCE values derived from the proposed NLRM_{red} (6 model parameters) and the original NLRM (15 model parameters) is effectively

negligible for practical purposes. Additionally, the simpler model structure would facilitate the computations and the process of reporting results in HCM-6 applications. The current version of the HCM includes a set of large tables for obtaining EC-PCE values for capacity analyses. Often the user must interpolate values in the tables. These tables could be substituted with simpler equations developed in this chapter. These can be used by analysts or developers of the Highway Capacity Software.

Another major finding is the simpler structure of the proposed CAF model facilitates the interpretation of the EC-PCE values and their relationship with the main influencing factors defined in the HCM-6 EC-PCE methodology. This is in contrast to the original CAF model used in the HCM-6 research, which has a relatively complex model structure which makes interpretation difficult. The proposed CAF model was comprised of two main contributors assumed to be independent of each other: (1) truck percentage effect, and (2) combined effect of grade and distance. Note that this assumption may not be valid for traffic conditions not analyzed using the HCM-6 VISSIM model. The additive property of these contributors may facilitate the estimation of capacity, CAF, and EC-PCE values. This chapter provided a set of graphs showing the marginal changes produce by each of these contributors on the traffic metrics. These graphs can be used by analyst and engineers to better understand the trade-offs of the truck percentage, grade, distance, and truck composition type in the design and operation of freeways.

CHAPTER 6

IMPACT OF CAPACITY DEFINITION ON THE HCM-6 PASSENGER CAR EQUIVALENT VALUES

6.1 Introduction

The HCM-6 equal capacity methodology for freeway segments is based entirely on VISSIM microsimulation model results aggregated over one-minute intervals. In particular, the VISSIM microsimulation model is used to estimate the capacity of 1,274 scenarios defined by combinations of truck percentage, grade, and grade distance levels as described in Section 3.2.3. These capacity values represent the main input to calculate the capacity adjustment factors (CAFs), which are subsequently used to calculate the HCM-6 EC-PCE values.

However, there are three major concerns related to the microsimulation model approach used in the HCM-6 methodology. First, the HCM-6 EC-PCE methodology assumed a capacity definition inconsistent with the rest of the HCM-6. Secondly, the microsimulation model was not calibrated to any capacity value. This is critical because the capacity is an input to the PCE calculation. Lastly, the HCM-6 methodology aggregated the data at a different level than that used in the rest of the HCM-6 and, indeed, for every previous HCM release.

The main objective of this chapter is to estimate EC-PCE values for basic freeway segments consistent with the standard assumptions underlying the HCM-6. Specifically, this chapter will examine the effect on HCM-6 PCE values when:

- 1) The standard HCM-6 definition of freeway capacity is used;

- 2) The standard HCM-6 aggregation of data (e.g., 15 minutes) is used;
- 3) The underlying microsimulation model is calibrated to the HCM-6 capacity definition; and
- 4) The underlying microsimulation approach follows standard calibration and usage protocols.

The goal is to quantify what, if any, changes occur in the HCM-6 CAF and PCE values when standard definitions are used. The goal is also to improve the core PCE methodology of the HCM-6. This would allow the engineers and analysts to use PCEs compatible with the traffic metrics in the HCM-6 in terms of definitions and aggregation levels. It is hypothesized this would improve the reliability of the capacity and levels of service analyses. More importantly, the improvements proposed in this chapter to the HCM-6 EC-PCE methodology would also facilitate users to develop their own localized PCEs for situations outside of the HCM-6 analyses using the same replicable and comparable framework.

6.2 Issues with the HCM-6 EC-PCE Approach

The HCM-6 CAF/EC-PCE values are dependent on the VISSIM Version 4.4 simulation model. This version of VISSIM is no longer available from the developers. It is important to note no empirical data was used to calibrate or validate the results (Dowling et al., 2014a, 2014b; Yang, 2013; Zhou, 2018). This is a huge advantage from a modeling perspective; it takes significantly less time to model the 1,274 HCM-6 scenarios in comparison to collecting empirical data and developing statistically-based models. It is also amenable for modeling situations not covered by the original scenarios such as modeling the effects of commercial vehicles operating as connected and automated

vehicles (Hurtado-Beltran & Rilett, 2021). However, there are a number of issues related to the “all-simulation” approach adopted by the HCM-6 that require further analyses to ensure consistent and replicable results.

6.2.1 HCM-6 Capacity Definition

Interestingly, in the HCM-6 EC-PCE research, the developers chose to define capacity as the 95th percentile of the maximum one-minute average flow-rate for the given scenario (Dowling et al., 2014a, 2014b; Yang, 2013). This is the first instance, to the authors’ knowledge, the HCM used

- 1) an aggregation level other than 15-minutes to calculate a traffic flow metric; and
- 2) used a capacity definition related to the 95th percentile of maximum flow.

In the HCM-6, the capacity for basic freeway and multilane highway segments is defined as “*a maximum flow rate associated with the occurrence of some type of breakdown, which results in lower speeds and higher densities*” (HCM, 2016, p. 12-7).

The same manual included a section to estimate the capacity from the field that takes into account a similar capacity definition, “*Freeway segment capacity is the maximum 15-min flow rate (in passenger cars per hour per lane) that produces an acceptable ($\lambda\%$) rate of breakdown*” (HCM, 2016, p. 26-18). Moreover, a similar capacity definition can be found for various transportation facilities in the manual. For example, in weaving segments, the capacity is defined as the maximum flow rate for a 15-min analysis period (HCM, 2016, p. 13-22).

Previous studies have shown the EC-PCE values may differ depending on the data aggregation level used to estimate capacity. For example, it has been reported the EC-PCE values for four-lane freeways were, on average, 11% lower for data aggregation levels of 15 minutes as compared to the aggregation level of one-minute used in the original research (Zhou, Rilett, & Jones, 2019b). The authors found this difference was statistically significant at the 5% level of significance. Similar results were found if different definitions of capacity were used in the calculations. For example, the authors used the maximum flow rate (e.g., 100th percentile) instead of the 95th percentile used in the original research and they found the capacity values were, on average, 15.7 percent higher. This resulted in PCE values that were, on average, 8.8 percent lower than the HCM-6 approach. To date, no one has examined the effect of different aggregation levels and capacity definitions on the original HCM scenarios (e.g., six-lane freeway, all vehicle types have same maximum speed, etc.).

Figure 6-1 shows the effect of capacity definition and aggregation level on the simulated capacity values of the 1,274 scenarios using the same output of the HCM-6 microsimulation model. The x-axis represents the capacity values computed as the maximum flow rate and the y-axis represents the capacity values as the 95th percentile of the maximum flow rate (e.g., current approach). The red circles correspond to an aggregation level of 1 minute (e.g., current approach), while the blue crosses relate to an aggregation level of 15 minutes. It may be seen that both capacity definition and aggregation level affect the capacity values. If the 95% maximum flow definition at one-minute averages is used, the capacity values range from 820 to 2,300 veh/h/ln. In contrast, if the standard HCM-6 capacity definition, maximum flow rate at 15-minutes

averages, is used then the capacity values range from 763 to 2,012 veh/h/ln. The average difference on the simulated capacity values between the two definitions was found to be 10.7%. Interestingly, it was observed the capacity of mixed flow scenarios changed at a greater rate as compared to the passenger car only flow scenarios, 13.0% versus 6.2%, respectively. This explains why the CAF values are affected by the capacity definition and aggregation level even though the CAF is a ratio between the mixed flow and passenger car only flow capacities.

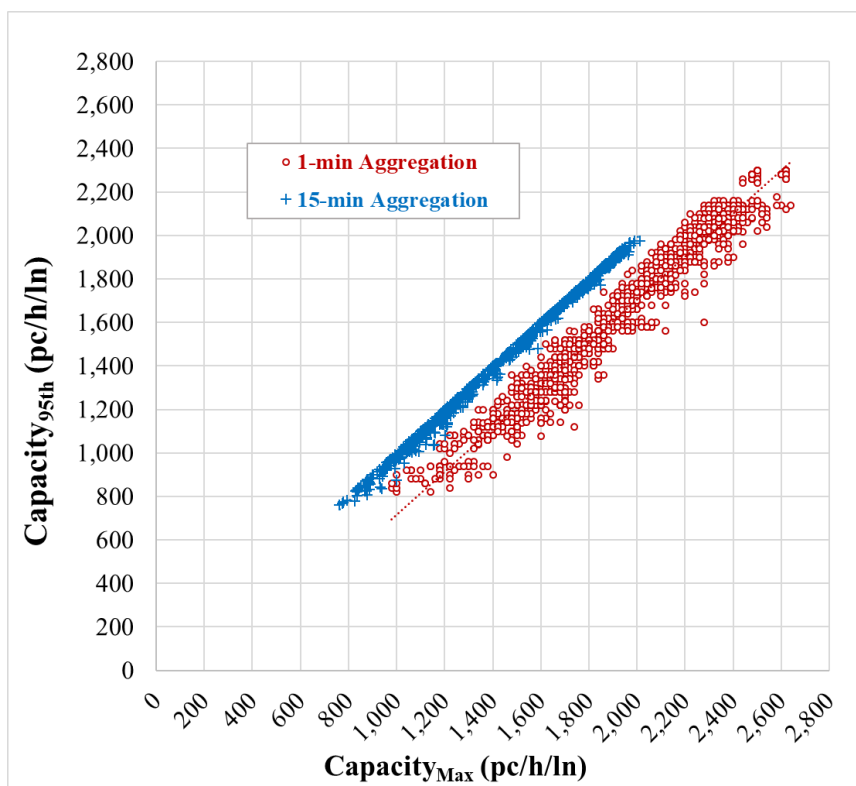


Figure 6-1. Effect of capacity definition and aggregation level on simulated capacity.

Therefore, it is the author's contention that care must be taken in comparing the capacity values found in the original EC-PCE research with other published capacity values based on larger aggregation levels. For example, in the HCM-6 mixed flow model,

the estimated CAF values (one-minute aggregation level) of the EC-PCE research are used to compute the mixed-flow capacity (*Equation 26-5, HCM, 2016*). This mixed-flow capacity is compared with the auto-only capacity (*Exhibit 12-6, HCM, 2016*) that was based on a larger aggregation level (15 minutes). It is expected by calculating the capacity using a consistent percentile of flow-rate and aggregation level with those used in the core methodologies for basic freeway and multilane highway facilities, EC-PCE values consistent with the other sections of the HCM-6 will be obtained.

6.2.2 *Model Calibration*

In the VISSIM microsimulation model the HCM-6 developers input operational and geometric characteristics of the vehicles (e.g., acceleration profiles, weight and power distributions, vehicle dimensions, etc.) based on previous research. The default Wiedemann 99 (car-following) and slow lane rules (lane-changing) were used to model the driving-behavior of the driver-vehicle units (Zhou, 2018). However, no empirical data was used to calibrate the driving-behavior of vehicles in the simulation.

It has been shown the VISSIM microsimulation capacity varies according to which VISSIM release is used. In one sense, this is not a problem as VISSIM 4.4 was used for the HCM-6. However, this version is no longer available nor supported by the microsimulation developer (PTV Group, 2019). For this reason, it is relatively easy to obtain capacity values that greatly differ from the base capacity values included in the HCM-6 without an adequate model calibration. For example, the HCM-6 capacity of basic freeway and multilane highway segments under base conditions ranges from 1,900 to 2,400 pc/h/ln and is a function of the free-flow speed and the facility type (HCM, 2016). These capacity values represent normal operating conditions across the US. Note

the HCM-6 base capacity for a freeway segment at 70 mph of free-flow speed is 2,400 pc/h/ln (*Exhibit 12-4, HCM, 2016*). In the HCM-6 research, the VISSIM microsimulation model results produced capacities as low as 2,059 pc/h/ln (VISSIM 11) or 2,275 pc/h/ln (VISSIM 20) for the base capacity conditions (Hurtado-Beltran & Rilett, 2021). It is easy to show this can negatively affect the calculation of CAF/EC-PCE values. It is hypothesized calibrating the underlying microsimulation model to the HCM definition of base capacity will lead to more consistent and, hopefully, accurate results.

6.2.3 Number of Microsimulation Replications for Each Scenario

The original EC-PCE research considered one single simulation run per scenario combination. This approach greatly reduced the number of simulation runs to complete the analysis. As the original researchers noted, this approach also drastically increased the noise or variability of the results (Dowling et al., 2014b). There is some debate in the literature on how many iterations, each with a new random seed number, should be conducted for a given scenario. The FHWA advocates using a single run for each scenario during the calibration process because it considers the variability produced by the driving behavior or the vehicle generation does not have a substantial impact on the results for a well-coded model (Wunderlich, Vasudevan, & Wang, 2019). Others, including the author of this chapter, advocate conducting multiple runs and then using the average, and the associated confidence intervals, for conducting the analysis (Spiegelman et al, 2011; Toledo & Koutsopoulos, 2004; Tufuor, Rilett, & Zhao, 2020). This is particularly important when modeling scenarios where minor changes can have major consequences – such as what occurs when modeling conditions on the edge of congestion. If only one replication is needed then intuitively running multiple runs and

averaging the results will not affect the final results. The only cost would be the extra time to conduct the simulations.

Note the original HCM researchers indicated the results, particularly related to the capacity values and the associated capacity adjustment factors (CAFs), had significant variation. As such, they made two adjustments in their methodology. The first was related to capacity. In particular, *“The 95th flow rate was selected in this research to avoid the noise due to the randomness in simulation”* (Yang, 2013). While this reduced the variability considerably, it did not completely remove the problem. Therefore, instead of using the CAF values directly to calculate the PCE the developers first calibrated regression models in order to identify a mathematical relationship between the simulated and estimated CAFs. The CAF estimates from these models were used to calculate the PCEs. It is hypothesized using a predefined number of simulations for each scenario, each using a different random number seed, will lead to microsimulation results that have much lower variation and higher consistency.

6.2.4 *Layout of Microsimulation Model*

Figure 1-3 shows a schematic of the underlying microsimulation model layout. It may be seen that the test bed includes an initial 12.8 km (8 miles) level section, followed by a central grade section of 9.7 km (6 miles), and a third level section of 1.6 km (1 mile). The grade of the central section varies according to the scenario (e.g., negative 6 degree to positive 6 degrees in increments of 1 degree) and it is on this central section where the microsimulation data is collected for the 1,274 scenarios. Note that virtual detectors are placed at various intervals on the central grade as shown in **Figure 1-3**. The data from these collectors are used to identify how grade and grade length affects various traffic

parameters including speed and capacity. In addition, the data for each scenario is collected concurrently. For example, a single run for a given input volume will collect information on the 0.4 km (0.25 mile) scenario, the 0.8 km (0.5 mile) scenario, etc.

It is hypothesized running all the grade length scenarios simultaneously might result in biased results. Specifically, it is argued shockwaves produced by vehicles upstream of a given detector might affect the traffic flow at the downstream detectors. This would be particularly true for commercial trucks on steep uphill grades where their operational performance is often characterized by a gradual reduction in speed until they reach “crawl speed” that is a function of grade value and the traveled distance (Al-Kaisy, 2006). This is, of course, less of an issue for passenger cars because their power/weight ratio is such that long, steep grades of the type in the analysis do not affect their ability to travel near the speed limit (Morris & Donnell, 2014).

Consequently, in this chapter each grade length scenario was run separately rather than concurrently. As an example, the 0.4 km (0.25 miles) length scenarios were all run with section 2 in **Figure 1-3** being 0.4 km (0.25 miles) and the 2.4 km (1.5 miles) length scenarios were run with section 2 in **Figure 1-3** being 2.4 km (1.5 miles) long. The goal is to verify the effect of the model layout on the results and how the proposed solution removes the problem.

To illustrate, **Table 6-1** shows the capacity values for a mixed traffic scenario defined by 30% truck percentage, +5% grade, and 30/70 SUT/TT truck composition type. The seven distance levels from 0.4 km (0.25 miles) to 8.1 km (5.00 miles) were evaluated considering two approaches: (1) independent runs (e.g., the model layout was modified according to the distance level using separate runs), and (2) single run (e.g., the seven

distance levels were evaluated in the same simulation run). Note the latter was the original approach used in the HCM-6 EC-PCE methodology. The mean capacity values, which were based on five experimental replications, differ between the two approaches. A paired t-test on the mean capacity values exposed this difference was statistically significant at $\alpha = 5\%$ for grades of 0.4 km (0.25 miles) and 0.8 km (0.5 miles). In other words, the capacity was higher for the shorter roadway segments when they were modeled separately. As would be expected the greatest differences occurred for the scenarios with the highest grades.

Table 6-1. Independent versus Single Runs on Capacity Values for a Mixed Traffic Scenario.

Scenario				Simulated Capacity (veh/h/ln)											
				Independent Runs						Single Run					
m	p	g	d	SR1	SR2	SR3	SR4	SR5	Mean	SR1	SR2	SR3	SR4	SR5	Mean
30/70 SUT/TT	30%	5%	0.25	1561	1541	1579	1564	1553	1560	1497	1509	1509	1508	1504	1506
30/70 SUT/TT	30%	5%	0.50	1517	1519	1533	1520	1525	1523	1511	1520	1500	1521	1505	1511
30/70 SUT/TT	30%	5%	0.75	1505	1509	1504	1513	1497	1506	1527	1519	1511	1504	1523	1517
30/70 SUT/TT	30%	5%	1.00	1509	1497	1531	1512	1527	1515	1504	1532	1500	1511	1533	1516
30/70 SUT/TT	30%	5%	1.50	1525	1508	1527	1507	1509	1515	1509	1517	1527	1499	1517	1514
30/70 SUT/TT	30%	5%	2.50	1516	1499	1531	1493	1509	1510	1517	1508	1528	1511	1504	1514
30/70 SUT/TT	30%	5%	5.00	1507	1532	1517	1496	1495	1509	1507	1532	1517	1496	1495	1509

Note: m = truck composition type; p = truck percentage; g = grade; d = distance (miles); SRi = simulation run *i*.

6.3 Proposed Approach for EC-PCE Estimation

The objective of the proposed approach is to use a capacity definition in the HCM-6 EC-PCE procedure consistent with the capacity definition for basic freeway segments in the HCM-6. The original protocols and assumptions were followed in this chapter except the simulated capacity was computed in agreement with the HCM-6 definition (e.g., using a 15-minute aggregation level). Moreover, the microsimulation model was calibrated to

match the base capacity for basic freeway segments at 70 mph (e.g., 2,400 veh/h/ln). Additionally, independent simulation runs and five experimental replications were performed for each scenario combination to improve the accuracy and reduce the variability of the results. A detailed discussion of the changes considered in the proposed approach is provided in the following sections.

6.3.1 Microsimulation Framework

This chapter used a microsimulation model in VISSIM 20 to obtain the simulated capacity of the 1,274 scenario combinations that comprised the HCM-6 EC-PCE procedure. The methodology adopted in this chapter, which is based on VISSIM 20, gave statistically similar results to the original results based on VISSIM 4.4 as shown in previous publications (Hurtado-Beltran & Rilett, 2021).

With the exception of the changes discussed above, all the original assumptions related to traffic demand vehicle types (e.g., passenger cars, single-unit trucks, and tractor-trailers), and operational characteristics (e.g., acceleration profiles, weight and power ratios, speed distributions, etc.) were kept the same. However, the vehicle input scheme was modified to ensure exact vehicle input over time intervals.

Although exact vehicle inputs were used in the original research, the time intervals used for vehicle generation (e.g., 60 minutes) and data aggregation (e.g., one minute) were incompatible to produce an exact vehicle generation as reported in the literature (Hurtado-Beltran & Rilett, 2021). Due to this, the proposed approach used a time interval of 15 minutes for both vehicle generation and data aggregation to reduce the variability of the results and to be consistent with the HCM-6 aggregation level.

In the original HCM-6 research, the scenario combinations related to the seven distance levels were analyzed in the same simulation run. To avoid the influence of the traffic shockwave at the detectors located upstream, the proposed approach considered independent simulation runs for each scenario combination. In addition, five experimental replications were used for each scenario combination. The number of experimental replications was determined based on the variability observed during the calibration process of the microsimulation model.

6.3.2 Model Calibration

The VISSIM 20 model was calibrated to match the HCM-6 base capacity of 2,400 pc/h/ln, which corresponds to a basic freeway segment at a free-flow speed (FFS) of 70 mph. It must be noted the driving behavior was not calibrated in the original research. Therefore, the capacity values tended to differ from *Exhibit 12-4* in the HCM-6. In this chapter, a gap sensitivity analysis based on the parameter CC1 (i.e., gap time) was performed for the model calibration. Default values of Wiedemann 99 for car-following, except the CC1 parameter, and slow lane rules for lane-changing were used as in VISSIM 20. The scenario combination used for the calibration of the model corresponds to a truck percentage of 0%, a grade of 0%, and distance of 0.4 km (0.25 miles), according to the base conditions in HCM-6.

In contrast to the original research that used the lowest simulation resolution available in VISSIM (e.g., 1 time step/simulation second), the proposed approach used a higher simulation resolution of 2 time steps/simulation second. Preliminary analyses revealed the lowest simulation resolution may have a significant impact on the capacity values. A paired t-test on the simulated capacity values confirmed the difference between

a simulation resolution of 2 and 10 time steps/simulation second was not statistically significant at $\alpha = 5\%$ considering the capacity definition and aggregation level of the proposed approach. Based on the previous finding, the simulation resolution was selected to reduce the required simulation time per run without compromising the accuracy of the results.

The results of the calibration process are shown in **Figure 6-2**. The horizontal axis represents the CC1 parameter value in seconds and the vertical axis the simulated capacity value in pc/h/ln. The gap sensitivity analysis explored CC1 values from 0.88 to 0.94 seconds. Note the default CC1 value in VISSIM 20 is 0.90 seconds. Five experimental replications were used to estimate the simulated capacity related to the explored CC1 values. The number of experimental replications was calculated using **Equation (6-1)** (Spiegelman et al, 2011). In this case, it was considered a standard deviation of 14 veh/h/ln, allowable error of 2%, level of significance of 5%, and five initial runs. Although the estimated number of simulation runs was 0.43, it was decided to use five experimental replications per scenario to consider a multi-run approach as suggested in the literature. It may be seen that the optimal CC1 better matching the base capacity was 0.92 seconds. This CC1 value was used to model the driving behavior for all 1,274 scenario combinations in the proposed approach.

$$N_m = \left(t_{1-\alpha/2, n-1} \frac{\sigma_m}{\varepsilon} \right)^2 \quad m = 1, \dots, M \quad (6-1)$$

Where:

N_m : Number of simulation runs for performance measure m .

M : Number of performance measures that are being considered by the user.

σ_m : Estimated standard deviation of performance measure m .

$t_{1-\alpha/2, n-1}$: t-statistic value for given significance level and number of simulation runs.

ε : Allowable error; this is often specified as a fraction of the mean value of the performance measure μ_m .

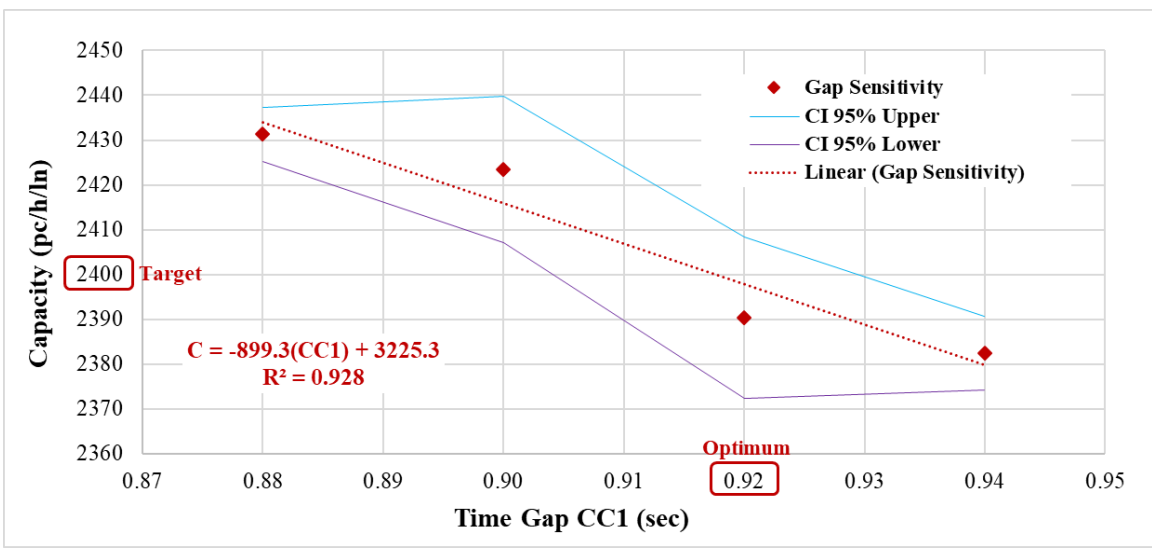


Figure 6-2. Gap sensitivity results used for model calibration.

6.3.3 Capacity Definition

The proposed approach used a consistent definition of capacity with the HCM-6. In this case, the capacity of each scenario combination was defined as the maximum hourly flow rate for a 15-minute aggregation level. The simulated capacity for each of the 1,274 scenarios was calculated using Equations (6-2) and (6-3). The simulated capacity was averaged over the experimental replications. Note that five experimental replications were used in this chapter.

$$C_{f,p,m,g,d} = \frac{\sum_{i=1}^n c_{i,f,p,m,g,d}}{n} \quad (6-2)$$

$$c_{i,f,p,m,g,d} = \text{Max}_{\substack{t=1,4 \\ r=1,9}} \{q_{f,t,p,m,g,d,r}\} \quad (6-3)$$

Where:

$C_{f,p,m,g,d}$: Simulated capacity at f flow type, p truck percentage level, m truck composition level, g grade level, d distance level, (veh/h/ln).

$c_{i,f,p,m,g,d}$: capacity for experimental replication i at f flow type, p truck percentage level, m truck composition level, g grade level, d distance level, (veh/h/ln).

n : Number of experimental replications for each scenario combination.

Max : Maximum value.

$q_{f,t,p,m,g,d,r}$: Flow rate for the f flow type at t time interval, p truck percentage level, m truck composition level, g grade level, d distance level, and r simulation volume level, based on 4 15-min interval traffic volume recorded by the detector (veh/h/ln).

6.3.4 CAF and PCE Estimation

The simulated capacity values, main input for the estimation of CAFs and PCEs, of all 1,274 scenario combinations were obtained using the calibrated VISSIM 20 model. These scenarios corresponded to a 30/70 SUT/TT truck composition type. These capacity values were used to calibrate the nonlinear regression (NLR) model used for fitting simulated and estimated CAF values (e.g., Steps 2 and 3 in the HCM-6 procedure). The nonlinear

regression model used in the HCM-6 is shown in **Equations (3-7) to (3-11)** (Dowling et al., 2014b; Zhou, Rilett, & Jones, 2019; Zhou, 2018).

This chapter adopted the same form of the nonlinear model (i.e., **Equation (3-7)**) as was used in the HCM-6. The parameters were estimated using a Generalized Reduced Gradient (GRG) approach (Lasdon, Fox, & Ratner, 1974). This is a nonlinear optimization method that uses an iterative process to optimize a target value. In this chapter, the target goal was to minimize the sum of squared errors between the simulated CAFs from Step 2 and the estimated CAFs from the non-linear regression model.

Finally, the CAF and PCE values for specific conditions of truck percentage, grade, and distance were estimated (e.g., Steps 4 and 5 in the HCM-6 procedure). The EC-PCEs ($EC - PCE_{2,p_s,m_s,g_s,d_s}$) at specific conditions of truck percentage p_s , grade g_s , and distance d_s , are calculated using **Equation (3-12)**.

6.4 Comparison of Estimated CAF Results

The CAFs were estimated for all 1,274 scenario combinations using the calibrated parameters and the nonlinear regression model shown in **Table 6-2** and **Equation (3-7)**, respectively. A comparison between the estimated CAFs for the proposed approach and the estimated CAFs for the original approach (e.g., HCM-6 results) are shown in **Figure 6-3**. The solid line represents the values estimated using the proposed approach and the dotted line represents the values from the HCM-6 methodology. The scenario number (horizontal axis) is given by **Equation (3-6)** and corresponds to a particular combination of truck percentage, grade, and distance used to compute the corresponding CAF. There were 14 truck percentage values (including 0%) and these are shown on the top of **Figure 6-3**. For a given truck percentage, the CAFs for grade and grade distance are shown in

order. The general form is a flat straight line for the negative and zero grade scenarios, followed by decreasing CAF values for the positive grade values. For both approaches, the CAF values decrease as truck percentage increases and this decrease is at a fairly linear rate. However, for the proposed approach the CAF values are, on average, 5.17% lower (ranging from 0.02% to 7.63%) than those of the original approach. It is hypothesized this occurs because, in contrast to the original approach, the proposed approach considered a different definition of capacity, uses the standard aggregation level of 15 minutes, uses a calibrated microsimulation model to match the HCM-6 base capacity for basic freeway segments, and uses state of the practice microsimulation approaches (e.g., multiple runs, finer step sizes, etc.).

Table 6-2. Calibrated NLRM Models.

Condition (30/70 SUT/TT)	Nonlinear Model Parameter (NLRM)											
	$\alpha_{1,2,m}^{Ta}$	$\beta_{1,2,m}^{Ta}$	$\gamma_{2,m}^{Ga}$	$\theta_{2,m}^{Ga}$	$\mu_{2,m}^{Ga}$	$\alpha_{2,m}^{Ga}$	$\phi_{2,m}^{Ga}$	$\eta_{2,m}^{Ga}$	$\alpha_{2,m}^{Da}$	$\beta_{2,m}^{Da}$	$\phi_{2,m}^{Da}$	R^2
HCM-6	0.53	0.72	8.0	0.126	0.030	0.69	12.90	1.0	1.72	1.71	-3.16	-
Proposed	0.56	0.59	8.0	0.127	0.070	0.69	10.63	1.0	1.72	1.71	-3.15	0.98

Note: The capacity adjustment factor for free-flow speed effect for the mixed flow is given by the following parameters: $\mu_{2,m}^{FSSa}=0.25$; $\rho_{2,m}^{FSS}=0.70$; $\beta_{2,m}^{FSS}=1.0$; $\phi_{2,m}^{FSS}=1.0$. This factor is equal to zero when the assumed free-flow speed is 112.65 km/h (70 mph), as the case in the original research. NLRM = nonlinear regression model (original model); SUT = single unit truck; TT = tractor-trailer.

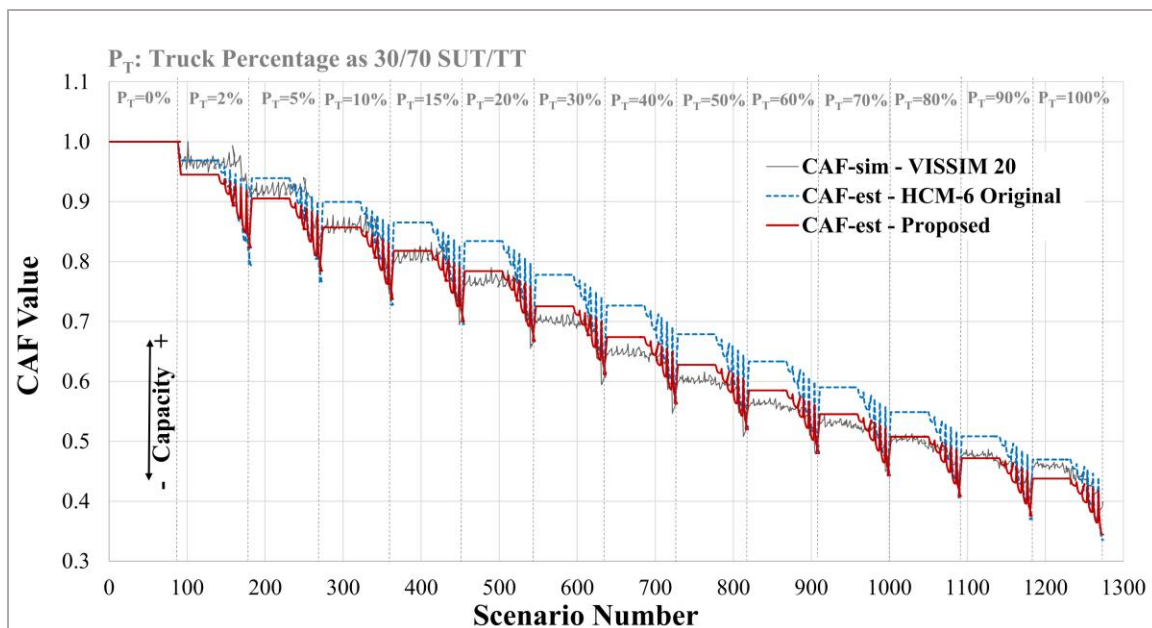


Figure 6-3. CAF values as a function of scenario number for the proposed and HCM-6 approaches.

6.5 Comparison of EC-PCE Results

A comparison of the EC-PCE values between the proposed approach and the original HCM-6 approach was performed. The EC-PCE values were estimated for ten levels of truck percentage (i.e., 10% to 100% in 10% increments), three levels of grade (i.e., 0%, +3%, and +6%), and three levels of distance (i.e., 0.8 km (0.5 mi), 1.61 km (1.0 mi), and 2.42 km (1.5 mi)). **Figure 6-4** shows the corresponding EC-PCE values as a function of truck percentage for the three levels of grade and three levels of distance for both the proposed approach and the HCM-6 values. The solid lines represent the proposed EC-PCE values and the dotted lines the HCM-6 EC-PCE values. The EC-PCE values were calculated using **Equation (4-12)**. Note any specific condition within the explored range of truck percentage, grade, and distance considered in the HCM-6 methodology can be computed using the model parameters provided in **Table 6-2**. On average, the EC-PCE

values for the proposed approach are 15.9% greater than those of the original HCM-6 approach indicating the current PCE values in the HCM may underestimate the impact of heavy trucks on traffic operations.

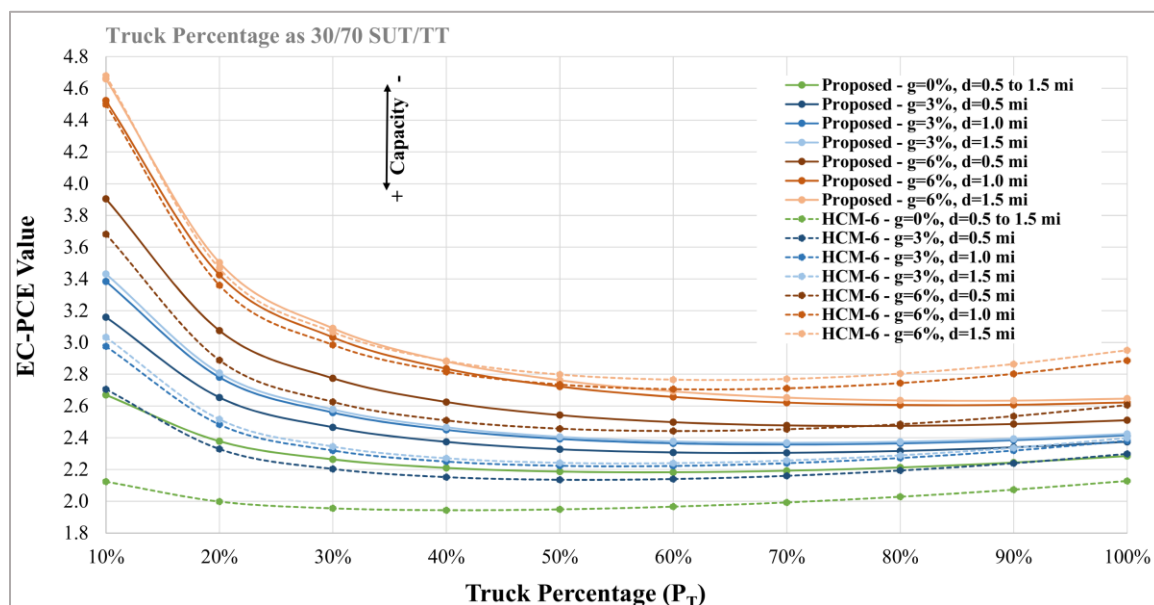


Figure 6-4. EC-PCE values for the proposed and HCM-6 approaches.

For both the proposed and original HCM-6 approaches, the maximum EC-PCE values occur at a truck percentage of 10%. In general, as grade and distance increase so does the EC-PCE. For higher truck percentages, the EC-PCE values for both approaches tend to decrease as truck percentage increases until the 40 percent value is reached. After this point, the EC-PCE values tend to increase at a decreasing rate with truck percentage. However, the latter increase is milder for the proposed approach. In general, the EC-PCE ranges from 2.2 to 4.7 for the proposed approach and from 1.9 to 4.7 for the original approach. It must be noted that the EC-PCE values for the proposed approach are slightly greater than the original approach, especially for the 0% and 3% grade values. This

0.0	0.125	3.9	2.6	3.1	2.3	2.7	2.1	2.5	2.0	2.4	2.0	2.3	2.0
	0.375	3.9	2.6	3.1	2.3	2.7	2.1	2.5	2.0	2.4	2.0	2.3	2.0
	0.625	3.9	2.6	3.1	2.3	2.7	2.1	2.5	2.0	2.4	2.0	2.3	2.0
	0.875	3.9	2.6	3.1	2.3	2.7	2.1	2.5	2.0	2.4	2.0	2.3	2.0
	1.25	3.9	2.6	3.1	2.3	2.7	2.1	2.5	2.0	2.4	2.0	2.3	2.0
	1.5	3.9	2.6	3.1	2.3	2.7	2.1	2.5	2.0	2.4	2.0	2.3	2.0
2.5	0.125	3.9	2.6	3.1	2.3	2.7	2.1	2.5	2.0	2.4	2.0	2.3	2.0
	0.375	5.1	4.1	3.6	2.9	3.0	2.5	2.7	2.3	2.5	2.2	2.4	2.1
	0.625	5.9	5.0	4.0	3.3	3.1	2.7	2.8	2.4	2.6	2.3	2.5	2.2
	0.875	6.3	5.5	4.1	3.5	3.2	2.8	2.9	2.5	2.7	2.4	2.6	2.3
	1.25	6.5	5.7	4.2	3.6	3.3	2.8	2.9	2.5	2.7	2.4	2.6	2.3
	1.5	6.5	5.8	4.2	3.6	3.3	2.8	2.9	2.6	2.7	2.4	2.6	2.3
3.5	0.125	3.9	2.6	3.1	2.3	2.7	2.1	2.5	2.0	2.4	2.0	2.3	2.0
	0.375	5.8	4.9	3.9	3.3	3.1	2.6	2.8	2.4	2.6	2.3	2.5	2.2
	0.625	6.9	6.3	4.4	3.9	3.4	3.0	3.0	2.6	2.8	2.5	2.6	2.4
	0.875	7.5	7.0	4.6	4.2	3.5	3.1	3.1	2.8	2.8	2.6	2.7	2.5
	1.25	7.8	7.4	4.8	4.3	3.6	3.2	3.1	2.8	2.9	2.6	2.7	2.5
	1.5	7.9	7.5	4.8	4.4	3.6	3.2	3.1	2.8	2.9	2.6	2.7	2.5
4.5	0.125	3.9	2.6	3.1	2.3	2.7	2.1	2.5	2.0	2.4	2.0	2.3	2.0
	0.375	6.5	5.8	4.2	3.6	3.3	2.8	2.9	2.6	2.7	2.4	2.6	2.3
	0.625	8.1	7.9	4.9	4.5	3.6	3.3	3.2	2.9	2.9	2.7	2.8	2.6
	0.875	8.9	8.9	5.2	5.0	3.8	3.6	3.3	3.1	3.0	2.8	2.9	2.7
	1	9.1	9.2	5.3	5.1	3.9	3.6	3.3	3.1	3.1	2.9	2.9	2.7
	1.5	9.1	9.2	5.3	5.1	3.9	3.6	3.3	3.1	3.1	2.9	2.9	2.7
5.5	0.125	3.9	2.6	3.1	2.3	2.7	2.1	2.5	2.0	2.4	2.0	2.3	2.0
	0.375	7.3	6.9	4.5	4.1	3.5	3.1	3.0	2.7	2.8	2.5	2.7	2.4
	0.625	9.5	9.8	5.5	5.3	4.0	3.8	3.4	3.2	3.1	2.9	2.9	2.8
	0.875	10.5	11.2	5.9	5.9	4.2	4.1	3.6	3.4	3.3	3.1	3.0	2.9
	1	10.8	11.6	6.1	6.1	4.3	4.2	3.6	3.5	3.3	3.2	3.1	3.0
	1.5	10.8	11.6	6.1	6.1	4.3	4.2	3.6	3.5	3.3	3.2	3.1	3.0
6.0	0.125	3.9	2.6	3.1	2.3	2.7	2.1	2.5	2.0	2.4	2.0	2.3	2.0
	0.375	7.7	7.5	4.7	4.4	3.6	3.2	3.1	2.8	2.9	2.6	2.7	2.5
	0.625	10.2	10.8	5.8	5.8	4.2	4.0	3.5	3.4	3.2	3.1	3.0	2.9
	0.875	11.5	12.5	6.4	6.5	4.4	4.4	3.7	3.7	3.4	3.3	3.2	3.1
	1	11.8	13.0	6.5	6.7	4.5	4.5	3.8	3.7	3.4	3.4	3.2	3.1
	1.5	11.8	13.0	6.5	6.7	4.5	4.5	3.8	3.7	3.4	3.4	3.2	3.1

Note: Prop. = proposed approach in this chapter; HCM = current HCM-6 approach.

6.6 Concluding Remarks

The objective of this chapter was to estimate EC-PCE values consistent with the HCM-6 capacity for basic freeway segments. It was hypothesized a capacity definition and aggregation level in agreement with the HCM-6 could produce more reliable PCE values for capacity and level of service analyses. The current PCE values in the HCM-6 were estimated considering an atypical definition of capacity (e.g., capacity as 95th percentile of the maximum flow rate) and aggregation level (e.g., one-minute) that differ from the standards observed to compute the traffic metrics in the HCM-6. It is important to assess to what extent the assumptions made in the original research can affect the PCE values published in the HCM-6.

One of the most significant findings to emerge from this chapter is the approach used to compute the capacity values in the HCM-6 procedure (e.g., Step 1) has a significant impact on the PCE results. This means the assumptions made in the original research regarding the capacity definition and aggregation level affect the PCE values shown in the HCM-6. As the PCE values are used to convert a mixed traffic stream into a passenger car stream, it is important the PCE values are based on the same capacity definition and aggregation level considered in the HCM-6 to produce comparable traffic metrics.

Another major finding is the approach proposed in this chapter produced greater PCE values as compared to the traditional approach, particularly for the lower grade and distance levels. This finding suggests the current PCE values in the HCM-6 may underestimate the effect of trucks in capacity and level of service analyses. The proposed approach addressed important issues identified in the original HCM-6 EC-PCE

methodology. It is argued the approach advocated in this chapter produces results more comparable and consistent with the underlying logic of the HCM-6. In particular, the proposed approach used a calibrated microsimulation model that targeted the base capacity for basic freeway segments in the HCM-6. Moreover, the capacity was computed using the same capacity definition (e.g., capacity as the maximum hourly flow rate) and aggregation level (e.g., 15 minutes) in agreement with the HCM-6. The PCE values from the proposed approach were, on average, 15.9% greater than those obtained in the original HCM-6 research. This finding is important because the proposed PCE values will produce more conservative capacity values and levels of service than the existing PCE values in the HCM-6 indicating the latter values may overestimate the capacity of basic freeway segments. Chapter 7 of this dissertation will consider a similar approach to the one exposed in this chapter as a part of the proposed methodology for EC-PCEs.

CHAPTER 7

IMPACT OF CAV TRUCK PLATOONING ON FOUR-LANE FREEWAY SEGMENTS IN WESTERN U.S.

7.1 Introduction

This chapter presents a new methodology to estimate EC-PCE values for generic purposes including CAV technologies. The proposed methodology will be illustrated by studying the deployment of CAV truck platooning on four-lane freeway segments in the Western U.S. As a part of the case study, two traffic conditions will be evaluated: (1) non-CAVs (e.g., only conventional cars and trucks) and (2) CAV truck platooning (only trucks operate as CAVs). A comparative analysis between both traffic conditions will provide insight about the potential impact of CAV truck platooning on the EC-PCE values and the capacity of four-lane freeways.

The proposed methodology will estimate EC-PCE values for basic freeway segments (four-lanes) that are consistent with the standard assumptions underlying the HCM-6 and will overcome the issues discussed in previous chapters of this dissertation. Specifically, the proposed methodology will consider the following improvements:

- 1) The standard HCM-6 definition of freeway capacity is used;
- 2) The standard HCM-6 aggregation of data (e.g., 15 minutes) is used;
- 3) The underlying microsimulation model is calibrated to the HCM-6 capacity values;
- 4) The underlying microsimulation approach follows standard calibration and usage protocols; and

- 5) A simpler regression model structure for fitting simulated and estimated data is used.

The goal is to demonstrate the proposed methodology developed in this dissertation can be suitable for exploring either conventional traffic situations or disruptive technologies such as CAVs. This would allow the engineers and analysts to use PCEs compatible with the traffic metrics in the HCM-6 in terms of definitions and aggregation levels. It is hypothesized this would improve the reliability of the capacity and levels of service analyses. More importantly, the EC-PCE methodology proposed in this chapter would also facilitate users to develop their own localized PCEs for situations outside of the HCM-6 analyses using the same replicable and comparable framework.

7.2 Operational Traffic Conditions in Western U.S.

The Western U.S. was selected as a case study because their operational conditions may differ from those assumed in the original HCM-6 EC-PCE research. In this regard, Zhou, Rilett and Jones (2019) argued the EC-PCE values published in the HCM-6 are not appropriate for the Western U.S. conditions. The HCM-6 EC-PCE values were developed for unrestricted three-lane freeway segments, a uniform free-flow speed (FFS) for passenger cars and trucks of 70 mph, a simplified truck composition type (e.g., only truck classes 5 and 8), and truck percentages up to 25%. The same EC-PCE value at 25% truck percentage is assumed for greater truck percentage values in the HCM-6. These conditions may not correspond to those that have been observed in western rural U.S.

For example, the Nebraska Department of Transportation (NDOT) reported Interstate 80 in Western Nebraska frequently experiences truck percentages between 25% and 60% (USDOT, 2015). High truck percentages have been also reported in other states

including Wyoming, Kansas, Nevada, and Texas (WYDOT, 2009; KDOT, 2015; NDOT, 2017; TxDOT, 2016). Moreover, it has been estimated truck percentages will continue to increase in the freeway system, reaching a 42% increase by 2040 (Mendez, Monje, & White, 2017).

Another important point is that most of the heavy trucks in Western U.S. are governed through the use of speed limiters that reduce their maximum operational speed considerably below the posted speed limit (Bishop, 2008). In addition, the interaction of high truck percentages and large speed differences promotes the formation of moving bottlenecks, negatively affecting the operational performance of freeways. This is especially critical on four-lane freeways (e.g., two-lanes per direction) which widely exist in the Western U.S (Zhou, Rilett, & Jones, 2019).

Therefore, care must be taken when the HCM-6 EC-PCE values are used to analyze freeway segments under the western rural US conditions. This was a main motivation for selecting this case study.

7.3 Data Description

The Nebraska Transportation Center (NTC) collected empirical traffic data at 13 sites on Interstate 80 between mileposts 177 and 399 in Nebraska. This data collection occurred from June to December 2015. The dataset is comprised of 48,903 valid vehicle records used to identify free-flow speed distributions for passenger cars, single unit trucks (SUT), and tractor trailers (TT). Free vehicles were defined as those are not in a moving bottleneck based on a 'critical headway' that ranged from 3 to 8 seconds. Further details of this dataset can be found elsewhere (Zhou, Rilett, Jones, & Chen, 2018). This empirical data, as representative of the western rural U.S. conditions (e.g., four-lanes

freeways, high truck percentages, and higher speed differentials), will serve as a basis to input the desired speed distributions and the truck length distributions in the microsimulation model.

Figure 7-1a shows the empirical free-flow speed (FFS) cumulative distributions for passenger cars (solid black line), single unit trucks (solid red line), and tractor trailers (solid blue line). In addition, it may be seen the uniform FFS of 70 mph assumed for cars and trucks in the HCM-6 EC-PCE methodology (gray dotted line), which drastically differs from the empirical data. Note the FFS for passenger cars, SUTs, and TTs are approximately normally distributed, and the average speed of SUTs and TTs are 7 mph and 10 mph lower than the average of passenger cars, respectively.

Figure 7-1b shows the empirical truck length cumulative distributions for single unit trucks (solid red line), and tractor trailers (solid blue line). For the Western U.S. the SUTs and TTs are modeled as having lengths that range from 30 to 45 ft for SUTs and from 50 to 95 ft for TTs. In contrast, the dotted lines correspond to the values used in the HCM-6 EC-PCE methodology where the SUTs and TTs are modeled as having the same length of 33 and 55 ft, respectively.

Figure 7-1c, d, e, and f show the operational characteristics used for modeling trucks in the HCM-6 EC-PCE methodology. These data were based on the NCHRP report 505 *'Review of Truck Characteristics as Factors in Roadway Design'* (2003). It is important to note the exact operational characteristics shown in the figures were used for modeling trucks in the VISSIM 20 model for both the non-CAV condition and the CAV truck platooning condition.

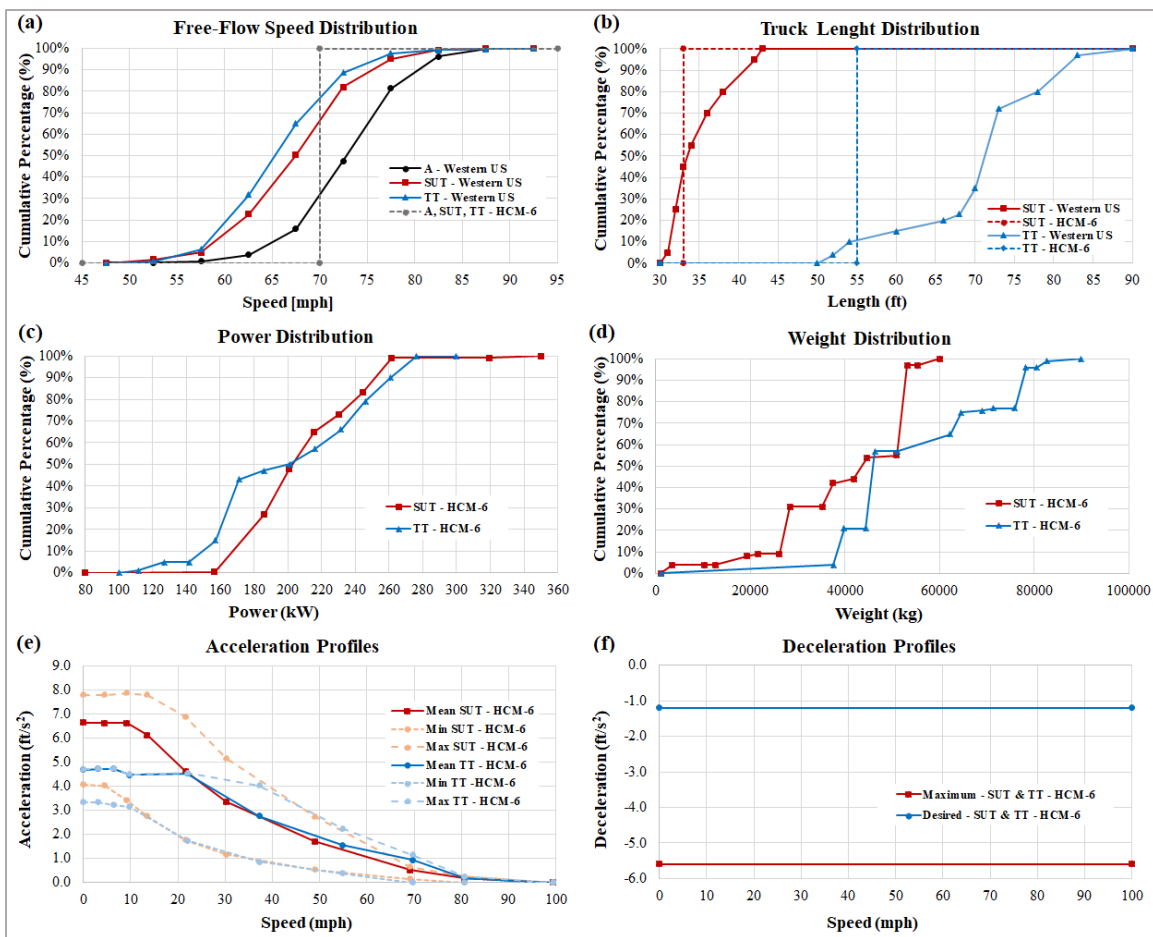


Figure 7-1. Truck attributes considered in the microsimulation model (Zhou, 2018; Dowling et al., 2014).

Thus, the Western U.S. conditions in this chapter refers to:

- 1) Four-lane freeways (e.g., two-lanes per direction).
- 2) Different free-flow speed distributions between vehicle types. Note the differences in speed distributions have been shown to be statistically significant (Zhou, 2018).
- 3) Empirical truck length distributions between truck types.

7.4 Microsimulation Model

Figure 7-2 shows a schematic of the underlying microsimulation model layout. The model layout corresponds to a unidirectional two-lane freeway segment. The test bed includes an initial 4.02 km (2.5 miles) level section, followed by a central grade section of variable length that is a function of the corresponding distance level of the explored scenario combination.

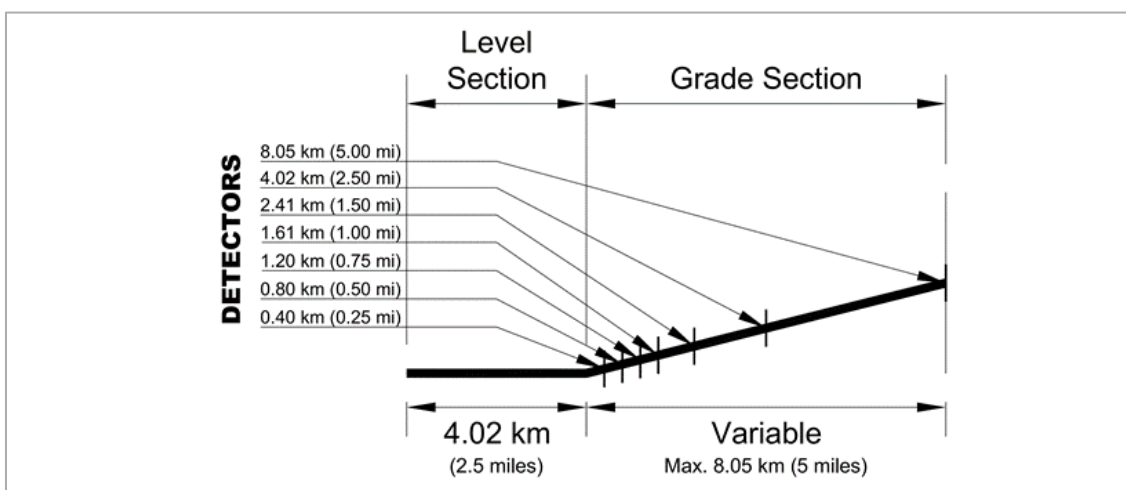


Figure 7-2. Schematic of the VISSIM model for EC-PCE estimation.

The length of the initial level section was reduced by approximately 70% compared to the HCM-6 test bed, in order to reduce the simulation running time. Preliminary experiments revealed approximately 90% of the platoon formation occurs at the 2.5 miles distance as shown in Appendix B of this dissertation (Hurtado-Beltran, Vakilzadian, & Rilett, 2020). It also was shown that shortening the length of the initial level section had no meaningful effect on the results. The grade of the central section varies according to the scenario (e.g., negative 6 degree to positive 6 degrees in increments of 1 degree) and it is on this central section where the microsimulation data is

collected for the 1,274 scenarios. Virtual detectors are placed on both lanes at various intervals on the central grade as shown in **Figure 7-2**. The data from these detectors are used to collect critical traffic data (e.g., speed, volume) so that the relationship between certain variables (e.g., grade, grade length) affect various traffic metrics including speed, flow rate, and capacity. In addition, the data for each scenario is collected independently. For example, the 0.4 km (0.25 miles) length scenarios were all run with section 2 in **Figure 7-2** being 0.4 km (0.25 miles) and the 2.4 km (1.5 miles) length scenarios were run with section 2 in **Figure 7-2** being 2.4 km (1.5 miles) long. The advantages of this scheme were discussed in Chapter 6 of this dissertation.

7.5 Model Calibration

The VISSIM 20 model was calibrated to match the base capacity values published in the HCM-6 for non-CAVs and CAVs. For the non-CAV condition, it was considered a base capacity of 2,400 pc/h/ln, which corresponds to a basic freeway segment at a free-flow speed (FFS) of 75 mph (*Exhibit 12-4*, HCM, 2016). In contrast, for the CAV condition, it was considered the CAV base capacity of 3,200 pc/h/ln that will be published in the forthcoming version of the HCM, HCM-6.1 (*Exhibit 26-15*). To estimate this CAV capacity, the HCM-6.1 assumed a maximum platoon size of 10 vehicles and an intraplatoon gap of 0.71 seconds. This cases study used the same assumptions for modeling the CAV truck platooning condition during the calibration process.

A gap sensitivity analysis based on the parameter CC1 (i.e., gap time) was performed for the model calibration. For the non-CAV condition, default values of Wiedemann 99 for car-following, except the CC1 parameter, and slow lane rules for lane-changing were used as in VISSIM 20. In contrast, default values of the ‘Aggressive

CoExist' driving behavior in VISSIM 20 were considered for the CAV condition, except the CC1 parameters and the platooning parameters. The scenario combination used for the calibration of the model corresponds to a truck percentage of 0%, a grade of 0%, and distance of 0.4 km (0.25 miles), in agreement with the base conditions in HCM-6.

In contrast to the original HCM-6 research that used the lowest simulation resolution available in VISSIM (e.g., 1 time step/simulation second), the proposed approach used a higher simulation resolution of 2 time steps/simulation second. Preliminary analyses revealed the lowest simulation resolution (e.g., 1 time step/simulation second) may have a significant impact on the capacity values. This is shown in Appendix C of this dissertation. A paired t-test on the simulated capacity values confirmed the difference between a simulation resolution of 2 and 10 time steps/simulation second was not statistically significant at $\alpha = 5\%$ considering the capacity definition and aggregation level of the proposed approach. Based on the previous finding, the simulation resolution was selected seeking to reduce the required simulation time per run without compromising the accuracy of the results. It is important to note that the simulation resolution was treated as a fixed calibration parameter as suggested in Appendix C.

The results of the calibration process are shown in **Figure 7-3**. The horizontal axis represents the CC1 parameter value in seconds and the vertical axis the simulated capacity value in pc/h/ln. Five experimental replications were used to estimate the simulated capacity related to the explored CC1 values. The gap sensitivity analysis explored CC1 values from 0.88 to 1.00 seconds for the non-CAV condition (**Figure 7-3a**), and from 0.80 to 0.94 seconds for the CAV condition (**Figure 7-3b**). The default

CC1 value in VISSIM 20 is 0.90 seconds which coincides with the optimal values obtained in the calibration process for both conditions. These CC1 values were used to model the driving behavior for all 1,274 scenario combinations that comprise each condition in the proposed methodology. **Table 7-1** shows the driving behavior parameters set for modeling the two conditions explored in this case study.

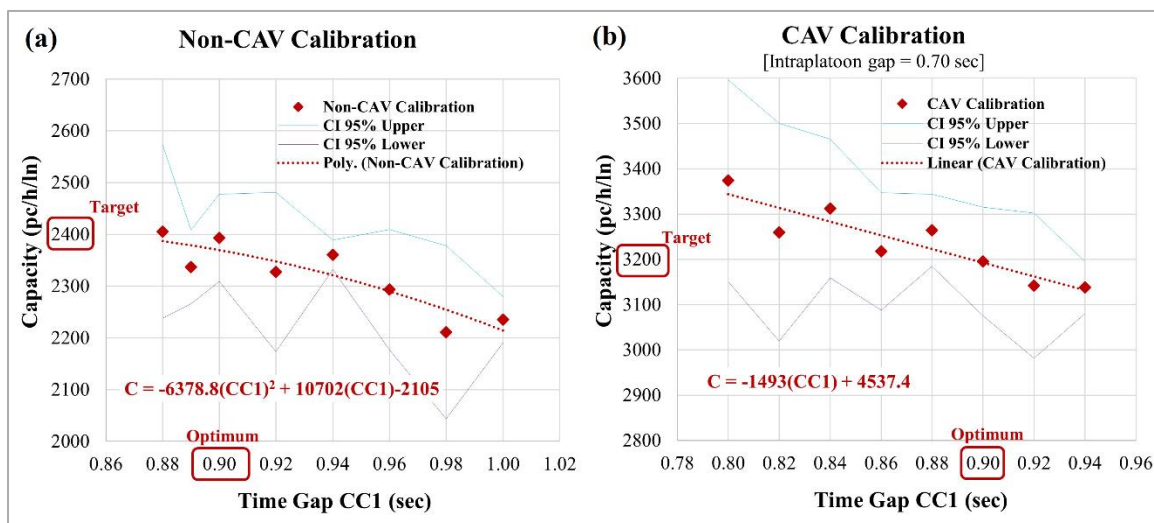


Figure 7-3. Gap sensitivity results used for the model calibration of: (a) non-CAV condition and (b) CAV truck platooning condition.

Table 7-1. Driving Behavior Parameters in VISSIM 20

Model	Parameter	Setting	
		Non-CAV	CAV Truck Platooning
Autonomous Driving	Enforce absolute braking distance	Unselected	Unselected
	Use implicit stochasticity	Selected	Unselected
	Platooning possible	Unselected	Selected
	Max. number of vehicles	-	10
	Max. desired speed	-	112.65 km/h (70 mph)
	Max. distance for catching up to a platoon	-	250 m
	Gap time	-	0.70 s
	Minimum clearance	-	1.00 m
Following	Look ahead	Min 0 m; Max 250 m	Min 0 m; Max 300 m
	Number of interaction objects & vehicles	2 & 99	10 & 10

	Look back distance	Min 0 m; Max 150 m	Min 0 m; Max 150 m
	Behavior during recovery from speed breakdown		
	Slow recovery	Unselected	Unselected
	Speed	60%	60%
	Acceleration	40%	40%
	Safety Distance	110%	110%
	Distance	200 m	200 m
	Standstill distance for static obstacles	Unselected	Unselected
	Wiedemann 99		
	CC0 standstill distance	1.5 m	2.0 m
	CC1 gap time	0.90 s (constant)	0.90 s (constant)
	CC2 following variation	4.0 m	0.0 m
	CC3 threshold for entering following	-8.0	-6.0
	CC4 negative following threshold	-0.35	-0.10
	CC5 positive following threshold	0.35	0.10
	CC6 speed dependency of oscillation	11.44	0.0
	CC7 oscillation acceleration	0.25 m/s ²	0.10 m/s ²
	CC8 standstill acceleration	3.5 m/s ²	4.0 m/s ²
	CC9 acceleration with 80 km/h	1.5 m/s ²	2.0 m/s ²
Car	Following behavior depending on the vehicle class	None	Same as conventional traffic for all vehicles
	General behavior	Slow lane rule	Slow lane rule
	Necessary lane change (own & trailing vehicle)		
	Maximum deceleration	-4.0 m/s ² & -3.0 m/s ²	-4.0 m/s ² & -4.0 m/s ²
	-1 m/s ² per distance	200 m & 200 m	100 m & 100 m
	Accepted deceleration	-1.0 m/s ² & -0.5 m/s ²	-1.0 m/s ² & -1.5 m/s ²
	Waiting time before diffusion	60 s	60 s
	Min. clearance (front/rear)	0.5 m	0.5 m
	To slower lane if collision time is above	11 s	11 s
	Safety distance reduction factor	0.60	0.75
	Maximum deceleration for cooperative braking	-3.0 m/s ²	-6.0 m/s ²
	Overtake reduced speed areas	Unselected	Unselected
	Advanced merging	Selected	Selected
	Vehicle routing decisions look ahead	Selected	Selected
	Cooperative lane change	Unselected	Selected
	Maximum speed difference	-	10.8 km/h
	Maximum collision time	-	10.0 s
	Rear correction of lateral position	Unselected	Unselected
	Desired position at free flow	Middle of lane	Middle of lane
Lateral	behavior		
	Observed adjacent lane(s)	Unselected	Unselected
	Overtake on same lane	Unselected	Unselected
	Exceptions for overtaking vehicles	None	None

Note: driving behavior parameters were input in VISSIM 20.

The proposed methodology, using VISSIM 20 with the parameter sets described above, was applied to estimate the EC-PCEs for the case study. Because the goal of the CAV condition is to explore the effect of CAV truck platooning on the capacity of freeway segments, it was assumed only trucks could operate in CAV mode and the truck operational characteristics were the same as the non-CAVs. In other words, the only

difference between the trucks in the non-CAV condition and the trucks in the CAV condition is the trucks in the latter scenario could form platoons based on CAV logic.

It must be noted that the microsimulation model was not calibrated to capture the effect of lateral constrictions imposed by the facility and the traffic stream. It has been reported in the literature that some factors such as lane width, number of lanes, lateral clearance, and oversize vehicles, affect the operational performance of freeways. In this regard, VISSIM 20 included some parameters to model the lateral behavior of the driver-vehicle units, especially to restrict the overtaking maneuvers depending on the lateral frictions in the same lane or adjacent lanes. However, the analysis of these parameters was outside the scope of the test cases presented in this dissertation. It should be noted that if the proper empirical data were available, it would be possible to calibrate and validate the model using the proposed methodology.

7.6 Proposed Procedure for the EC-PCE Estimation

The main steps of the proposed procedure for the estimation of EC-PCEs are basically the same as those for the HCM-6 EC-PCE methodology, except that Steps 1 and 3 consider the approaches evaluated in this dissertation. The proposed procedure for the estimation of EC-PCE values is shown in **Figure 7-4**.

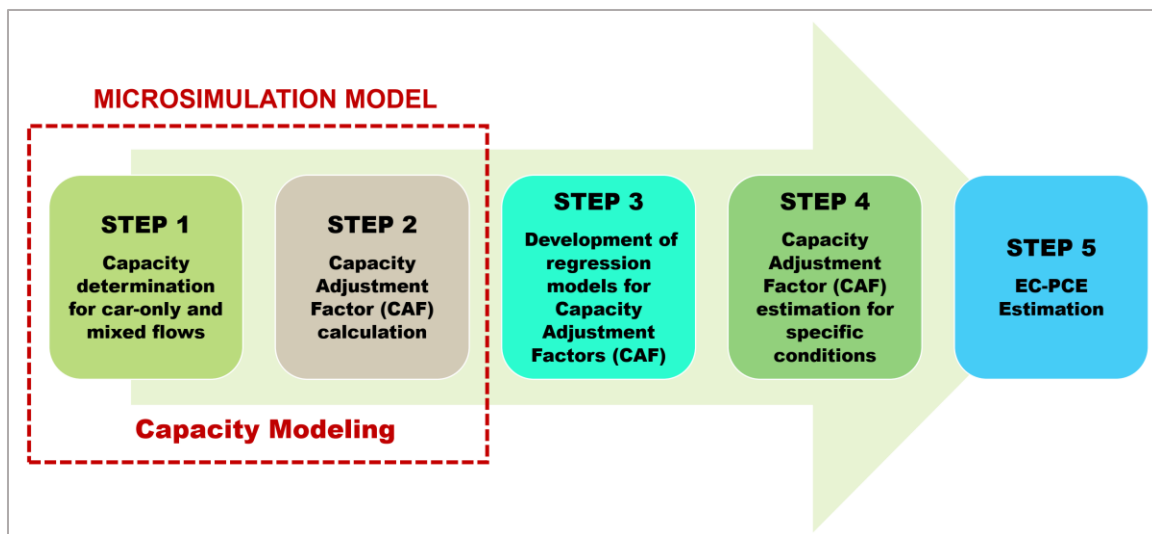


Figure 7-4. Proposed Process for EC-PCE estimation.

In Step 1, the simulated capacities, estimated using the calibrated VISSIM model, for both passenger car-only flow and mixed flow are identified for combinations of grade, grade distance, truck percentage, and vehicle fleet composition. In contrast to the original HCM-6 EC-PCE methodology, Step 1 uses a capacity definition (e.g., maximum flow rate) and data aggregation level (e.g., 15 minutes) in agreement with the HCM-6. In Step 2, the Capacity Adjustment Factors (CAFs) for all 1,274 scenarios estimated based on the VISSIM flow values from Step 1. A nonlinear regression model ($NLRM_{prop}$) is calibrated in Step 3 using the CAF values computed in Step 2 as input. Step 3 considers an alternative regression model structure (e.g., $NLRM_{prop}$) suitable for both non-CAV and CAV conditions as compared to the HCM-6 EC-PCE research. This $NLRM_{prop}$ is used to estimate CAF values as a function of the different truck percentage, vehicle composition, grade, and distance parameters analyzed in Step 1. In Step 4, these calibrated models are used to estimate CAFs. In Step 5, the EC-PCEs for specific combinations of truck

percentage, grade, and grade distance are estimated based on the CAF estimates from Step 4.

The procedure must be repeated for assessing each truck composition type considered in the analysis. For this case study, the empirical Western U.S. truck composition described above will be used for the EC-PCE estimation of both the non-CAV and CAV conditions. Typically, there are two approaches that have been used to account for the effect of trucks in the estimation of PCE values (Al-Kaisy, 2006): (1) an aggregate approach, and (2) a discrete approach. The aggregate approach provides PCE values based on the average operational performance of a typical fleet of trucks (e.g., combination of single unit trucks and tractor trailers). In contrast, the discrete approach divides the trucks into categories of performance and provides PCE values for each category. Note that the discrete approach was only used in the third version of the HCM (1985), while the aggregate approach has been consistently used in all the subsequent versions.

As the aggregate approach was used in the HCM-6 EC-PCE research, the proposed methodology presented in this Chapter will also assume the same treatment. However, it should be noted that the methodology can be used to analyze a single heavy vehicle type if desired by the user. This would allow to estimate PCEs for a specific heavy vehicle type which operational performance would greatly differ from the HCM assumptions, for instance, buses, recreational vehicles, or electric trucks. In this case, it is critical to perform an adequate calibration of the operational attributes of the subject vehicle in the microsimulation model, especially in terms of the weight to power ratio and acceleration and deceleration profiles.

Although most of the Steps have been discussed in previous chapters of this dissertation, this chapter will provide a detailed description of each Step of the proposed procedure, so the reader can readily follow the process and changes.

7.6.1 Step 1: Simulated Capacity Determination

In Step 1, the simulated capacity value of each scenario was obtained based on the VISSIM model output. Each scenario was simulated using five simulation replications and different random seeds. The same set of random seeds were used to evaluate all the scenarios. The input volume was gradually increased in increments of 50 veh/h/ln until reaching a volume capacity ratio of one. A total of 48 volume levels (e.g., 50, 100, 150, ..., 2,400 veh/h/ln) were considered in every run assuming a theoretical capacity of 2,400 veh/h/ln (e.g., HCM-6 base capacity). Each volume level consisted of 15 minutes of vehicle loading to achieve a steady-state condition and 15 minutes of steady-state for data collection. As a result, the simulation period comprised a total of 24 hours per scenario (e.g., 0.5 hour per volume level by 48 volume levels). It is important to note that the volumes were input following the protocols recommended in Appendix A of this dissertation to ensure ‘exact’ vehicles inputs in agreement with the data aggregation level (15 minutes). Similar to the original HCM-6 EC-PCE methodology, the scenarios were defined by a combination of the following factors:

- flow-rate types (f) either passenger car-only or mixed traffic flow,
- 13 levels of truck percentage (p) from 2% to 100%,
- 13 levels of grade (g) from -6% to 6%, and
- 7 levels of grade distance (d) from 0.40 km (0.25 mi) to 8.05 km (5.00 mi).

In total, there are 91 scenarios for the passenger car-only flow condition (e.g., 13 levels of grade x 7 levels of distance), and 1,183 scenarios for the mixed-traffic flow condition (e.g., 13 levels of truck percentage x 13 levels of grade x 7 levels of distance). The VISSIM model output consisted of the space mean speed and the flow rate collected at each detector per 15 minute interval in agreement with the HCM-6 data aggregation level. These outputs are used to compute the hourly flow rate, at 15 minute averages, for each combination using **Equations (7-1)** and **(7-2)**, respectively.

$$q_{f,t,p,m,g,d,r} = V_{f,t,p,m,g,d,r} * 4 \quad (7-1)$$

Where:

$q_{f,t,p,m,g,d,r}$: Flow rate for the f flow type at t time interval, p truck percentage level, m truck composition level, g grade level, d distance level, and r simulation volume level based on 15-min interval traffic volume recorded by the detector, (veh/h/ln).

$V_{f,t,p,m,g,d,r}$: 15-min interval traffic volume recorded by the detector for the f flow type at t time interval, p truck percentage level, m truck composition level, g grade level, d distance level, and r simulation volume level, (veh/min/ln).

$\bar{v}_{f,t,p,m,g,d,r}$: 15-min interval space mean speed for the f flow type at t time interval, p truck percentage level, m truck composition level, g grade level, d distance level, and r simulation volume level, (mph).

The proposed methodology uses a consistent definition of capacity with the HCM-6. In this case, the capacity of each scenario combination was defined as the maximum hourly flow rate for a 15 minute aggregation level. The simulated capacity for

each of the 1,274 scenarios was calculated using **Equations (7-1)** and **(7-2)**. The simulated capacity was averaged over the experimental replications. Five experimental replications were used in this case study.

$$C_{f,p,m,g,d} = \frac{\sum_{i=1}^n c_{i,f,p,m,g,d}}{n} \quad (7-2)$$

$$c_{i,f,p,m,g,d} = \underset{r=1,48}{\text{Max}}_{t=1} \{q_{f,t,p,m,g,d,r}\} \quad (7-3)$$

Where:

$C_{f,p,m,g,d}$: Simulated capacity at f flow type, p truck percentage level, m truck composition level, g grade level, d distance level, (veh/h/ln).

$c_{i,f,p,m,g,d}$: capacity for experimental replication i at f flow type, p truck percentage level, m truck composition level, g grade level, d distance level, (veh/h/ln).

n : Number of experimental replications for each scenario combination.

Max: Maximum value.

$q_{f,t,p,m,g,d,r}$: Flow rate for the f flow type at t time interval, p truck percentage level, m truck composition level, g grade level, d distance level, and r simulation volume level, based on one 15-min traffic volume recorded by the detector (veh/h/ln).

The hourly flow-rate and speed values can serve to populate scatter plots that describe this fundamental relationship. Each speed-flow scatter plot contains 240 pairs of flow-rate and speed values (e.g., 1 interval x 48 volume levels x 5 simulation runs).

Figure 7-5 through **Figure 7-7** are examples of speed-flow scatter plots for specific

scenario combinations that show the observations used to calculate the capacity values for every experimental replication (e.g., SR1 to SR5).

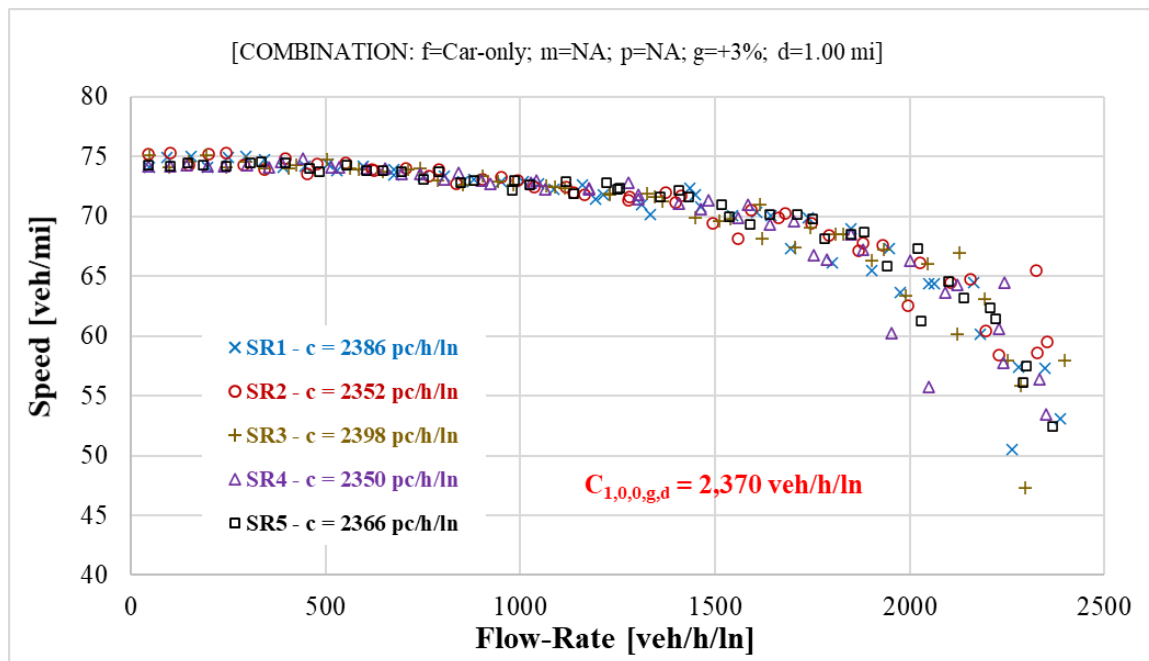


Figure 7-5. Passenger car only flow-speed scatter plot (grade 3%, distance 1 mi).

Figure 7-5 shows the speed versus flow-rate graph for the passenger car-only flow, 3% grade, and 1.61 km (1.0 mi) distance scenario. In general, it may be seen that after the breakpoint the speed decreases with the flow rate at an increasing rate. Using **Equation (7-2)**, the definition of capacity for the proposed methodology, the capacity is found to be 2,370 veh/h/ln. As was assumed in the case study that only trucks would operate as CAVs for the CAV truck platooning condition, the capacity values for the passenger car-only scenarios (e.g., 91 scenarios) will be the same for both the non-CAV and CAV conditions.

Figure 7-6 shows the speed versus flow-rate graph for the same conditions as **Figure 7-5** but for the mixed-traffic flow condition and a 20% truck percentage. It may

be seen that the speed decreases at a linear rate with the flow rate. A breakpoint occurs at approximately 400 veh/h/ln and the capacity value for this scenario combination is estimated to be 1,892 veh/h/ln.

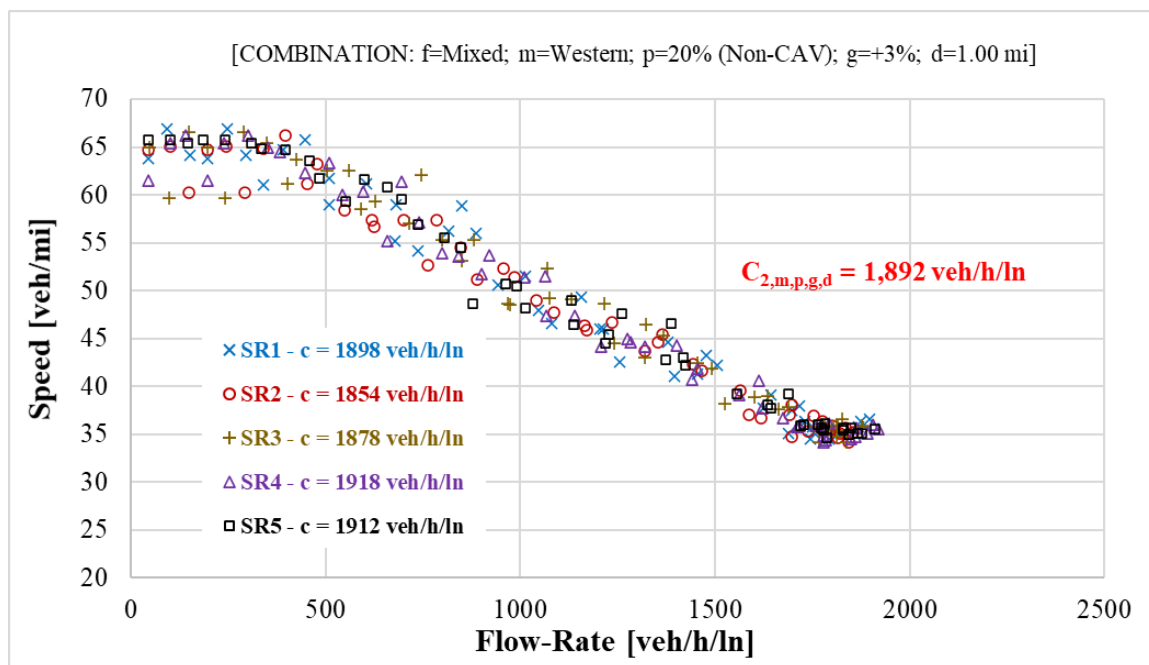


Figure 7-6. Mixed traffic flow-speed scatter plot for non-CAV condition (20% truck percentage, 3% grade, and 1 mi distance).

Figure 7-7 shows the speed-flow curve for the CAV condition for the same conditions as **Figure 7-6**. It may be seen that the breakpoint occurs at a higher flow value (e.g., 500 veh/h/ln). As well, the CAV capacity (e.g., 1,990 veh/h/ln) is approximately 5.2% percent higher than the equivalent non-CAV capacity (e.g., 1,892 veh/h/ln). It is hypothesized the higher capacity occurs due to the deployment of CAV truck platoons in the traffic stream, which vehicles present shorter headways, and reduced stochasticity as compared to non-CAVs.

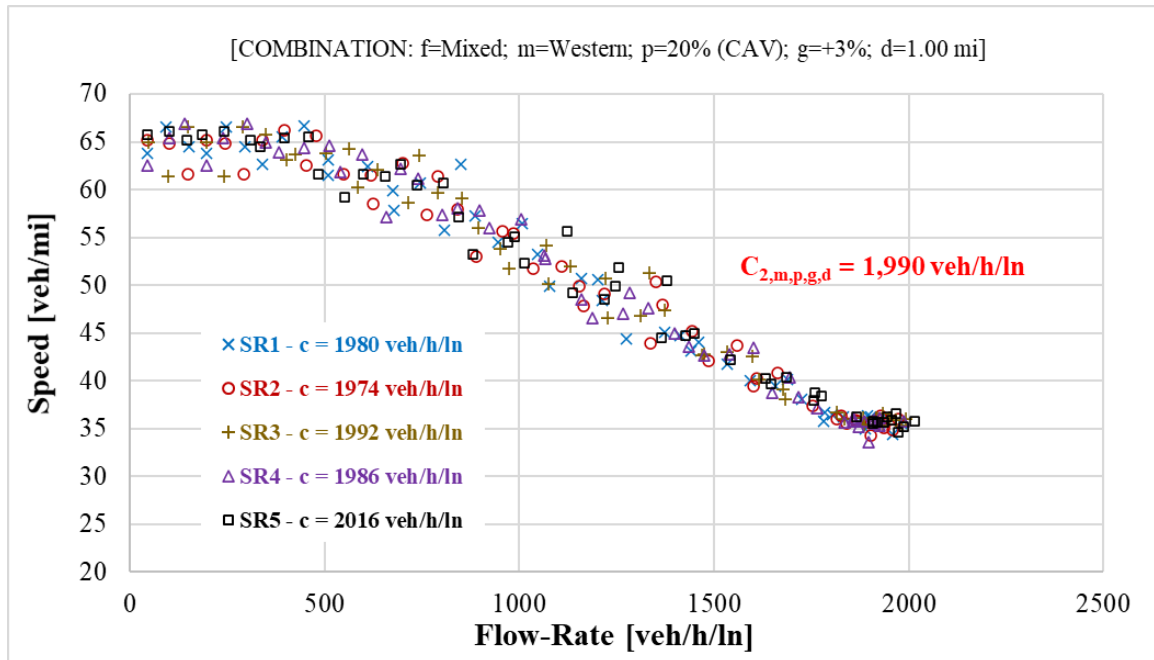


Figure 7-7. Mixed traffic flow-speed scatter plot for CAV condition (20% truck percentage, 3% grade, and 1 mi distance).

7.6.2 Step 2: Simulated CAFs Computation

In this step, the capacity adjustment factors (CAFs) for each scenario are calculated using the simulated capacity results from Step 1. These are calculated for the mixed flow and passenger car-only flow scenarios using **Equations (7-4)** and **(7-5)**, respectively. These equations use the capacity of each scenario obtained from the flow-density scatter plots from Step 1.

$$CAF_{2,p,m,g,d} = \frac{C_{2,p,m,g,d}}{C_{1,0,0,g,d}}; \forall p = 1, P; \forall m = 1, M; \forall g = 1, G; \forall d = 1, D \quad (7-4)$$

$$CAF_{1,0,0,g,d} = \frac{C_{1,0,0,g,d}}{C_{1,0,0,g,d}} = 1; \forall g = 1, G; \forall d = 1, D \quad (7-5)$$

Where:

$CAF_{2,p,m,g,d}$: Capacity adjustment factor for the mixed flow at p truck percentage level ($P = 13$), m truck composition level ($M = 3$), g grade level ($G = 13$), d distance level ($D = 7$).

$CAF_{1,0,0,g,d}$: Capacity adjustment factor for the auto-only flow at g grade level ($G = 13$), d distance level ($D = 7$).

$C_{2,p,m,g,d}$: Capacity for the mixed flow at p truck percentage level, m truck composition level, g grade level, d distance level, (veh/h/ln).

$C_{1,0,0,g,d}$: Capacity for the auto-only flow at g grade level, d distance level, (veh/h/ln).

To illustrate, consider the scenario defined by mixed flow ($f=2$), 20% truck percentage ($p=5$), 30/70 SUT/TT truck composition ($m=1$), +3% grade ($g=10$), and 1.61 km (1.0 mi) distance ($d=4$). The passenger-car only and mixed traffic scatter plots for this situation were shown in **Figure 7-5** and **Figure 7-6**, respectively. Using **Equation (7-4)** the Capacity Adjustment Factor for this situation ($CAF_{2,5,1,10,4}$) is 0.798 (1,892/2,370). The process is analogous for the CAV condition. This calculation is repeated for the other 1,273 scenarios using either **Equation (7-4)** or **(7-5)**, as appropriate, for the given flow type.

The CAF values computed in this step (e.g., CAF-sim) for both the non-CAV and CAV truck platooning conditions are shown in **Figure 7-8**. The x-axis represents the scenario number. Each specific scenario number is calculated using **Equation (7-6)** and is a function of the truck percentage, grade, and distance. There were 14 truck percentage values (including 0%) and these are shown on the top of **Figure 7-8**. The thin red line

represents the simulated CAFs from the non-CAV condition and the thin blue line the simulated CAFs from the CAV condition. The thick red and blue lines represent the estimated CAF values discussed later in Step 4. For a given truck percentage, the CAFs for grade and grade distance are shown in order. The general form is a flat straight line for the negative and zero grade scenarios, followed by decreasing CAF values for the positive grade values.

$$n = 91 * p + (g - 1) * 7 + d \quad (7-6)$$

Where:

n : Scenario number.

p : Ordinal number of truck percentage level, $p = 1, 2, \dots, P$, means 2-100% truck percentage.

P : Total levels of truck percentage, $P = 13$.

g : Ordinal number of grade level, $g = 1, 2, \dots, G$, means -6% to 6% grade.

G : Total levels of grade, $G = 13$.

d : Ordinal number of distance level (the level of detector location), $d = 1, 2, \dots, D$, means 0.40-8.05 km (0.25-5.00 mi).

D : Total levels of distance (detector location), $D = 7$.

7.6.3 Step 3: Regression Models Development

To perform a fair comparison between the non-CAV condition and the CAV truck platooning condition, the estimated CAFs should be obtained using the same regression model structure. This chapter proposed a nonlinear regression model with 8-model parameters to be calibrated using the simulated CAF values as input. The proposed

nonlinear regression model (NLRM_{prop}) is based on the reduced nonlinear regression model (NLRM_{red}) developed in Chapter 5 of this dissertation. However, the proposed regression model adds the same polynomial form for the truck percentage effect developed in Chapter 3 of this dissertation for the CAV condition. This decision was based on the assumption that the NLRM_{prop} model can be suitable for both non-CAV and CAV truck platooning conditions. The proposed regression model is shown in **Equation (7-7)**.

$$CAF_{2,p,m,g,d,FFS} = CAF_{1,0,0,g,d} + \alpha_{12,m,FFS}^{T_a} * (p_s)_p^{\beta_{12,m,FFS}^{T_a}} + \alpha_{22,m,FFS}^{T_a} * (p_s)_p^{\beta_{22,m,FFS}^{T_a}} + \alpha_{2,m,FFS}^{G_a} * (g_s)_g^{\beta_{2,m,FFS}^{G_a}} * \left[1 - \alpha_{2,m,FFS}^{D_a} * e^{\beta_{2,m,FFS}^{D_a} * (d_s)_d} \right] * D \quad (7-7)$$

Where:

$CAF_{2,p,m,g,d}$: Capacity adjustment factor for the mixed flow ($f = 2$) at p truck percentage level, m truck composition level, g grade level, d distance level, and FFS free-flow speed.

$CAF_{1,0,0,g,d}$: Capacity adjustment factor for the auto-only flow at g grade level, d distance level. This value is assumed to be 1.

$(p_s)_p$: Truck percentage at p truck percentage level (between 0 and 1).

$(g_s)_g$: Grade at g grade level (between -0.06 and 0.06).

$(d_s)_d$: Distance of grade at d distance level (mile).

D : Dummy variable, if $(g_s)_g > 0$ then $D = 1$, otherwise $D = 0$.

$\alpha_{12,m,FFS}^{T_a}$, $\alpha_{22,m,FFS}^{T_a}$, $\beta_{12,m,FFS}^{T_a}$, $\beta_{22,m,FFS}^{T_a}$, $\alpha_{2,m,FFS}^{G_a}$, $\beta_{2,m,FFS}^{G_a}$, $\alpha_{2,m,FFS}^{D_a}$, $\beta_{2,m,FFS}^{D_a}$:

Parameters for capacity adjustment factor for truck percentage effect (T_a), grade effect (G_a), and distance effect (D_a).

The proposed model has eight parameters and a dummy variable (D) related to whether the section being analyzed has a grade that is positive or non-positive. It may be seen when the grade is positive the explanatory variables are truck percentage (p), grade (g), and distance (d). Conversely, when the grade is negative or level, truck percentage (p) is the only explanatory variable. Although the truck percentage effect has a polynomial form, this effect is still independent of the combined effect of grade and distance as was discussed in Chapter 5 of this dissertation. In addition, the free-flow speed (FFS) and the truck composition type (m) effects are set constant for all situations. This is similar to the original HCM-6 nonlinear regression model (NLRM).

7.6.4 Step 4: CAFs Estimation for Specific conditions

In this step, the CAFs for the mixed flow scenarios are estimated for specific conditions (CAF_{2,p_s,m_s,g_s,d_s}). The parameters of interest are truck percentage p_s , grade g_s , and distance d_s . These estimated CAFs are obtained using **Equation (7-7)** based on the estimators obtained from the regression model calibration (Step 3).

7.6.5 Step 5: EC-PCEs Estimation

In the last step of the methodology, the EC-PCEs ($EC - PCE_{2,p_s,m_s,g_s,d_s}$) at specific conditions of truck percentage p_s , grade g_s , and distance d_s , are calculated using **Equation (7-8)**.

$$EC - PCE_{2,p_s,m_s,g_s,d_s} = \frac{1 - (1 - p_s) * CAF_{2,p_s,m_s,g_s,d_s}}{p_s * CAF_{2,p_s,m_s,g_s,d_s}} \quad (7-8)$$

Where:

$EC - PCE_{2,p_s,m_s,g_s,d_s}$: EC-PCE for the mixed flow at truck percentage p_s , truck composition m_s , grade g_s , and distance d_s .

CAF_{2,p_s,m_s,g_s,d_s} : Capacity adjustment factor for the mixed flow at truck percentage p_s , truck composition m_s , grade g_s , and distance d_s .

p_s : Truck percentage (between 0 and 1).

7.7 Calibrated Regression Model Results

The calibrated nonlinear regression model (NLRM_{prop}) for the non-CAV condition and the CAV truck platooning condition are shown in **Equations (7-9)** and **(7-10)**, respectively. These equations were used to calculate the estimated CAF values for the mixed traffic condition for both analyses. The calibrated parameters were estimated using the Generalized Reduced Gradient (GRG) method (Lasdon, Fox, & Ratner, 1974) where the target goal was to minimize the sum of squared errors between the simulated CAFs obtained in Step 2 and the estimated CAFs given by the proposed regression model shown in **Equation (7-7)**.

- CAFs for the Non-CAV condition ($m = \textit{Western US}$):

(7-9)

$$CAF_{mix} = 1 - 8.498 * (p_s)^{1.13} + 8.007 * (p_s)^{1.18} - 7.119 * (g_s)^{1.30} * [1 - 1.382 * e^{-2.55*(d_s)}] * D$$

- CAFs for the CAV condition ($m = \textit{Western US}$):

(7-10)

$$CAF_{mix} = 1 - 8.335 * (p_s)^{1.22} + 8.173 * (p_s)^{1.29} - 8.119 * (g_s)^{1.30} * [1 - 1.382 * e^{-2.55*(d_s)}] * D$$

The above equations can be used in combination with **Equation (7-8)** to estimate the EC-PCE value directly for a given scenario. Note an EC-PCE can be calculated for any combination of truck percentage, grade, and distance using the calibrated regression models. For example, consider the scenario defined by an 34% truck percentage ($p_s=0.34$), a +4.1% grade ($g_s=0.041$), a distance of 0.875 mi ($d_s=0.875$), for the CAV condition under Western U.S. conditions. Using **Equation (7-10)** the Capacity Adjustment Factor for this situation (CAF_{mix}) is 0.690. Using this value as input in **Equation (7-5)**, the EC-PCE is estimated to be 2.32. Note that using **Equation (7-9)** the EC-PCE value is 2.71 for the non-CAV condition.

Table 7-2 shows the statistics calculated for assessing the goodness-of-fit of the calibrated regression models. For the non-CAV condition, the statistics expose a very good fit with an approximate R-squared value of 0.98 for the calibrated model shown in **Equation (7-8)**. Although the goodness-of-fit statistics for the CAV truck platooning condition is slightly poorer (e.g., R-squared value of 0.93), as revealed by the residual standard error (S) and the coefficient of determination (R^2), its performance is very close to the non-CAV condition. Note these R-squared values are higher than those discussed in Chapter 4 of this dissertation, especially for the CAV condition.

Table 7-2. Goodness-of-Fit Statistics for Estimated CAF values

Statistic	Non-CAV Condition	CAV Truck Platooning Condition
	NLRM _{prop}	NLRM _{prop}
SSE	1.037	1.119
SST	43.86	16.57
N	1274	1274
P	8	8
$S = \sqrt{MSE}$	0.029	0.030

R_{adj}^2	0.98	0.93
MAPE	3.50%	2.70%

Note: $NLRM_{prop}$ = proposed nonlinear regression model; SSE = sum of squared error; SST = sum of squared total; N = number of observations; P = number of regression parameters; S = residual standard error; R_{adj}^2 = adjusted coefficient of determination; MAPE = mean absolute percentage error.

7.8 Comparison of Estimated CAF Results

The estimated CAF results were estimated using the calibrated regression models shown in **Equations (7-9)** and **(7-10)** for the non-CAV and CAV conditions, respectively. A comparison between the estimated CAFs for the CAV condition and the estimated CAFs for the non-CAV condition (e.g., conventional traffic) are shown in **Figure 7-8**. The thick blue line represents the CAV condition and the thick red line the non-CAV condition. The scenario number (horizontal axis) is given by **Equation (7-6)** and corresponds to a particular combination of truck percentage, grade, and distance was used to compute the corresponding CAF. For the non-CAV condition, the CAF values decrease as truck percentage increases and this decrease is at a fairly linear rate. In contrast, for the CAV condition the CAF values decrease as the percentage of trucks increase until a 50% truck percentage is reached. After this point, the CAF values increase with the truck percentage. For truck percentages of less than 10 percent, the CAF values are similar to the non-CAV condition. It is hypothesized this occurs because there are less opportunities for truck platoon formation. Interestingly, when trucks are 100 percent of the vehicle stream the CAF values are approximately 16.3 percent lower than the CAF for passenger cars at level grade conditions. That is, a traffic stream with 100% CAV will have a maximum vehicle flow rate of 2,009 veh/h/ln as compared to the 100% passenger cars scenario (e.g., 2,400 veh/h/ln) under the Western U.S. conditions. Taking as reference the truck percentage interval from 10% to 100% (scenarios 274 to 1274), the CAF values for

the CAV condition are, on average, 25.4% higher (ranging from 0.1% to 92.8%) than those of the non-CAV condition.

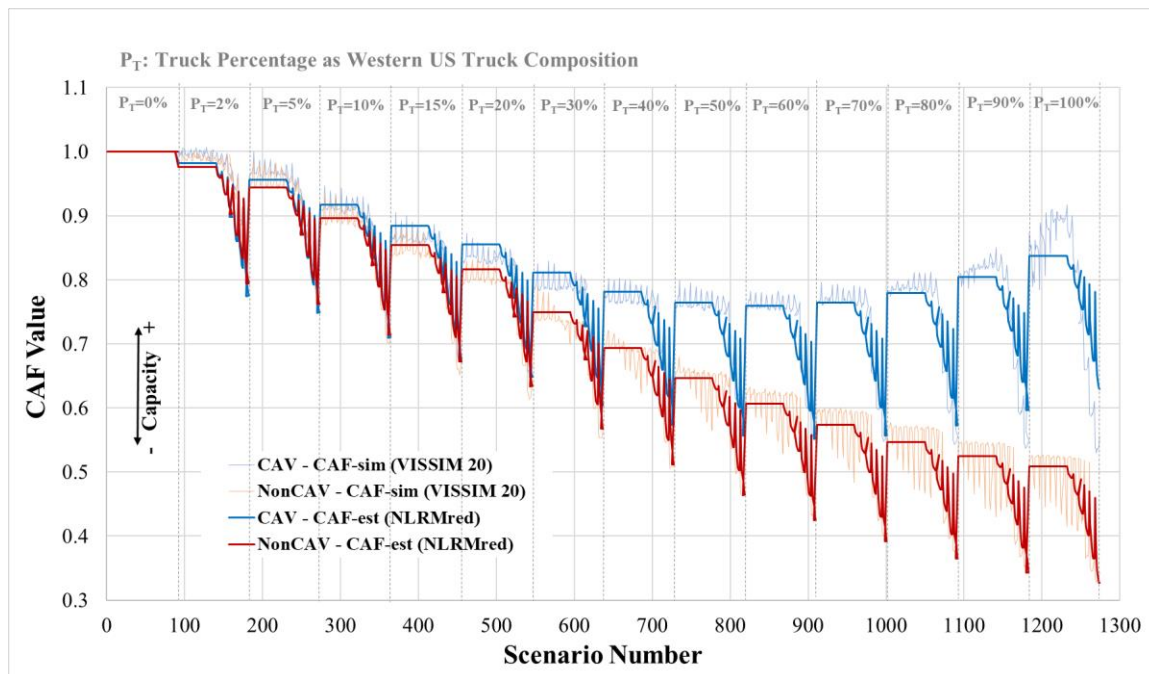


Figure 7-8. CAF values for four lane freeways as a function of scenario number: CAV and non-CAV scenarios.

7.9 Comparison of EC-PCE Results

The EC-PCE values were estimated for ten levels of truck percentage (i.e., 10% to 100% in 10% increments), grade (i.e., 0%, +3%, and +6%), and distance (i.e., 0.8 km (0.5 mi), 1.61 km (1.0 mi), and 2.42 km (1.5 mi)). **Figure 7-9** shows the corresponding EC-PCE values as a function of truck percentage for the three levels of grade and three levels of distance for both the CAV condition and the non-CAV condition. The solid lines represent the CAV truck platooning EC-PCE values and the dotted lines the non-CAV (e.g., only conventional traffic) EC-PCE values. The EC-PCE values were calculated using **Equation (7-8)**. Any specific condition within the explored range of truck

percentage, grade, and distance considered in the proposed methodology can be computed using the calibrated CAF models shown in **Equations (7-9) and (7-10)**. On average, the EC-PCE values for the CAV condition are 24.4% lower than those of the non-CAV condition indicating the CAV technology lessens the impact of heavy trucks on traffic operations of four-lane freeways in the Western U.S.

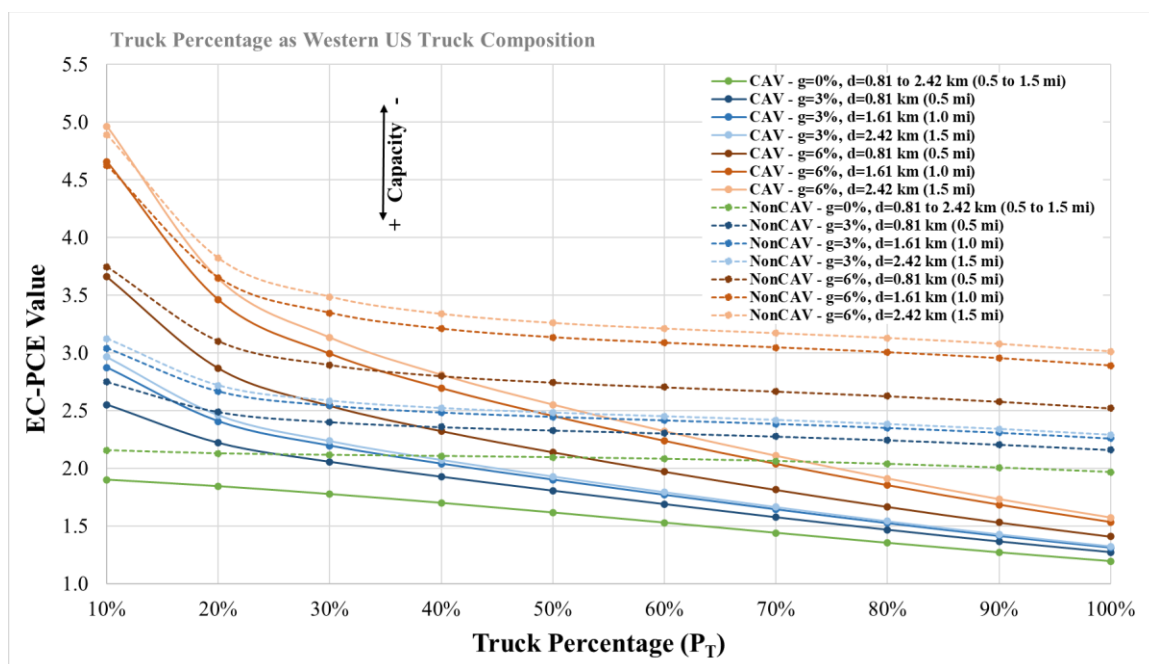


Figure 7-9. EC-PCE values for four-lane freeways as a function of truck percentage: CAV and non-CAV scenarios.

For both the CAV and non-CAV conditions, the maximum EC-PCE values occur at a truck percentage of 10%. These values range from 1.9 to 4.9. In general, as grade and distance increase so does the EC-PCE. For higher truck percentages, the EC-PCE values for the non-CAV condition tend to decrease as truck percentages increases. After a 50% truck percentage value this decrease occurs at a mild rate. In general, the EC-PCE ranges from 2.0 to 4.9 for the non-CAV condition. Similarly, for the CAV condition the EC-PCE

decrease at a smaller rate as percentage of trucks increase. However, the EC-PCE shows a more noticeable decrease for the CAV condition ranging from 1.2 to 4.7. As would be expected from the earlier analysis, as truck percentage approaches 100 percent the EC-PCE value approaches 1.

Interestingly, the PCE values for the non-CAV condition under the Western U.S. (e.g., four-lane freeways) were, on average, 7.5% higher compared to those that were published in the HCM-6. These results were consistent with the results reported by Zhou, Rilett, and Jones (2019) in the analyses of moving bottlenecks on four-lane freeways. This finding suggests that the PCE values reported in the HCM-6, which were based on six-lane freeways (three-lanes per direction) and the set of assumptions discussed in Chapter 3 of this dissertation, may underestimate the effect of trucks in capacity and level of service analyses for the western rural U.S. This means that the actual capacity and level of service value that can be observed in this region could be lower than the values given by the core methodologies of the HCM-6.

In summary, the CAV technology increases capacity for a given scenario under the Western U.S. conditions, all else being equal, and this results in corresponding lower EC-PCE values. The increase in capacity for a given scenario is a function of the grade, grade length, and percentage trucks in the scenario. This comparison is for trucks equipped with CAV technology. It is hypothesized if the passenger cars also had CAV platoon technology then the capacity increase shown in **Figure 7-9** would be even greater. However, it is unclear how the EC-PCE values would change without a detailed simulation study, which is beyond the scope of this chapter.

7.10 Concluding Remarks

The objective of this chapter was to analyze the effect of CAV truck platooning on four-lane freeway segments using the new EC-PCE methodology proposed in this dissertation. It was argued the proposed methodology produces more consistent and comparable capacity, CAF, and EC-PCE values to be used in the core methodologies of the HCM-6. The proposed methodology was illustrated taking as a case study the western rural U.S. This region is characterized by four-lane freeways, high truck percentages, and significant speed differentials between cars and trucks that violate various assumptions considered in the original HCM-6 EC-PCE research. In the case study, empirical data (e.g., Western U.S.) was used to estimate EC-PCEs for two traffic conditions: (1) non-CAVs and (2) CAV truck platooning. A VISSIM 20 model was calibrated to match the HCM-6.1 capacity values (e.g., 2,400 pc/h/ln for non-CAVs and 3,200 pc/h/ln for CAVs) to ensure comparable metrics with the HCM-6. In addition, a simpler nonlinear regression model suitable for non-CAVs and CAVs scenarios was used to perform a fair comparison between the two conditions. It is important to note this model showed a very good fit in both cases. Finally, the impact of CAV technology on freeway capacity was quantified using the estimated CAF values and the resulting EC-PCE values.

Not surprisingly, it was found CAV truck platoons have the potential to increase capacity on four-lane freeway segments, all else being equal. This finding was consistent to that for six-lane freeways discussed in Chapter 3 of this dissertation. In this case study, the EC-PCE values for the CAV truck platooning condition, which assumed a 100% CAV market penetration rate for trucks, were approximately 24.4% lower, on average,

than those for the non-CAV condition. In other words, CAV trucks have a lower impact on freeway operations than non-CAV trucks.

In addition, it was found CAV truck platooning has the greatest effect when the truck percentage is greater than 30 percent. For truck percentage values below this cut-off, the metrics tended to show similar values between the non-CAV and CAV conditions. It was hypothesized this occurred because the proportion of CAV trucks was such that the resulting truck platoons, and associated truck platoon size, were not enough to influence the capacity of the freeway segment. This finding indicates CAV trucks may have the greatest impact in areas that have higher percentage truck values such as in the Western U.S.

Another interesting finding was that the PCE values for non-CAVs (e.g., only conventional vehicles) under the Western U.S. condition were higher than the published values in the HCM-6. This implies that the capacity and level of service values obtained from the core methodologies in the HCM-6 would be overestimated for the western rural U.S. It is recommended to explore to what extent the traffic metrics that have been considered for the analysis of freeway segments in the HCM-6 could be representative of the Western U.S. conditions, given that a significant part of the underlying research in the HCM has been mostly focused on other US regions such as the East or West coast. This would help to improve the reliability of the capacity and level of service analyses for the freeway system located in this important region of the U.S. where the proportion of trucks in the traffic demand has been reported above the average U.S. values.

An additional benefit of the proposed methodology is that the same procedure can be used to obtain PCE values for a single heavy vehicle type (e.g., buses, recreational

vehicles, etc.). The case study that was used to illustrate the proposed methodology considered the effect of trucks using an aggregate approach as occurred with the original HCM-6 EC-PCE methodology. This is that the effect of trucks on the traffic stream was derived from a specific combination of trucks (e.g., empirical Western US truck composition). However, heavy vehicles can be also treated using a discrete approach where they are divided into categories of performance, and the PCE values are estimated for each category. The proposed methodology is flexible enough to be used for this purpose. Under this approach, it will be needed to calibrate the operational characteristics of the subject heavy vehicle type (e.g., weight and power distributions, acceleration/deceleration profiles, etc.) in the microsimulation model. This is critical for the reliability of the PCE results.

Despite the various advantages provided by the proposed approach, there are some important limitations that require further review. For example, the microsimulation model was not calibrated to capture the effect of lateral constrictions on the traffic stream. It has been reported in the literature that some factors such as lane width, number of lanes, lateral clearance, and oversize vehicles, affect the operational performance of freeways. In this regard, the driving behavior in VISSIM 20 includes some parameters for modeling the lateral behavior of vehicles. However, these model parameters have not been sufficiently explored while modeling the behavior of vehicles under lateral frictions. An adequate modeling of the lateral effect is important because it has been reported that CAVs would be less sensitive to the lateral conditions of freeways compared to conventional vehicles. This would represent another benefit of CAV technologies on the capacity of freeways that should be further explored.

It is recommended to perform a similar sensitivity analysis as discussed in Chapter 3 of this dissertation to explore the effect market penetration rate, platoon truck type, lane restriction, and platoon size. It is hypothesized the effect of these variables will be different for four-lane freeways as compared to six-lane freeways. This was not explored due to time constraints. In addition, it is recommended some driving behavior and operational characteristics such as interplatoon spacing, platoon forming logic, weight and power distributions, acceleration profiles, etc., be studied. These parameters were not studied in this chapter due to the lack of empirical data related to these topics. This is an area of potential research that would further help transportation agencies as they begin the transition to CAV operations.

Finally, it was observed most of the capacity values in the set of scenario combinations occurred at saturated flow conditions (e.g., queue discharge flow). Although the proposed methodology calibrated the microsimulation model targeting an empirical capacity value (e.g., HCM-6 base capacity), the simulated capacity of each scenario was computed using a deterministic approach (e.g., maximum flow rate) as occurred in the original HCM-6 research (e.g., 95th percentile of the maximum flow rate). This deterministic approach does not ensure the capacity values are taken from undersaturated flow conditions as suggested in the HCM-6 (e.g., maximum prebreakdown flow rate). It is hypothesized a stochastic method for computing the capacity values of each scenario (e.g., breakdown capacity method) could yield different capacity and EC-PCE values. It is recommended to explore the extent a stochastic determination of capacity may change EC-PCE results. In this regard, it is recommended to calibrate the microsimulation model taking as a reference not only the base capacity

value but also the corresponding speed-flow curve for basic freeway segments used in the HCM-6 (e.g., *Exhibit 12-7*). The reliability and consistency of the EC-PCE values will improve to the extent that the capacity of each scenario is better estimated.

CHAPTER 8

CONCLUDING REMARKS AND RECOMMENDATIONS

This chapter provides a synopsis of the main findings of the research presented in this dissertation. A special emphasis is given on those results that correspond to the objectives of this research. Finally, a section that provides recommendations for future research is also included.

8.1 Concluding Remarks

Passenger car equivalencies (PCEs) are used to account for the effect of different vehicle types on capacity and quality of service of a mixed traffic stream. In the current version of the Highway Capacity Manual, Sixth Edition (HCM-6), the equal capacity passenger car equivalencies (EC-PCE) methodology was used to estimate EC-PCEs for heavy trucks on freeway and multilane highway segments. These EC-PCEs are widely used in the HCM-6 to convert a mixed traffic stream of passenger cars and trucks to a single uniform passenger car stream for purpose analysis.

The EC-PCEs for freeway segments were estimated using a microsimulation-based methodology where the capacity of the mixed-traffic and car-only flow scenarios were modeled. It is important to note the HCM-6 EC-PCE methodology has a large number of assumptions including those related to vehicle speed (e.g., all vehicles travel at the same uniform free-flow speed of 70 mph), vehicle type (e.g., two types of trucks: single unit and semitrailer), weight and power ratios, driving behavior (e.g., Wiedemann 99 model, slow lane rules, etc.), operating conditions (e.g., three-lanes per direction, no lane restriction, etc.), capacity definition (95th percentile of the maximum flow rate), and

aggregation level (one minute). Therefore, care must be taken in using the EC-PCE values published in the HCM when these key assumptions are not appropriate for a particular analysis.

It was argued in this dissertation the HCM-6 EC-PCE procedure can be used to analyze novel traffic situations including those related to CAV technologies. However, the following issues have been identified with the current HCM-6 EC-PCE methodology:

- 1) The EC-PCEs were estimated under assumptions atypical of past HCM releases including a new definition of capacity (e.g., 95th percentile of the maximum flow rate) and a new data aggregation level (e.g., one minute). These assumptions affect the consistency of the results with the traffic metrics used in the HCM-6.
- 2) The microsimulation model used for capacity modeling was originally developed for a VISSIM version no longer available, affecting the experimental replication of the procedure. In addition, the microsimulation model was not calibrated to target an empirical capacity value (e.g., HCM-6 base capacity for basic freeway segments) to produce compatible outputs with the HCM-6. This is critical because the capacity is an input to the EC-PCE calculation.
- 3) The nonlinear regression model used in the original HCM-6 research for fitting simulated and estimated data has a relatively complex model structure that makes the interpretation difficult of the traffic metrics and the process of reporting results. Equally important, the model structure is not flexible enough for modeling new traffic situations such as CAV truck platooning. This is

critical because the original regression model structure may limit the potential of the methodology to analyze further traffic situations.

The main objective of this dissertation was to develop a new microsimulation-based methodology that can be used with the current Highway Capacity Manual (HCM-6) for capacity modeling and the estimation of CAF and EC-PCE values at freeway and multilane highway segments. Another major objective was to demonstrate how the proposed approach can be further used to analyze new traffic situations such as the deployment of CAV truck platooning on freeways. The following sections provides a summary of the findings for each specific objective defined in this dissertation.

8.1.1 Use the Exact HCM-6 EC-PCE Methodology for Exploring CAV Truck Platooning

This dissertation argued that to understand the potential impact on the freeway system of CAV technologies, analyses should be conducted using the standard US methodological framework. Consequently, the exact Highway Capacity Manual, Sixth Edition (HCM-6) equal capacity passenger car equivalencies (EC-PCE) methodology was used to estimate capacity and EC-PCEs for CAV truck platoons on freeway segments.

It was found EC-PCE values for CAV trucks are, on average, 34.3% lower as compared to the values for non-CAV trucks, indicating CAV platoons can have a positive effect on freeway capacity. The amount of decrease is a function of a number of CAV operational assumptions and these were studied through a sensitivity analysis. This analysis demonstrated the effect of CAV truck platoons can be modeled using the standard HCM-6 approach. However, a number of issues were identified that required

further assessment including a need for consistent metrics, a more robust microsimulation framework, and a more flexible and simpler regression model structure.

8.1.2 Assess the Convenience of Alternative Regression Model Structures

The HCM-6 EC-PCEs for freeway segments were estimated using a microsimulation-based methodology where the capacity of the mixed-traffic and car-only flow scenarios were modeled. A nonlinear regression model (NLRM) was used to develop capacity adjustment factor (CAF) models using the microsimulation data as input. The NLR model has a complex model structure and includes 15 model parameters. This dissertation developed alternative and simpler regression models of CAFs needed to derive the EC-PCE values in the HCM-6 methodology for freeway and multilane highway segments.

It was found simpler regression models provided similar results as those obtained with the current NLRM model. Additionally, it was found the current NLRM model may not be adequate for analyzing CAV traffic conditions. It was concluded if the HCM-6 EC-PCE methodology is expected to be used to analyze traffic conditions beyond the scope of the HCM-6, it is important to perform a deeper assessment of the form and error of the regression models used in fitting the simulated and estimated data.

8.1.3 Propose Simpler Equations to Calculate and Interpret CAFs and EC-PCEs

It was hypothesized because of the complexity of the existing 15 parameter model structure, the HCM-6 EC-PCE values were reported using a set of tables (e.g., HCM-6, Exhibits 12-26, 12-27, and 12-28). These tables are used to identify the required EC-PCE values for a given scenario (e.g., grade, grade distance, truck composition, and truck

percentage). This dissertation proposed a simpler nonlinear regression model with 6 model parameters that can be used for the estimation of CAF values and EC-PCE values for freeway and multilane highway segments under conventional traffic.

It was found the proposed model can readily substitute the original model with little loss in fidelity. Equally important, the CAF formulae developed in this dissertation can be used to calculate EC-PCE values directly, obviating the need for the HCM-6 EC-PCE tables and interpolations. In addition, the marginal effects of the two main contributors in the proposed CAF model, truck percentage and combined effect of grade and distance, were discussed in this dissertation. This provides the user with a better understanding of the trade-offs between capacity, CAF, and EC-PCE values and the parameters that affect them.

8.1.4 Propose a New Microsimulation Framework and Evaluate its Impact on HCM-6 EC-PCEs

The current HCM-6 EC-PCEs were estimated under assumptions atypical of past HCM releases including a new definition of capacity (e.g., 95th percentile of the maximum flow rate) and a new data aggregation level (e.g., one minute). It is important to assess to what extent these assumptions may affect the PCE values published in the HCM-6.

Consequently, this dissertation compared the HCM-6 EC-PCEs, and associated capacity adjustment factors (CAF), with values developed using the HCM-6 EC-PCE methodology with historic HCM assumptions. In addition, the microsimulation model was calibrated to match the HCM-6 base capacity value for freeway segments to ensure consistent and comparable results.

It was found the EC-PCE values from the proposed approach were, on average, 15.9% greater than those obtained in the original research. This finding suggests the values published in the HCM-6 could underestimate the effect of trucks in capacity and level of service analyses. Moreover, this analysis demonstrated the capacity definition, the data aggregation level, and the calibration of the microsimulation model have a significant impact on the EC-PCE results. These aspects must be considered when the HCM-6 EC-PCE methodology is used to analyze further traffic scenarios.

8.1.5 Develop an Improved EC-PCE Methodology for Novel Traffic Scenarios

An improved methodology that addresses the limitations of the HCM-6 EC-PCE methodology was developed. In contrast to the HCM-6 methodology, the proposed methodology used consistent metrics to the HCM-6, a replicable procedure based on a calibrated VISSIM model, and a more flexible and simpler regression model structure for fitting simulated and estimated data. The proposed regression model is easy to interpret and facilitate the process of reporting results (e.g., analytical equations instead of tables and interpolated values). The improved methodology can be used to estimate CAF and EC-PCE values for novel traffic scenarios including those related to CAV technologies.

The improved methodology was illustrated using the Western U.S. conditions as a case study. Two traffic conditions were explored: (1) non-CAVs and (2) CAV truck platooning. It was demonstrated the proposed procedure was able to estimate CAF and EC-PCE values for non-CAV and CAV conditions.

It was found CAV truck platoons have the potential to increase capacity on four-lane freeway segments, all else being equal. The EC-PCE values for the CAV truck platooning condition, which assumed a 100% CAV market penetration rate for trucks,

were approximately 24.4% lower, on average, than those for the non-CAV condition. In other words, CAV trucks have a lower impact on freeway operations than non-CAV trucks. In addition, it was found CAV truck platooning has their greatest effect when the truck percentage is greater than 30 percent. For truck percentage values below this cut-off, the metrics tended to show similar values between the non-CAV and CAV conditions. This finding indicates that CAV trucks may have the greatest impact in areas that have higher percentage truck values such as the Western U.S.

The new techniques proposed in this dissertation for capacity modeling and EC-PCE estimation are expected to be applied for any traffic condition beyond the scope of the HCM-6. The proposed approach will provide a more flexible and repeatable procedure that can be used by engineers and traffic agencies for generic purposes. It is vital all the future capacity and EC-PCE analyses are performed using the same standard methodological framework to produce comparable results that can be applied consistently into the core methodologies described in the HCM-6.

8.2 Future Research

In some chapters of this dissertation, the analyses were performed considering a 30/70 SUT/TT truck composition type, the most common in the rural U.S. The same procedure can be repeated for the remaining truck composition types considered in the HCM-6 (e.g., 50/50 SUT/TT and 70/30 SUT/TT). However, as was discussed in Chapter 5 of this dissertation, there are only small differences on the EC-PCE values between the three truck composition types according to the HCM-6 assumptions. Note this point may not be valid for other traffic conditions. Another related point is that the proposed methodology could be used to estimate PCE values for a specific heavy vehicle type using a discrete

approach. This would allow to obtain PCE values for vehicles with physical attributes and operational performance that greatly differ from those that were assumed in the HCM-6, for instance, recreational vehicles and electric trucks.

This dissertation assumed the same weight and power distributions developed in the original HCM-6 research for conventional trucks to be used for the CAV truck platooning condition. These distributions are a critical element for modeling the behavior of trucks at steep grade conditions having an important impact on the results. It is suggested to perform a further review of the weight and power distributions to ensure they are representative of the behavior of CAV trucks in real scenarios. This was not done due to the lack of empirical data.

It is recommended to perform a further review of the effect of lateral frictions while modeling the driving behavior of the driver-vehicle units. The microsimulation model used in the proposed methodology was not calibrated to capture the effect of lateral constrictions given by the facility and the traffic stream. It has been reported in the literature that some factors such as lane width, number of lanes, lateral clearance, and oversize vehicles, affect the operational performance of freeways. An adequate modeling of the lateral effect is important because it is expected that CAVs would be less sensitive to the lateral frictions compared to conventional vehicles which would provide more capacity to the freeway facility.

Another recommendation is to perform a deeper assessment of the form and error of the regression models be conducted when the HCM-6 EC-PCE methodology is used to analyze traffic conditions beyond the scope of the HCM-6 (e.g., restricted lanes, two-

lanes, EVs, etc.). It is possible a different model structure than the one proposed in this dissertation might provide better results.

Interestingly, it was found that the PCE values that were published in the HCM-6 may underestimate the effect of trucks in capacity and level of service analyses. This finding was consistent with six-lane freeways and four-lane freeways. The approach proposed in this dissertation, which was based on more consistent metrics with the HCM-6, produced greater PCE values compared to the original HCM-6 EC-PCE procedure. This means that that the capacity and level of service values obtained from the core methodologies in the HCM-6 would be overestimated, especially for the western rural U.S. It is recommended to explore to what extent the traffic metrics that have been considered for the analysis of freeway segments in the HCM-6 could be representative of different regions in the U.S. This would help to improve the reliability of the capacity and level of service analyses for the freeway system, especially where the presence of trucks is above the average U.S. values.

Lastly, it was observed most of the capacity values in the set of scenario combinations occurred at saturated flow conditions (e.g., queue discharge flow). Although the proposed approach calibrated the microsimulation model targeting an empirical capacity value (e.g., HCM-6 base capacity), the simulated capacity of each scenario was computed using a deterministic approach (e.g., maximum flow rate) as occurred in the original HCM-6 research (e.g., 95th percentile of the maximum flow rate). This deterministic approach does not ensure the capacity values are taken from undersaturated flow conditions as suggested in the HCM-6 (e.g., maximum prebreakdown flow rate). It is hypothesized a stochastic method for computing the

capacity values of each scenario (e.g., breakdown capacity method) could yield different capacity and EC-PCE values. It is recommended to explore the extent to which a stochastic determination of capacity may change EC-PCE results. In this regard, it is recommended to calibrate the microsimulation model taking as a reference not only the base capacity value but also the corresponding speed-flow curve for basic freeway segments used in the HCM-6 (e.g., *Exhibit 12-7*). The reliability and consistency of the EC-PCE values will improve to the extent the capacity of each scenario is better estimated.

REFERENCES

- AASHTO. 2011. *A policy on geometric design of highways and streets*. Washington, DC: AASHTO.
- ACEA (European Automobile Manufacturers Association). 2017. “*What is truck platooning? European automobile manufacturers association.*” Accessed December 12, 2019.
https://www.acea.be/uploads/publications/Platooning_roadmap.pdf.
- Aghabayk, K., Sarvi, M., Young, W., & Kautzsch, L. 2013. *A novel methodology for evolutionary calibration of Vissim by multi-threading*. In Australasian Transport Research Forum (Vol. 36, No. 1, pp. 1-15).
- Al-Kaisy, A., Jung, Y., & Rakha, H. 2005. *Developing passenger car equivalency factors for heavy vehicles during congestion*. Journal of transportation engineering, 131(7), 514-523.
- Al-Kaisy, A. F., Hall, F. L., & Reisman, E. S. 2002. *Developing passenger car equivalents for heavy vehicles on freeways during queue discharge flow*. Transportation Research Part A: Policy and Practice, 36(8), 725-742.
- Al-Kaisy, A. 2006. *Passenger car equivalents for heavy vehicles at freeways & multilane highways: some critical issues*. ITE Journal, 2006(3), 40-43. Accessed January 4, 2021. <https://scholarworks.montana.edu/xmlui/handle/1/3489>.
- Alecsandru, C., Ishak, S., & Qi, Y. 2012. *Passenger car equivalents of trucks on four-lane rural freeways under lane restriction and different traffic conditions*. Canadian Journal of Civil Engineering, 39(10), 1145-1155.

- AVS (Automated Vehicles Symposium). 2019. *Trucking Automation: Deployment Challenges and Opportunities – Part 2*. 2019 Breakout Sessions. Orlando, FL. Jul. 15-18, 2019. Accessed Feb. 18, 2020.
<https://www.automatedvehiclessymposium.org/avs2019/program/breakouts>.
- Barceló, J. 2010. *Fundamentals of traffic simulation*. New York: Springer.
- Benekohal, R. F., & Zhao, W. 2000. *Delay-based passenger car equivalents for trucks at signalized intersections*. Transportation Research Part A: Policy and Practice, 34(6), 437-457.
- Bevly, D., et al. 2017. *Heavy truck cooperative adaptive cruise control: Evaluation, testing, and stakeholder engagement for near term deployment: Phase two final report*. Technical Rep. Washington, DC: USDOT, Federal Highway Administration.
- Bishop, R. 2008. *Safety Impacts of Speed Limiter Device Installations on Commercial Trucks and Buses*. Transportation Research Board, Washington, D.C.
- Bourke, P. Interpolation methods. Miscellaneous: projection, modelling, rendering, 1(10), 1999.
- Bujanovic, P., and T. Lochrane. 2018. "Capacity predictions and capacity passenger car equivalents of platooning vehicles on basic segments." J. Transp. Eng. Part A: Syst. 144 (10): 04018063. <https://doi.org/10.1061/JTEPBS.0000188>.
- Chandler, R. E., Herman, R., & Montroll, E. W. 1958. *Traffic dynamics: studies in car following*. Operations research, 6(2), 165-184.
- Chitturi, M. V., & Benekohal, R. F. 2008. *Effect of Work zone length and speed difference between vehicle types on delay-based passenger car equivalents in*

- work zones*. In 87th Annual Meeting of the Transportation Research Board, Washington, DC.
- Delignette-Muller, Laure, M., & Dutang, C. 2015. "*fitdistrplus: An R Package for Fitting Distributions*." *Journal of Statistical Software* 64.4: 1-34.
- Dowling, R., Skabardonis, A., & Alexiadis, V. 2004. *Traffic analysis toolbox volume III: guidelines for applying traffic microsimulation modeling software*. No. FHWA-HRT-04-040.
- Dowling, R., G. List, B. Yang, E. Witzke, and A. Flannery. 2014a. *Incorporating truck analysis into the highway capacity manual*. Washington, DC: Transportation Research Board.
- Dowling, R., G. List, B. Yang, E. Witzke, and A. Flannery. 2014b. *Trucks in the freeway analyses of the highway capacity manual*. Raleigh, NC: Institute for Transportation Research and Education.
- Dowling, R., List, G., Yang, B., Witzke, E. and Flannery, A. 2014c. *Freeway Analysis Procedure for Mixed Flows on Constant Grades (Working Paper #2)*. Institute for Transportation Research and Education. September 15, 2014.
- Elefteriadou, L., Torbic, D., & Webster, N. 1997. *Development of passenger car equivalents for freeways, two-lane highways, and arterials*. *Transportation Research Record*, 1572(1), 51-58.
- Fan, H. S. 1990. *Passenger car equivalents for vehicles on Singapore expressways*. *Transportation Research Part A: General*, 24(5), 391-396.
- Fellendorf, M., & Vortisch, P. 2010. *Microscopic traffic flow simulator VISSIM*. In *Fundamentals of traffic simulation* (pp. 63-93). Springer, New York, NY.

- Fitzpatrick, D., G. Cordahi, L. O'Rourke, C. Ross, A. Kumar, and D. Bevly. 2016. *Challenges to CV and AV applications in truck freight operations*. Washington, DC: Transportation Research Board.
- Fransson, E. 2018. *Driving behavior modeling and evaluation of merging control strategies-A microscopic simulation study on Sirat Expressway*.
- Gao, Y. 2008. *Calibration and comparison of the VISSIM and INTEGRATION microscopic traffic simulation models*. Master Thesis, Virginia Tech.
- Guanetti, J., Y. Kim, and F. Borrelli. 2018. "Control of connected and automated vehicles: State of the art and future challenges." *Annu. Rev. Control* 45 (Jan): 18–40. <https://doi.org/10.1016/j.arcontrol.2018.04.011>.
- Gunst, R. F., & Webster, J. T. 1975. *Regression analysis and problems of multicollinearity*. *Communications in Statistics-Theory and Methods*, 4(3), 277-292.
- Hallmark, S., D. Veneziano, and T. Litteral. 2019. *Preparing local agencies for the future of connected and autonomous vehicles*. Rep. No. MN/RC 2019-18. St Paul, MN: Minnesota DOT.
- Harwood, D. W. 2003. *Review of truck characteristics as factors in roadway design* (Vol. 505). Transportation Research Board.
- HCM (Highway Capacity Manual). 1965. Highway research board. Washington DC: HCM.
- HCM (Highway Capacity Manual). 2016. Transportation research board. Washington DC: HCM.

- Hendrickson, C., and L. Rilett. 2017. "Traffic simulation and transportation engineering." *J. Transp. Eng., Part A: Syst.* 143 (12): 01817002.
<https://doi.org/10.1061/JTEPBS.0000091>.
- Huber, M. J. 1982. *Estimation of passenger-car equivalents of trucks in traffic stream* (discussion and closure) (No. 869).
- Hurtado-Beltran, A., & Rilett. 2019. *The Importance of Stochasticity on Microsimulation Model Output*. Presented at the 99th Transportation Research Board Annual Meeting, Washington DC, January 12-16, 2020. Paper No. 20-05777, Poster Session 1653.
- Hurtado-Beltran, A., Vakilzadian, H., & Rilett, L. R. 2020. *Impact of the Entry Time Model on Connected and Automated Vehicle (CAV) Platoon Formation*. In 2020 IEEE International Conference on Electro Information Technology (EIT) (pp. 655-662). IEEE.
- Hurtado-Beltran, A., & Rilett, L. R. 2021. *Impact of CAV Truck Platooning on HCM-6 Capacity and Passenger Car Equivalent Values*. *Journal of Transportation Engineering, Part A: Systems*, 147(2), 04020159.
<https://doi.org/10.1061/JTEPBS.0000492>.
- Hurtado-Beltran, A., & Rilett, L. R. 2021. *An Alternative Regression Model Structure for the HCM-6 Equal Capacity Passenger Car Equivalency Methodology*. Washington, DC: Transportation Research Record, Forthcoming.
- Husch, D. & Albeck, J. 2004. "SimTraffic 6 User Guide. Version 6," Trafficware, Albany, CA.

- Janssen, R., H. Zwijnenberg, I. Blankers, and J. Kruijff. 2015. *Truck platooning driving the future of transportation*. Hague, Netherlands: Netherlands Organization for Applied Scientific Research.
- Kang, S., H. Ozer, and I. L. Al-Qadi. 2019. *Benefit cost analysis (BCA) of autonomous and connected truck (ACT) technology and platooning*. Reston, VA: ASCE.
- Kansas Department of Transportation (KDOT). 2015. *Traffic Flow Map, Kansas State Highway System*.
- Keller, E. L., & Saklas, J. G. 1984. *Passenger car equivalents from network simulation*. *Journal of Transportation Engineering*, 110(4), 397-411.
- Kittelson & Associates. 2019. "*HCM CAV CAFs: Capacity adjustment factors for connected and autonomous vehicles in the highway capacity manual*." In Proc., Presentation at the 17th National Transportation Planning Applications Conf. Salem, OR: Oregon Dept. of Transportation.
- Kong, D., & Guo, X. 2016. "*Analysis of vehicle headway distribution on multi-lane freeway considering car-truck interaction*," *Advances in Mechanical Engineering*, 8(4), 1687814016646673.
- Konstantinopoulou, L., A. Coda, and F. Schmidt. 2019. "*ENSEMBLE: Enabling safe multi-brand truck platooning for Europe*." In Proc., Presentation at the Automated Vehicles Symp., 15–18. Brussel, Belgium: European Commission.
- Krammes, R. A., & Crowley, K. W. 1986. *Passenger car equivalents for trucks on level freeway segments*. *Transportation Research Record*, (1091).
- L'ecuyer, P. 1988. "*Efficient and portable combined random number generators*," *Communications of the ACM*, 31(6), 742-751.

- Lasdon, L. S., R. L. Fox, and M. W. Ratner. 1974. "Nonlinear optimization using the generalized reduced gradient method: *Revue française d'automatique, informatique, recherche opérationnelle*." *Recherche opérationnelle* 8 (3): 73–103.
- Li, J.J. 2017. *Simulate Stochastic Vehicle Arrivals & Compare VISSIM Stochastic vs Exact Inputs*. <https://www.linkedin.com/pulse/simulate-stochastic-vehicle-arrivals-compare-vissim-vs-li> Accessed Oct. 08, 2018.
- Li, L., & Chen, X. M. 2017. "Vehicle headway modeling and its inferences in macroscopic/microscopic traffic flow theory: A survey," *Transportation Research Part C: Emerging Technologies*, 76, 170-188.
- Li, S. E., Y. Zheng, K. Li, L. Wang, and H. Zhang. 2017. "Platoon control of connected vehicles from a networked control perspective: Literature review, component modeling, and controller synthesis." In *IEEE transactions on vehicular technology*. Piscataway, NJ: IEEE.
- Lieberman, E., & Rathi, A. K. 1997. *Traffic simulation. Traffic flow theory*.
- List, G., Roupail, N., and Yang, B. 2014. *PCE Values for Single Grades*. Raleigh, NC: Institute for Transportation Research and Education. December 18, 2014.
- Luttinen, R. T. 1996. "Statistical analysis of vehicle time headways," Helsinki University of Technology.
- Mahdavian, A., A. Shojaei, and A. Oloufa. 2019. "Assessing the long and mid-term effects of connected and automated vehicles on highways' traffic flow and capacity." In *Proc., Int. Conf. on Sustainable Infrastructure*, 263. Reston, VA: ASCE. <https://doi.org/10.1061/9780784482650.027>.

- Makridis, M., K. Mattas, B. Ciuffo, M. A. Raposo, T. Toledo, and C. Thiel. 2018. *"Connected and automated vehicles on a freeway scenario. Effect on traffic congestion and network capacity."* In Proc., 7th Transport Research Arena TRA. Vienna, Austria: Transport Research Arena.
- Mannering, F., Kilareski, W., & Washburn, S. 2007. *"Principles of highway engineering and traffic analysis,"* John Wiley & Sons.
- Maurya, A. K., Dey, S. & Das, S. 2015. *"Speed and time headway distribution under mixed traffic condition,"* Journal of the Eastern Asia Society for Transportation Studies, 11, 1774-1792.
- McHale, G. 2019. *"FHWA level 1 truck platooning research program."* In Proc., Presentation at the Automated Vehicles Symp., 15–18. Washington, DC: USDOT, Federal Highway Administration.
- Mendez, V. M., C. A. Monje, Jr., and V. White. 2017. *Beyond Traffic: Trends and Choices 2045—A National Dialogue About Future Transportation Opportunities and Challenges.* In *Disrupting Mobility, Impacts of Sharing Economy and Innovative Transportation on Cities* (G. Meyer, and S. Shaheen, eds.), Springer International Publishing, Cham, Switzerland, pp. 3–20.
- MnDOT. 2008. *"Advanced CORSIM Training Manual,"* SEH No. A-MNDOT0318.00, Minnesota Department of Transportation.
- Moridpour, S. 2014. *Evaluating the time headway distributions in congested highways.* Journal of Traffic and Logistics Engineering Vol, 2(3).
- Morris, C. M., & Donnell, E. T. 2014. *Passenger car and truck operating speed models on multilane highways with combinations of horizontal curves and steep grades.*

Journal of Transportation Engineering, 140(11), 04014058.

[https://doi.org/10.1061/\(ASCE\)TE.1943-5436.0000715](https://doi.org/10.1061/(ASCE)TE.1943-5436.0000715).

Nevada Department of Transportation (NDOT). 2017. *2017 Vehicle Classification Distribution Report*.

Okura, I., & Sthapit, N. 1995a. *Microscopic Headway Method of Estimating Passenger Car Equivalents*. In Proceedings of Infrastructure Planning (Vol. 17).

Okura, I., & Sthapit, N. 1995b. *Passenger car equivalents of heavy vehicles for uncongested motorway traffic from macroscopic approach*. Doboku Gakkai Ronbunshu, 1995 (512), 73-82.

Olstam, J. J., & Tapani, A. 2004. *Comparison of Car-following models* (Vol. 960). Linköping: Swedish National Road and Transport Research Institute.

PCT (Python Core Team). 2015. *Python: A dynamic, open source programming language*. Python Software Foundation. URL <https://www.python.org/>.

PTV (Planung Transport Verkehr). 2018. *VISSIM 10 user manual*. Karlsruhe, Germany: PTV AG.

PTV (Planung Transport Verkehr). 2019a. *PTV VISSIM & VISWALK 2020: Release notes* (last modified: 2019-10-09). Karlsruhe, Germany: PTV AG.

PTV (Planung Transport Verkehr). 2019b. *VISSIM 20 user manual*. Karlsruhe, Germany: PTV AG.

PTV Group. 2021. *PTV Vissim & PTV Viswalk Service Pack Download Area*. Accessed January 11, 2021. http://cgi.ptvgroup.com/cgi-bin/en/traffic/vissim_download.pl.

- Raj, P., Sivagnanasundaram, K., Asaithambi, G., & Ravi Shankar, A. U. 2019. *Review of methods for estimation of passenger car unit values of vehicles*. Journal of Transportation Engineering, Part A: Systems, 145(6), 04019019.
- Rakha, H., Ingle, A., Hancock, K., & Al-Kaisy, A. 2007. *Estimating truck equivalencies for freeway sections*. Transportation research record, 2027(1), 73-84.
- RCT (R Core Team). (2013). *R: A language and environment for statistical computing*. R Foundation for Statistical Computing, Vienna, Austria. URL <http://www.R-project.org/>.
- Rilett, L. R. 2020. "Using simulation to estimate and forecast transportation metrics: Lessons learned." In Proc., CIGOS 2019, Innovation for Sustainable Infrastructure, 23–33. New York: Springer.
- Rossen, V. G. 2018. "Autonomous and cooperative vehicles and highway capacity." Accessed September 28, 2019. <https://essay.utwente.nl/76615/>.
- Roy, R., & Saha, P. 2018. *Headway distribution models of two-lane roads under mixed traffic conditions: a case study from India*. European transport research review, 10(1), 3.
- Sharma, M., & Biswas, S. 2020. *Estimation of Passenger Car Unit on urban roads: A literature review*. International Journal of Transportation Science and Technology.
- Sheather, S. 2009. *A modern approach to regression with R*. Springer Science & Business Media.

- Shi, L., and P. Prevedouros. 2016. "Autonomous and connected cars: HCM estimates for freeways with various market penetration rates." *Transp. Res. Procedia* 15 (Jun): 389–402. <https://doi.org/10.1016/j.trpro.2016.06.033>.
- Sparmann U. 1978. *Spurwechselforgänge auf zweispurigen BAB-Richtungsfahrbahnen*. Forschung Straßenbau und Straßenverkehrstechnik, Heft 263, Bonn.
- Spiegelman, C., E. S. Park, and L. R. Rilett. 2011. *Transportation statistics and microsimulation*. Boca Raton, FL: CRC Press.
- Stanek, D. 2019. *A procedure to estimate the effect of autonomous vehicles on freeway capacity*. Washington, DC: Transportation Research Board.
- Sukennik, P. 2018. *Micro-simulation guide for automated vehicles*. Karlsruhe, Germany: PTV Group.
- Texas Department of Transportation (TxDOT). 2016. *2016 Texas Truck Flow Band Map*.
- Toledo, T., & Koutsopoulos, H. N. (2004). Statistical validation of traffic simulation models. *Transportation Research Record*, 1876(1), 142-150.
- TSS. 2006. "AIMSUN 5.1 Microsimulator user's manual Version 5.1," TSS-Transport Simulation Systems, S.L.
- TTC (Toyota Tsusho Corporation). 2019. "Truck platooning project in Japan." In Proc., Presentation at the Automated Vehicles Symp., 15–18. Tokyo: Ministry of Economy, Trade and Industry.
- Tufuor, E., Rilett, L. R., & Zhao, L. 2020. *Calibrating the Highway Capacity Manual Arterial Travel Time Reliability Model*. *Journal of Transportation Engineering, Part A: Systems*, 146(12), 04020131. <https://doi.org/10.1061/JTEPBS.0000451>.

- Urbanik, T., A. Tanaka, B. Lozner, E. Lindstrom, K. Lee, S. Quayle, and S. Sunkari. 2015. *Signal timing manual*. Washington, DC: Transportation Research Board.
- U.S. Department of Transportation (USDOT). 2015. *Traffic Flow Map of the State Highways*. State of Nebraska.
- Van Aerde, M., & Yagar, S. 1984. *Capacity, speed and platooning vehicle equivalents for two-lane rural highways*. TRB.
- Virginia Department of Transportation (VDOT). 2020. *Vissim User Guide Version 2.0*. VDOT Traffic Engineering Division. Virginia Department of Transportation.
- Washburn S., & Ozkul, S. 2013. *Heavy Vehicle Effects on Florida Freeways and Multilane Highways*, FDOT Contract BDK77 977-15 (UF Project 00093817).
- Webster, N., & Elefteriadou, L. 1999. *A simulation study of truck passenger car equivalents (PCE) on basic freeway sections*. Transportation Research Part B: Methodological, 33(5), 323-336.
- Wiedemann, R. 1974. *Simulation des Strassenverkehrsflusses*.
- Wiedemann, R., & Reiter, U. 1992. *Microscopic traffic simulation: the simulation system MISSION, background and actual state*. Project ICARUS (V1052) Final Report, 2, 1-53.
- Wunderlich, K. E., Vasudevan, M., & Wang, P. 2019. *TAT Volume III: Guidelines for Applying Traffic Microsimulation Modeling Software 2019 Update to the 2004 Version* (No. FHWA-HOP-18-036). United States. Federal Highway Administration. Accessed January 7, 2021.
- Wyoming Department of Transportation (WyDOT). 2009. *Interstate 80 Tolling Feasibility Study, Phase 2*. Final Report.

- Yang, B. 2013. *“On the HCM’s treatment of trucks on freeways.”* Master thesis, Dept. of Civil Engineering, North Carolina State University.
- Yeung, J. S., Wong, Y. D., & Secadiningrat, J. R. 2015. *Lane-harmonised passenger car equivalents for heterogeneous expressway traffic.* Transportation Research Part A: Policy and Practice, 78, 361-370.
- Zhou, J. 2018. *“Effects of moving bottlenecks on traffic operations on four-lane level freeway segments.”* Doctoral dissertation, Dept. of Civil and Environmental Engineering, Univ. of Nebraska-Lincoln.
- Zhou, J., Rilett, L., Jones, E., & Chen, Y. 2018. *Estimating passenger car equivalents on level freeway segments experiencing high truck percentages and differential average speeds.* Transportation Research Record, 2672(15), 44-54.
- Zhou, J., L. Rilett, and E. Jones. 2019a. *Estimating passenger car equivalent using the HCM-6 PCE methodology on four-lane level freeway segments in western US.* Washington, DC: Transportation Research Record.
- Zhou, J., Rilett, L., & Jones, E. 2019b. *Sensitivity analysis of speed limit, truck lane restrictions, and data aggregation level on the HCM-6 passenger car equivalent estimation methodology for western US conditions.* Transportation research record, 2673(11), 493-504.

GLOSARY AND KEY ABBREVIATIONS

Basic Freeway Segment – freeway section where the traffic flow is uninterrupted. A basic freeway segment is outside the influence of on and off ramps for at least 1,500 feet.

CAF – capacity adjustment factor. This factor is defined as a ratio of mixed traffic flow capacity to passenger car-only flow capacity.

Capacity – maximum sustainable flow rate that can pass a given point of the road system during a specified time period under prevailing roadway, environmental, traffic, and control conditions.

CAV – connected and automated vehicles. These vehicles are capable of both autonomous driving and connectivity with other entities of the transportation system (e.g., vehicles, road infrastructure, etc.). It was assumed that CAVs have Cooperative Adaptive Cruise Control, which takes advantage of the communication exchange to form platoons with harmonized speeds and shorter gaps between them.

Density – number of vehicles occupying a road lane per unit length at a given instant (e.g., veh/mi/ln, veh/km/ln).

EC-PCE – equal capacity passenger car equivalent. It represents the passenger car equivalents that were estimated for the current version of the Highway Capacity Manual. These passenger car equivalents were estimated using capacity as the impedance metric of reference.

Flow Rate – equivalent hourly volume that would occur if a sub hourly flow (e.g., peak 15-minute flow) was sustained for an entire hour.

Gap – time interval between the passage of consecutive vehicles moving in the same stream, measured between the rear of the lead vehicle and the front of the following vehicle.

HCM-6 EC-PCE – original methodology for the estimation of equal capacity passenger car equivalents in the 6th edition of the Highway Capacity Manual.

HCM-6 – 6th edition of the Highway Capacity Manual.

Headway – time interval between passage of consecutive vehicles moving in the same stream, measured between corresponding points (e.g., front bumper) on successive vehicles.

Microsimulation – virtual representation of the traffic system where the driver-vehicle unit represent the fundamental entity of analysis.

MLRM – multivariate linear regression model.

NLRM – nonlinear regression model.

PCE – passenger car equivalent. It represents the number of passenger cars that would produce the same effect on the traffic flow as a given vehicle type (e.g., trucks). A passenger car equivalent is a factor used to convert a mixed traffic stream of passenger cars and trucks into a single uniform traffic stream of passenger cars.

Spacing – distance between vehicles moving in the same lane, measured between corresponding points (front to front) of consecutive vehicles.

Speed – time rate of change of distance.

Space Mean Speed – arithmetic mean of the speed of those vehicles occupying a given length of road at a given instant.

Truck Platooning – linking of two or more trucks in convoy using connectivity technology and automated driving support systems.

Uninterrupted Flow – traffic flow conditions where vehicles traversing a length of roadway are not required to stop by any cause external to the traffic stream.

VISSIMTM – a microscopic traffic microsimulation software package abbreviated from “Verkehr In Städten - SIMulationsmodell” (German for “Traffic in cities - simulation model”).

Volume – number of vehicles passing a point per unit of time (e.g., veh/hour/ln, veh/day).

APPENDIX A

THE IMPORTANCE OF STOCHASTICITY ON MICROSIMULATION

MODEL OUTPUT

A.1 Introduction

One of the most important characteristics of a microsimulation is the ability to model the temporal and spatial nature of traffic demand. Every microsimulation has a vehicle generation model that determines how and when the driver-vehicle units are introduced in the simulation. This model typically allows for both exact volumes, where the exact number of vehicles are generated, and stochastic volumes where the number of vehicles generated follows a statistical distribution.

While stochastic vehicle generation is often used in practice, there is very little information in the literature on how this option affects the results. More importantly, the characteristics of the stochasticity applied in most microsimulation models are unknown to the user because the underlying code is proprietary. In addition, the documentation is often inadequate with respect to understanding the exact theory underlying the modeling approach. There is a paucity of studies examining the potential impacts on simulation outputs between stochastic and exact vehicle generation. The only exception was an informal study that had neither interpretations nor conclusions (Li, 2017). It is important engineers understand the logic behind the underlying theory of the microsimulation model and be aware of the extent to which the stochastic component in the vehicle generation model may have an influence on the variables of interest in the

microsimulation. This need has been recognized in previous publications (Hendrickson & Rilett, 2017).

This study will examine one component of microsimulation models – stochasticity of vehicle generation. Most of the commercial microsimulation packages available today allow the user to associate stochasticity to some simulation inputs including traffic volumes. The stochastic condition is usually the default option for the user. However, how this option impacts vehicle generation is rarely well documented. In this study, the analysis will be focused on the vehicle generation model, using the software VISSIM 10 as a study case since it is widely used by engineers and researchers in the transportation engineering field. It should be noted the characteristics of the stochasticity in the vehicle generation model of VISSIM are unknown because they have not been published either by the developer or through a formal study. This study will analyze the stochastic component of vehicle generation and provide equations that relate VISSIM inputs to the resulting vehicle generation characteristics. In addition, two examples, for interrupted and uninterrupted flow conditions, are included to demonstrate the effect on performance measures when the user chooses between stochastic and exact vehicle inputs.

The methodological approach of this study is based on microsimulation models and several statistical analyses. Three microsimulation case studies, including the PCE model of the HCM-6, are used for assessing the potential impacts on some performance measures when different vehicle generation approaches are used. A simple regression analysis is performed to determine the relationship between the expected coefficient of variation and stochastic vehicle inputs. Additionally, a statistical analysis between the

exact versus stochastic outputs doing a paired t-test is conducted. The range of stochastic volumes that may affect the results of the analyzed performance measures are identified. It should be noted this methodology will be performed considering traffic modeling as a static assignment (based on vehicle inputs).

It is hypothesized the stochasticity has a significant impact on the simulation outputs by varying the number of potential interactions of driver-vehicle units in the simulation. This will support the importance of indicating, in any microsimulation study, the conditions in which the driver-vehicle units were deployed in order to make a satisfactory interpretation of the simulation results. In sum, this study emphasizes the need to have a deep understanding of the underlying logic of microsimulation models, to document the parameter sets chosen in a microsimulation study, and to calibrate the models to local conditions.

Three scenarios in VISSIM 10 were produced with the aim of addressing the following four specific objectives:

- 1) identify the best-fit distributions of stochastic volumes and time headways (scenario 1),
- 2) explore the variability of the stochastic vehicle input (scenario 1),
- 3) estimate the impact of the stochastic volume on performance measures at interrupted flow (scenario 2) and uninterrupted flow conditions (scenario 3), and
- 4) demonstrate whether stochastic and exact vehicle inputs are sensitive to the associated time intervals (scenario 1). The three scenarios are described in more detail in the following sections.

A.1 Underlying Theory of Stochasticity in Vehicle Generation

A.1.1 Scenario (1) for Exploring Stochasticity

To identify the underlying theory of the stochastic component in vehicle generation, a basic case in VISSIM 10 was used consisting of a single-lane link. The relevant characteristics and parameters of the model are shown below:

- One-lane at level (unidirectional); length = 1,609 m (1 mi); and width = 3.65 m (12 ft).
- Vehicle composition = Passenger-car only (100: Car).
- Desired speed = 120 km/h (75 mph).
- Behavior type = urban motorized (default Wiedemann 74).

The urban motorized link type was selected for this scenario because this allows a more reduced time headway between successive vehicles at the selected desired speed compared to the freeway link type (based on default settings of VISSIM 10). This is relevant because it drastically reduced the number of “stuck” vehicles that occur at the link entrance for moderate to high volume levels. The problem with “stuck” vehicles (recognized as simulation errors) is they cannot be counted as simulated vehicles because they would not be introduced in the network, although they were generated by the code. However, this study is focused on how the vehicle generation model supplies vehicles in the simulation, so it was critical that all vehicles generated enter the network.

Specifically, this model was used to measure the variability produced by the stochastic vehicle input on simulated volumes and time headways and its sensitivity to the time interval size. In this case, the generated vehicles at the entry of the link were

collected using the output files. Due to the massive number of simulation runs performed in the analysis, a Python routine was created to extract, from the vehicle input data files, the total number of generated vehicles for each simulation run (PCT, 2015).

Each combination of simulation runs was composed of a stochastic vehicle input (V) and a time interval size (T). Five levels of vehicle inputs (from 150 to 2,400 vph) and four levels of time intervals (from 60 to 3,600 seconds) were considered for this analysis (see **Table A-2**). It is important to note the user must give the vehicle input in terms of vehicles per hour (vph), regardless the time interval size which is given in seconds and may be a fraction of or larger than an hour. In total, 20,000 simulations were deployed considering 1,000 simulation runs per combination. A different seed number per simulation run (from 1 to 1,000 with $\Delta=1$) was used to guarantee unlike generations of stochastic volumes.

Additionally, the best fit distributions for stochastic volumes and time headways were explored. To do this, the Akaike and Schwarz's Bayesian information criteria in addition to the Kolmogorov-Smirnov, Cramer-von Mises, and Anderson-Darling goodness-fit-statistics were estimated. In this regard, smaller values of the previous statistics are preferred in determining the best fit distribution (Delignette-Muller, Laure, & Dutang, 2015). From the same scenario for exploring stochasticity, the combination V1200-T3600 (stochastic vehicle input = 1,200 vph, time interval = 3,600 s, and 1,000 simulation runs) was selected as a basis to identify the best-fit distributions. The combination represents a moderated traffic volume where no stuck vehicles were observed in the set of simulation runs.

A.1.2 Results of Distributions for Stochastic Volumes and Time Headways

Table A-1 shows the statistics of the applied criteria that were calculated to identify the best-fit distributions (smaller values are preferred). It was found the theoretical lognormal distribution fit both stochastic volumes and time headways (for stochastic and exact vehicle inputs). These findings are consistent with other previous studies where time headways were calibrated based on field data (Moridpour, 2014; Roy & Saha, 2013).

Table A-1. Applied Criteria for Best-fit Distributions on: (a) Stochastic Volume and (b) Time Headways.

Criteria	Probability Distribution				
	Normal	Lognormal	Gamma	Weibull	Exponential
(a) Stochastic Volume					
Goodness-of-fit statistics					
Kolmogorov-Smirnov statistic	0.026	0.025	0.024	0.078	-
Cramer-von Mises statistic	0.079	0.052	0.059	1.707	-
Anderson-Darling statistic	0.438	0.326	0.344	11.105	-
Goodness-of-fit criteria					
Akaike's Information Criterion	9997.4	9996.7	9996.6	10137.7	-
Bayesian Information Criterion	10007.3	10006.5	10006.5	10147.5	-
(b) Time Headways					
Goodness-of-fit statistics					
Kolmogorov-Smirnov statistic	0.205	0.130	0.130	0.133	0.179
Cramer-von Mises statistic	16.949	3.464	5.979	5.255	5.083
Anderson-Darling statistic	94.185	22.117	36.036	34.283	37.687
Goodness-of-fit criteria					
Akaike's Information Criterion	6196.5	4816.8	5048.2	5101.3	5142.4
Bayesian Information Criterion	6206.8	4827.1	5058.5	5111.6	5147.5

The histograms of stochastic volumes and time headways can be seen in **Figure A-1**. The histogram of stochastic volumes comprises 1,000 simulation runs with $V=1,200$ vph and $T=60$ -min. The histogram reveals a mean value equal to 1198.6 vph and a standard deviation of 35.81 vph. Although the stochastic vehicle input was 1,200 vph. In this case, the user could expect volumes as low as 1,104 vph or as high as 1,316 vph depending on the selected seed number in the simulation. On the other hand, the histogram of time headways has a mean value of 3 s, and the most frequent value is around 1 s, which is consistent with its statistical distribution. The VISSIM manual (PTV, 2018) indicates the time headways are obtained from a negative exponential distribution. However, the behavior found in the lower values makes the data better fit a log-normal distribution (see **Figure A-1**). It is important to note no examples of either histograms were found in the literature.

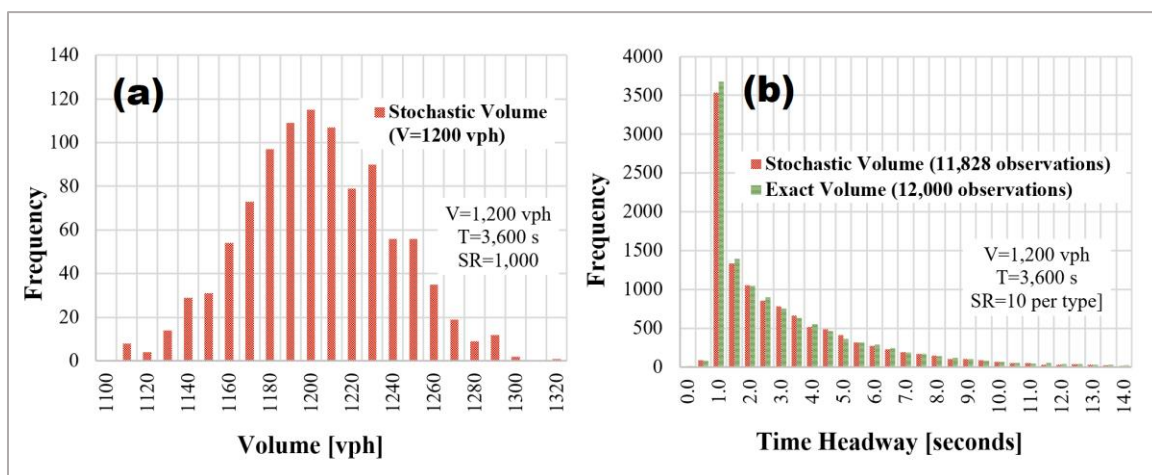


Figure A-1. Example of histograms for (a) stochastic volumes and (b) time headways

A.1.3 Results of Variability of Stochastic Volumes

The descriptive statistics of each combination of volume and time interval are shown in **Table A-2**. The variability of stochastic volumes changes according to the target volume defined as the expected number of generated vehicles within the associated time interval. Due to this, the measures of central tendency are given in terms of vehicles per time interval size (veh/T). By comparing the combinations V1200-T1800 and V600-T3600 in **Table A-2** it can be observed the standard deviations are the same because the combinations refer to the same proportion of expected vehicles (e.g., 600 vehicles). This is a key point to understanding the variability of stochastic volumes in VISSIM because it suggests this variability depends on the expected number of generated vehicles within the time interval regardless of the time interval size.

Table A-2. Descriptive Statistic of the Analyzed Stochastic Vehicle Input Combinations

Combination	n	Target Volume [veh/T]	Mean [veh/T]	Median [veh/T]	Mode [veh/T]	StdDev [veh/T]	CV [%]	Min	Max	Kurtosis	Skewness
V2400-T3600	1000	2400	2396.8	2393.0	2391	49.33	2.06	2246	2555	-0.01	0.08
V2400-T1800	1000	1200	1198.3	1197.5	1193	35.82	2.99	1104	1316	-0.16	0.06
V2400-T600	1000	400	398.9	399.0	406	19.97	5.01	340	454	-0.26	-0.01
V2400-T60	1000	40	39.8	39.0	39	6.13	15.41	21	60	0.05	0.20
V1200-T3600	1000	1200	1198.6	1198.0	1198	35.81	2.99	1104	1316	-0.17	0.07
V1200-T1800	1000	600	598.7	600.0	606	24.59	4.11	520	679	-0.15	-0.05
V1200-T600	1000	200	199.7	200.0	202	14.01	7.02	161	241	-0.20	0.02
V1200-T60	1000	20	20.1	20.0	20	4.33	21.57	7	34	0.23	0.34
V600-T3600	1000	600	598.9	600.0	606	24.57	4.10	520	679	-0.17	-0.04
V600-T1800	1000	300	299.4	300.0	292	17.33	5.79	247	352	-0.14	-0.02
V600-T600	1000	100	100.2	100.0	97	9.88	9.87	72	133	-0.09	0.11
V600-T60	1000	10	10.1	10.0	9	3.13	31.09	2	23	0.17	0.42
V300-T3600	1000	300	299.5	300.0	307	17.31	5.78	247	352	-0.15	-0.02
V300-T1800	1000	150	150.3	150.0	145	12.01	7.99	116	182	-0.27	0.05

V300-T600	1000	50	50.2	50.0	51	6.93	13.79	30	75	0.13	0.20
V300-T60	1000	5	5.0	5.0	5	2.22	43.93	0	14	0.35	0.45
V150-T3600	1000	150	150.4	150.0	152	12.00	7.98	116	182	-0.28	0.05
V150-T1800	1000	75	75.3	75.0	74	8.65	11.48	48	113	0.32	0.19
V150-T600	1000	25	25.2	25.0	24	4.94	19.63	11	42	0.18	0.33
V150-T60	1000	2.5	2.5	2.0	2	1.53	62.32	0	10	0.82	0.66

Note: V = input volume [vph]; T = simulation time interval [s]; CV = coefficient of variation; n = sample size (equal to number of simulation runs).

The coefficient of variation is a measure of dispersion defined as the ratio of the standard deviation to the mean, usually expressed as percentage (Spiegelman, Park, & Rilett, 2011). It was found the correlation between the coefficient of variation and stochastic volumes follows a non-linear trend that decreases as the stochastic target volume increases (see **Figure A-2**). However, there is still an important variation for high volumes. For example, taking as reference an input volume of 2,400 veh/T, the coefficient of variation (CV) is around 2%, which represents a variation of ± 49 veh/T (considering one standard deviation).

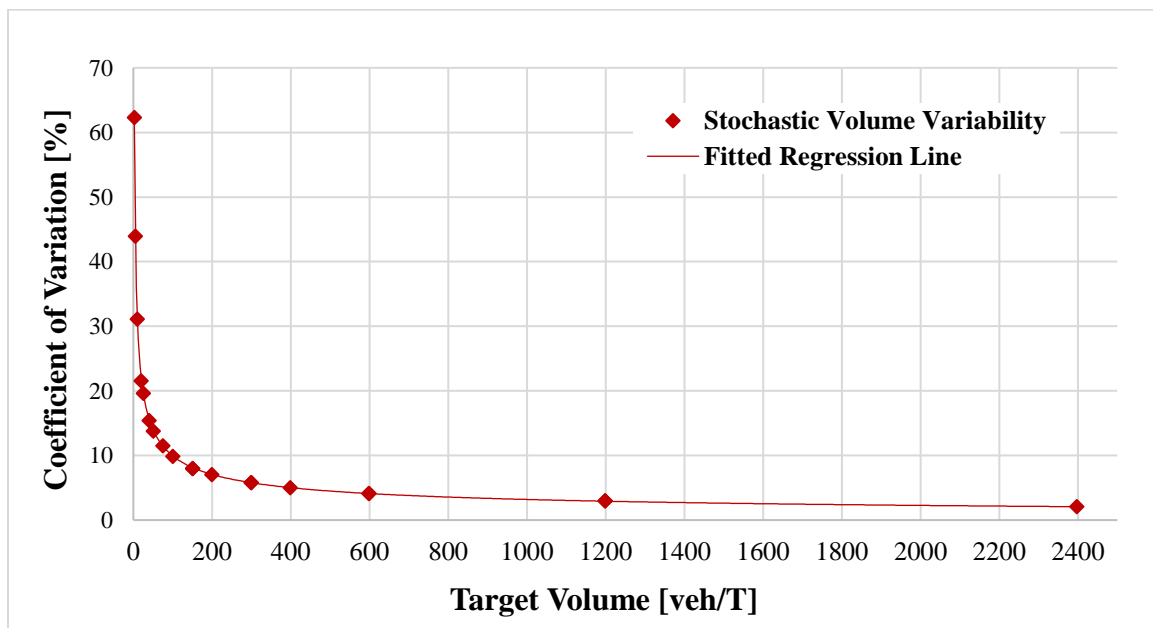


Figure A-2. Variability of stochastic input volumes.

These findings were complemented with a simple regression analysis using R software between both variables to define their mathematical relationship (RCT, 2013). In the regression model, the coefficient of variation was considered the response variable and the stochastic volume the exploratory variable. Box-Cox transformation was applied to the exploratory variable in order to fit the data. **Equation (A-1)** shows the transformed regression model obtained from this analysis. As can be seen in the regression model, the coefficient of variation seems to be inversely proportional to the square root of the stochastic volume.

$$CV = \frac{\beta_1}{\sqrt{V_T}} + \epsilon \quad (\text{A-1})$$

Where:

CV : coefficient of variation in percentage.

V_T : stochastic target volume in veh/T.

β_1 : estimator coefficient of the predictor.

ϵ : error.

Equation (A-2) can be derived from the transformed regression model. It shows the variance of stochastic volumes is approximately equal to the stochastic vehicle input. For example, if the stochastic vehicle input were equal to 1,600 vph considering a time interval of 15-min (which would represent 400 generated vehicles in the time interval), it would be expected the variance would be 400 vehicles² or a standard deviation of 20 vehicles (square root of 400 vehicles²) within the 15-min time interval.

$$Var \approx V_T \quad (\text{A-2})$$

Where:

Var : variance of stochastic target volume within the time interval T in veh^2/T^2 .

V_T : stochastic target volume in veh/T .

The probability distribution consistent with **Equation (A-2)** is a Poisson distribution, which has a mean value equal to the variance. The Poisson distribution is usually used to model the number of arrivals in a given time interval when the waiting time between arrivals is small and independent (Spiegelman, Park, & Rilett, 2011). Therefore, it can be stated that in VISSIM 10 the total number of stochastic vehicles introduced in a simulation within a time interval are given by a Poisson distribution. This is important because it illustrates the logic behind the vehicle generation model but is not included in the VISSIM 10 literature.

A.1.4 Results of Variability in Exact Volumes

As was mentioned in previous sections, the exact volume is only exact for the entire time interval associated with the vehicle input. It is important to add the exact volumes would be exact only if the continued interval check mark is unselected (PTV, 2018). In this case, the user must create as many time intervals as necessary, not just for different volumes and vehicle compositions, but to guarantee exact volumes in a time period of interest.

For fractions of the associated time interval, exact volumes may behave following similar patterns as stochastic volumes. For example, **Figure A-3** shows a comparison of the standard deviations of generated vehicles between stochastic and exact volumes, considering 15-min fractions of a 60-min time interval. In total, 50 simulation runs were deployed using an input volume of 1,200 vph; theoretically, a mean of 300 vehicles

would be expected per 15-min fraction. As can be seen in the graphs, the variability of exact volumes in fractions of the time interval may be even slightly higher than the one shown by stochastic volumes (depending on the seed numbers). This is important because in many simulation studies it is a common practice to use a 60-min interval for vehicle inputs and a 15-min interval for data aggregation to compute the outputs. Therefore, this finding supports the recommendation of using a time interval size for vehicle inputs in concordance to the interval size for data aggregation to guarantee an expected behavior in the generation of vehicles if exact volume is required.

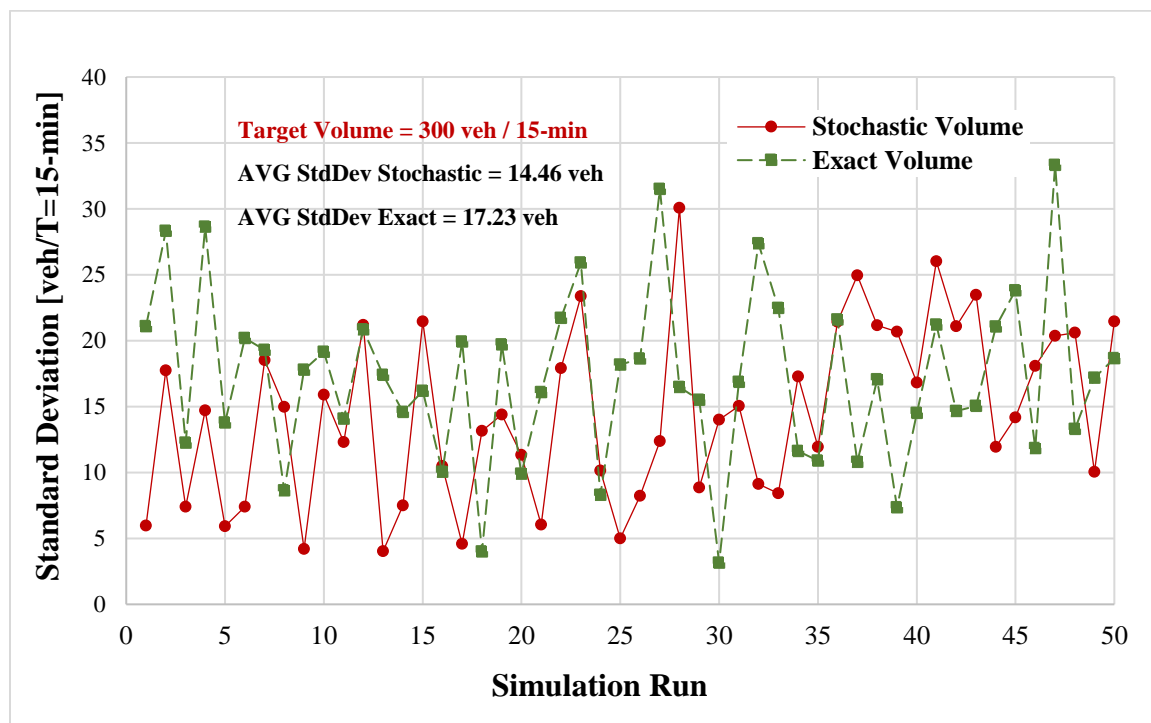


Figure A-3. Example of existing stochasticity in fractions of the time interval.

A.2 Impact of Stochasticity on Performance Measures

A.2.1 Scenarios (2 & 3) for Assessing Impact on Performance Measures

With the aim of measuring the effect of the vehicle input type on the traffic performance measures, two scenarios were elaborated in VISSIM 10 accounting for the interrupted and uninterrupted flow conditions. The theoretical characteristics of each traffic flow type can be found elsewhere (Lieberman & Rathi, 1997). In both cases, the effect on performance measures was evaluated by comparing the results from simulations where the only difference was if the volumes were stochastic or exact. It was hypothesized the difference between the outputs given by both volume types would be statistically significant; in other words, the null hypothesis was the difference would be equal to zero because, at present, they have been used indistinctly. A description and a brief explanation of these scenarios are given in the following sections.

A.2.2 Interrupted Flow Case (Scenario 2)

This scenario was similar to the previous scenario used for exploring stochasticity with the difference that a fixed signal control was added close to the end of the link. **Figure A-4a** shows the schematic of this scenario with the location of the signal control. The relevant characteristics and parameters are provided below:

- One-lane at level (unidirectional); length = 1,676 m (1 mi); and width = 3.65 m (12 ft).
- Vehicle composition = Passenger-car only with uniform distribution (only Toyota Yaris).
- Desired speed = 56 km/h (35 mph) with uniform distribution.

- Behavior type = urban motorized (default Wiedemann 74).
- Signal control settings: Cycle = 120 s; 2 phases; Green = 56 s; and Change Period = 4 s.
- Time interval = 15-min for deploying volumes, and 15-min for data aggregation.

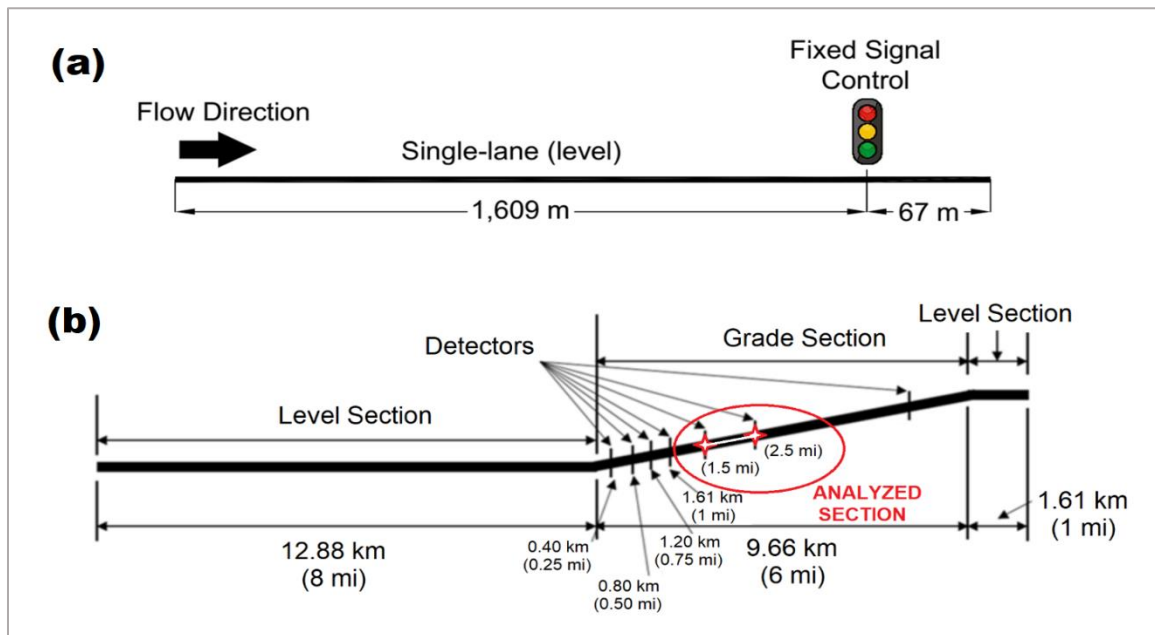


Figure A-4. Schematic of scenarios for (a) interrupted and (b) uninterrupted flow (modified from Zhou, 2018).

This scenario considered a uniform distribution of vehicle composition and desired speed to reduce the sources of variability in the traffic simulation that could have an influence on the estimation of performance measures. Besides, all the generated vehicles had the same geometry and operational features, and they were traveling through the link with a constant speed and the same driving behavior. Theoretically, the unique sources of variability were given by the vehicle input type (comparing stochastic versus exact) and the applied seed number.

The procedures described in the HCM-6 consider an analysis period of 15-min to calculate the performance measures in signalized intersections, and other publications recommend considering the same interval size to calculate the simulation outputs (HCM, 2016; Dowling & Alexiadis, 2004). Due to this, the analyzed performance measures in this model were calculated using a time interval of 15-min for deploying the input volumes (for both stochastic and exact conditions) and the same interval size for data aggregation. This is important because it was observed in the previous scenario and related studies that the performance measures are sensitive to the data aggregation size and the time interval associated with the vehicle input (Zhou, 2018).

A total of 2,000 simulation runs (2 vehicle input types x 10 volume levels x 100 seed numbers) were executed to compare the performance measures produced while choosing between stochastic or exact vehicle inputs. The values of the performance measures compared in the analysis had the same volume level and seed number but different vehicle input type (stochastic or exact). Ten volume levels (from 120 to 1,200 vph) related to theoretical volume to capacity ratios of 10, 33, 50, 67, 75, 80, 85, 90, 95, and 100% were considered. The simulation period of each simulation run was 21 hours accounting for one-hour for vehicle loading to achieve a steady state and 20-hours of steady state with a constant volume controlled by 15-min time intervals (80 observations per simulation run). In the case of the exact vehicle input, this means VISSIM generated an exact number of vehicles for every single interval; for instance, if the exact vehicle input was 800 vph, 200 vehicles were exactly generated at the end of each 15-min interval. In contrast with the exact type, the stochastic vehicle input is not sensitive to the time interval size, as was exposed by the model for exploring stochasticity; however, the

same time interval scheme was used for the set of simulation runs with stochastic volumes. Thus, 160,000 observations were obtained in this model to calculate the performance measures that served as a basis for the comparison between both types of vehicle inputs.

A.2.3 Uninterrupted Flow Case (Scenario 3)

For this traffic flow condition, a similar VISSIM model was used as compared to the one considered in the HCM-6 to obtain the simulated capacity adjustment factors (CAFs) with which the equal capacity passenger cars equivalence (EC-PCEs) are estimated for freeway segments and multilane highways (Zhou, 2018; Dowling et al., 2014; Yang, 2013). With this model, it was evaluated if the stochastic volume had a significant impact on performance measures at uninterrupted flow by comparing stochastics versus exact outputs. A complete and detailed description of the EC-PCE (HCM-6) model can be found elsewhere (Zhou, 2018). The relevant characteristics and parameters are given below:

- General conditions:
 - Three-lane unidirectional freeway segment; total length = 24.14 km (15 mi); and total width = 10.97 m (36 ft).
 - Desired speed = 113 km/h (70 mph) with uniform distribution.
 - Behavior type = freeway (default Wiedemann 99 and slow-lane rules for lane-changing).
 - Time interval = 60-min for deploying volumes and 1-min for data aggregation.
- Specific conditions:

- Grade section = +1%.
- Vehicle composition = Mixed traffic (90% passenger-car and 10% 30SUT/70TT).

The schematic of this scenario appears in **Figure A-4b**. The model layout was divided into three segments: (1) initial level section, (2) central grade section, and (3) ending level section. The central grade section included a set of eight detectors (data collection points) that were used to collect the vehicle data. In this case, the performance measures were estimated for one-mile length using the detectors located at 2.4 km (1.5 mi) and 4.0 km (2.5 mi) from the beginning point of the central grade section. Additionally, two travel time detectors (vehicle travel time measurements) were placed at the same points for measuring travel times and delays. The analyzed performance measures were calculated using a time interval of 60-min for deploying the input volumes (for both stochastic and exact types) and an interval size of 1-min for data aggregation. It must be pointed out the same interval sizes have been used to calculate capacity and density in the EC-PCE (HCM-6) model.

A total of 200 simulation runs (2 vehicle input types x 100 seed numbers) were executed to compare the selected performance measures while choosing between stochastic or exact vehicle input type. The values of the performance measures compared in the analysis had the same volume level and seed number but different vehicle input type (stochastic or exact). Nine volume levels (from 240 to 2,400 vph) from theoretical volume to capacity ratios of 10, 25, 50, 75, 80, 85, 90, 95, and 100% were considered. The simulation period of each simulation run was 36 hours (3-hours x 9 volume levels) accounting for one-hour of vehicle loading to achieve a steady state, one-hour of steady

state at the volume level for data collection, and one-hour of vehicle unloading. Hence, 108,000 observations (60 1-min observations x 9 volume levels x 100 seed numbers x 2 vehicle input types) were obtained to calculate travel times and delays that served as a basis for the comparison between both types of vehicle inputs.

A.2.4 Results of the Impact of Stochasticity on Performance Measures

Another important objective of this study was to define if the stochasticity in the vehicle generation model may have a statistically significant impact on performance measures at interrupted and uninterrupted flow conditions. This potential impact was measured through a paired t-test assuming a difference of zero in the null hypothesis by comparing the outputs from stochastic and exact vehicle inputs. In both conditions, it was found the impact of the stochasticity on the analyzed performance measures is statistically significant considering a confidence level of 95%. In general, the impact on performance measures is more evident from moderate to high volumes before reaching the capacity in the system. These results are summarized in **Table A-3** and **Table A-4**.

Table A-3. Descriptive Statistic and Paired t-test of Performance Measures at Interrupted Flow Conditions.

Performance Measure Statistics	Vehicle Input Volume V [vph]									
	V=120		V=400		V=600		V=800		V=900	
	Exact	Stoch.	Exact	Stoch.	Exact	Stoch.	Exact	Stoch.	Exact	Stoch.
Average Queue Length [m]										
Mean	2.9	2.9	13.1	13.1	24.7	24.9	48	50.4	85	115.2
StdDev	0.75	0.95	1.88	2.58	3.22	4.72	9.4	16.9	29.31	77.82
CV [%]	25.6	32.9	14.3	19.7	13.1	18.9	19.6	33.5	34.5	67.5
p-value (t-test)	0.004		0.95		5.6x10 ⁻⁴		2.1x10 ⁻²⁹		1.7x10 ⁻²¹⁶	
Number of Queue Stops										
Mean	15.3	15.4	58.9	58.9	99	99.6	159.4	163.1	227.5	268.1

StdDev	3.06	4.15	6.98	9.47	9.97	14.26	17.99	31.91	44.02	108.96
CV [%]	20	27	11.8	16.1	10.1	14.3	11.3	19.6	19.3	40.6
p-value (t-test)	0.14		0.55		1.8x10 ⁻³		7.8x10 ⁻²¹		7.2x10 ⁻¹⁹⁸	
Average Delay per Vehicle [s]										
Mean	16.5	16.3	18.8	18.8	21.1	21.2	25.9	26.5	34.7	42.2
StdDev	3.78	3.99	2.43	2.61	2.3	2.52	3.4	4.95	8.13	20.15
CV [%]	22.9	24.5	12.9	13.9	10.9	11.9	13.1	18.6	23.4	47.7
p-value (t-test)	1.0x10 ⁻⁴		0.8		0.44		9.0x10 ⁻²²		1.9x10 ⁻¹⁹⁷	
	V=960		V=1020		V=1080		V=1140		V=1200	
	Exact	Stoch.	Exact	Stoch.	Exact	Stoch.	Exact	Stoch.	Exact	Stoch.
Average Queue Length [m]										
Mean	386.4	369.1	419.3	418.3	421.2	420.9	421.9	421.8	422.2	422.2
StdDev	79.17	106.5	36.53	39.62	28.92	28.91	23.79	23.78	20.5	20.25
CV [%]	20.5	28.9	8.7	9.5	6.9	6.9	5.6	5.6	4.9	4.8
p-value (t-test)	2.2x10 ⁻⁵²		9.0x10 ⁻⁶		0.08		0.45		0.92	
Number of Queue Stops										
Mean	613.6	589.6	648.3	647	650.4	650.1	651.2	651.1	651.6	651.6
StdDev	94.91	130.61	45.73	49.47	36.32	36.43	29.95	30.19	26.46	26.13
CV [%]	15.5	22.2	7.1	7.6	5.6	5.6	4.6	4.6	4.1	4
p-value (t-test)	4.3x10 ⁻⁶⁶		7.7x10 ⁻⁶		0.0504		0.34		0.67	
Average Delay per Vehicle [s]										
Mean	146.6	188.2	270.3	268.9	275	274.7	276.8	276.6	277.7	277.6
StdDev	52.06	89.11	40.88	43.47	31.74	32.29	27.06	27.23	24.19	24.1
CV [%]	35.5	47.3	15.1	16.2	11.5	11.8	9.8	9.8	8.7	8.7
p-value (t-test)	≈ 0		1.1x10 ⁻¹³		0.0011		0.011		0.055	

Note: sample size of each vehicle input volume type was n=8000 for interrupted flow.

Although several performance measures were analyzed for the interrupted flow condition and similar results were found on them, **Table A-3** only shows the three performance measures considered more relevant for this traffic flow type. For example, in terms of average queue length, the greatest difference in the mean value (based on 8,000 observations) appears for the vehicle input volume of 900 vph. This means 75% of the theoretical volume to capacity ratio (v/c) assuming a theoretical capacity of 1,200 vph. The difference is statistically significant and consistent through the volume range from 600 to 1,020 vph (50% to 85% of v/c). A comparison of mean values and standard deviations of delay between stochastic and exact volumes for the ten volume levels are

depicted in **Figure A-5**. It must be noted that, in most of the cases, the variability of the performance measures for stochastic volumes is consistently larger than those given by the exact volumes.

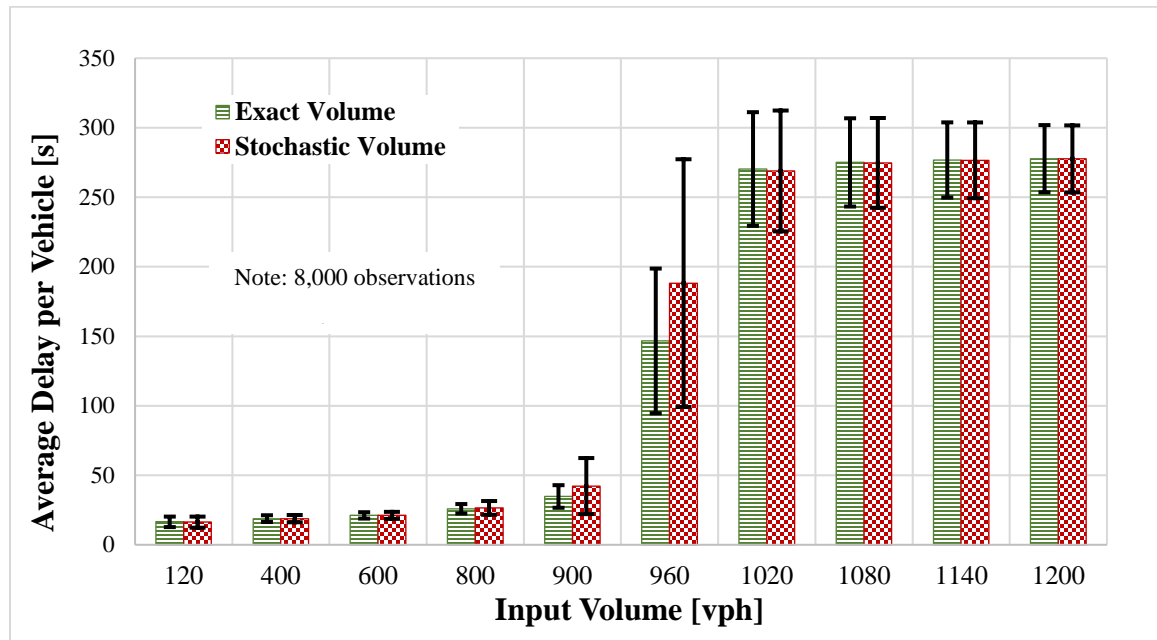


Figure A-5. Means and standard deviations of average delay from scenario 2.

On the other hand, average delay and average travel time were the analyzed performance measures for the uninterrupted flow condition. The difference given by the vehicle input type in the average delay is statistically significant and consistent through the volume range from 240 to 2,160 vph (10% to 90% of v/c assuming a theoretical capacity of 2,400 vph). A similar pattern is observed for average travel time; however, the variability is considerably lower than those obtained for average delay. In general, the variability for the uninterrupted flow condition is less evident compared to the interrupted flow, although the observed differences are still statistically significant. It is important to note that this scenario (3) presents more sources of stochasticity that may affect the

results; for instance, the fact that the vehicle composition is mixed traffic with variable geometry and performance. However, the comparison between the performance measures poured by both vehicle input types was applied to observations with the same simulation conditions (e.g., seed number, volume level, time interval, data aggregation, etc.). In theory, the unique difference in terms of model inputs was the vehicle input type.

Table A-4. Descriptive Statistic and Paired t-test of Performance Measures at Uninterrupted Flow Conditions.

Performance Measure Statistics	Vehicle Input Volume V [vph]									
	V=120		V=240		V=600		V=1200		V=1800	
	Exact	Stoch.	Exact	Stoch.	Exact	Stoch.	Exact	Stoch.	Exact	Stoch.
Average Delay [s]										
Mean	-	-	0.44	0.51	0.5	0.52	0.95	0.85	3.68	2.96
StdDev	-	-	0.59	0.66	0.43	0.42	0.85	0.6	2.84	2.33
CV [%]	-	-	134.7	131.6	71.3	80	89.7	71.3	77	78.6
p-value (t-test)	-		4.1x10-12		0.0002		7.5x10-17		3.0x10-53	
Average Travel Time [s]										
Mean	-	-	51.84	51.91	51.91	51.93	52.38	52.28	55.16	54.44
StdDev	-	-	0.59	0.67	0.43	0.42	0.74	0.38	2.83	2.33
CV [%]	-	-	1.1	1.3	0.8	0.8	1.7	1.2	5.1	4.3
p-value (t-test)	-		3.7x10-12		0.0002		5.6x10-16		9.2x10-53	
Performance Measure Statistics	V=1920		V=2040		V=2160		V=2280		V=2400	
	Exact	Stoch.	Exact	Stoch.	Exact	Stoch.	Exact	Stoch.	Exact	Stoch.
	Average Delay [s]									
Mean	5.46	4.58	8.47	7.78	14.5	14.1	15.9	15.7	16.12	16.33
StdDev	4.01	3.28	5.76	5.46	7.92	7.90	8.00	7.94	8.06	8.13
CV [%]	73.6	71.6	68.0	70.2	54.5	55.8	50.5	50.5	50.0	49.8
p-value (t-test)	4.8x10-38		2.0x10-11		0.0113		0.4135		0.1567	
Average Travel Time [s]										
Mean	56.94	56.07	59.95	59.27	65.99	65.61	67.31	67.19	67.58	67.79
StdDev	4.0	3.27	5.73	5.44	7.89	7.86	7.97	7.91	8.03	8.10
CV [%]	7.0	5.80	9.56	9.17	12.0	12.0	11.8	11.8	12.0	11.9
p-value (t-test)	6.9x10-38		1.9x10-11		0.0111		0.4091		0.1565	

Note: sample size of each vehicle input volume type was n=6000 for uninterrupted flow.

A.3 Concluding Remarks

The general purpose of the current study was to examine the stochastic component of the vehicle generation model using the software VISSIM 10 as a test case. Three scenarios were used for exploring the underlying logic of stochastic volumes and for assessing the potential impacts derived from this stochasticity on some performance measures at interrupted and uninterrupted flow conditions. A simple regression analysis was performed to determine the relationship between the expected coefficient of variation and stochastic vehicle inputs. Additionally, a statistical analysis based on paired t-test (exact versus stochastic outputs) allowed identification of the range of stochastic volumes and volume to capacity ratios that may affect the results of the analyzed performance measures.

One important finding to emerge from this study is that the stochastic component of the vehicle generation model in VISSIM 10 shows a variance approximately equal to the target stochastic volume within the associated time interval, which is consistent with a Poisson distribution. Because of this, the coefficient of variation of stochastic volumes declines in a non-linear manner as vehicle demand increases. Moreover, it was found that the theoretical lognormal distribution fit both stochastic volumes and time headways. It is vital the user understand the theory behind the demand generation in order to make a proper interpretation of the results.

In terms of exact volumes, there is stochasticity present within the time interval in which they are deployed. The exact volumes are only exact for the entirety of the associated time interval. If a fraction of the time interval is considered for analysis, the simulated volumes may behave as stochastic volumes. Due to this, it is suggested to use a

time interval size for deploying exact volumes at most the length of the time interval considered for the data aggregation used in the computation of simulation outputs. Note this point will be considered as a part of the proposed microsimulation framework in Chapter 6 and 7 of this dissertation.

Another major finding is the stochasticity of vehicle generation may have an impact on performance measures, particularly from moderated to high volumes before reaching the capacity in the system. For the analyzed performance measures at both interrupted and uninterrupted flow conditions, statistically significant differences were found at 95% confidence level while choosing between exact or stochastic volumes. Note because HCM-6 has begun using microsimulation to analyze capacity it is important to understand how vehicles are generated (Zhou, 2018). The larger variability associated with stochastic volumes would require setting an adequate number of simulation runs to guarantee consistency in the results.

These findings enhance our understanding of the stochastic component of the vehicle generation model in microsimulations, a key model of the traffic building block that has not been well documented. The evidence suggests any traffic microsimulation study must indicate the conditions in which the volumes were deployed (e.g., vehicle input type, time interval size, data aggregation interval, etc.) to ensure that others may replicate the experiments.

The generalizability of these results is subject to certain limitations. For instance, the results are valid only for traffic modeling as a static assignment, which is based on vehicle inputs and routing proportions. Further work needs to be done to explore the stochastic component in the dynamic assignment scheme, although it is suspected the

behavior could be similar. On the other hand, an important part of the analysis was performed considering default simulation parameters and uniform distributions on some attributes of the driver-vehicle units that may not be valid in other simulation studies. Moreover, this research was based on VISSIM 10, future studies on the current topic are therefore recommended to explore the stochasticity in other commercial microsimulation packages.

APPENDIX B

IMPACT OF THE ENTRY TIME MODEL ON CAV PLATOON FORMATION

B.1 Introduction

The majority of microsimulation packages use the exponential time headway model to introduce the driver-vehicle units in the network because it is easy to code, has low processing demand, and if there are no platooning effects in the network, it fits standard traffic flow theory. However, various empirical studies have shown that time headways can follow different statistical distributions depending on traffic conditions as was discussed in the literature review of this dissertation. The purpose of this study is to analyze the effect of the entry time model used in the vehicle generation on connected and automated vehicle (CAV) platoon formation on freeways. Two entry headway distributions were explored: (1) the exponential headway model that is used in VISSIM (note that the user cannot change the distribution of the entry time model); and (2) the lognormal headway model that is frequently observed when there are moderate to high levels of congestion. The goal is to determine if the distribution of the entry time model has a significant impact on the simulation outputs when freeway segments are analyzed under the operation of CAV platoon formation. In addition, it is important to examine how the CAV platoon formation behaves as a function of the freeway distance. The latter will help to determine an appropriate distance before the data collection section in the HCM-6 EC-PCE model.

The methodology applied in this study is comprised of three main steps. First, the time headway models of both exponential and lognormal distributions were used to develop vehicle entry times. The vehicle type and desired speed were also defined externally using random variates and input modeling approaches for controlling their influence on the results of the experimental replications (runs). The only difference between the two simulated scenarios were the vehicle entry times for each simulated vehicle. The next step was to run the traffic simulation models in VISSIM 20 using the two sets of inputs. The COM interface was used to control vehicle generation in the simulation. The function ‘AddVehicle()’ was coded in a Python script to generate the vehicles with the calculated stochastic attributes (PTV, 2019). In the last step, the simulation output from each scenario were processed to identify the CAV platoon metrics as a function of distance from the entry node. Statistical analyses were performed with the aim of determining any difference between the two scenarios in terms of platoon size and platoon frequency. A brief description of the study is provided below.

B.2 Methodology

B.2.1 Microsimulation Model and Testbed

As the targeted simulation outputs are related to CAV platoon formation, VISSIM 20 was used in this study due to its CAV and platoon modeling capabilities. The layout of the microsimulation test network is depicted in **Figure B-1**.

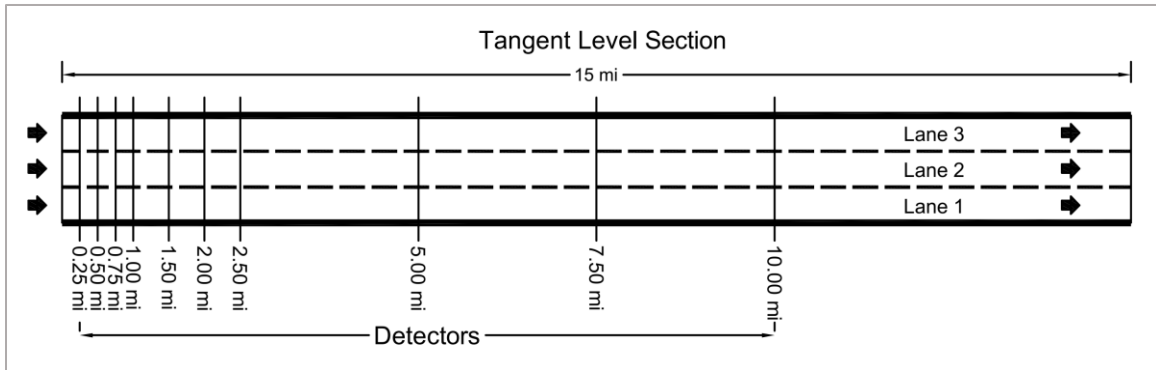


Figure B-1. Schematic of the microsimulation model.

The testbed contains ten data collection points, each covering the three lanes, that were used to obtain platoon size and platoon frequency information. Note that a similar test network was used in the latest version of the *Highway Capacity Manual* (HCM-6) to simulate the capacity of freeway segments (HCM, 2016). This test network has a large number of assumptions including those related to vehicle types, operational capabilities, and driving behavior that were discussed in this dissertation. Unless otherwise noted, all of the HCM-6 assumptions were followed in this study. The key assumptions that were considered for this study are the following:

- Unidirectional three-lane freeway segment.
- Volume to capacity ratio (V/C) of 0.75 assuming a theoretical capacity of 2,400 veh/h/ln.
- Vehicle composition: 50% passenger cars (A) and 50% tractor-trailers (TTs).
- All passenger cars (A) operating as non-CAVs.
- All TTs operating as CAVs (assuming 100% market penetration rate)
- Empirical desired speed distributions on level terrain under western rural U.S.

- Driving behavior: (a) 'Wiedemann 99' (default) for non-CAVs, and (b) 'Aggressive CoExist' for CAVs.
- Maximum platoon size of seven trucks (only CAVs can perform platoon formation).
- External vehicle generation using the COM interface.
- Total simulation period of 60 min divided in 15 min for warming period, 15 min for data collection, 15 min to extend steady state, and 15 min for vehicle unloading.
- Data aggregation of 15 min for computing the simulation outputs.

Note that to aid the analysis the input traffic variables, including desired speed distributions, volume-to-capacity ratio, and vehicle composition were selected to favor platoon formation. For example, according to the platoon-forming logic set in the traffic simulator, a speed differential between successive CAVs is required in order to allow for a CAV truck to approach a CAV platoon. Therefore, the empirical speed distribution assumed in this analysis will create the speed differential required for platoon formation. Moreover, a moderate traffic volume will facilitate platoon formation because there is an ample presence of potential vehicles for CAV platooning; and there is still room for lane changing, so the CAVs can encounter each other in the mixed traffic stream to form a new platoon. Consequently, the assumed volume to capacity ratio will facilitate these conditions. Additionally, a vehicle composition of 50%-50% for non-CAVs and CAVs, respectively was chosen because it allowed for the maximum amount of interaction between both vehicle types, all else being equal.

B.2.2 Time Headway Models

Two time-headway distributions were explored in this study: (1) exponential distribution (a.k.a. negative exponential) and (2) lognormal distribution. The following assumptions were considered for the time headway model.

- The OD volumes are exact. In other words, there is no variation in volumes. If a given OD input volume is 1800 veh/h/ln, then exactly 1800 vehicles will enter the network in an hour.
- The vehicle lane that a given vehicle enters the network is based on equal probability (e.g., given there are three lanes the probability of selecting any one lane is 1/3).
- Each lane has identical time headway distribution (e.g., lognormal or exponential).

In both cases, the time headways were calculated assuming that the entry traffic flow is 1,800 veh/h/ln. This implies that exactly 450 vehicles per lane would be generated per 15-min simulation period. To guarantee exact traffic volumes within the time interval of interest, it is necessary to adjust the time headways. For example, if 450 vehicles will be generated for a 15-min time interval, the 450 time headways must add up to exactly 15 min (or 900 sec). **Equation (B-1)** has been used to calculate a factor that allows adjusting the set of time headways (Lieberman & Rathi, 1997). The same approach was used in this study to ensure the exact vehicle generation.

$$K = \frac{T}{\sum_{i=1}^N h_i} \tag{B-1}$$

where:

K : adjustment factor for exact vehicle generation within the time interval T .

T : time interval associated with the exact traffic vehicle input, seconds.

N : total number of generated vehicles within the time interval T .

h_i : time headway for the subject vehicle i , seconds.

The random numbers used to feed the headway models that will be explained below were obtained using the generator proposed by L'Ecuyer (1988) that combines three multiplicative congruential generators. The same generator was used to model the stochasticity of vehicle type and desired speed.

B.2.2.1 Exponential Time Headways

The random variates for the exponential time headway model were calculated using the quantile function, also known as the inverse transform function, as shown in **Equation (B-2)** (Lieberman & Rathi, 1997; Luttinen, 1996).

$$h_i = (H - h_{min}) * [-\ln(1 - R_i)] + h_{min} \quad (\text{B-2})$$

where:

h_i : time headway exponentially distributed for the subject vehicle i , seconds.

H : mean time headway computed as the reciprocal of the traffic flow input, seconds.

h_{min} : minimum expected time headway, seconds.

R_i : random number $\sim U[0,1]$ for the subject vehicle i .

For the scenarios explored, the mean time headway (H) was set to equal 2 seconds by definition (e.g., entry flow is 1,800 veh/h/ln). The minimum time headway (h_{min}) was

set to 0.9 sec. This is in agreement with the default value of the VISSIM parameter CC1 (time headway) which defines the safety distance between successive vehicles (PTV, 2019).

To illustrate, **Table B-1** shows an example of the summary statistics of the exponential time headway model (first row). The statistics were calculated for the set of time headways corresponding to Lane 1 (outermost lane) and Run 1 (first simulation run).

Table B-1. Summary Statistics for a Sample of Time Headways.

Headway Model	Mean	Sd	Min	Max	Rate	MLEs	
						MeanLog	SdLog
Exponential	2.000	1.110	0.903	6.724	0.500	-	-
Lognormal	2.000	0.346	1.358	3.208	-	0.679	0.166

Note: Sd = Standard Deviation; MLEs = Maximum Likelihood Estimators.

Figure B-2 shows the histogram of the exponential time headway model for this set. The exponential time headways for the remaining lanes and simulation runs were calculated using the exact headway distribution model but considering different random numbers. As can be seen, the shifted mean (mean headway minus the minimum headway, this was $2.0 - 0.9 = 1.1$ sec) and the standard deviation of the exponential model was approximately the same ($1.10 \approx 1.11$) in concordance with the theoretical properties of the exponential distribution. Additionally, the mean headway of the exponential time headway model was equal to 2 sec which corresponds to the input hourly traffic volume. The minimum headway observed in the set was 0.9 seconds, which satisfied the minimum time headway defined in the analysis of 0.9 sec.

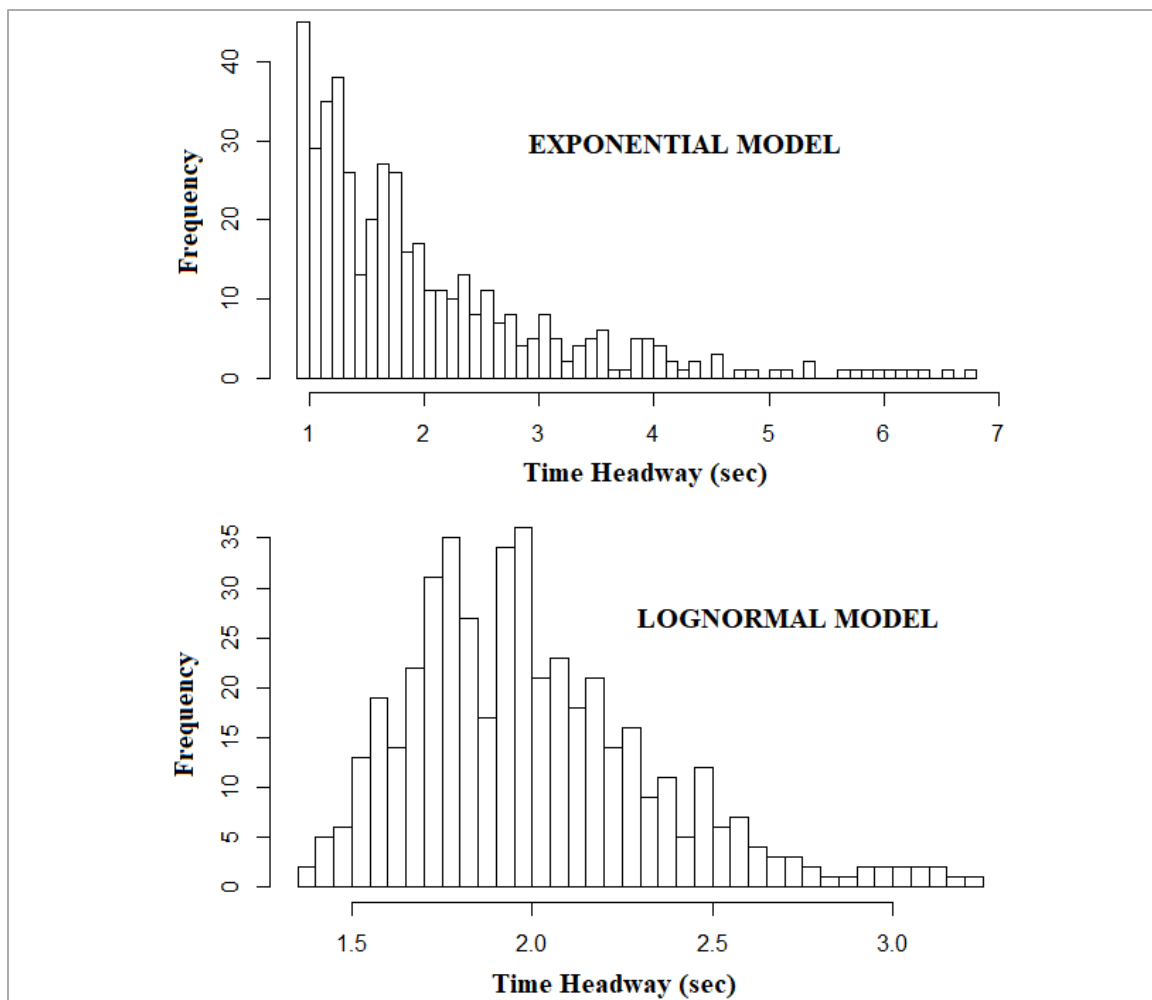


Figure B-2. Histograms for lognormal and exponential time headway models.

B.2.2.2 Lognormal Time Headways

The lognormal distribution does not have an inverse-transform function to generate random variates. In this study, the random variates for the lognormal time headway model were calculated using the expression shown in **Equation (B-3)**, which was solved using statistical software (Luttinen, 1996).

$$h_i = \left[\exp(\mu + \sigma * \Phi^{-1}(R_i)) \right] + h_{min} \quad (\text{B-3})$$

$$\mu = \log\left(\frac{[H-h_{min}]^2}{\sqrt{[H-h_{min}]^2 + \sigma_H^2}}\right) \quad ; \quad \sigma^2 = \log\left(1 + \frac{\sigma_H^2}{[H-h_{min}]^2}\right)$$

where:

h_i : time headway lognormal distributed for the subject vehicle i , seconds.

H : mean time headway computed as the reciprocal of the traffic flow input, seconds.

h_{min} : minimum expected time headway, seconds.

σ_H : desired standard of deviation of the expected time headways, seconds.

R_i : random number $\sim U[0,1]$ for the subject vehicle i .

Φ : standard normal distribution function.

μ, σ^2 : parameters of the lognormal distribution.

A mean time headway (H) of 2 sec and a minimum time headway (h_{min}) of 0.9 sec were used for the lognormal headway model, in agreement with the target traffic flow and the exponential headway model described previously. On the other hand, this approach also requires the user to input the standard deviation of the expected time headways. Previous studies have reported that U.S. multilane freeway segments that have lognormally distributed headways have observed standard deviations (σ_H) that were approximately 50% of the observed mean (Maridpour, 2014). Consequently, this study assumed a desired standard deviation (σ_H) of 0.55 sec (e.g., 50% of 1.1 sec).

An example of the summary statistics of the lognormal time headway model is shown in the second row of **Table B-1**. As occurred with the exponential model, the statistics were also calculated for the set of time headways corresponding to Lane 1 (outermost lane) and Run 1 (first simulation run). **Figure B-2** shows the histogram of the lognormal time

headway model for the same set. The same approach was applied for the remaining lanes and simulation runs but different random numbers were used. The mean headway of the lognormal time headway model was equal to 2 sec which corresponds to the input hourly traffic volume. The minimum headway observed in the set was 1.358 sec, which satisfies the minimum time headway defined in the analysis of 0.9 sec.

B.2.3 Stochastic Attributes Definition

B.2.3.1 Vehicle Type

The study considered two vehicle types: passenger car and tractor-trailer. As the assumed vehicle composition for the explored scenarios was 50%-50%, the vehicle type (VT) was sampled using a uniform distribution $R_i \sim U[0,1]$, as shown in **Equation (B-4)**.

$$VT = \begin{cases} A, & 0 \leq R_i < 0.5 \\ TT, & 0.5 \leq R_i < 1.0 \end{cases} \quad (\text{B-4})$$

The vehicle type was computed independently for each of the three lanes. Due to the stochasticity of the procedure, the overall vehicle composition was A=50.96% and TT=49.04%. Note that the same vehicle composition was used for all of the scenarios explored and simulation runs.

B.2.3.2 Desired Speed

The desired speed attribute for the driver-vehicle units was determined stochastically using empirical continuous distributions. Free-flow speed data collected at 13 sites on Interstate 80 between mileposts 177 and 399 in Nebraska was used. Further details of this dataset can be found elsewhere (Zhou, 2018). This dataset served to define the empirical continuous distribution of the desired speed of each vehicle type. The empirical cumulative distribution

functions (CDFs) of both passenger cars and tractor-trailers are depicted in **Figure B-3**. Note that the same values of desired speed for each driver-vehicle unit were used for all of the scenarios explored and simulation runs.

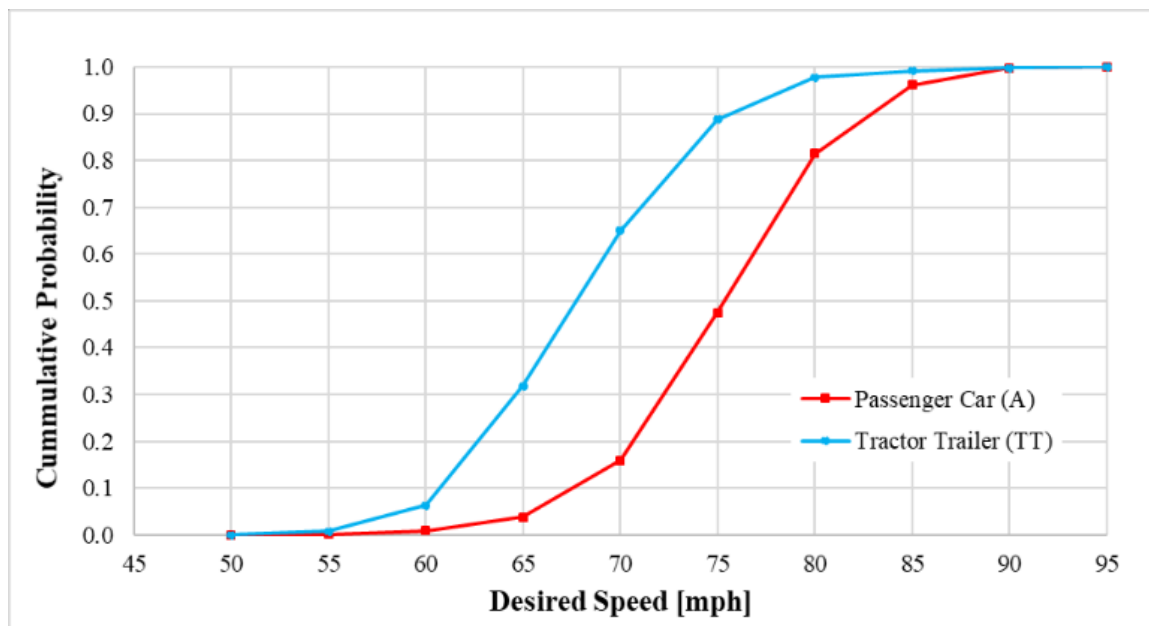


Figure B-3. Empirical CDFs of desired speed.

B.2.4 Simulation Runs

The number of simulation runs was defined considering a preliminary set of three simulation runs. The standard deviation of the platoon frequency that was found at the ten data collection points was used to calculate the minimum number of runs. It was assumed an allowable error (ϵ) of eight platoons, which represents 5% of the observed mean platoon frequency after 10 miles (approximately 160 platoons). Considering a two-sided t-test at a level of significance $\alpha = 0.05$, the number of simulation runs for the analysis was found to be greater than four (4) with a power of the test of 90%. Therefore, five runs were run for each scenario.

B.2.5 Simulation Output Processing

In order to identify the CAV truck platoons at the ten detector locations, the output simulation file 'data collection (raw data)' (*.mer) was generated from VISSIM 20. For each driver-vehicle unit, the entry times at the detector, the lane, and the vehicle type were extracted from the above file. This data was used to identify each CAV truck platoon that passed the given detector location. Depending on the prevalent speed, it was found that the time headway between successive CAV trucks in platoon mode ranged approximately from 1.1 to 1.3 seconds at 70 to 45 mph, respectively. This time headway range and the maximum number of trucks in the platoon (e.g., seven) served as thresholds to create an algorithm to filter and process the data. The aim was to collect the platoon frequency (number of platoons) and platoon size (number of CAV trucks in the platoon), at each of the ten detector locations for the 15-min time interval at steady-state conditions.

B.3 Results and Discussion

B.3.1 Platoon Formation

This study compared the exponential and lognormal entry time models to explore their impact on CAV platoon formation at isolated freeway segments. **Figure B-4** shows the CAV platoon formation, in terms of platoon frequency (vertical axis) and platoon size, as a function of distance (horizontal axis), ranging from 0 to 10 miles, for both the exponential and lognormal time headway models. Each line corresponds to a particular combination of time headway model and platoon size. The solid lines represent the exponential time headway model and the dotted lines the lognormal time headway model. Note that the notation 'EX' stands for the exponential model and 'LN' for the lognormal model; on the

other hand, the notation 'PS#' denotes the platoon size. For example, the symbol 'LN-PS7' refers to the lognormal time headway condition and a platoon size of seven CAV trucks.

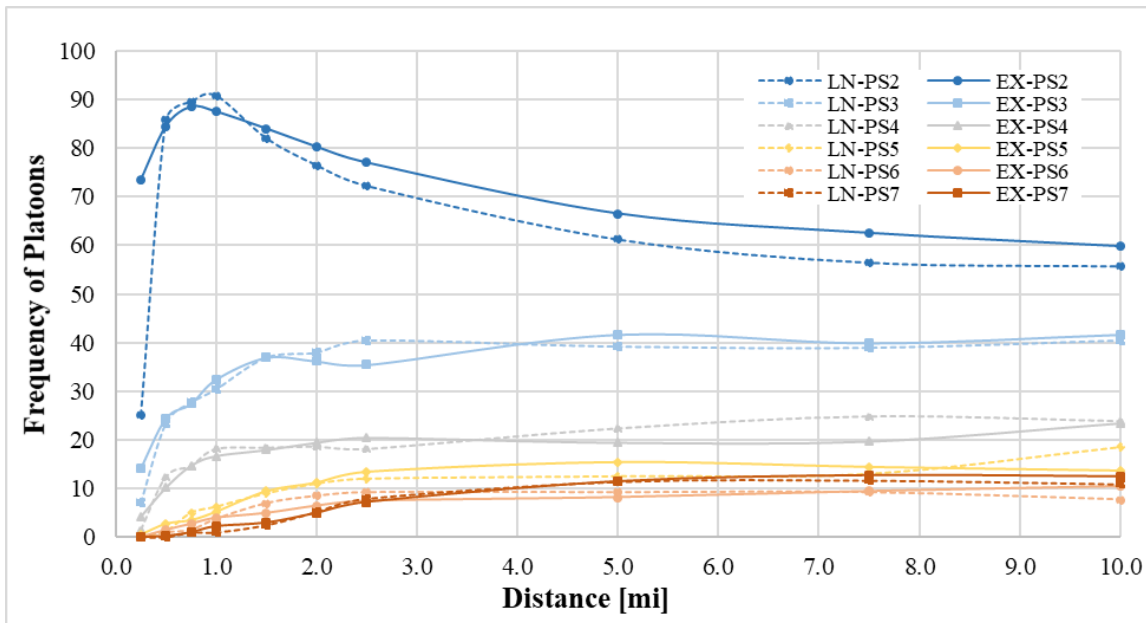


Figure B-4. Platoon formation for lognormal and exponential time headway models.

Not surprisingly, at the beginning of the freeway segment (0.25 mile-detector), the majority of the CAV truck platoons were comprised of two (approximately 80%) or three trucks (approximately 15%) for the exponential and lognormal conditions. Note that the platoon frequency values at 0.25 begin to diverge, this phenomenon will be discussed later. For the platoon size of two trucks, the platoon frequency drastically increased as the distance of the freeway segment increased until a maximum value was reached somewhere between 0.5 and 1.0 miles. After this point, the number of platoons of two started a gradual decrease because platoons of larger size began to appear in the system. It was hypothesized that this was due to the following CAV trucks joining the platoon and from small platoons forming a larger platoon. The increasing trend of platoon frequency for platoon sizes of

three to seven trucks showed an inflection point between 1.0 and 2.5 miles. After this point the platoon size distribution was approximately steady.

It should be noted that between 7% and 8% of the CAV truck platoons in the system reached the maximum platoon size of seven trucks at distances greater than 2.5 miles. Similarly, based on the assumptions considered in this study, approximately 80% of the platoons showed a moderate to low platoon size of fewer than five trucks even though the theoretical maximum value of seven trucks was input. It is expected that different traffic characteristics might produce a different proportion of platoon sizes in the traffic stream.

In general, it may be seen that the exponential and lognormal conditions tended to show a similar trend in platoon formation. The only exception was at the first detector (e.g., at the 0.25 mile marker). This finding suggests that the entry time model effect on CAV platoon formation is minimal and only occurs in the first 0.25 miles of the test network. It is recommended that if the HCM approach, and associated test network, is used to model CAV technologies that the vehicles travel at least 0.5 miles before platoon data is collected.

B.3.2 Platoon Frequency

The platoon frequency was measured as the number of CAV truck platoons observed at a given detector over a 15-minute aggregation level. The mean platoon frequency (vertical axis) as a function of distance (horizontal axis) for both the exponential and lognormal conditions is shown in **Figure B-5**. The red solid line represents the exponential time headway model, and the blue dotted line represents the lognormal time headway model. The mean platoon frequency was calculated by averaging, from the set of simulation runs, the number of platoons observed at each of the detectors.

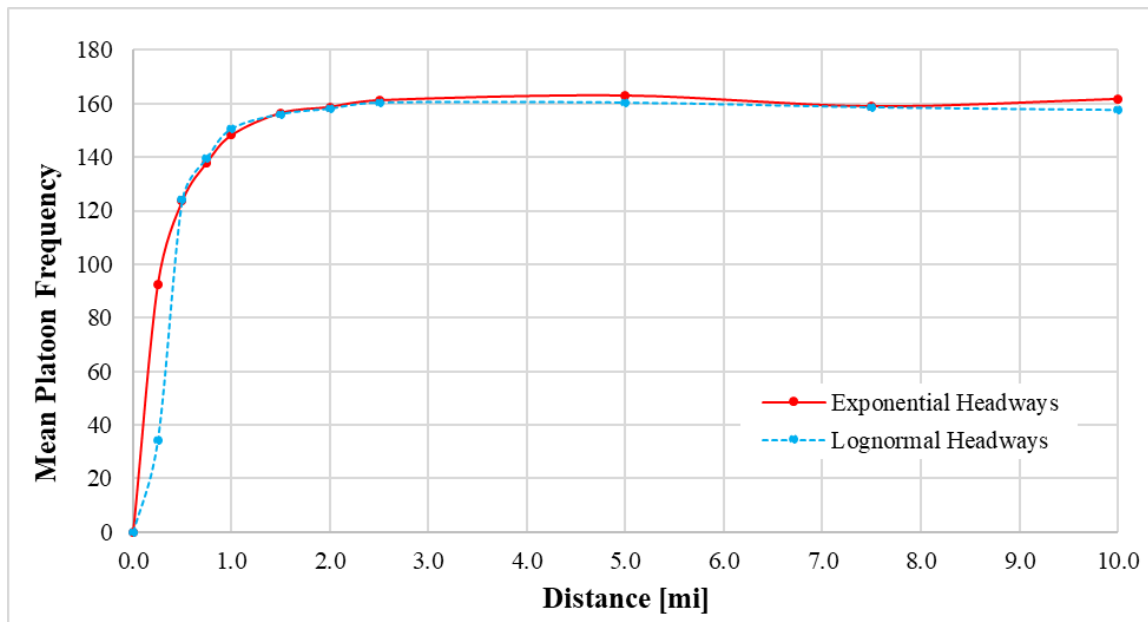


Figure B-5. Mean platoon frequency as a function of distance: exponential and lognormal models.

It can be seen that the mean platoon frequency for both conditions was approximately the same when the distance was greater than 0.5 miles. For both conditions, the highest mean platoon frequency was approximately 160 platoons, and this occurred at the 2.0-mile mark. There was an inflection point at the 1.0-mile detector which represents approximately 93.8% of the highest mean platoon frequency.

Interestingly, at the 0.25-mile detector, there is a noticeable difference in platoon frequency between the exponential and lognormal scenarios. The lognormal condition had a mean platoon frequency of 34 platoons (15.0% of the highest mean platoon frequency) as compared to the exponential condition that had 93 platoons (58.1% of the highest mean platoon frequency). It was hypothesized that the shorter time headways of the exponential model facilitated a faster platoon formation because, two successive CAV trucks would theoretically enter the network closer in distance to each other. Therefore, platoons could

form earlier in the simulation. However, after the 0.25 mile point the effect of the entry time model disappeared. At the 0.5-mile marker both the exponential and lognormal models revealed a similar mean platoon frequency. A two-sided paired t-test on mean platoon frequency values revealed that the time headway model does not produce a significant effect on platoon frequency in the microsimulation model at $\alpha = 5\%$.

B.3.3 Platoon Size

The platoon size was defined as the average number of CAV trucks that comprised each platoon observed at the detector locations considering a 15-min aggregation level. **Figure B-6** shows the mean platoon size as a function of distance (for both the exponential and lognormal conditions). The red solid line represents the exponential time headway model, and the blue dotted line represents the lognormal time headway model. The mean platoon size was calculated by averaging, from the set simulation runs, the platoon size observed at the detectors. It can be seen that the mean platoon size for both conditions was approximately the same for all locations on the test network. In contrast to the abrupt increase shown by the mean platoon frequency, the mean platoon size revealed a gradual increase as the distance factor increased. For both conditions, the minimum and maximum mean platoon sizes were approximately 2.30 (0.25-mile detector) and 3.45 (10.0-mile detector) trucks, respectively. Note that the maximum platoon size was, by definition, seven trucks. It can be observed an inflection point at the 2.5-mile detector in which the mean platoon size represented approximately 90% of the maximum mean platoon size. After this point, the platoon size continues to grow but at a decreasing rate as compared to the situation before the inflection point. It was hypothesized that this gradual increase was due to the travel distance required by the following CAV trucks to reach the existing CAV

truck platoons. A two-sided paired t-test on mean platoon size values revealed that the entry time model does not produce a significant effect on platoon size in the microsimulation model at $\alpha = 5\%$.

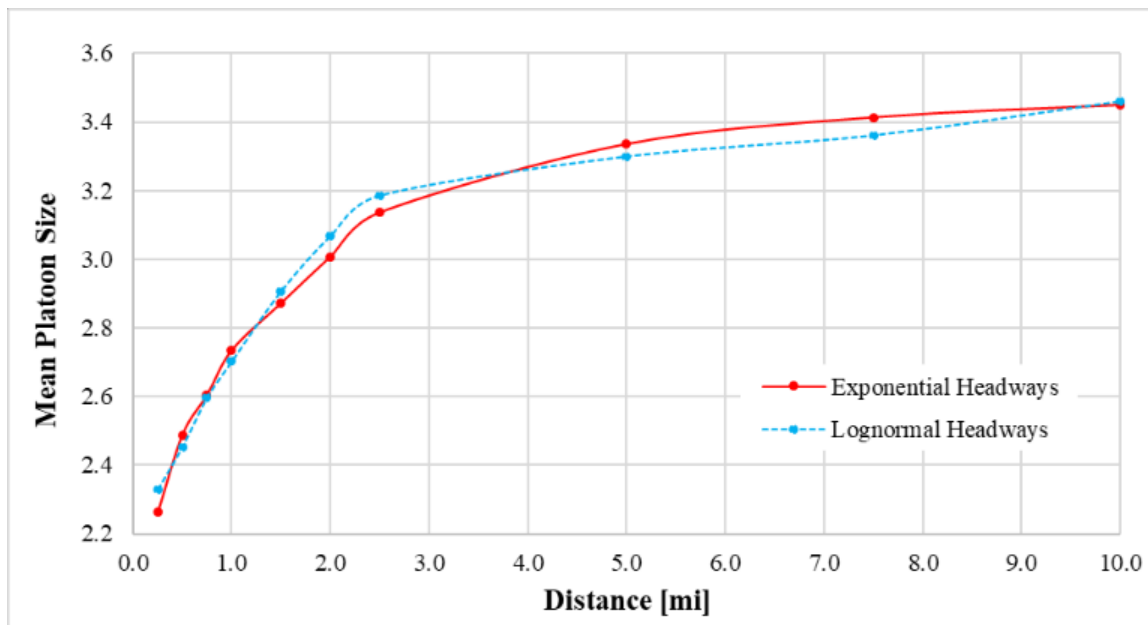


Figure B-6. Mean platoon size as a function of distance: exponential and lognormal models.

It must be noted that according to the platoon-forming logic in VISSIM 20, two existing platoons cannot be combined to form a greater single platoon. Only faster isolated vehicles with CAV capabilities can join an existing platoon and this occurs when a CAV vehicle approaches a platoon from the rear. It is important to highlight that this platoon-forming logic impedes the appearance of greater platoon sizes in the traffic stream. It is important to note that the maximum platoon size that is input to the simulation does not ensure that most of the platoons observed in the simulation will reach this maximum. Instead, the distribution of platoon size results from a complex interaction between various traffic and operational factors, including traffic flow, vehicle

composition, market penetration rate, speed distribution, volume-to-capacity ration, platoon attributes, etc.

B.4 Concluding Remarks

This study explored the effect of the entry time model used in vehicle generation on CAV platoon formation on isolated freeway segments. There is no discussion in the literature about the effects of the entry time model on the results of traffic microsimulation studies.

One of the most significant findings to emerge from this study is that the distribution of the entry time model did not affect the CAV platoon formation based on the assumptions stated in this study. Although the entry model had a minimal effect at the beginning of the link, it is hypothesized that this effect was rapidly removed by the driving-behavior logic that takes control of the driver-vehicle unit once it is traveling along the link.

Another major finding is that the CAV platoon formation may require longer travel distances to obtain the highest values of platoon frequency and platoon size. According to the assumptions of this study, the mean platoon frequency required approximately a distance of 2.5 miles to achieve the greatest platoon frequency. At this point, the platoon size was approximately 90% of the greatest mean platoon size. Although the maximum platoon size set in the study was seven CAV trucks, the greatest mean platoon size observed after 10 miles was only 3.45 trucks. The analyst should be aware that the maximum platoon size does not guarantee that most platoons will reach this size, but rather the interaction of various operational and traffic factors.

On the other hand, it is hypothesized that the current platoon-forming logic in the VISSIM 20 microsimulation model may limit the appearance of greater platoons than

those that could be observed in practice. For example, in the simulation, two successive CAV platoons of two vehicles each cannot merge to form a single platoon of four vehicles as would be expected to occur in reality. It is also recommended that microsimulation models include outputs relative to those vehicles that participate in CAV platoon formation at following and approaching states to facilitate user identification for analysis purposes.

Further work needs to be done to explore other statistical distributions for the entry time model. For example, many models assume that vehicles enter the network following a uniform distribution. It is recommended that a sensitivity analysis be performed to explore the effect of other parameters on CAV platoon formation, such as desired speed, vehicle composition, market penetration rate, driving behavior, platoon-forming logic, weight and power distributions, acceleration profiles, etc. This is an area of potential research that would further help transportation agencies as they begin the transition to CAV operations.

APPENDIX C

IMPACT OF THE SIMULATION RESOLUTION ON MICROSIMULATION MODEL OUTPUT

C.1 Introduction

Typically, a traffic microsimulation is a stochastic (there is variability in attributes and behavior), a dynamic (system state change in time), and a discrete (change at fixed points in time) model. The simulation resolution is a simulation parameter that is related to the dynamic and discrete nature of the microsimulation model. This simulation resolution determines the number of times that the dynamic objects in the simulation (e.g., vehicles, pedestrians, signal controls, etc.) are recalculated during the simulation run. A high simulation resolution will result in a more realistic and detailed model but will demand more computational resources and longer simulation run time (PTV, 2019). Some microsimulation guidelines have recommended that low simulation resolutions should be used only for preliminary analysis and reserve the highest resolutions for the final microsimulation model (VDOT, 2020). However, the simulation resolution parameter has received little attention in traffic microsimulation studies and its implications on the results are not entirely known.

In the current version of the Highway Capacity Manual (HCM-6), equal capacity passenger car equivalents (EC-PCE) for basic freeway segments were obtained using a microsimulation model approach (HCM, 2016). Specifically, a VISSIM microsimulation model was used for modeling the capacity of 3,822 traffic scenario combinations that served as main inputs for the EC-PCE values that were published in the HCM-6. To the

author's knowledge, this is the first time that the HCM uses a microsimulation model approach for capacity modeling. Interestingly, the HCM-6 EC-PCE microsimulation model used the lowest simulation resolution that is available in VISSIM (Dowling et al., 2014). There is no discussion on how the simulation resolution was selected nor the implications of this selection on the results of the HCM-6 EC-PCE microsimulation model. In this regard, it is important to evaluate if the existing simulation resolution has a significant impact on the capacity values, so other may replicate the experiments or evaluate novel traffic scenarios using the HCM-6 EC-PCE approach.

The main objective of this study is to analyze the impact of the simulation resolution on the capacity values obtained with the HCM-6 EC-PCE microsimulation model. A simulation resolution sensitivity was performed to compare the simulated capacity of 84 traffic scenario combinations that were simulated using the original HCM-6 EC-PCE protocols in VISSIM 20. It is hypothesized that the simulation resolution may affect the simulation outputs, so it should be treated as a calibration parameter in the microsimulation model to ensure consistent outputs. This is important to make possible the experimental replication of the results obtained from the microsimulation model.

C.2 Methodology

The main purpose of this study is to perform a simulation resolution sensitivity on the simulated capacity values obtained with the HCM-6 EC-PCE microsimulation model. This study used the same microsimulation model assumptions that were used in the original HCM-6 EC-PCE research. Five simulation resolutions were explored in VISSIM 20 including the simulation resolution of 1 second (i.e., 1 time step/simulation second) that was selected for the HCM-6 EC-PCE approach. In addition, two capacity definitions

were also explored to process the VISSIM model outcomes: (1) capacity as the 95th percentile of the maximum flow rate (e.g., HCM-6 EC-PCE capacity definition), and (2) capacity as the maximum flow rate (e.g., traditional capacity definition). The goal was to determine how that simulation resolution may affect the results in both capacity definitions.

The methodology applied in this study is comprised of three main steps. First, the microsimulation model in VISSIM was used to simulate a set of traffic scenario combinations under the explored simulation resolutions. The next step was to develop flow-density scatterplots based on the VISSIM model outputs. These scatterplots were the basis to calculate the simulated capacity for each scenario combination considering the two definitions of capacity explored in this study. Lastly, the comparisons between the results from the explored simulation resolutions and capacity definitions were conducted using standard statistical theory.

C.2.1 Traffic Scenario Combinations

A total of 84 scenario combinations were evaluated for exploring the impact of the simulation resolution on the HCM-6 EC-PCE VISSIM model results. The scenarios were defined by a combination of the following factors:

- 2 flow-rate types (f) either passenger car-only or mixed traffic flow,
- 3 levels of truck percentage (p), 5%, 10%, and 20%,
- 3 levels of grade (g), 0% (level terrain), 3% (rolling terrain), 6% (mountainous terrain),
- 7 levels of grade distance (d) from 0.25 mi to 5.00 mi.

- 1 level of truck composition type (m), 30/70 SUT/TT.

Therefore, there were 21 scenarios for the passenger car-only flow condition (e.g., 3 levels of grade x 7 levels of distance), and 63 scenarios for the mixed-traffic flow condition (e.g., 3 levels of truck percentage x 3 levels of grade x 7 levels of distance x 1 level of truck composition type).

C.2.2 Simulation Resolution Sensitivity

Five simulation resolutions were explored: (1) 1.0 second (1 time step/simulation second) (e.g., HCM-6 EC-PCE approach), (2) 0.5 seconds (2 time-steps/simulation second), (3) 0.33 seconds (3 time-steps/simulation second), (4) 0.2 seconds (5 time steps/simulation second), and (5) 0.1 seconds (10 time steps/simulation second). Note that the simulation resolution ranges from 1 to 20 time-steps/simulation second in VISSIM 20 (1).

C.2.3 Time per Run

The time per run is the time required to complete a single simulation run. This time depends on the characteristics and performance of the computer that is used to execute the VISSIM model. Due to the HCM-6 EC-PCE methodology is comprised of a total of 3,822 scenario combinations is important to estimate in advance the time that would be required to complete the whole set of simulations. For example, by knowing the mean time per run, the analyst could estimate the time that would be required to complete the total set of simulations and the number of computers needed to meet a time frame.

In this case, the time per run was calculated as the average time from 120 simulation runs (12 scenario combinations x 10 replications). The timestamp from the simulation run list in VISSIM was used to calculate the time elapsed by each simulation

run. The fastest time per run is achieved considering the lowest simulation resolution (e.g., 1 second). This time was used as a reference to calculate a relative time per run, which specifies how many times the time per run with higher resolutions is greater than the time given by the lowest resolution.

C.3 Discussion and Results

C.3.1 Simulated Capacity Results

The impact of the simulation resolution on the simulated capacity results of the HCM-6 EC-PCE VISSIM model are shown in **Figure C-1** and **Figure C-2**. Two capacity definitions were explored to estimate the simulated capacity based on the VISSIM 20 model outputs: (1) capacity as the 95th percentile of the maximum flow rate which corresponds to the HCM-6 EC-PCE capacity definition (**Figure C-1**), and (2) capacity as the maximum flow rate which corresponds to the theoretical capacity definition (**Figure C-2**). In both graphs, the y-axis represents the simulated capacity in veh/h/ln and the x-axis represents the scenario number. Each specific scenario number is calculated using **Equation (C-1)** and is a function of the truck percentage, grade, and distance. Each line in the graph represents a different simulation resolution value. The red solid line corresponds to the simulated resolution of 1 second that was used in the HCM-6 EC-PCE approach. The dotted lines correspond to higher simulation resolutions from 0.5 to 0.1 seconds.

$$n = 21 * p + (g - 1) * 7 + d \quad (\text{C-1})$$

Where:

n : Scenario number.

p : Ordinal number of truck percentage level, $p = 1, 2, \dots, P$, means 5%, 10%, and 20% truck percentage.

P : Total levels of truck percentage, $P = 3$.

g : Ordinal number of grade level, $g = 1, 2, \dots, G$, means 0%, 3%, and 6% grade.

G : Total levels of grade, $G = 3$.

d : Ordinal number of distance level (the level of detector location), $d = 1, 2, \dots, D$, means 0.25-5 mi.

D : Total levels of distance (detector location), $D = 7$.

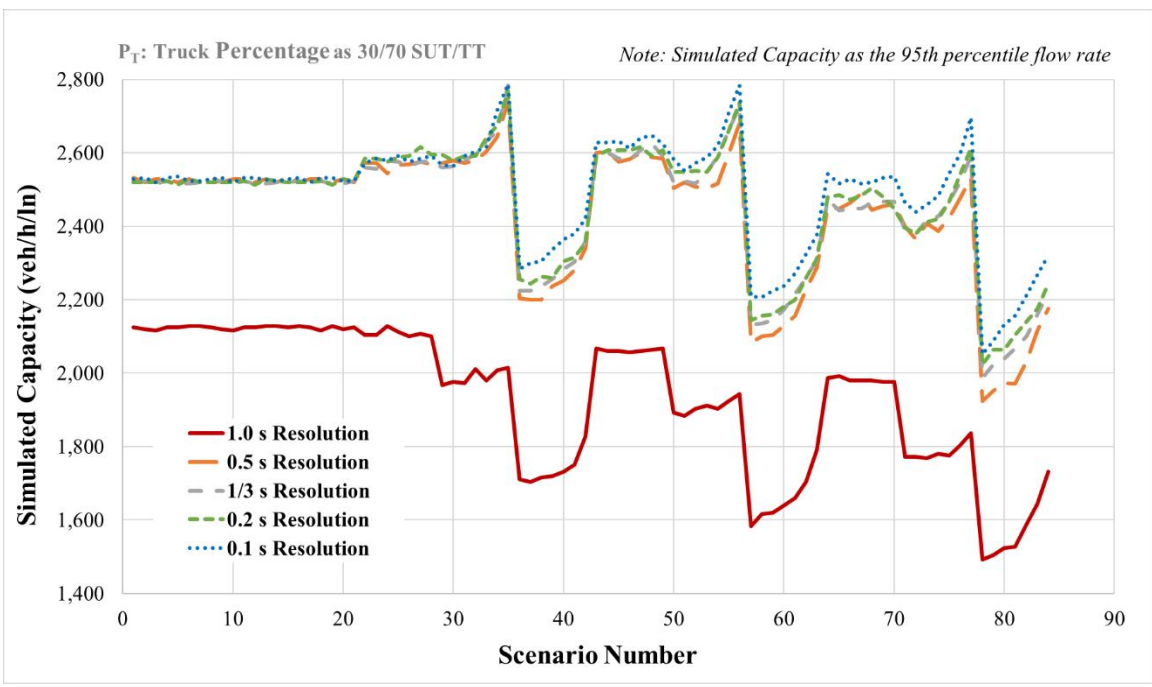


Figure C-1 Impact of simulation resolution on simulated capacity (as 95th percentile of maximum flow rate).

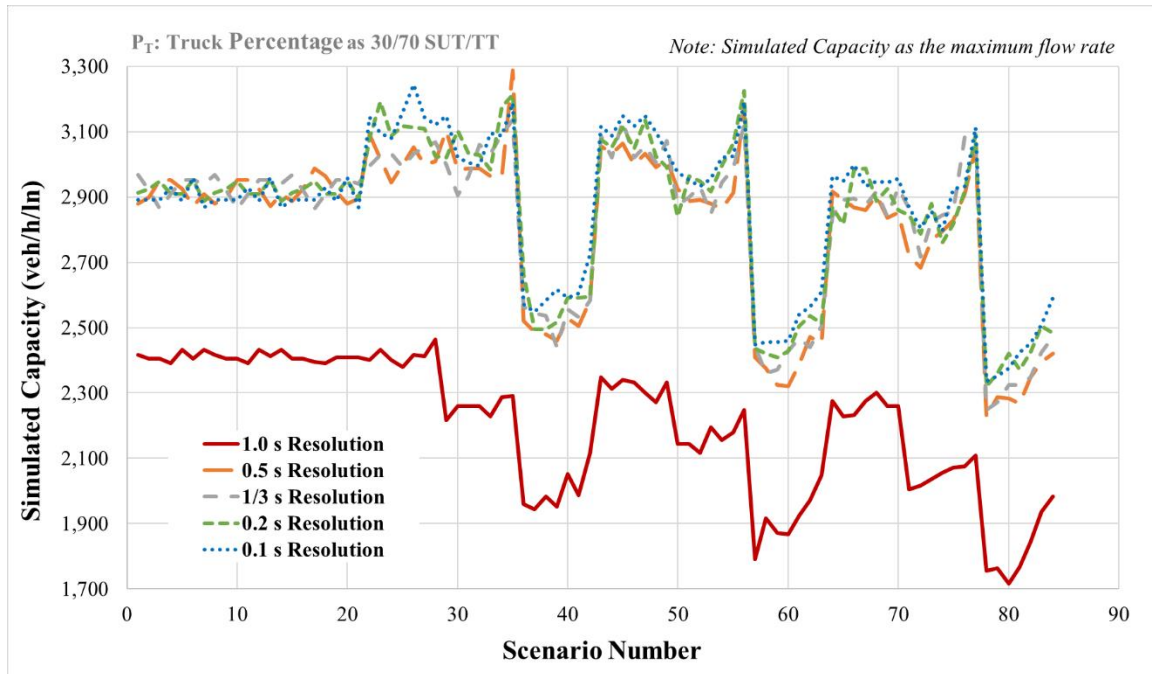


Figure C-2 Impact of simulation resolution on simulated capacity (as maximum flow rate).

It may be seen that the simulated capacity values obtained with the simulation resolution of 1 second (e.g., HCM-6 EC-PCE approach) greatly differ from those obtained with higher simulation resolutions for both capacity definitions. Interestingly, the simulated capacity obtained with simulation resolutions from 0.5 to 0.1 seconds shows similar results. It must be noted that the simulated capacity was calculated as the mean value of the ten simulation runs that were performed for each scenario combination. This approach greatly reduced the variability in the simulated capacity results produced by the stochastic component of the VISSIM model.

Table C-1 shows the results of a two-sided t-test on the simulated capacity values based on the 84 scenario combinations that were performed for exploring each simulation resolution. It may be seen that the difference between the capacity values given by the

simulation resolutions of 1 second and 0.5 seconds are statistically significant at a 5% level of significance. In contrast, the difference between the capacity values obtained with higher simulation resolutions from 0.5 to 0.1 seconds is not statistically significant at a 5% level of significance. These results were consistent for both capacity definitions. In addition, a paired t-test on 12 capacity values (defined as maximum flow rate) at the 5-mile detector (same detector) shows that the difference between the simulation resolutions of 0.5 and 0.1 seconds was not statistically significant at a 5% level of significance.

Table C-1 Descriptive Statistics and two-sided t-test of Explored Simulation

Resolutions.

Statistic	Simulation Resolution (SR)							
	SR=1.0 s	SR=0.5 s	SR=0.5 s	SR=0.33 s	SR=0.33 s	SR=0.2 s	SR=0.2 s	SR=0.1 s
(a) 95 th								
Mean	1931	2433	2433	2450	2450	2461	2461	2491
StdDev	192.6	188.6	188.6	173.7	173.7	169.0	169.0	154.1
Observations	84	84	84	84	84	84	84	84
Pooled Variance	36348		32884		29375		26156	
df	166		166		166		166	
t Stat	-17.05		-0.60		-0.42		-1.21	
p-value (two-tail)	0.000		0.549		0.675		0.229	
t Critical (two-tail)	1.97		1.97		1.97		1.97	
(b) Max.								
Mean	2203	2807	2807	2828	2828	2851	2851	2870
StdDev	207.2	251.9	251.9	243.7	243.7	238.1	238.1	231.9
Observations	84	84	84	84	84	84	84	84
Pooled Variance	53200		61420		58025		55237	
df	166		166		166		166	
t Stat	-16.95		-0.55		-0.63		-0.52	
p-value (two-tail)	0.000		0.581		0.530		0.603	
t Critical (two-tail)	1.97		1.97		1.97		1.97	

Note: (a) 95th = capacity as the 95th percentile of the maximum flow rate; (b) Max = capacity as the maximum flow rate; df = degrees of freedom; StdDev = standard deviation.

As was expected, the simulated capacity values obtained as the 95th percentile of the maximum flow rate (e.g., HCM-6 EC-PCE capacity definition) are lower than those obtained as the maximum flow rate (e.g., theoretical capacity definition). On average, the simulated capacity values defined as the 95th percentile of the maximum flow rate are 12.4% lower than the simulated capacity values defined as the maximum flow rate using VISSIM 20. It is important to note that scenarios 1 to 7 in **Figure C-1** correspond to the base capacity conditions (e.g., passenger car only and level grade conditions) for a basic freeway segment. According to the HCM-6, the base capacity for a freeway segment at 70 mph of free-flow speed is 2,400 pc/h/ln; however, the VISSIM model of the HCM-6 EC-PCE research produces an average capacity of 2,123 pc/h/ln for the same conditions. It is easy to show that this can negatively affect the results of HCM-6 EC-PCE research.

Another interesting point is that higher simulation resolutions (e.g., ≤ 0.5 seconds) can yield capacity values as high as 2,800 veh/h/ln observing the original assumptions of the HCM-6 EC-PCE VISSIM model (e.g., default Wiedemann 99 and slow lane rules) as shown in **Figure C-1**. This indicates that if higher simulation resolutions are to be used in the HCM-6 EC-PCE VISSIM model, a model calibration targeting an empirical value of capacity (e.g., the HCM-6 base capacity) must be performed. This will improve the accuracy of the simulated capacity values and will ensure the results can be reproduced and repeated by others regardless of the inherent uncertainties of the microsimulation model.

C.3.2 Flow-Density Scatterplots Results

In the HCM-6 EC-PCE methodology, the simulated capacity values for each scenario combination are obtained from the flow-density scatterplots (e.g., Step 1 in the

methodology). The flow-density scatterplots were developed for the 84 scenario combinations and for the five simulation resolutions explored in this study; in other words, 420 flow-density scatterplots were developed in this study. To illustrate, **Figure C-3** shows four flow-density scatterplots that correspond to simulation resolutions of 1 second (i.e., HCM-6 approach), 0.5 seconds, 0.2 seconds, and 0.1 seconds considering the same traffic scenario combination. This scenario combination corresponds to the following conditions: mixed traffic flow, 20% truck percentage, 3% grade, and 1.0-mile distance.

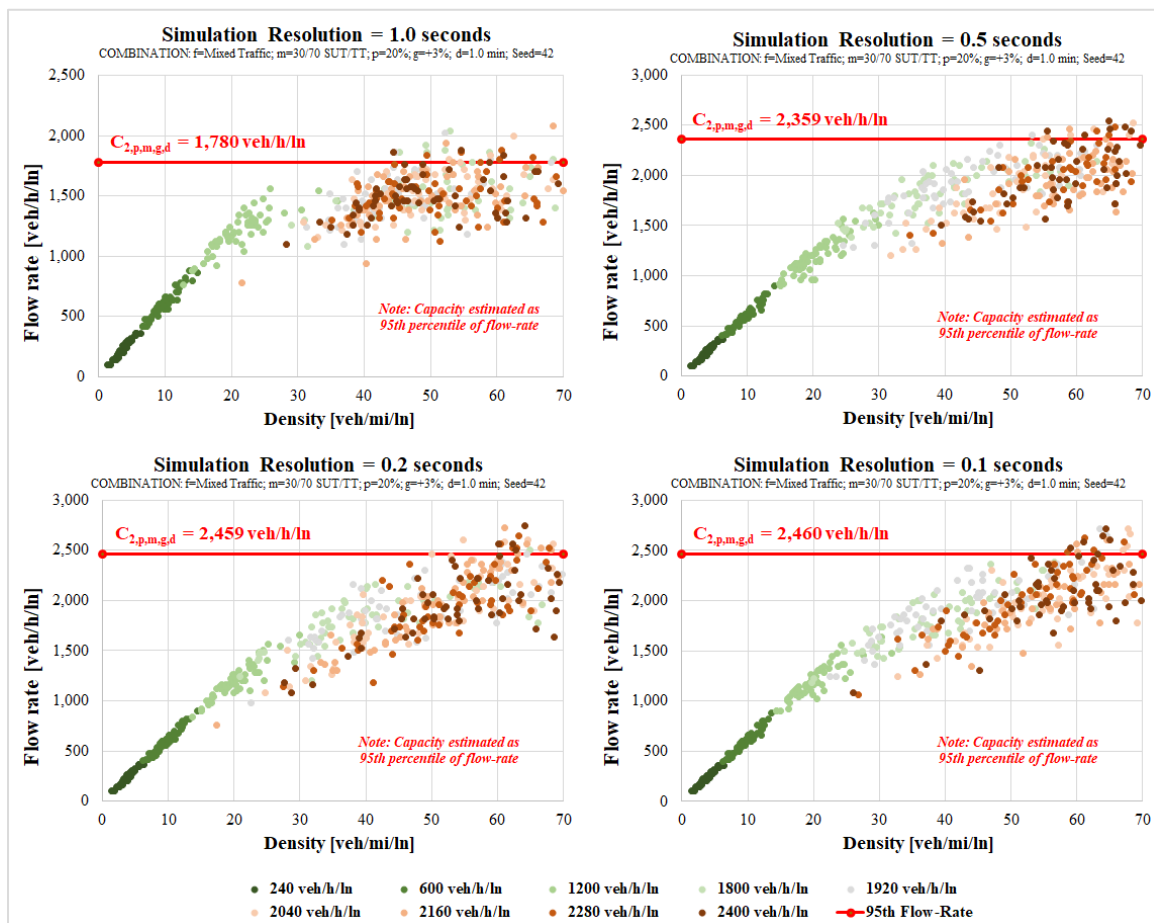


Figure C-3 Flow-density scatterplots as a function of simulation resolution.

It may be seen that the flow-density scatterplot related to the simulation resolution of 1 second (e.g., HCM-6 approach) shows a different trend as compared to the scatterplots related to higher simulation resolutions. In the former scatterplot (i.e., 1 second simulation resolution), an abrupt traffic breakdown appears at an approximate density value of 25 veh/mi/ln and a relative lack of flow-density pairs can be observed between density values of 25 and 35 veh/h/ln. In contrast, the flow-density scatterplots developed for higher simulation resolutions show a smoother transition for the traffic breakdown from density values of 25 veh/h/ln to the flow-density pairs related to the maximum flow-rate values. It is hypothesized that higher simulation resolutions (e.g., \leq 0.5 seconds) in the HCM-6 EC-PCE VISSIM model will allow detecting small variations in the flow-density-speed relationship exposing a more accurate and realistic behavior of the traffic stream.

C.3.3 Time per Simulation Run Results

As was explained previously, a higher simulation resolution in the microsimulation model will require a longer time per simulation run because the position of the dynamic objects in the simulation is recalculated more frequently demanding more computational resources. **Figure C-4** shows the relative time per simulation run as a function of the simulation resolution value. The relative time was estimated regarding the lowest simulation resolution available in VISSIM 20 (e.g., 1 second = 1 time step/simulation second). Consequently, the relative time per run for the simulation resolution of 1 second (e.g., HCM-6 approach) is equal to one. It may be seen that as the simulation resolution value decrease (i.e., more time steps per simulation second) the relative time per run increases at an increasing rate. For example, for a simulation resolution of 0.1 second, the

relative time per run is approximately 8 times greater than the time required to execute a run with the lowest simulation resolution of 1 second.

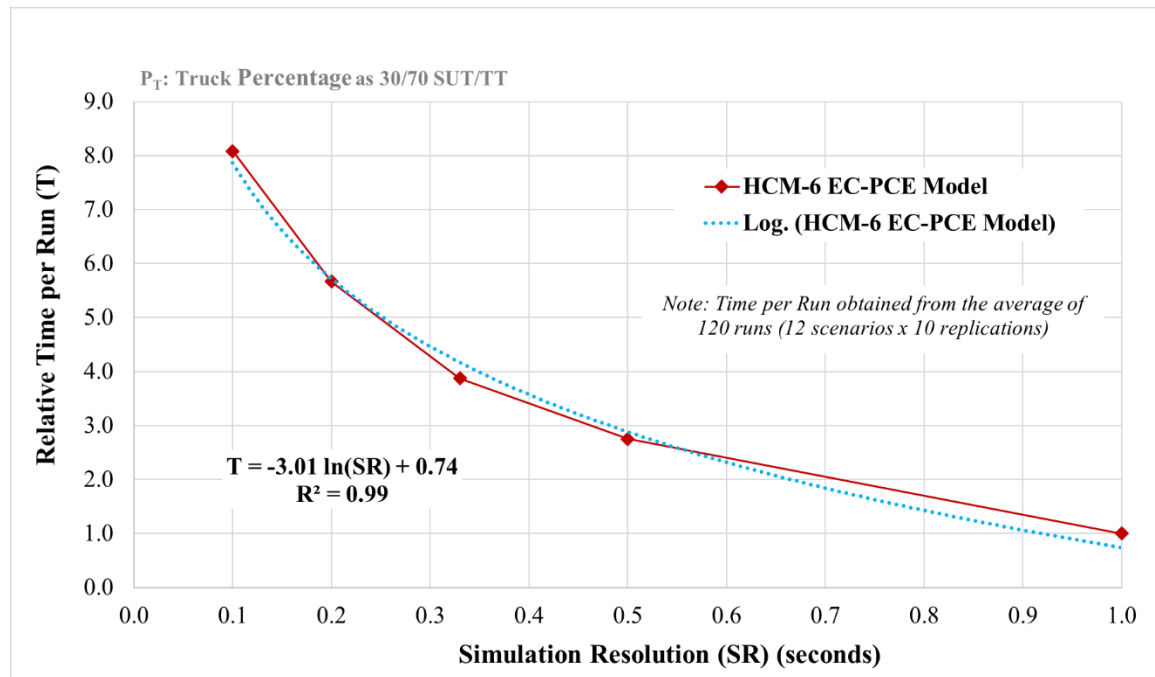


Figure C-4. Relative time per run as a function of simulation resolution.

In this research, the mean time per simulation run that was found in the HCM-6 EC-PCE VISSIM model with a simulation resolution of 1 second was 24 minutes, using a processor Intel® Core™ i7 @ 3.07 GHz with 8.00 GB ram. This implies that a higher simulation resolution of 0.1 seconds will require, on average, 192 minutes to execute one simulation run. Given that the HCM-6 EC-PCE methodology is comprised of 3,822 scenario combinations, running the total set of scenarios would require 12,230 hours (i.e., ≈ 510 days) of simulation time considering only a single simulation run per scenario. Evidently, this time will vary depending on the specific computer capabilities used in a particular experiment. For this reason, it is important to select a simulation resolution to calibrate the HCM-6 EC-PCE VISSIM model that allows the analyst to perform the

experiments within a reasonable time frame based on the technological resources available in the research, but at the same time ensuring enough accuracy on the model results.

C.4 Concluding Remarks

The objective of this study was to analyze the impact of the simulation resolution on the capacity values obtained with the HCM-6 EC-PCE microsimulation model. Interestingly, the original HCM-6 EC-PCE research used the lowest simulation resolution in VISSIM (e.g., 1 time step/simulation second) for modeling the capacity values of 3,822 traffic scenario combinations that served to estimate the EC-PCE values that appear in the HCM-6. There is no discussion about the implications of this selection and how it may affect the experimental replication of the HCM-6 EC-PCE methodology. A simulation resolution sensitivity was performed to compare the simulated capacity of 84 traffic scenario combinations that were simulated using the original HCM-6 EC-PCE protocols in VISSIM 20.

One of the most significant findings to emerge from this study is that the simulation resolution parameter has a significant impact on the simulated capacity values obtained with the HCM-6 EC-PCE microsimulation model. This implies that a different simulation resolution would yield different capacity values for the same traffic scenario combination. In this sense, it is recommended to calibrate the HCM-6 EC-PCE microsimulation model to match an empirical capacity value while considering a fixed simulation resolution. It is important to emphasize that the simulation resolution used to calibrate the model should be documented as a calibration parameter to facilitate that others may replicate the experiments.

Another interesting finding is that the difference between the capacity values obtained with a simulation resolution of 1 second (e.g., HCM-6 approach) and those with higher simulation resolutions (e.g., 0.5, 0.3, 0.2, 0.1 seconds) was statistically significant at a 5% level of significance. In contrast, the difference between the simulated capacity values obtained with higher simulation resolutions, from 0.5 to 0.1 seconds, was not statistically significant at a 5% level of significance. These findings were consistent with both capacity definitions explored in this study. It is important to note that the simulation resolution of 0.5 seconds may produce similar results as those obtained with the higher simulation resolutions with a significant reduction of the required simulation time. This is important because further traffic scenarios beyond the scope of the HCM-6 could be simulated considering a simulation resolution of 0.5 seconds without significant loss in fidelity and accuracy as compared to more demanding simulation resolutions, although this should be corroborated for microsimulation model versions other than VISSIM 20.

Interestingly, the HCM-6 EC-PCE microsimulation model produced capacity values that were not consistent with those that appear in the HCM-6. In the HCM-6, the capacity for basic freeway segments is defined as the maximum flow rate observed during a sustained period of 15 minutes. However, the HCM-6 EC-PCE research defined the capacity as the 95th percentile of the maximum one-minute average flow-rate for the given scenario. As was shown in this study, the capacity values defined as the maximum flow rate were, on average, 14.2% greater than the capacity values defined as the 95th percentile of the maximum flow rate. Previous studies have also shown that the aggregation level has a significant impact on the capacity values (Zhou, Rilett, & Jones, 2019). It is important that the HCM-6 EC-PCE methodology uses a consistent definition

of capacity and aggregation level, so the capacity values obtained from the microsimulation model can be compared with those in the HCM-6. Note that the mixed flow model included in the HCM-6 (*Equation 26-1*) compares the HCM-6 EC-PCE capacity with the base capacity values for basic freeway segments (*Exhibit 12-4*). It is clear that both capacity sources must be compatible.